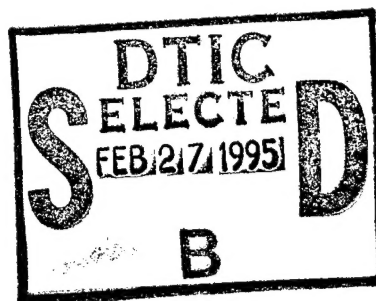**US Army Corps
of Engineers**
Waterways Experiment
Station

Nonlinear, Incremental Structural Analysis of Olmsted Locks: Phase III

by Chris A. Merrill, Barry D. Fehl, Sharon Garner

DTIC
SELECTED
FEB 27 1995
B

19950221 015

The contents of this report are not to be used for advertising, publication, or promotional purposes. Citation of trade names does not constitute an official endorsement or approval of the use of such commercial products.

Nonlinear, Incremental Structural Analysis of Olmsted Locks: Phase III

by Chris A. Merrill, Barry D. Fehl, Sharon Garner

U.S. Army Corps of Engineers
Waterways Experiment Station
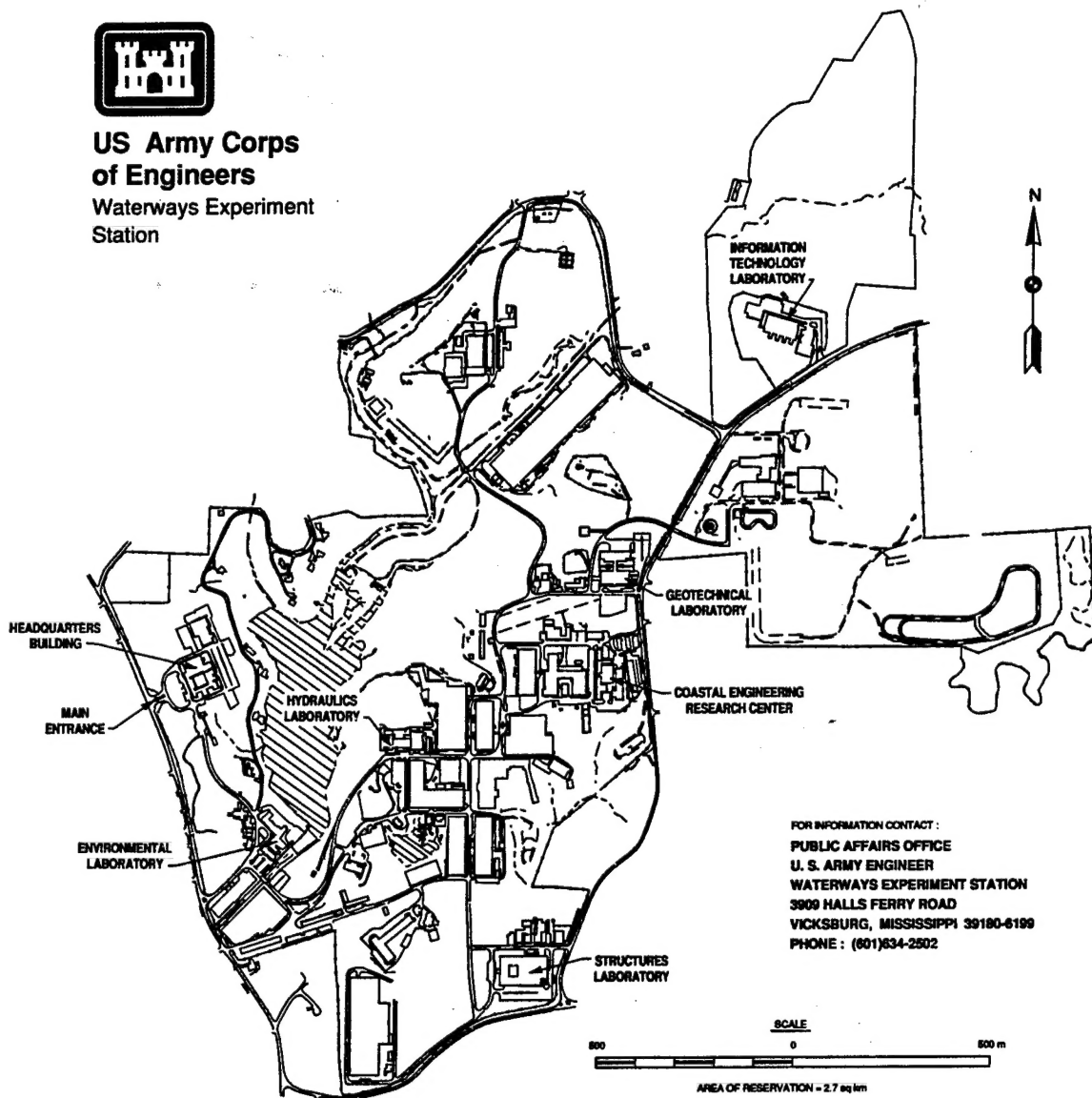3909 Halls Ferry Road
Vicksburg, MS 39180-6199

Final report

DTIC QUALITY INSPECTED 4

US Army Corps
of Engineers
Waterways Experiment
Station

N

INFORMATION
TECHNOLOGY
LABORATORY

HEADQUARTERS
BUILDING

MAIN
ENTRANCE

HYDRAULICS
LABORATORY

GEOTECHNICAL
LABORATORY

COASTAL ENGINEERING
RESEARCH CENTER

ENVIRONMENTAL
LABORATORY

STRUCTURES
LABORATORY

FOR INFORMATION CONTACT :
PUBLIC AFFAIRS OFFICE
U. S. ARMY ENGINEER
WATERWAYS EXPERIMENT STATION
3909 HALLS FERRY ROAD
VICKSBURG, MISSISSIPPI 39180-6199
PHONE : (601)634-2502

SCALE

500   0   500 m

AREA OF RESERVATION = 2.7 sq km

Contents

List of Figures

List of Tables

Preface

The work described in this report was conducted for the U.S. Army Engineer District, Louisville, by the Computer-Aided Engineering Division (CAED), Information Technology Laboratory (ITL), and the Structural Mechanics Division (SMD), Structures Laboratory (SL), U.S. Army Engineer Waterways Experiment Station (WES). The investigation was authorized by DD form 448, MIPR No. RMB-92-800, dated 3 Jun 1992.

The investigation was accomplished under the general supervision of Dr. N. Radhakrishnan, Director, ITL; Mr. Bryant Mather, Director, SL; and Mr. James T. Ballard, Assistant Director, SL, and under the direct supervision of Mr. H. Wayne Jones, CAED, and Dr. Robert L. Hall, SMD. This report was prepared by Mr. Chris A. Merrill, CAED, Mr. Barry D. Fehl, CAED, and Ms. Sharon Garner, SMD. The authors acknowledge Mr. Byron McClellan and Mr. Jeff Bayers, CEORL-ED-DS, for their support and encouragement during the performance of the work described herein.

The work contained in this report is a portion of the Phase III, Nonlinear, Incremental Structural Analysis (NISA) Study of the Olmsted Locks. Analyses of a typical culvert valve monolith and the lower miter gate monolith were also performed as a part of the Phase III Study. The Phase III Study was a combined effort of Ms. Sharon Garner of the WES Structures Laboratory, Messrs. Chris Merrill and Barry Fehl of ITL, and, working under contract to WES, Mr. Randy James and Dr. Robert Dunham of ANATECH Research Corporation. The entire Phase III NISA Study was a closely coordinated effort which included review meetings attended by representatives from Headquarters, the Ohio River Division, and the Louisville District. The Phase III NISA Study was a part of a larger WES effort on the Olmsted Project with Mr. Glenn Pickering of the WES Hydraulics Laboratory acting as the point of contact.

At the time of publication of this report, Director of WES was Dr. Robert W. Whalin. Commander was COL Bruce K. Howard, EN.

Conversion Factors, Non-SI to SI Units of Measurement

Non-SI units of measurement used in this report can be converted to SI units as follows:

Multiply	By	To Obtain
Btu (International Table) per pound (mass) · degree Fahrenheit	4,186.8	joules per kilogram kelvin
Btu (International Table) inch per hour · square inch · degree Fahrenheit	20.7688176	watts per meter kelvin
calories per gram	4.184	kilojoules per kilogram
Fahrenheit degrees	5/9	Celsius degrees or kelvins[1]
feet	0.3048	meters
inches	25.4	millimeters
kips (force) per inch-	1.213659	kilonewtons per meter
miles (U.S. statute)	1.609347	kilometers
pounds (force) per square inch	0.006894757	megapascals
pounds (mass) per cubic foot	16.01846	kilograms per cubic meter
pounds (mass) per cubic inch	27,679.899	kilograms per cubic meter

[1] To obtain Celsius (C) temperature readings from Fahrenheit (F) readings, use the following formula: $C = (5/9)(F - 32)$. To obtain kelvin (K) readings, use $K = (5/9)(F - 32) + 273.15$.

1 Introduction

Background

The Olmsted project will be located on the Ohio River at mile 964.4 and will have two locks (on the right bank) and a dam to control the river during low flow periods. The lock will be designed as a W-frame type structure and each chamber of the locks will be approximately 110 ft wide and 1,200 ft long.[1] The project was authorized for construction by the Water Resources Development Act of 1988.

In September 1989, the U.S. Army Engineer District, Louisville, requested that the U.S. Army Engineer Waterways Experiment Station (WES) perform a nonlinear, incremental structural analysis (NISA) to evaluate the constructability of the unprecedented W-frame structure. WES performed a NISA as requested using guidance from Engineer Technical Letter (ETL) 1110-2-324 (USACE 1990). NISA is a finite element process which utilizes the general purpose code ABAQUS (Hibbit, Karlsson, and Sorensen 1988), along with software developed by ANATECH Research Corp. which models the nonlinear effects of various material properties. This software is implemented by ABAQUS by its user subroutine UMAT and is discussed in detail in reports developed at WES (Garner and Hammons 1991) and ANATECH (ANATECH Research Corp. 1992).

As a result of the NISA performed by WES a report was published (Garner et al. 1992) documenting the data used, procedures, and results of the work. After a brief introduction the report presents the data with respect to the material properties used and various items concerning input into the analysis. The remainder of the report discusses the analyses and results of Phase I and Phase II of the Olmsted NISA study. Phase I of the study focused on evaluation of two different placement methods and verification through limited three-dimensional (3-D) analyses and two-dimensional (2-D) out-of-plane analyses. An evaluation was then made in

---

[1]   A table of factors for converting non-SI to SI units of measurement is given on page xv.

Phase II of the study on the two concrete mixtures being considered by evaluating bounds to the creep and shrinkage curves as required in ETL 1110-2-324. The results from Phase II were then used to validate the results obtained in Phase I.

Upon completion of Phases I and II, a determination was made based on the conclusions and recommendations of the first two phases that further analyses could be performed which would demonstrate that more cost-effective construction methods were achievable. In a meeting of personnel of U.S. Army Corps of Engineers Headquarters (HQ), the Ohio River Division (ORD), the Louisville District (ORL), and WES in April 1992, it was determined and directed that WES should perform a third phase (Phase III) of NISA work which would support changes to more cost-effective construction methods and evaluate the construction of the lower miter gate monolith and a culvert valve monolith. From that directive, WES developed a proposed scope of work that was agreed to by the Louisville District and which is described below.

Objective

The primary objective of the Phase III NISA study for the Olmsted locks was to evaluate proposed changes in construction methods that would provide tangible cost savings to the project but that would not compromise the integrity of the structure. A secondary objective was to further consider some areas in which questions remained and to verify that these areas will not be cause for concern during construction of the project.

Scope

The analyses in this portion of the Phase III study were performed on a typical chamber monolith. The finite element mesh and associated dimensions used in the chamber monolith analyses are shown in Figure 1. The lift placement sequence is shown in Figure 2. The finite element mesh shown in the two figures is identical to the mesh used in Phases I and II with the exception of the area around the gallery of the center wall. The width of the center wall gallery was increased to 36 ft from 8 ft during the course of the Phase II study. From the results of the Phase II analyses it was determined that all remaining analyses could be performed using the conditions of load case 5, which contains minimum creep and maximum shrinkage, for mixture 11. It was also decided to use plane stress formulation in the analyses. A brief description of the scope of each set of analyses to be performed is described in the following paragraphs.
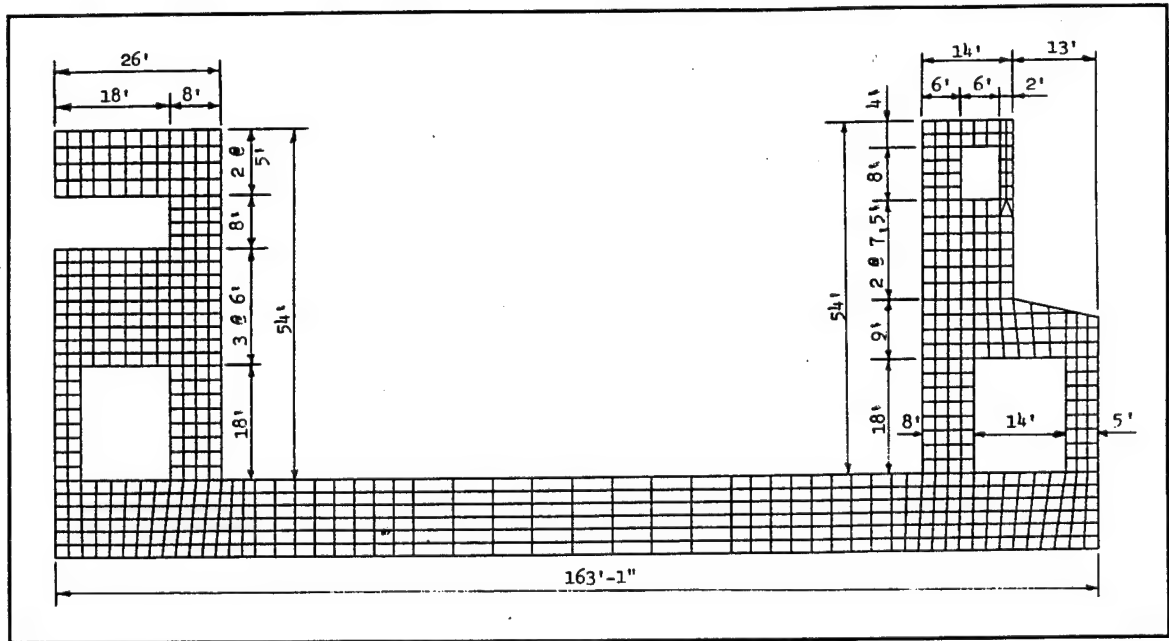
Figure 1.   Geometry and finite element mesh of a typical chamber monolith
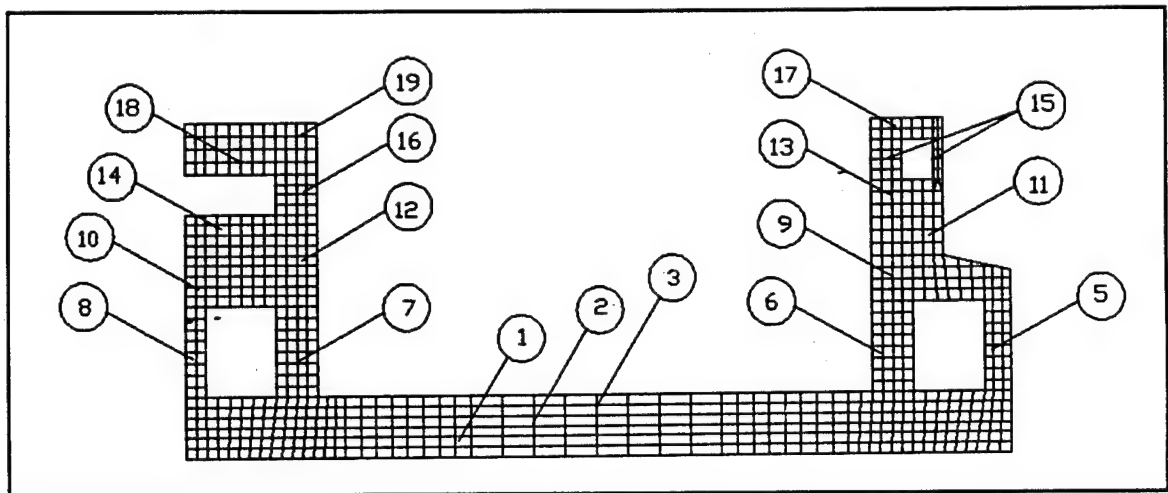
Figure 2.   Lift placement sequence and finite element mesh of a typical chamber monolith

Start time and insulation requirements

Without the benefit of additional analyses, the specifications for the Olmsted project would have required insulation for any concrete placed during the winter months between Nov 1 and Apr 1. An analysis was performed based on these specifications and then an analysis was performed using the period from Dec 1 to Mar 1 for insulation requirements. The first two analyses were performed using an insulating value of R equal to 4, but a subsequent analysis used an R value of 2. Additional analyses

were performed to study the effects of cold fronts (i.e. a sudden drop in temperature) on surface stresses and to evaluate reducing the insulation period from 90 to 30 days. These additional analyses included varying start times in an attempt to model the most detrimental case.

Placement intervals and lift heights

Two analyses of the center wall were performed using increased lift heights and a 5-day placement interval. In the first analysis a 60 °F placement temperature was maintained throughout the analysis. In the second analysis the concrete placement temperature was kept at the ambient temperature at the time of placement. These analyses were performed to determine if it was possible to receive cost savings through increasing the lift heights.

Placing temperature

Analyses were performed which varied the placing temperature from the original 60 °F used in Phases I and II to one analysis with a 70 °F placing temperature and another analysis with a placing temperature based on the ambient conditions. The three analyses were compared to assist in understanding the trends in the behavior due to changes in the placing temperature and to determine the maximum allowable placing temperature.

Miscellaneous Items

During the course of the study, questions were raised on various items which were part of the analysis and were subsequently added to the scope of the NISA study. These items included the addition of an extreme ambient condition, varying the time of set of the concrete, evaluating the method of applying the stress-free temperature, and looking at changing the interval of the slab placements. In addition, an analysis was performed on the chamber monolith using an updated version of the constitutive and cracking model to verify that its behavior was satisfactory.

Additional Phase III studies

Three other reports are under preparation at present (1994) covering other aspects of the Phase III study. The first report covers how to implement reinforcement in the finite element program ABAQUS (program used in performing a NISA) and illustrates how reinforcement affects the behavior of a structure by showing how results are altered by inclusion of reinforcement in an analysis of the chamber monolith. The second report is on a 3-D analysis of the wall of monolith L-17, which is a tainter valve monolith, and will primarily investigate any out-of-plane cracking problems that may occur due to the location of the tainter valve pit within the

monolith. Finally, the third report will document work performed on monolith L-19, the lower miter gate monolith, to identify any problem areas which may exist in this massive monolith. A number of 2-D analyses were performed on the monolith to gauge the behavior of the monolith, and several modifications were made in the construction methods based on results of the 2-D analyses. Finally, a 3-D analysis was performed to determine differences in the structural behavior compared to the 2-D analyses performed.

2 Winter Placement and Insulation Requirements

Summary of Analyses

The goal of the winter placement study was to determine the minimum insulation requirements necessary to protect the chamber monolith from cracking due to exposure to cold ambient temperatures.

The study of winter placement requirements was conducted in four parts.

a. Initially three parameters were investigated: start and ending dates for insulation, age of concrete at removal of insulation, and thickness of insulation (as R value). The start-of-construction date for these analyses was Oct 1, and all analyses used the average daily ambient temperature curve shown in Figure 3.

b. The next three analyses used the minimum insulation requirements determined from the previous analyses. In these analyses the average ambient daily temperature was modified to model cold fronts, and two methods were used to model the air elements in enclosed culverts.

c. The next two analyses imposed more rigorous conditions on the floor section. In these analyses the start-of-construction time was shifted to allow the removal of insulation in January, near the lowest point in the average ambient temperature curve. In each case, a cold front was simulated immediately upon removal of the insulation.

d. The two final two analyses used a starting date of Oct 1 and the extreme ambient curve developed in Chapter 4.

In all analyses, concrete was placed at ambient temperature until 40 °F, the minimum temperature for placement, was reached. Film coefficients used to allow heat loss at exposed surfaces in the heat transfer analyses
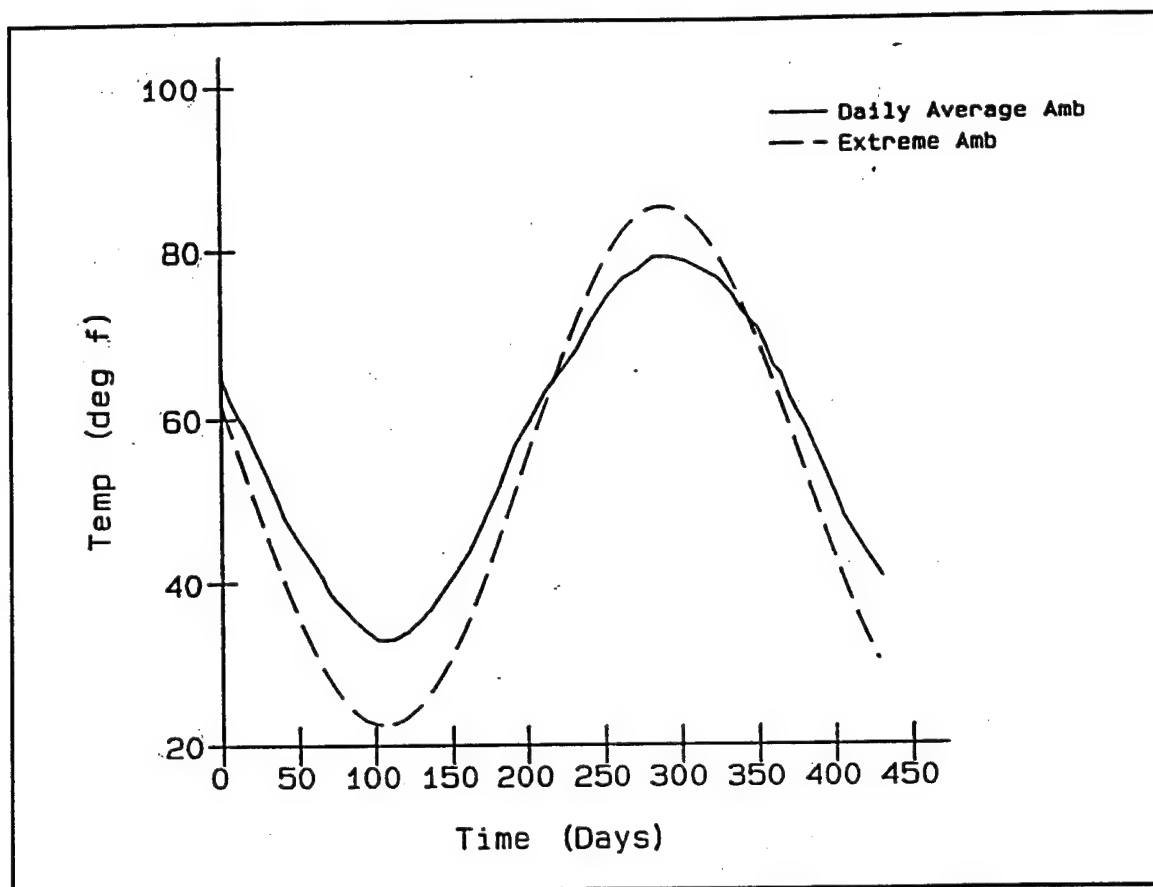
Figure 3.   Ambient temperature curves used in winter placement analyses

are given in Table 1. Assumptions made in calculating these film coeffi-
cients can be found in a previous report (Garner et al. 1992). The lift
placement sequence used in the analyses is shown in Figure 2. Unless
otherwise noted, the lift placement schedule given in Table 2 was used in
the analyses.

Table 1
Film Coefficients for Heat Transfer Analyses

			Film Coefficients, Btu/day-In.^{2}-°F			
			Insulation + Forms		Insulation Only	
Time Period	Concrete	Forms	R = 2 (h - ft^2 - °F/Btu)	R = 4 (h - ft^2 - °F/Btu)	R = 2 (h - ft^2 - °F/Btu)	R = 4 (h - ft^2 - °F/Btu)
Oct	0.5552	0.1350	NA	NA	NA	NA
Nov - Apr	0.6998	0.1421	0.05223	0.04305	0.07446	0.0567
May	0.5387	NA	NA	NA	NA	NA
Jun - Sep	0.4727	NA	NA	NA	NA	NA

Table 2
Lift Placement Schedule

Lift	Placement Day	Ambient Temperature °F	Lift	Placement Day	Ambient Temperature °F
1	Oct 1	65.0	11	Dec 10	37.5
2	Oct 11	60.5	12	Dec 15	36.5
3	Oct 21	57.0	13	Dec 20	35.5
5	Oct 26	53.0	14	Dec 25	34.5
6	Oct 31	50.5	15	Dec 30	34.0
7	Nov 5	48.0	16	Jan 4	33.3
8	Nov 10	42.0	17	Jan 9	33.0
9	Nov 30	40.8	18	Jan 14	33.0
10	Dec 5	39.0	19	Jan 19	33.3

Maximum and Minimum Insulation Requirements

Maximum and minimum winter placement requirements as suggested by the Louisville District are given in Table 3. Insulation variables used in the first four winter placement analyses are given in Table 4.

When discussing temperatures across a section, the term "temperature differential" will be used to refer to the difference between the maximum and minimum temperatures across the section at a given time. Normally, for several weeks after placement and during the cool months of the year the maximum temperature occurs at the center of a symmetrical section or the base of a thin floor, while outer surface temperatures are at cooler ambient temperatures. During the summer, temperatures at the center of a

Table 3
Maximum and Minimum Winter Placement Requirements

Condition	Start Date	End Date	Age At Removal (days)	R (h - ft² - °F/Btu)
Minimum requirements	Dec 1	Mar 1	30	2
Maximum requirements	Nov 1	Apr 1	90	4

Table 4
Winter Placement Analyses, Part 1 Insulation Parameters

Analysis	Insulation Dates	R (h - ft^2 - °F/Btu)	Age of Removal (days)
1	Nov 1 - Apr 1	4	90
2	Nov 1 - Apr 1	2	90
3	Dec 1 - Mar 1	2	90
4	Dec 1 - Mar 1	2	30

wall or at the base of a thin floor that has already undergone hydration of its cementious material may be cooler, with the maximum temperature occurring at the surface of the concrete. This difference in temperatures results in differences in strains across a section. For instance, at the interior of a recently placed thick wall section, elevated temperatures will result in expansive strains, while at the cooler surface the concrete will attempt to contract. Restraint of these surface contractions provided by the hot expanding center of the section can result in tensile stresses and cracking.

Temperatures are given at nodes and stresses at integration points. Both node and element numbers increase from left to right and from bottom to top. Adjoining nodes or elements are numbered sequentially from left to right.

Temperature histories across floor section 3 are plotted along with average ambient temperatures for the four analyses in Figure 4. The sudden drops in temperature at the concrete surface (node 3641) at 110 days in Figures 4a, b, and c occurred when insulation was removed and surface temperatures dropped to the ambient temperature. Just prior to removal of the insulation, the difference in temperature between the surface of the concrete and the average ambient temperature was 15 °F in analysis 1, 8 °F in analysis 2, and 7 °F in analysis 3. Since all analysis 4 floor concrete was greater than 30 days old prior to Dec 1, no insulation was used on the floor, and no sudden changes in surface temperature occurred in Figure 4d. Long-term temperature differentials in the floor were not affected by insulation. As soon as the surface temperature returned to ambient, temperature differentials in all analyses were similar. At 300 days, the temperature differential across the floor section was approximately 20 °F in all four analyses.

Horizontal stress histories at section 3 for the four analyses are plotted in Figure 5. Maximum stresses for this section for each analysis are given in Table 5. For all analyses with insulation, the maximum tensile stress occurred near the center of lift 3 when insulation was removed. Maximum stress decreased with length of insulation period and R value. This
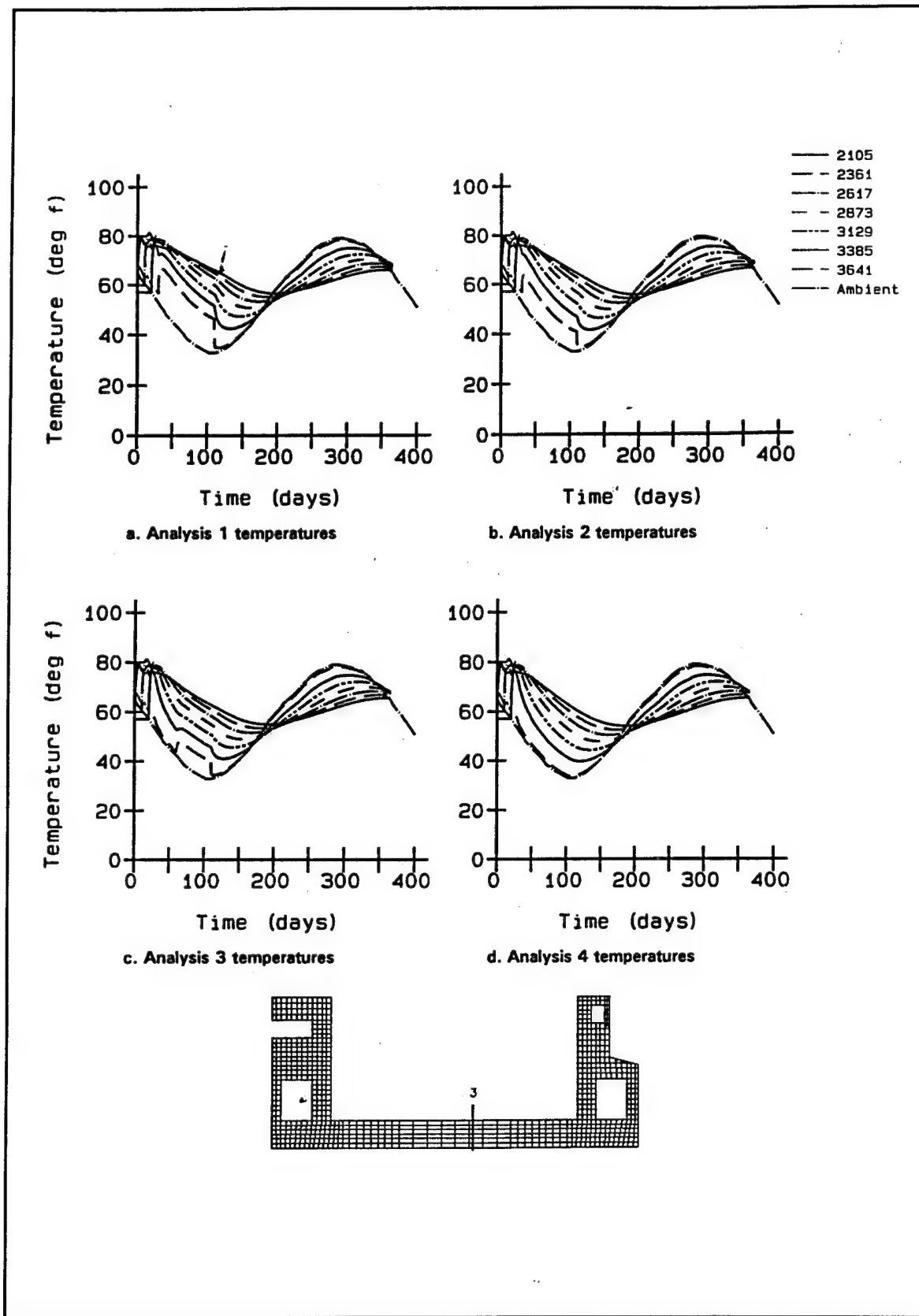
Figure 4.   Nodal temperatures at section 3, winter placement analyses 1 through 4
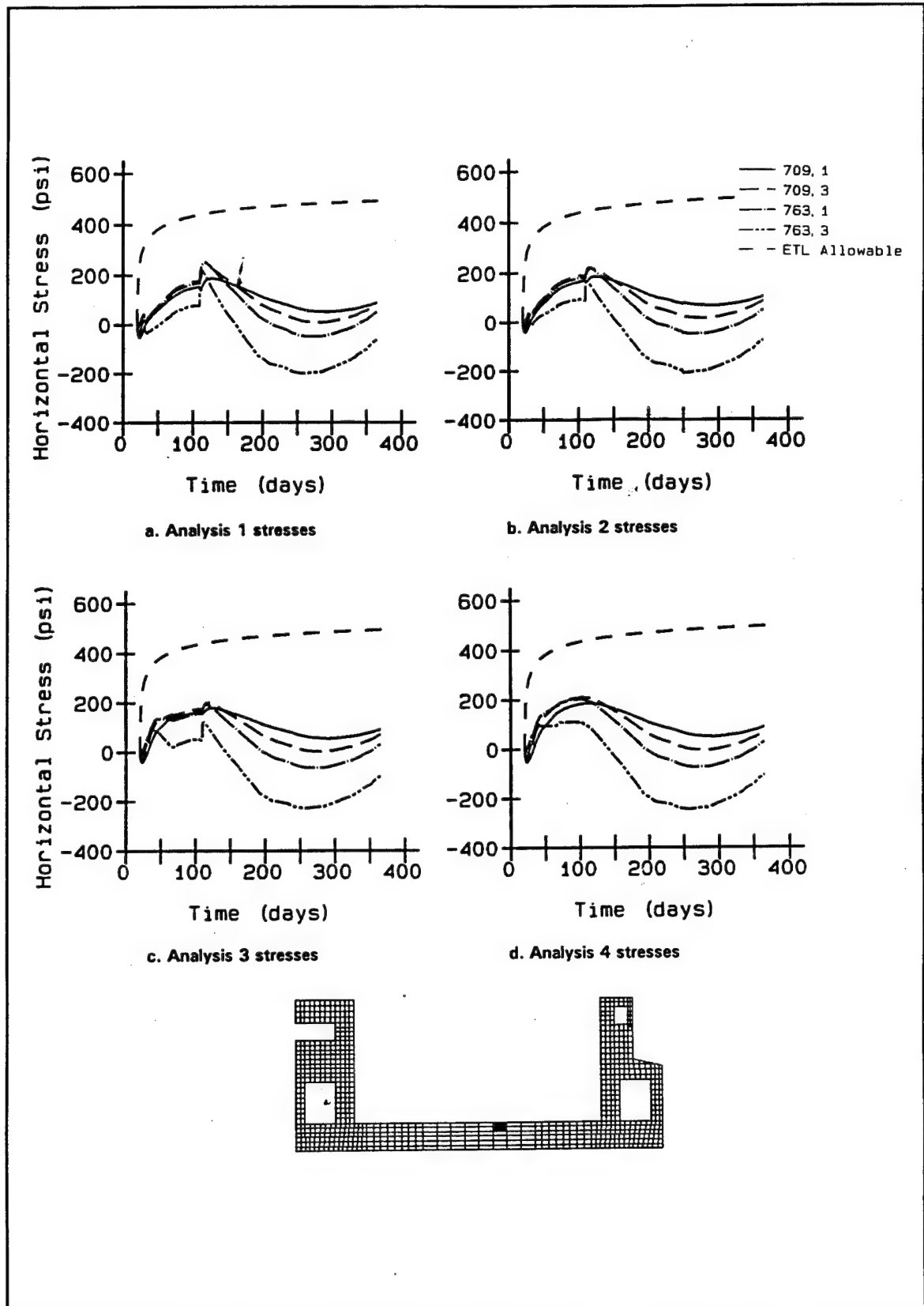
Figure 5.   Horizontal stresses, floor section 3, winter placement analyses 1 through 4

Table 5
Maximum Tensile Stresses, Section 3, Analyses 1 Through 4

Analysis	Element	Point	Stress (psi)	ETL Allowable (psi)	Percentage of Allowable
1	763	1	252.7	442.3	57.1
2	763	1	218.1	442.3	49.3
3	763	1	210.2	443.0	48.4
4	709	3	211.4	434.4	48.7

is because surface temperatures were maintained at an artificially high value during the insulation period and dropped to near ambient when insulation was removed, resulting in immediate tensile stresses. The magnitude of the temperature drop and the resulting tensile stress increased with thickness of insulation and length of insulation period. In analysis 4, where no insulation was used, the maximum tensile stress occurred at 87 days after the start of construction. In all of the first four analyses, maximum tensile stress in the floor never exceeded 57.1 percent of the ETL allowable stress.

Air in enclosed culverts in these four analyses was simulated using air elements with an ETL-specified conductivity of 1,000 Btu-in./day-in.^{2}-°F which has been corrected to h = 0.03 Btu-in./day-in.^{2}-°F. Because this produced inaccurate results in wall areas near culverts, wall stresses for the first four analyses are not discussed.

Analyses with Cold Fronts

Minimum insulation requirements from the previous analyses were used in the next three analyses in which cold fronts were simulated at 65, 95, 115, and 135 days after the start of placement. Cold fronts were simulated by dropping the ambient temperature 30 deg below the average ambient over a period of 12 hr and allowing it to rise to the average curve over the next 2.5 days. The scheduling of cold fronts was designed to subject the insulated concrete to adverse conditions shortly after the removal of insulation. The first cold front occurred 45 days after the placement of the last floor lift, but prior to removal of floor insulation placed in November and just prior to the removal of lift 6 insulation. The cold front at 95 days occurred when lift 9 insulation was removed, the cold front at 115 days corresponded to removal of the lift 13 insulation, and the cold front at 135 days coincided with removal of the lift 17 insulation.

Temperature histories from the first analysis, floor section 3, are shown in Figure 6. Cold fronts tended to cause sudden drops in surface temperature to approximately 10 deg above ambient, but no long-term effects were observed for the 12-ft-thick floor section. Surface temperatures returned to ambient as the cold fronts ended, and temperature gradients across the section were similar to those in the previous analysis 4 by day 150. Stresses across section 3, lift 3, for this period are shown in Figure 7. The maximum stresses during each cold front occurred near the surface and ranged from 377.5 psi (87.7 percent of ETL allowable) at 95 days to 285.7 psi at 135 days. Maximum floor stresses for this analysis are given in Table 6.
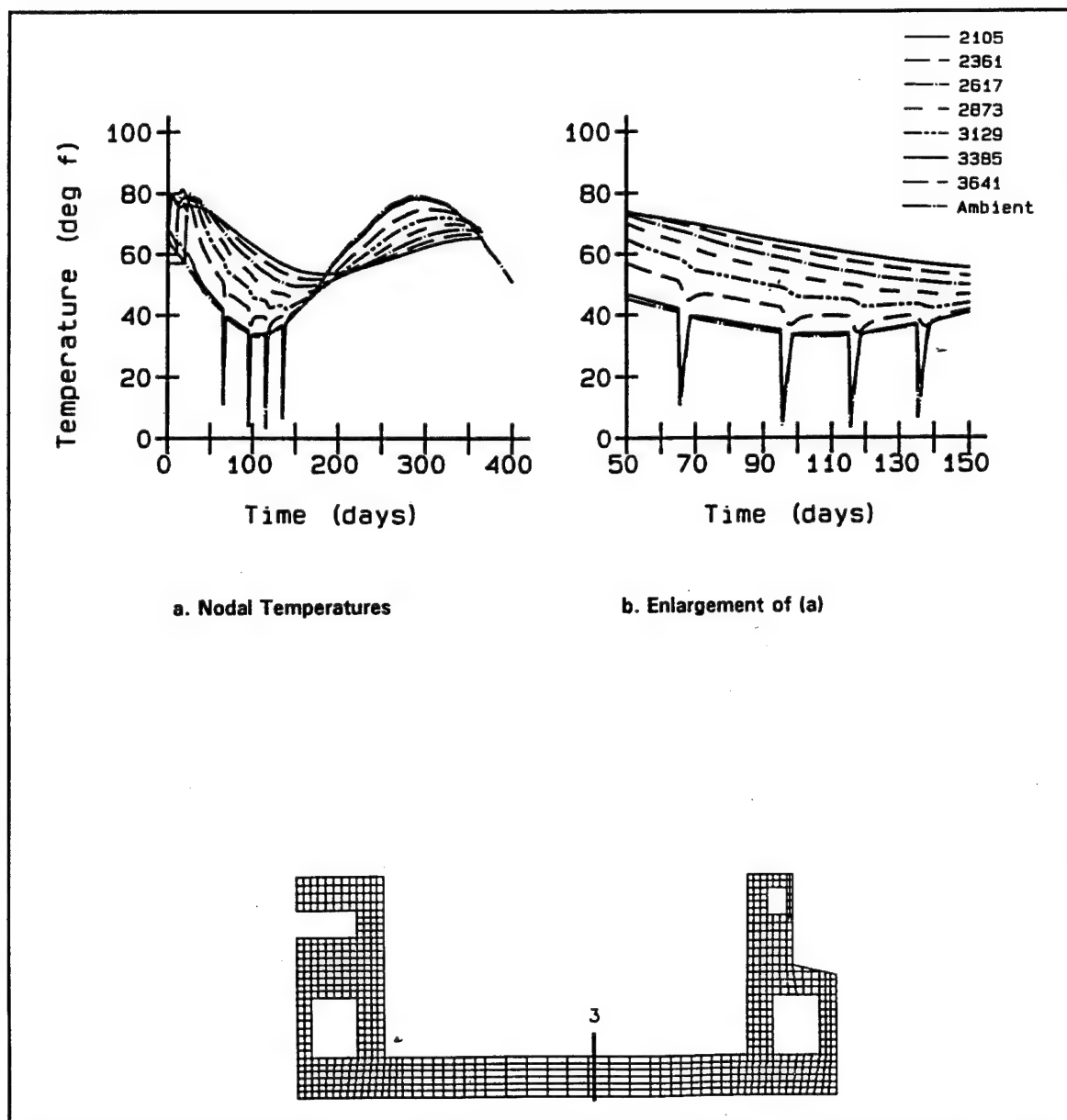
Figure 6.   Nodal temperatures, floor section 3, winter analysis with cold fronts
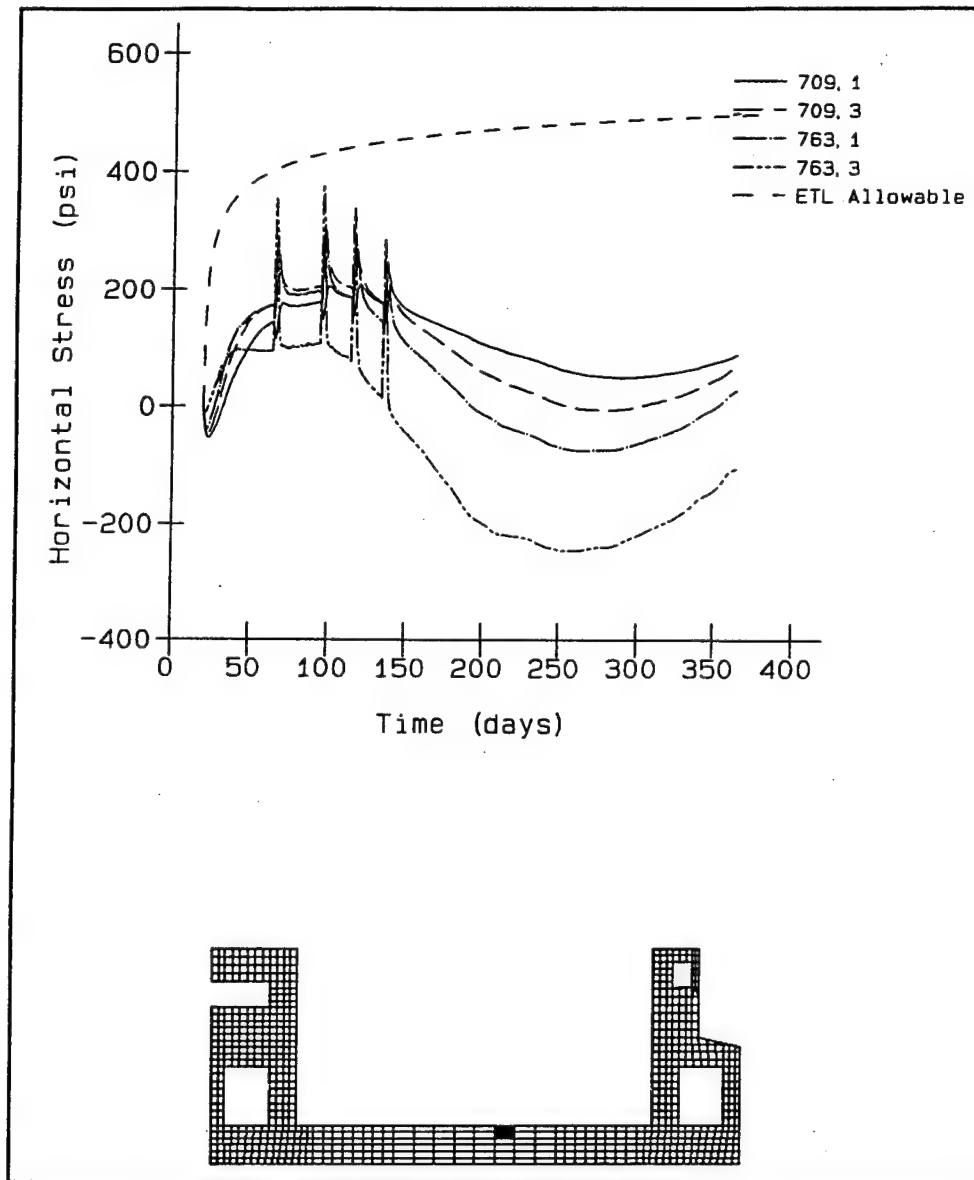
Figure 7.   Maximum horizontal stresses, floor section 3, winter analysis
with cold fronts

**Table 6
Maximum Tensile Stresses, Section 3, Winter Analyses with
Cold Fronts**

Day	Element	Point	Stress (psi)	ETL Allowable (psi)	Percentage of Allowable
65	763	3	354.2	404.7	87.5
95	763	3	377.5	430.6	87.7
115	763	3	341.1	441.9	77.2
135	763	3	285.7	450.5	63.4

In the next two analyses, two methods were used to simulate air in closed culverts. ETL 1110-2-324 recommends using air elements with the properties specified in Table 7. This method may be overly conservative since it assumes no heat loss in the out-of-plane direction and cannot account for heat loss through the plywood culvert covers at the ends of a monolith. In the first analysis, air was modeled according to the ETL, as air elements with a thermal conductivity of 0.03 Btu-in./day-in.^{2}-°F. In the second analysis, a very small film coefficient (0.01 Btu/in.^{2}-day-°F) was used on all inside culvert surfaces. Culverts were assumed to be covered as soon as surrounding insulation was placed. In accordance with the specifications, culvert covers remained in place after insulation was removed in both analyses.

Table 7
Recommended Air Properties

Property	Value
Density, lb/in.^{3}	4.5E-5
Specific heat, Btu/lb-°F	0.24
Thermal conductivity, Btu-in./day-in.^{2}-°F	0.03

Temperature histories across lift 12 for the two analyses are shown in Figure 8. Since temperatures at the outer face of the concrete were approximately ambient after removal of the insulation in both analyses, only the outer face temperature history from the analysis using air elements has been plotted. Temperatures at the center of lift 12 were somewhat higher in the first analysis than in the second analysis, with a maximum difference of about 5 °F at 200 days. Temperatures at the outer surface for both analyses dropped to ambient when the insulation was removed at 110 days. At 114 days, just after insulation was removed and just prior to the cold front at 115 days, the temperature differential across the section was 37.7 °F in the first analysis and 36.6 °F in the second analysis. Minimum surface temperatures during cold fronts were 13.03 °F at 115 days and 15.4 °F at 135 days, or approximately 9 to 10 deg above the ambient. Because of the elevated center temperature in the first analysis, temperature differentials throughout the winter months were greater in the first analysis than in the second. However, the elevated center temperatures resulted in smaller temperature differentials for the first analysis during summer months. At 285 days, roughly the peak of the ambient temperature curve, the temperature differential was 15.7 °F in the first analysis and 18.2 °F in the second analysis.

Temperature histories across the center wall culvert are shown in Figure 9. Temperatures across lift 8 (nodes 4609 and 4613) were close to uniform by 30 days after placement, while small temperature differentials can
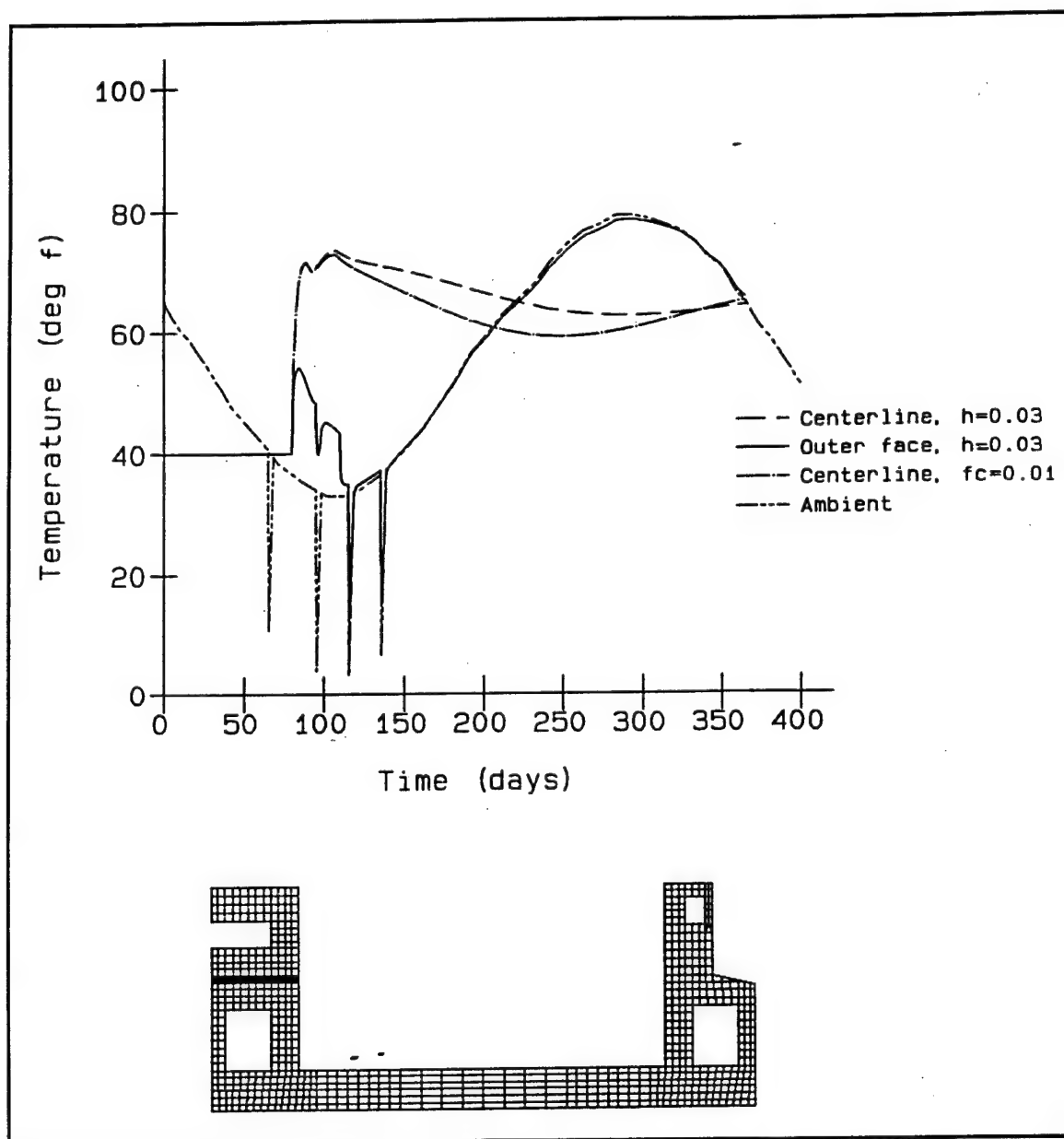
Figure 8. Nodal temperatures at center and outer face of center wall, lift 12, winter analyses modeling culverts with air elements and low film coefficients

be observed across lift 7 (nodes 4625, 4629, and 4633), which was 8 ft thick. Temperatures in lift 8 are somewhat higher in the first analysis than in the second. This indicates that using air elements rather than film coefficients to simulate closed culverts results in higher temperatures at the interior of the culvert and higher temperatures along the inside face of lift 7. This in turn resulted in slightly higher temperature differentials across lift 7. At 90 and 200 days, temperature differentials across lift 7 were roughly 9 °F in the first analysis and 7 °F in the second analysis. Lift 7 insulation was removed at 70 days, so the 65-day cold front had little affect
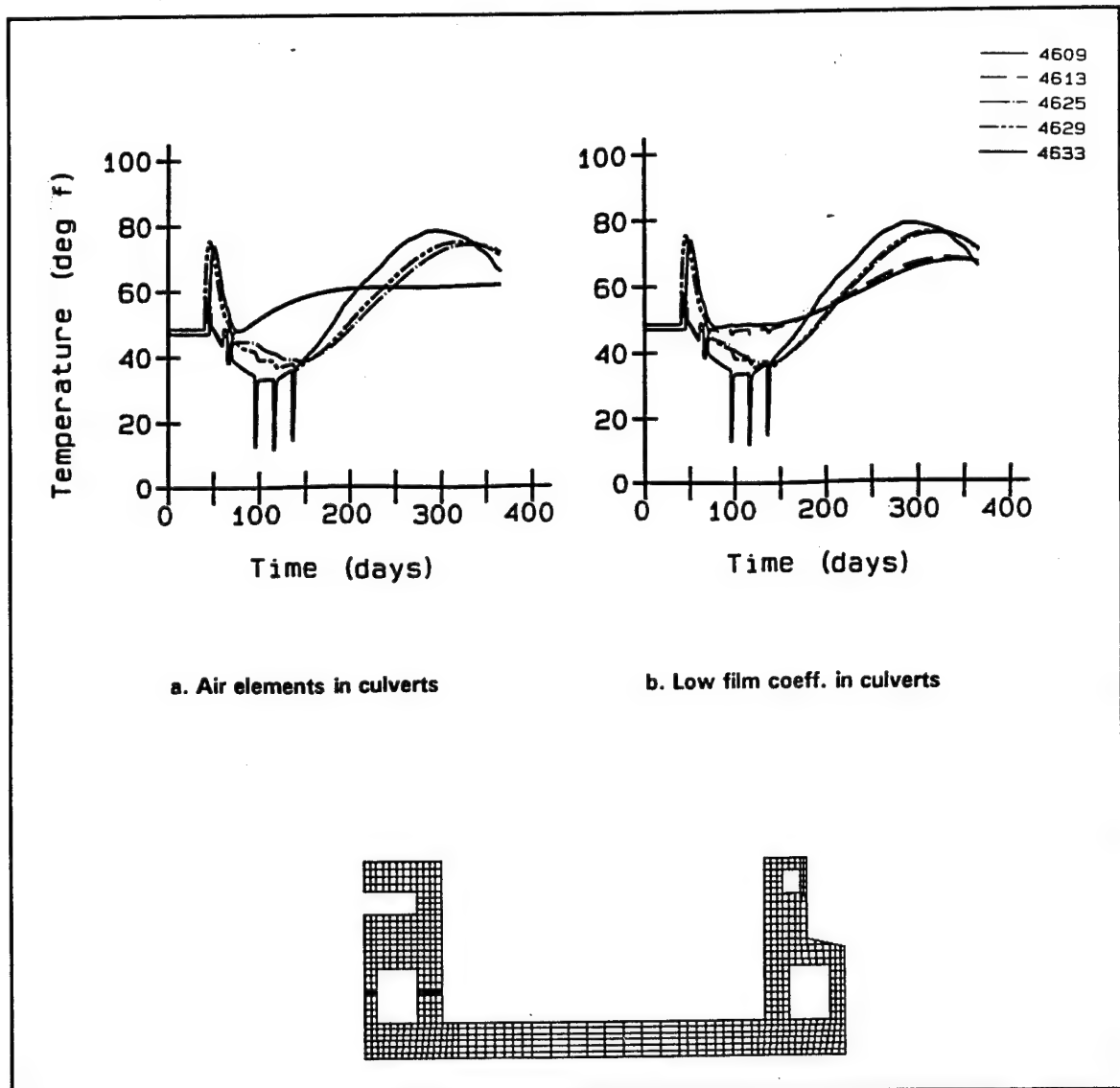
Figure 9. Nodal temperatures across center wall culvert, winter placement analyses using air elements and low film coefficients at culverts

on surface temperatures. At 95 days, surface temperatures dropped to 12.6 °F, or 8.6 °F above ambient. Similar drops occurred at 115 and 135 days.

Temperatures across the center of lift 5 for the analysis using air elements are shown in Figure 10. Immediately after placement, center temperatures climbed to 72.4 °F, while surface temperatures were at ambient, resulting in a 17 °F differential. However, temperatures became more uniform across this 6-ft section by 30 days after placement. Throughout the rest of the analysis, temperature differences between the center and outer nodes were less than 6 °F. For this uninsulated lift, outer surface temperatures dropped to roughly 8 to 10 °F above ambient during cold fronts.
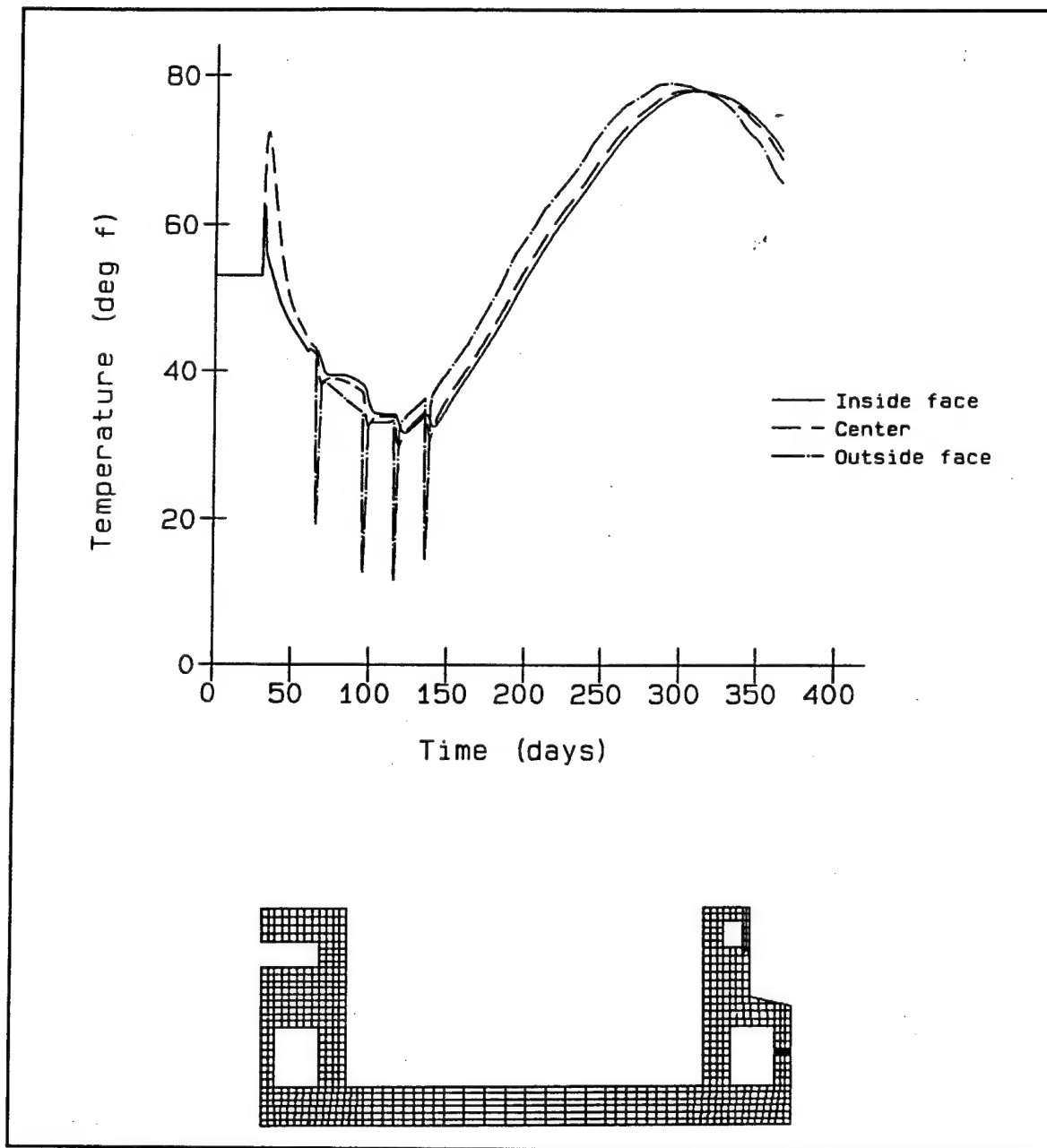
Figure 10.   Temperatures across lift 5, analysis using air elements at culverts

Wall stresses were low throughout the two analyses. The highest tensile stresses tended to occur above and at the right-hand corner of the center wall gallery, in lift 10, and at the surface of exposed concrete during cold fronts. Maximum principal stresses in element 1315, integration point 2, over the center wall gallery are compared for the two analyses in Figure 11; maximum principal stresses at the corner of the gallery (element 1222, integration point 2) are compared in Figure 12; and maximum principal stresses at the center of lift 10 are compared in Figure 13. Stresses in these figures are given in Table 8. In general, stresses at these
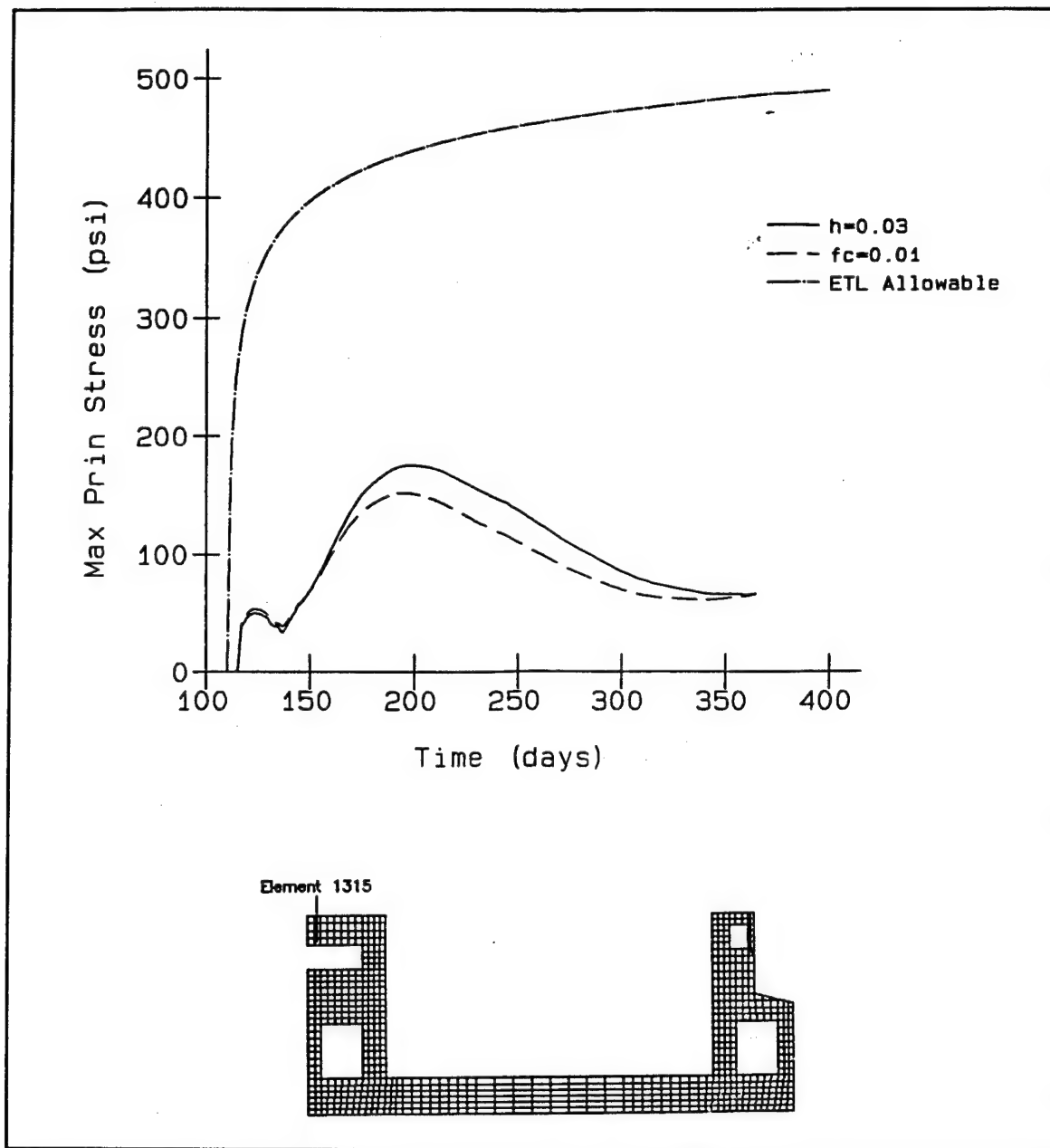
18

Figure 11. Maximum principal stress, element 1315, integration point 2, analyses using air elements and low film coefficients at culverts

points were higher at earlier times during the analysis using low film coefficients at culvert interior surfaces, but the maximum stresses in the analysis using air elements represented a higher percentage of the ETL allowable stress. However, results from both methods were similar for these analyses.

The effect of cold fronts on stresses near the surface of the concrete in the analysis using air elements can be seen in Figures 14 and 15. Due to the placement schedule, lift 5 concrete remained uninsulated throughout
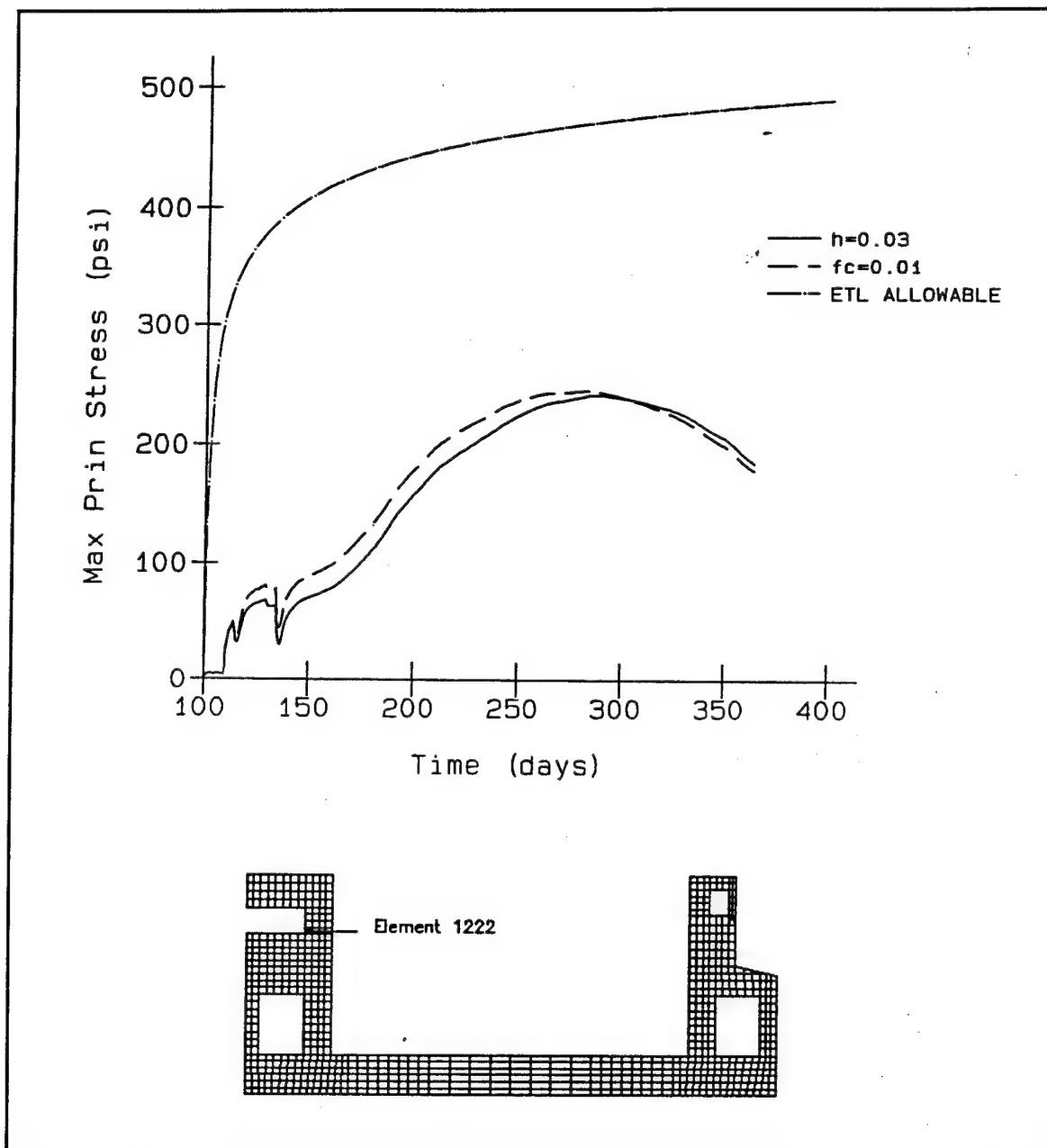
Figure 12.   Maximum principal stress, element 1222, integration point 2, analyses using air elements and low film coefficients at culverts

the analysis. An initial stress peak at the surface of lift 5 can be observed at day 33, shortly after placement, and further peaks occur at each cold front. Lift 11 concrete was insulated at placement and insulation was removed at day 105. An initial stress peak occurred shortly after placement; the tensile stress peak at 95 days was low since the concrete was still insulated; another peak occurred at 105 days when the insulation was removed; and the largest peak occurred at 115 days.
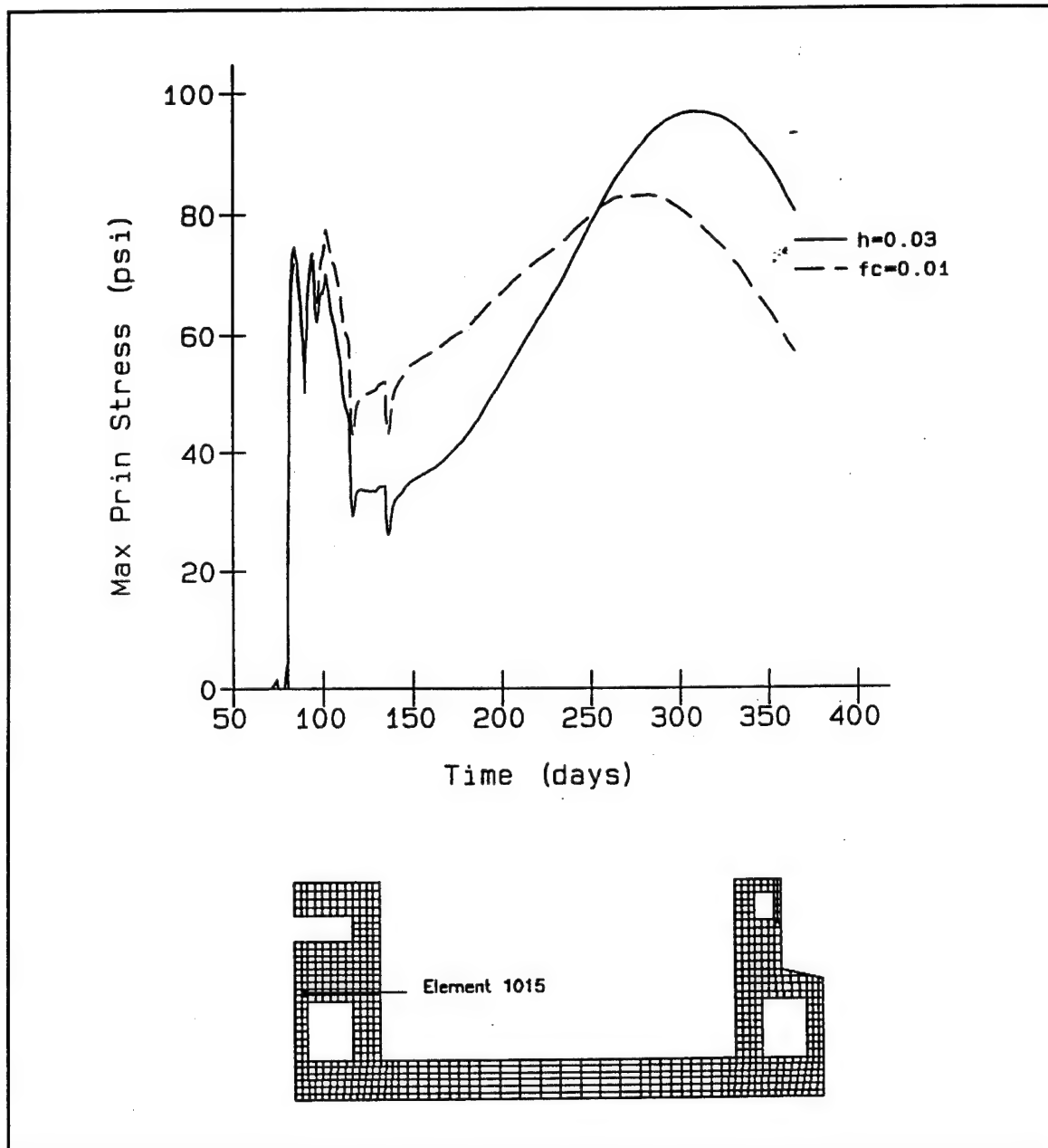
Figure 13.   Maximum principal stress, element 1015, integration point 3, analyses using air elements and low film coefficients at culverts

However, maximum principal stress at the surface of wall lifts was always low when compared with the ETL allowable, and the allowable stress has not been plotted. Since results for the two winter analyses were almost identical in these areas, only surface stresses for the analysis using air elements have been plotted.

Table 8
Maximum Principal Stresses In Walls, Winter Analyses with Cold Fronts

Analysis	Element	Point	Stress (psi)	ETL Allowable (psi)	Percentage of Allowable
Air elements	1015	3	96.5	374.5	25.8
Low fc[1]	1015	3	82.9	476.2	17.4
Air elements	1222	2	241.3	471.4	51.2
Low fc	1222	2	245.3	470.1	52.2
Air elements	1315	2	175.1	437.7	40.0
Low fc	1315	2	151.8	435.5	34.9

[1] fc, film coefficient

Additional Floor Insulation Analyses

The first seven winter placement analyses provided a thorough study of placement using the daily average ambient temperature curve and of the effects of cold fronts on wall sections. However, since maximum tensile stresses in all analyses occurred in the floor, two analyses were carried out to provide additional information on floor insulation requirements.

In the first analysis, construction was started on Nov 22, insulation was placed on Dec 1 and was removed from the floor surface on Jan 1 during the coldest time of the year. Concrete age at removal was 30 days. The concrete was subjected to a cold front immediately upon removal of the insulation. In the next analysis, construction was started on Nov 1, insulation was placed on Dec 1 and was removed from the floor upper surface at the end of January at a concrete age of 90 days. The concrete was then immediately subjected to a cold front. Stresses in the top lift at section 3 from the two analyses are shown in Figures 16 and 17 and compared with the ETL allowable stress in Table 9. Maximum stresses occurred at the upper surface of the floor for both analyses. Maximum stress from the first analysis exceeded the ETL allowable, while maximum stress from the second analysis is less than 80 percent of the ETL allowable. This indicates that 30 days of insulation is not adequate to protect the floor from the effects of extreme winter temperatures.
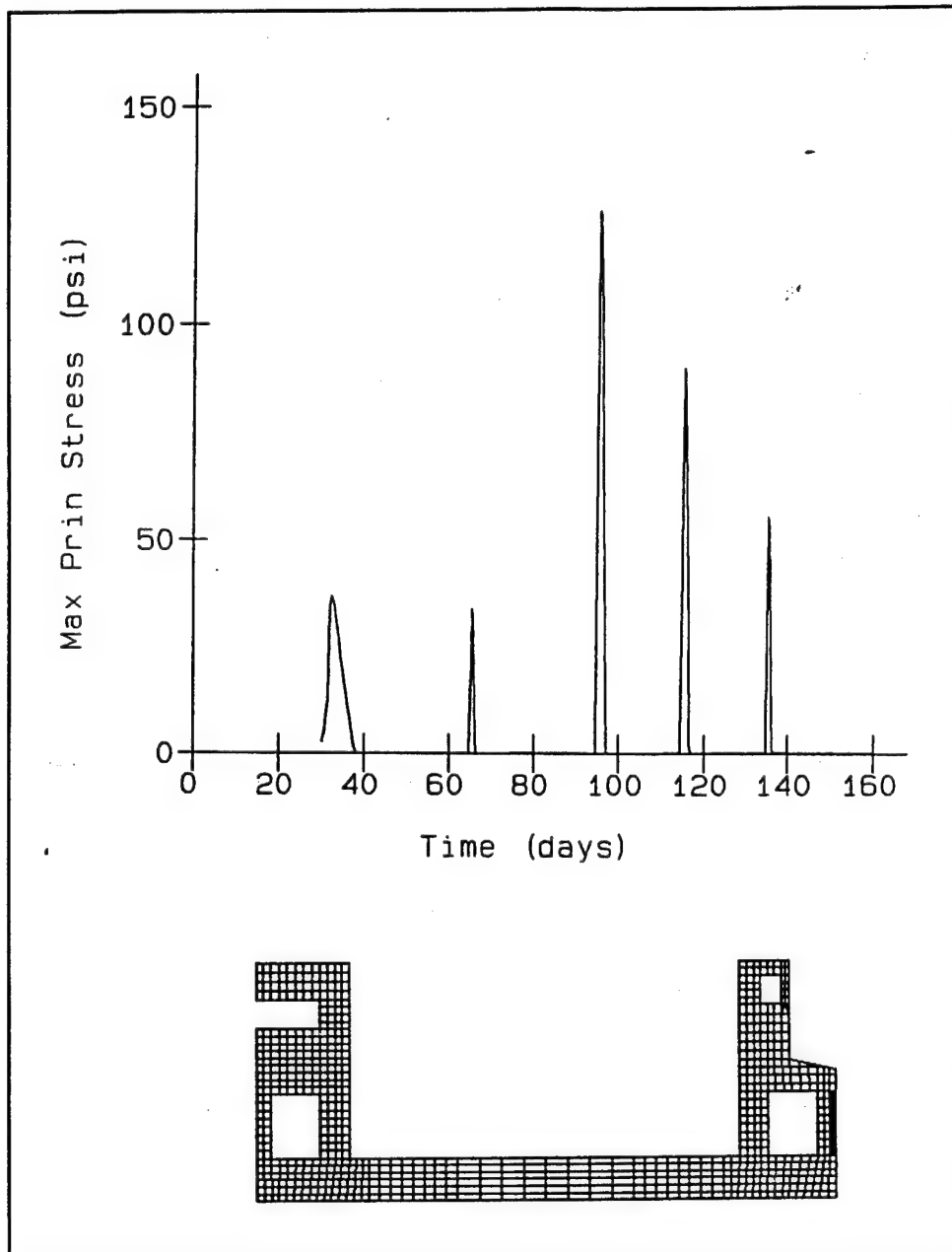
Figure 14.   Maximum principal stress at lift 5 outer surface, analysis using air elements at culverts

Extreme Ambient Temperature Curve

Since the average daily ambient temperature curve was based on daily temperatures averaged over 30 years, two additional analyses were run to determine if cracking would occur during an unusually cold winter. These analyses used the extreme daily ambient temperature curve shown in Figure 3 and developed in Chapter 4. The minimum temperature for this curve was 22.5 °F, while minimum temperature for the daily average
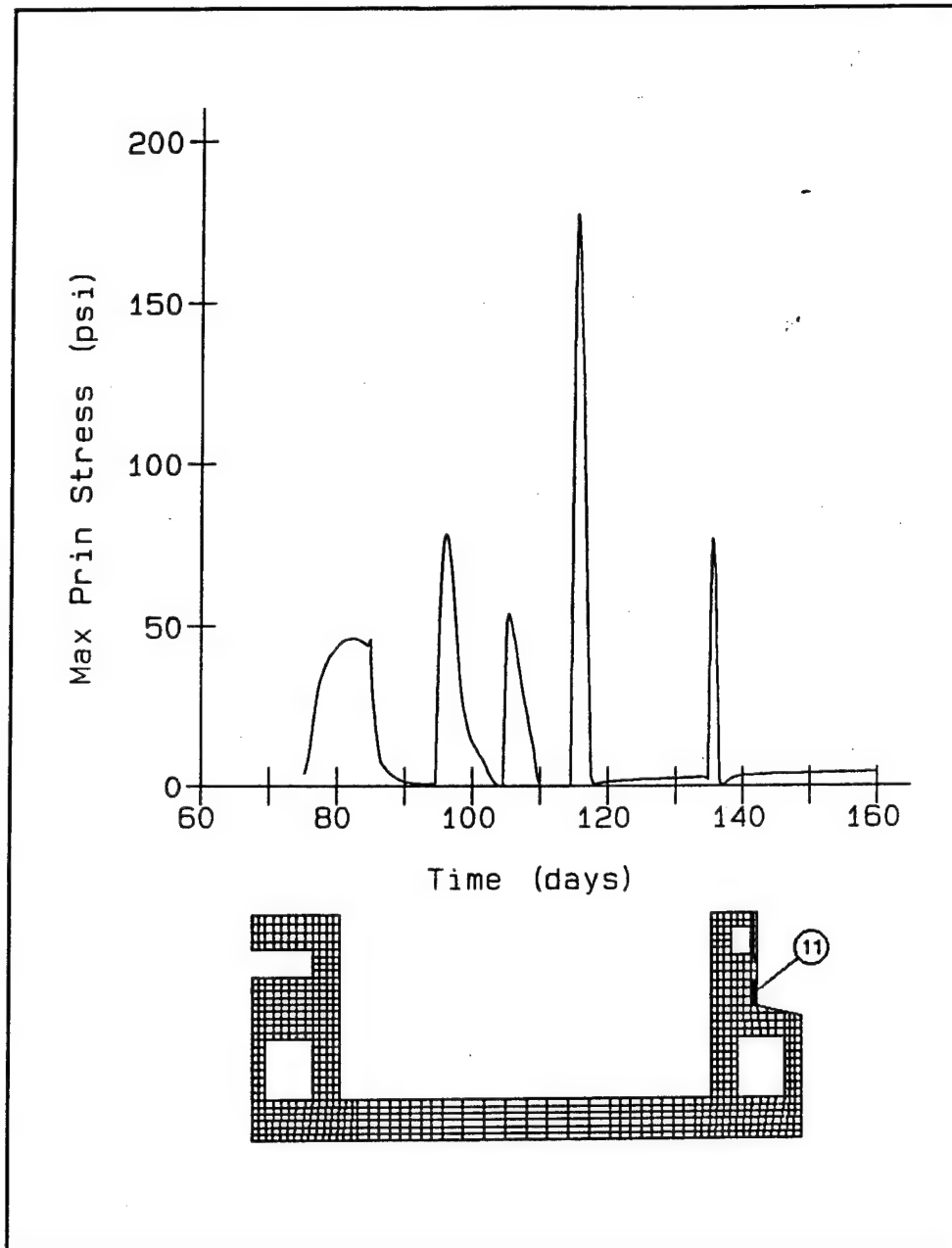
Figure 15.   Maximum principal stress at lift 11 outer surface, analysis
               using air elements at culverts

ambient temperature curve used in all other analyses was 33 °F. Insula-
tion with R = 2.0 h-ft^2-°F/Btu was applied starting Dec 1 and removed
when the concrete age reached 30 days. Culverts were closed throughout
the analysis after insulation was applied, and air within culverts was modeled
using air elements with a thermal conductivity of 0.03 Btu-in./day-in.^{2}-°F.
In the first analysis, the extreme ambient curve was used without cold
fronts. Stresses at floor section 3 from this analysis are plotted against
stresses at this location from Winter Placement Analysis 4, which uses the
average daily ambient temperature curve, in Figure 18. Stresses for the
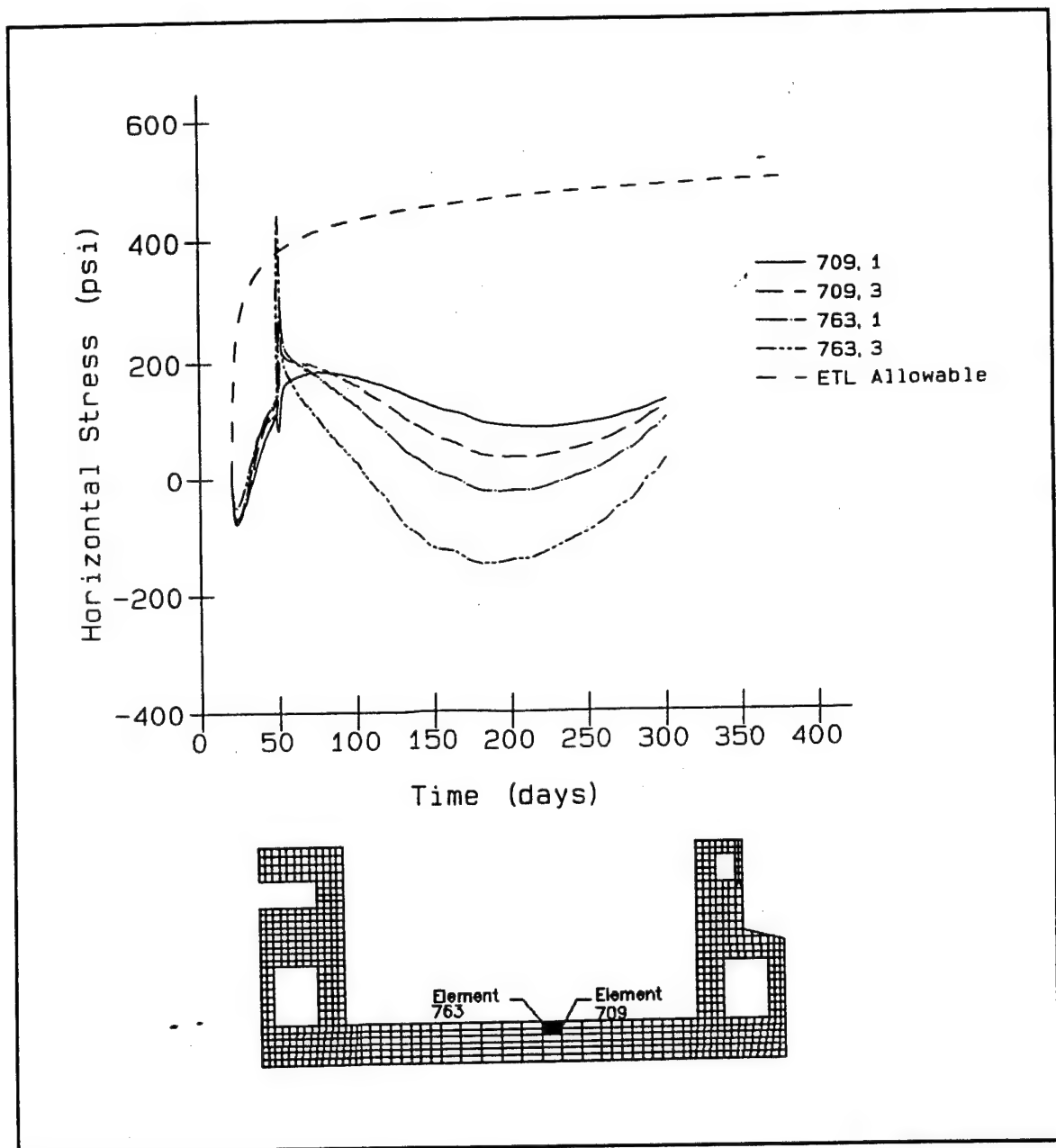
Figure 16.   Horizontal stress, section 3, lift 3, insulation to 30 days age

two analyses are compared with the ETL allowable in Table 10. The maximum horizontal stress in element 709, integration point 3, increased approximately 15 percent when the extreme daily ambient curve was used rather than the average daily ambient curve.

In the next analysis, cold fronts were simulated at 65, 95, 115, and 135 days after the start of concrete placement. Maximum horizontal stresses in element 763, integration point 3, are compared with the ETL allowable stress in Figure 19 and Table 11. The ETL allowable was
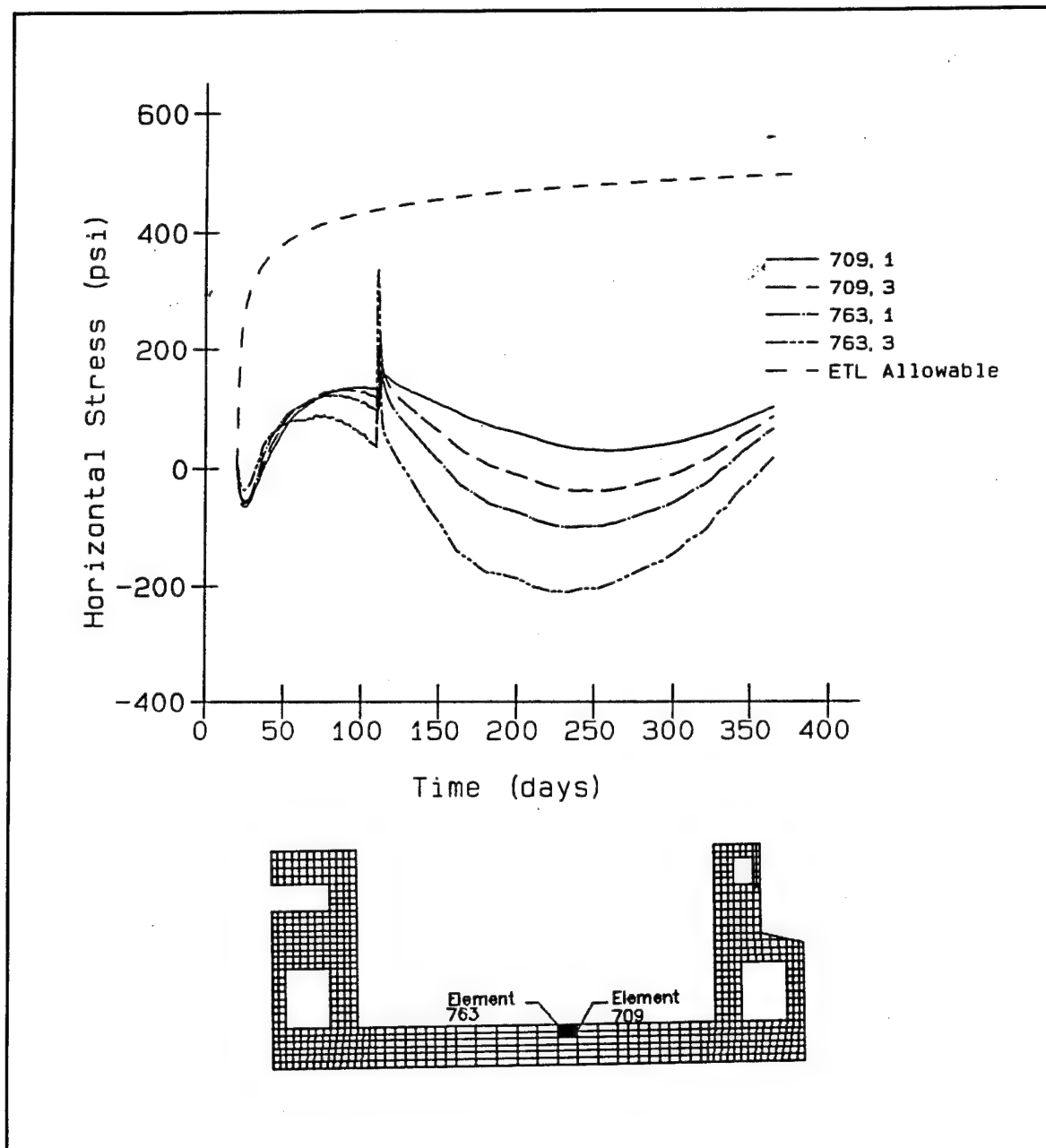
Figure 17.   Horizontal stress, section 3, lift 3, insulation to 90 days age

Table 9 Maximum Tensile Stresses, Section 3, Floor Analyses with Cold Fronts					
Analysis	Element	Point	Stress (psi)	ETL Allowable (psi)	Percentage of Allowable
30 day age	763	3	441.1	382.6	115.0
90 day age	763	3	336.8	439.3	76.7
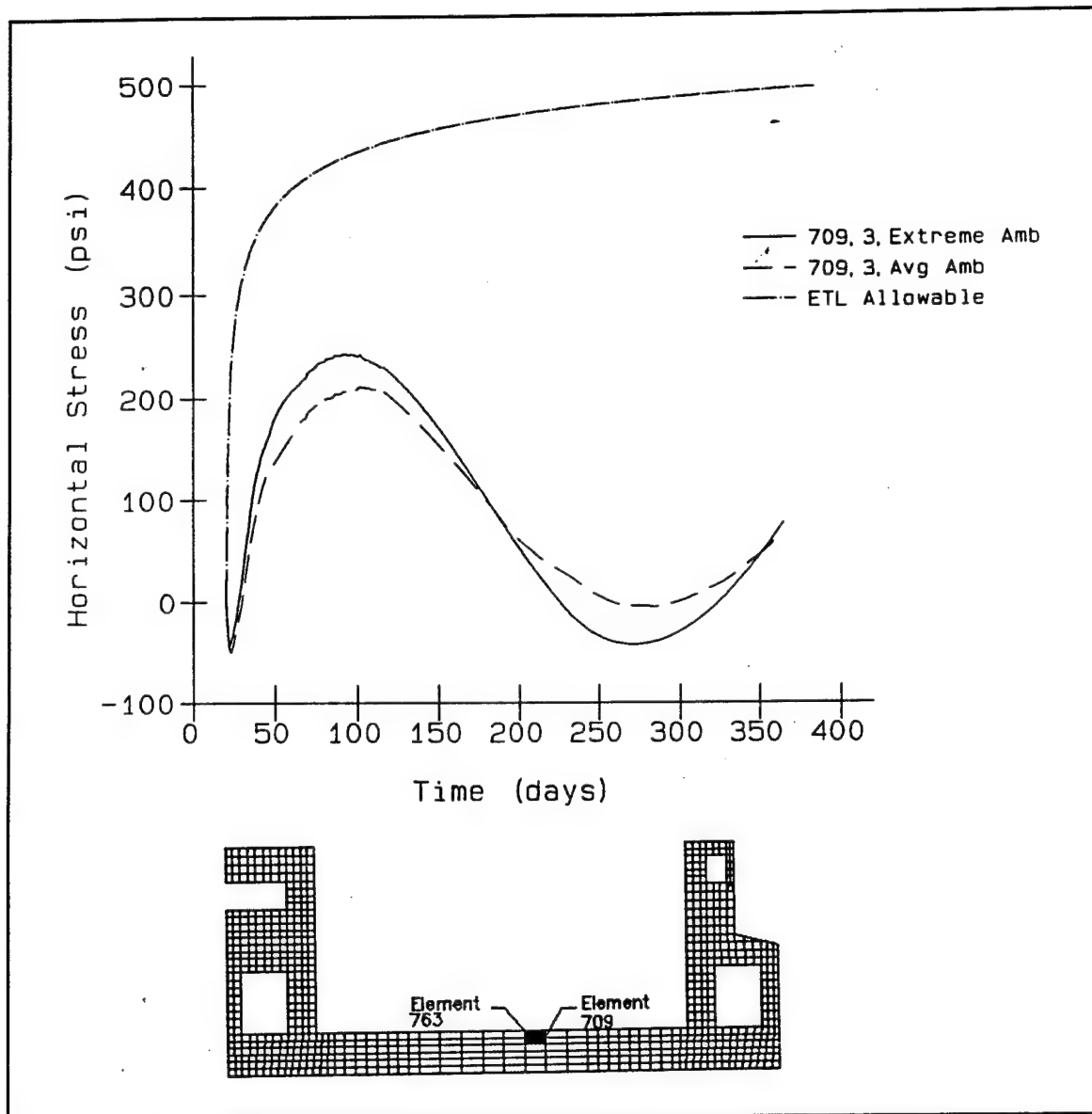
Figure 18.   Horizontal stress, section 3, lift 3, average and extreme ambient temperature curves

exceeded by predicted stress at 66.5 days and 76.7 percent of the allowable stress was reached at 95.5 days. This provides further confirmation that 30 days of winter insulation is not adequate to protect the floor against unacceptable stress levels.

Stress peaks also occurred at the surface when insulation was removed and during cold fronts. However, these stress peaks were low when compared with the ETL allowable and have not been plotted. Maximum principal stresses around the gallery and in lift 10 are compared with those from the previous Winter Placement Analysis using air elements in Figures 20-22. Stresses from these plots are given in Table 12. In each case maximum

Table 10
Maximum Horizontal Stress in Floor, Daily Average and Extreme Ambient Curves

Analysis	Element	Point	Stress (psi)	ETL Allowable (psi)	Percentage of Allowable
Average ambient	709	3	211.4	434.3	48.7
Extreme ambient	709	3	243.7	427.9	57.0
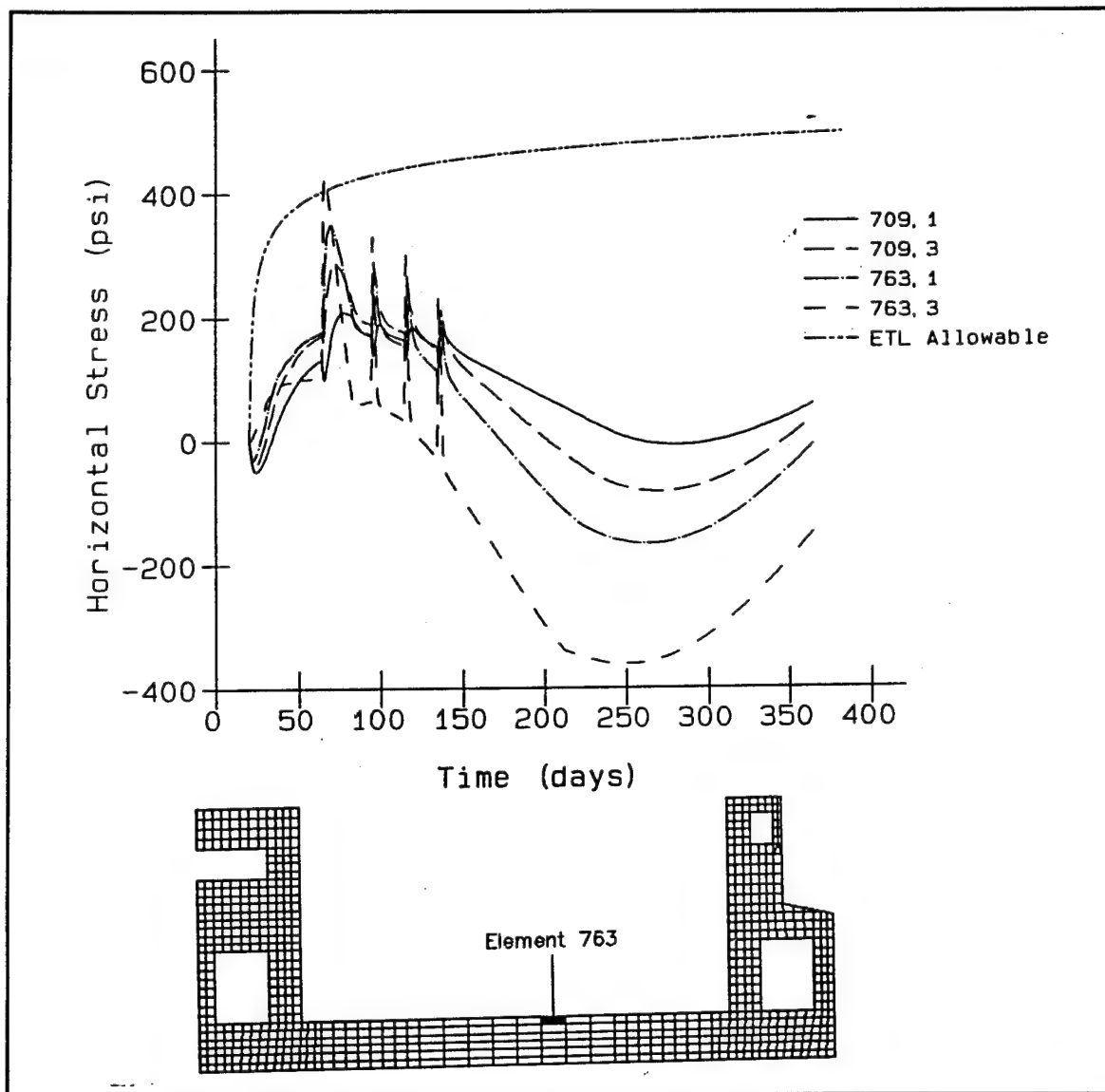
Figure 19. Maximum horizontal stress, element 763, integration point 3, extreme ambient curve with cold fronts

Table 11
Maximum Horizontal Stresses at Top of Floor, Extreme Ambient Analysis with Cold Fronts

Element	Point	Stress (psi)	Day	ETL Allowable (psi)	Percentage of Allowable
763	3	427.8	66.5	405.9	105.4
763	3	330.4	95.5	430.6	76.7
763	3	300.5	115.5	441.8	68.0
763	3	235.7	135.5	450.4	52.3

principal stress was increased approximately 20-30 percent when the extreme ambient temperature curve was used in place of the average ambient curve.

Conclusions

Modeling closed culverts with air elements as suggested in ETL 1110-2-324 rather than using a low film coefficient at all interior surfaces results in higher temperatures at the interior of culverts, larger temperature differentials across wall sections, and wall stresses that represent a larger percentage of the ETL allowable stress. Results from the two methods are similar enough that the ETL method does not appear to be overly conservative, although either method should produce acceptable results.

During cold fronts, temperatures at the surface of the concrete can drop to 8 to 10 °F below ambient, or well below freezing. However, stresses calculated in the walls were within acceptable limits when wall insulation was removed at an age of 30 days. Maximum wall stresses from the winter analyses occurred at the lower corner of the center wall gallery and were approximately 50 percent of the ETL allowable stress. Surface stresses were always well below ETL allowable stresses, even when cold fronts were simulated. Based on these analyses, insulation to a concrete age of 30 days seems to be adequate for chamber monolith walls.

Maximum horizontal stresses in the floor remained at acceptable levels for all winter analyses using the daily average ambient temperature curve and an October 1 start-of-placement date. However, when later placement times were simulated in conjunction with a cold front at the time that insulation was removed and a concrete age at removal of 30 days, horizontal stresses near the surface of the floor exceeded the ETL allowable. When the insulation was removed at an age of 90 days, the maximum horizontal stress near the surface of the floor was only about 77 percent of the ETL
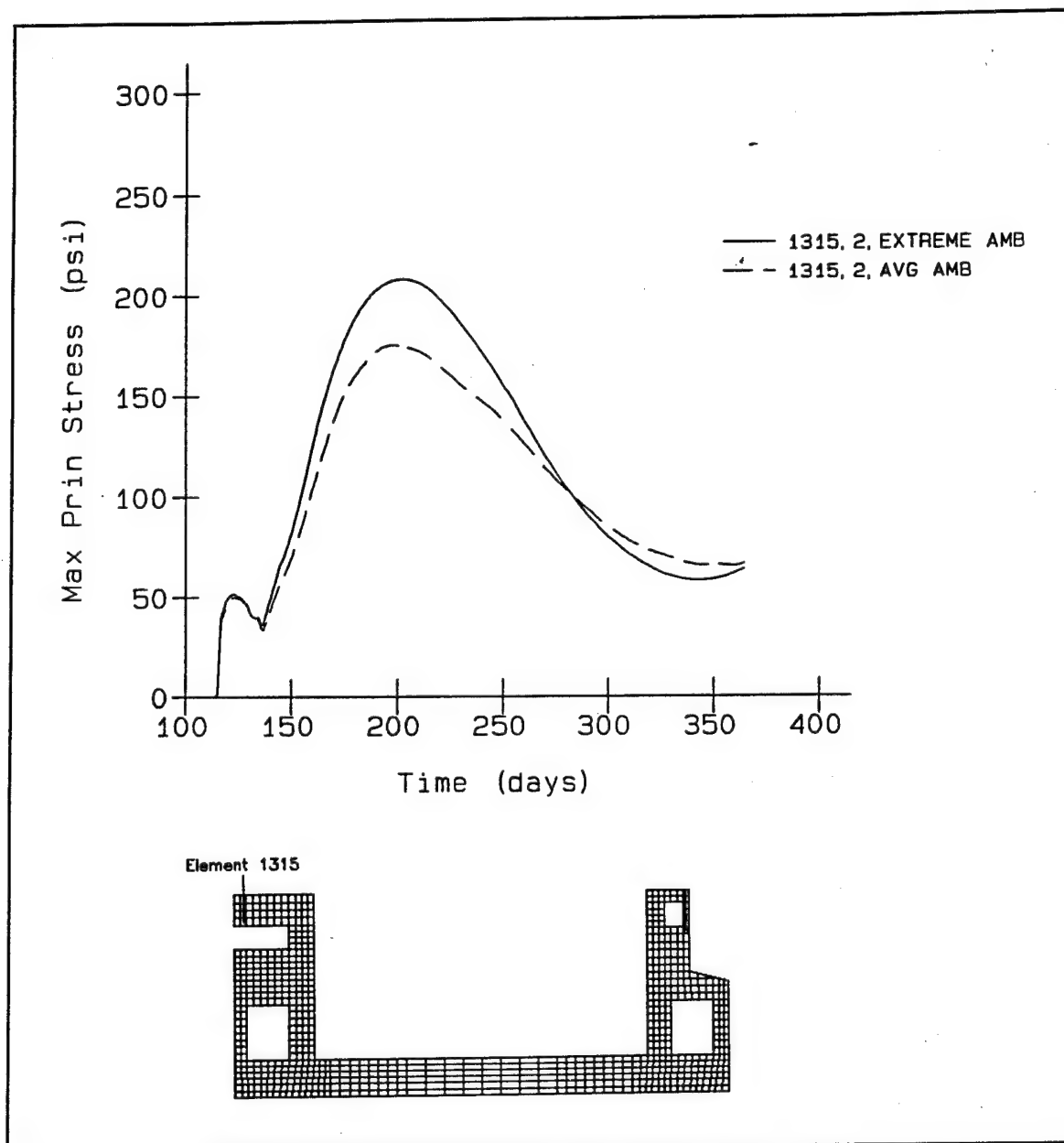
Figure 20.   Maximum principal stress, element 1315, integration point 2, average and extreme ambient temperature curves
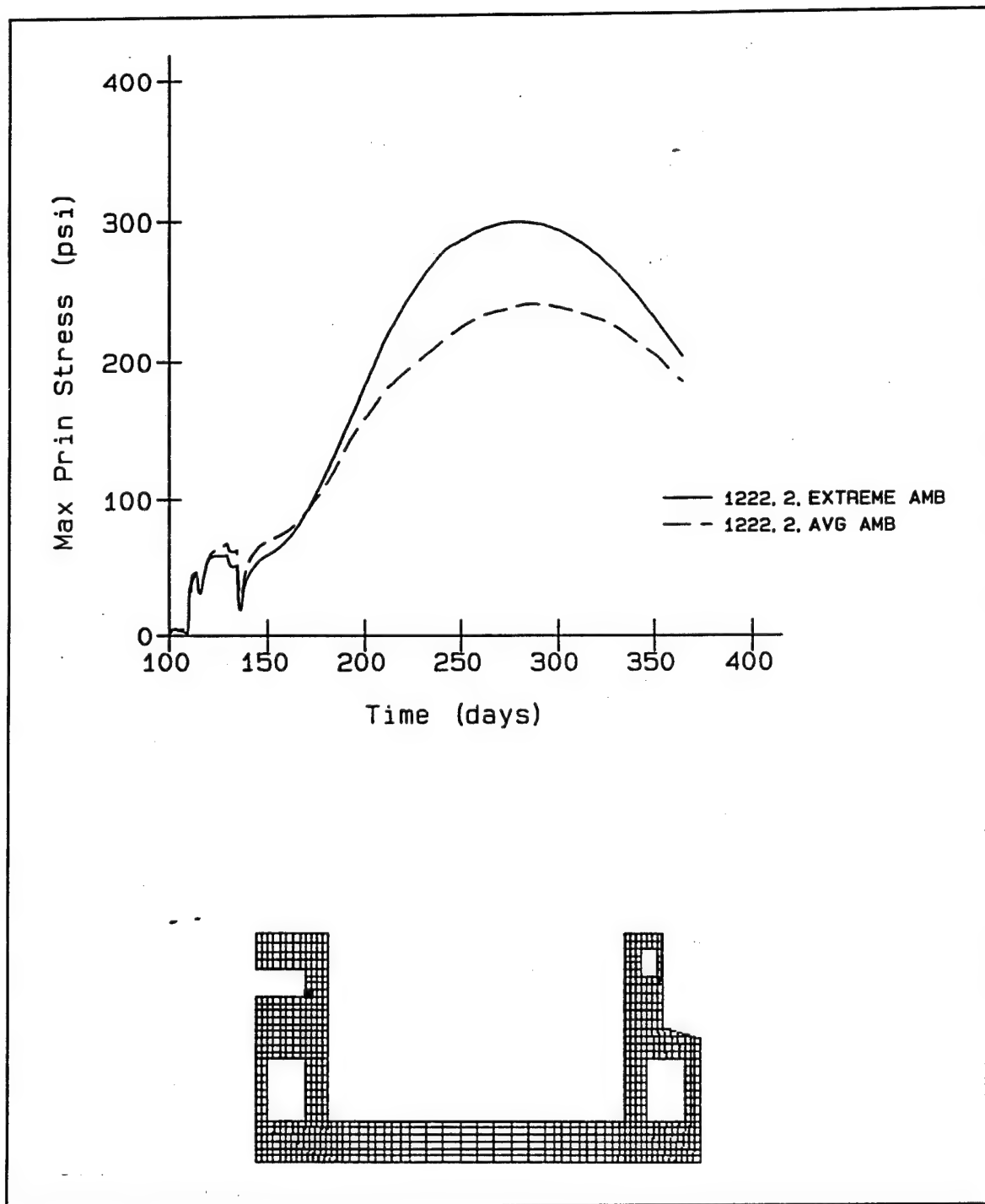
Figure 21. Maximum principal stress, element 1222, integration point 2, average and extreme ambient temperature curves
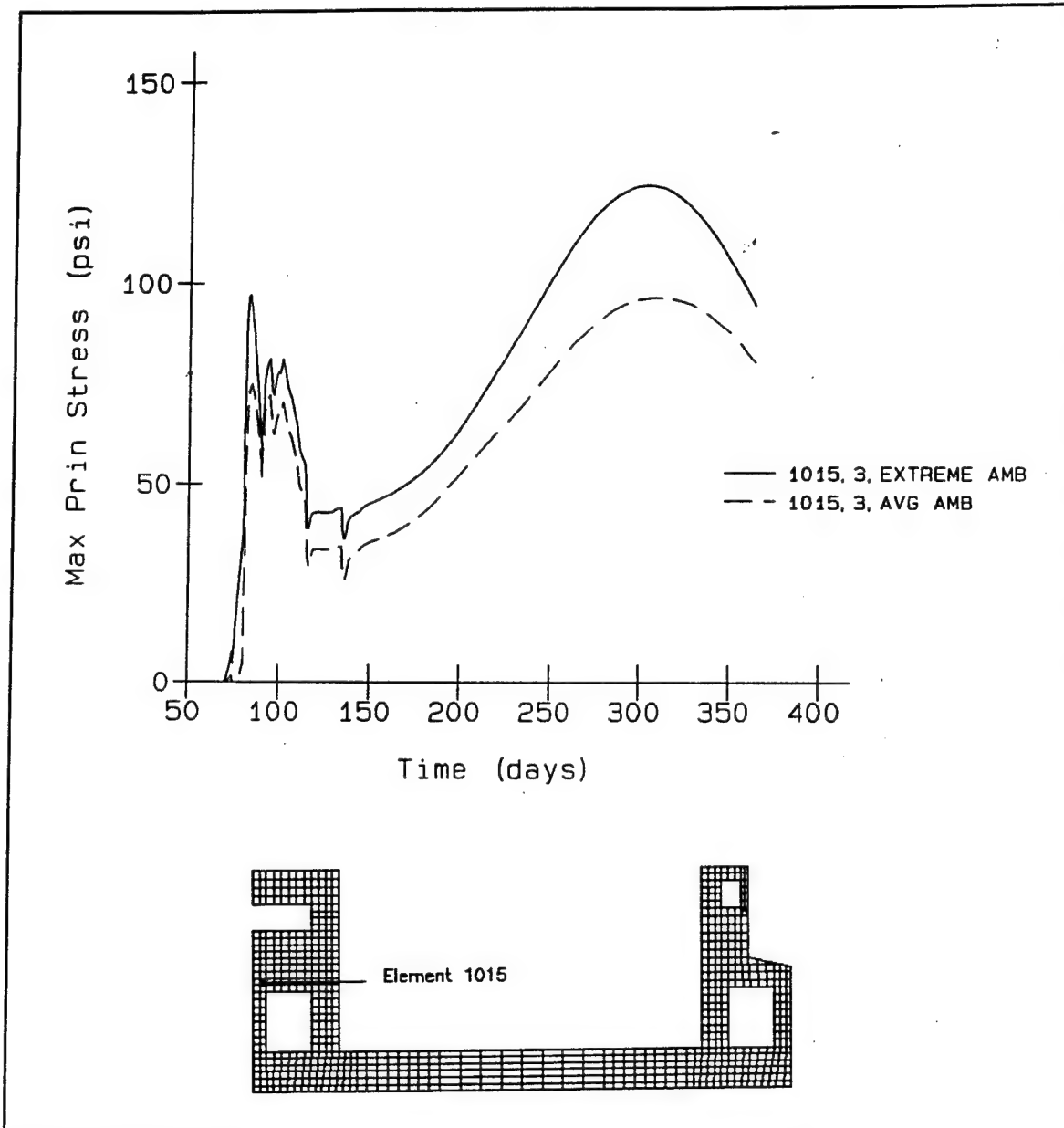
Figure 22.   Maximum principal stress, element 1015, integration point 3, average and
extreme ambient temperature curves

Table 12
Maximum Principal Stresses in Walls, Average and Extreme Ambient Analyses

Analysis	Element	Point	Stress (psi)	ETL Allowable (psi)	Percentage of Allowable
Average ambient	1015	3	96.5	480.7	20.0
Extreme ambient	1015	3	124.7	479.7	26.0
Average ambient	1222	2	241.4	471.0	51.3
Extreme ambient	1222	2	299.3	469.2	63.8
Average ambient	1315	2	175.1	437.7	40.0
Extreme ambient	1315	2	208.0	439.8	47.3

allowable stress. Based on these analyses, winter floor insulation should remain in place until the concrete has reached an age of 90 days.

Analyses of an uninsulated floor using the extreme daily ambient temperature curve rather than the daily average ambient resulted in higher horizontal stresses hear the top of the floor, but all floor stresses remained within the ETL allowable. When cold fronts were simulated, maximum horizontal stresses near the surface of the floor exceeded the ETL allowable. This provides further evidence that 90 days of insulation is preferable for the chamber monolith floor.

Wall stresses were within the ETL allowable when the extreme ambient temperature curve with cold fronts was used. The maximum stress occurred at the corner of the center wall gallery and was approximately 64 percent of the ETL allowable stress.

3 Chamber Monolith Wall Analyses

Purpose of Analyses

Chamber monolith wall analyses were conducted to answer the following questions.

a. All previous analyses were based on maximum wall lift heights of 5 to 6 ft. Additional analyses were required to determine if doubling the maximum wall lift height would result in unacceptable stresses.

b. Vertical cracking along the outer wall of chamber monolith culverts has been observed in other Corps structures. This cracking is probably due to the restraint of out-of-plane strains caused by shrinkage and thermal effects. A three-dimensional analysis of the monolith outer wall was conducted to determine the potential for this type of cracking.

Increased Lift Heights

Two analyses were run to determine the effect of increasing lift heights in the center wall. Both analyses used the lift arrangement shown in Figure 23, a Jun 20 start-of-placement date, and 5 days between lift placements. In the first analysis, a maximum placement temperature of 60 °F was used. In the next analysis, lifts were placed at ambient temperature. Placement schedule and temperatures for the two analyses are shown in Table 13.

The primary areas of concern for these two analyses were the thick center wall section comprised of lifts 10 and 12 and the area surrounding the gallery. It was expected that changing the height of lift 10 from 6 to 12 ft would result in increases in temperature and stress in the thick center section. Because the outer wall of the gallery was so thin when compared
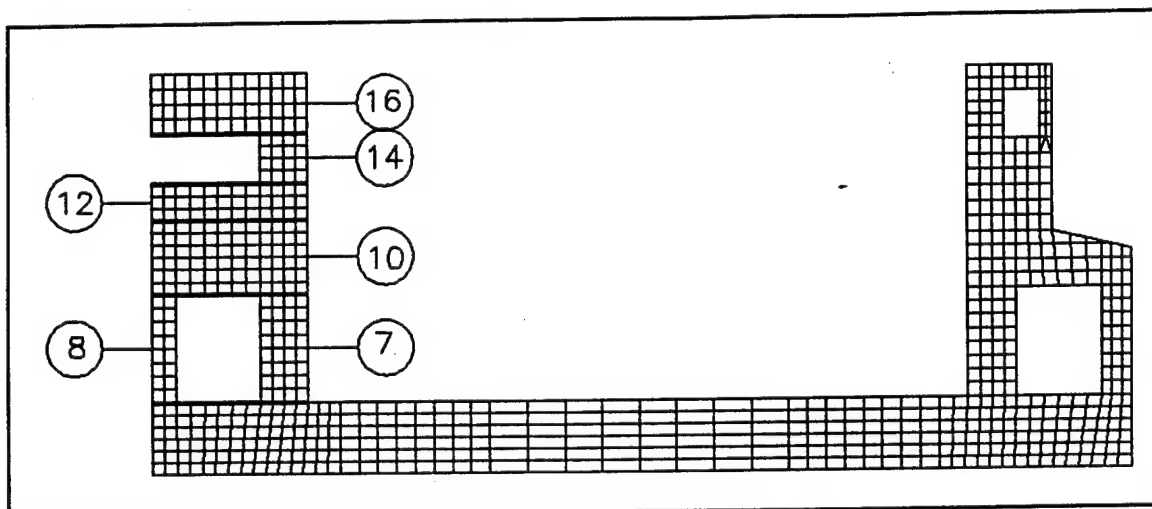
Figure 23.   Lifts for increased lift height analyses

Table 13 Placement Dates and Temperatures, Center Wall Analyses			
Lift	Day	Run 1 Temperature (°F)	Run 2 Temperature (°F)
7	30	60	79.0
8	35	60	78.8
10	40	60	78.5
12	45	60	77.0
14	50	60	77.5
16	55	60	76.0

with this section, it was anticipated that it would cool much faster than the center section, possibly resulting in high tensile stresses in this area.

Temperatures at nodes across the center of lifts 10 and 12 are shown for the two increased lift height analyses and for the load case 5 analysis (Garner et al. 1992) in Figure 24. When viewing temperature plots, remember that node numbers increase from left to right and bottom to top. The maximum temperature in the load case 5 analysis was 91 °F at the center of the wall. Maximum temperatures for the two new analyses were 101.1 °F for the 60 °F placement and 113.9 °F for the ambient placement at the center of the wall. Temperature differentials across the section were higher in the increased lift height analyses than in the load case 5 analysis for the first 50 days after placement. At later times, temperature differentials were similar for the three analyses. The temperature differential
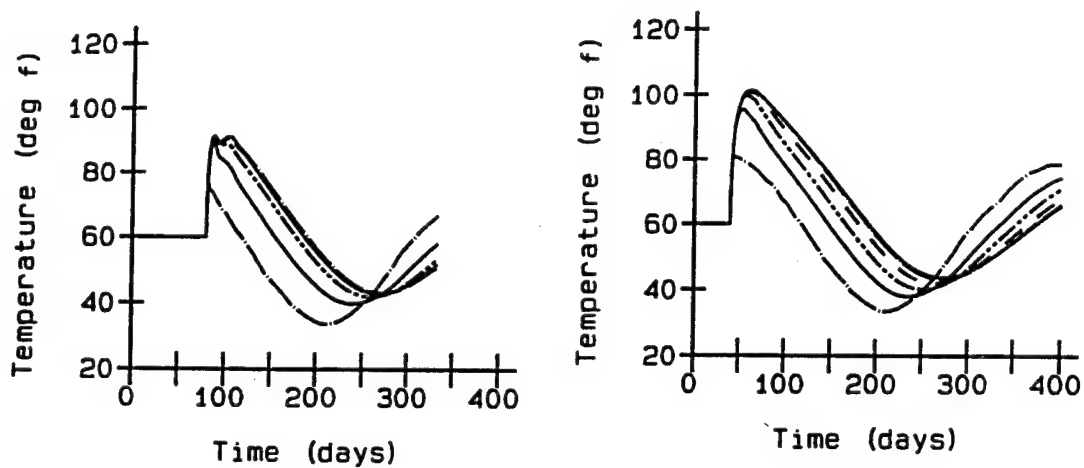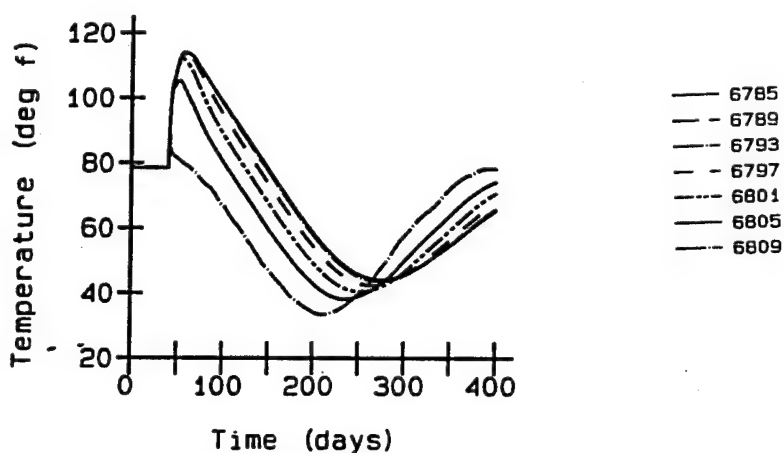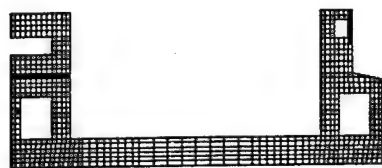
Figure 24. Temperatures at center wall center section, load case 5, and increased lift height analyses

in the ambient placement analysis was slightly higher than that in the 60 °F placement analysis at day 150 (31 °F as opposed to 28 °F). However, by day 325 the temperature differential across the section was approximately 15.5 °F in all three analyses.

Temperatures at nodes along the top of lift 10 are compared for the three analyses in Figure 25. Once again, maximum temperatures and early time temperature differentials varied, but temperature differentials across the section were approximately 24 °F in all three analyses by day 200.

In both analyses, stresses were low when compared with ETL allowable stresses. In the first analysis, peak stresses in the thick wall section consisting of lifts 10 and 12 occurred at the top of lift 10 rather than at the center of the section. Stress peaks in this area occurred approximately 10 days after placement and again approximately 350 days after the start-of-construction date. Stresses at 350 days are much lower for the analysis with ambient placement. Maximum tensile stresses at the top center element of lift 10 for the two analyses are compared with results from load case 5 in Figure 26 and Table 14. Although the load case 5 analysis was run for only 333 days, stress from this analysis at this time was slightly higher than that for the increased lift height analysis with a 60 °F placement. When the concrete was placed at ambient temperature the location of peak stress shifted from the top of lift 10 to the center of the section consisting of lifts 10 and 12. In the plot of maximum principal stresses in elements along the center of the two lifts (Figure 27) stresses at this location were highest in the load case 5 analysis. This may be due to the smaller gallery used in load case 5, which caused the outer gallery wall lift to be much more massive, impeding heat loss through the gallery. Stresses were approximately 50 percent higher in the ambient placement increased lift height analysis than in the analysis with a 60 °F placement temperature. Stresses are listed in Table 15. The highest wall stresses in each analysis occurred at the lower right-hand corner of the gallery opening. Stresses at this location were slightly higher in the analysis with a 60 °F maximum placement temperature. Maximum principal stresses at this location are shown in Figure 28 and listed in Table 16. Load case 5 stresses are not given at this location because of the differences in the gallery in the two analyses.

It would appear from these plots that the magnitude of peak stresses is approximately the same in both analyses, but the location of peak stresses shifts from the top to the center of lift 10 when the placement temperature is changed from 60 °F to ambient temperature. All stresses are well below the ETL allowable.
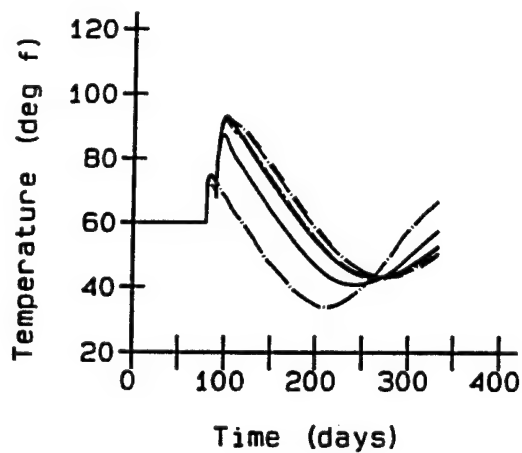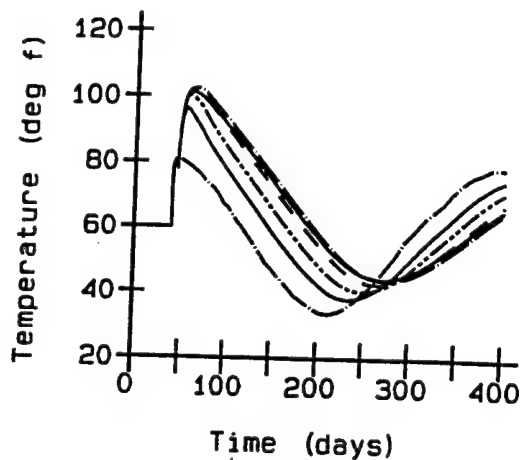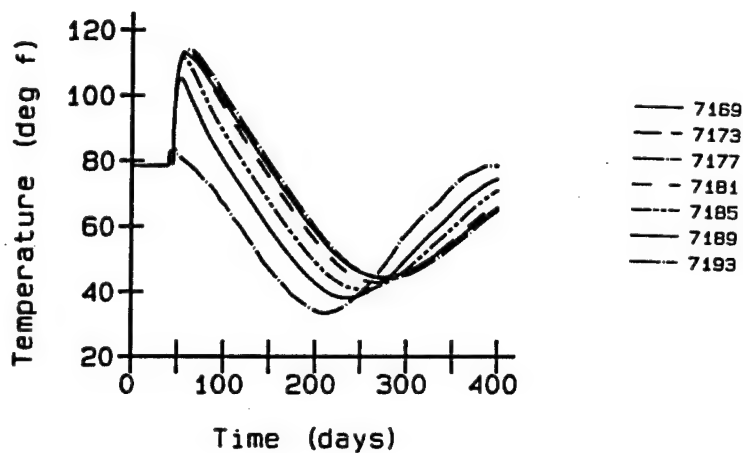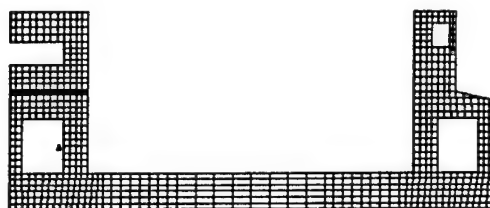
Figure 25.   Temperatures at top of lift 10, load case 5, and increased lift height analyses
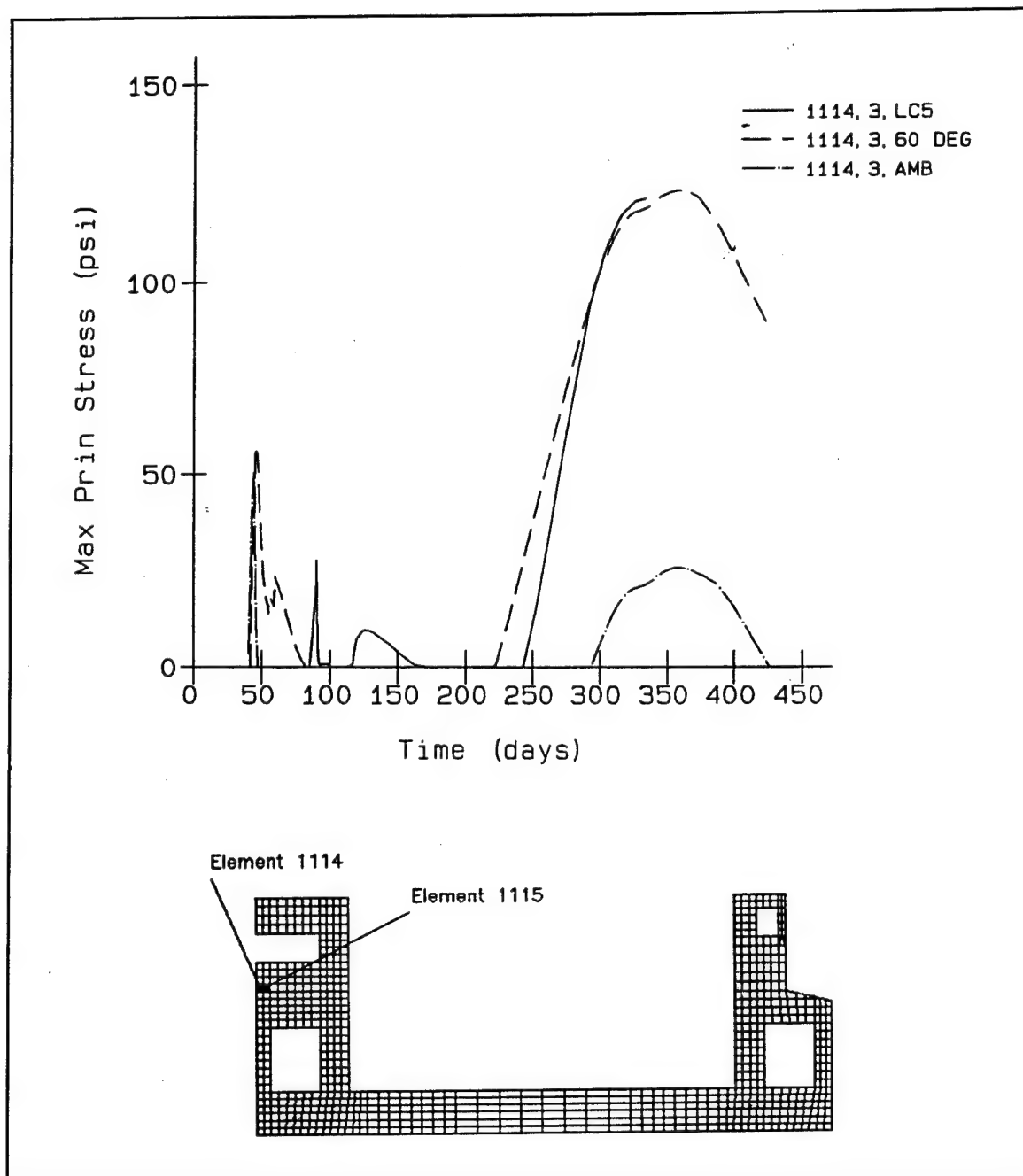
Figure 26. Maximum principal stresses at top of lift 10, load case 5, and increased lift height analyses

Table 14
Maximum Principal Stresses at Top of Lift 10, Increased Lift Height Analyses

Analysis	Element	Point	Stress (psi)	Day	ETL Allowable (psi)	Percentage of Allowable
Load case 5	1114	3	121.3	332.5	482.9	25.1
60 °F placement	1114	3	118.8	332.5	488.3	24.3
Ambient placement	1114	3	21.4	332.5	488.3	4.3
60 °F placement	1114	3	123.3	357.5	491.3	25.0
Ambient placement	1114	3	26.0	357.5	491.3	5.0

Three-Dimensional (3-D) Analyses

The grid for the 3-D analysis consisted of one half of the monolith outer wall and an adjoining floor section, shown in Figure 29. Since culvert wall stresses are not greatly affected by stresses at the center of the monolith floor, a section of floor only long enough to give an accurate temperature distribution was included. Also, since the outer wall concrete above lift 9 does not greatly affect stresses in the outer culvert wall, lifts above lift 9 were modeled as pressure loads applied at the appropriate times. A 20-ft-deep section of soil extending 10 ft beyond the outer boundaries of the concrete was included for the heat transfer analysis, a constant temperature was specified at the base of the soil, and adiabatic boundaries were used at the sides of the soil, at the symmetric centerline of the wall, and at the inside face of the floor. Soil and piles were modeled as springs in the stress analysis, and roller boundaries were used at the symmetric centerline of the monolith and at the inside face of the floor section.

For this analysis, wall concrete was placed at 5-day intervals at ambient temperature. The start-of-placement date was Jun 20. Maximum principal stresses in the outer culvert wall were similar to those in a 2-D analysis. Stresses at the face of the concrete reached a peak shortly after placement, while stresses at the interior were initially close to zero and increased for approximately 20 days after placement. In general, maximum principal stresses throughout the analysis were less than 25 psi. A plot of stresses along a column of elements at the outer surface of lift 5 (Figure 30) indicates that maximum stresses were reached at 32.5 days, or 2.5 days after placement. These stresses are similar to the stresses along
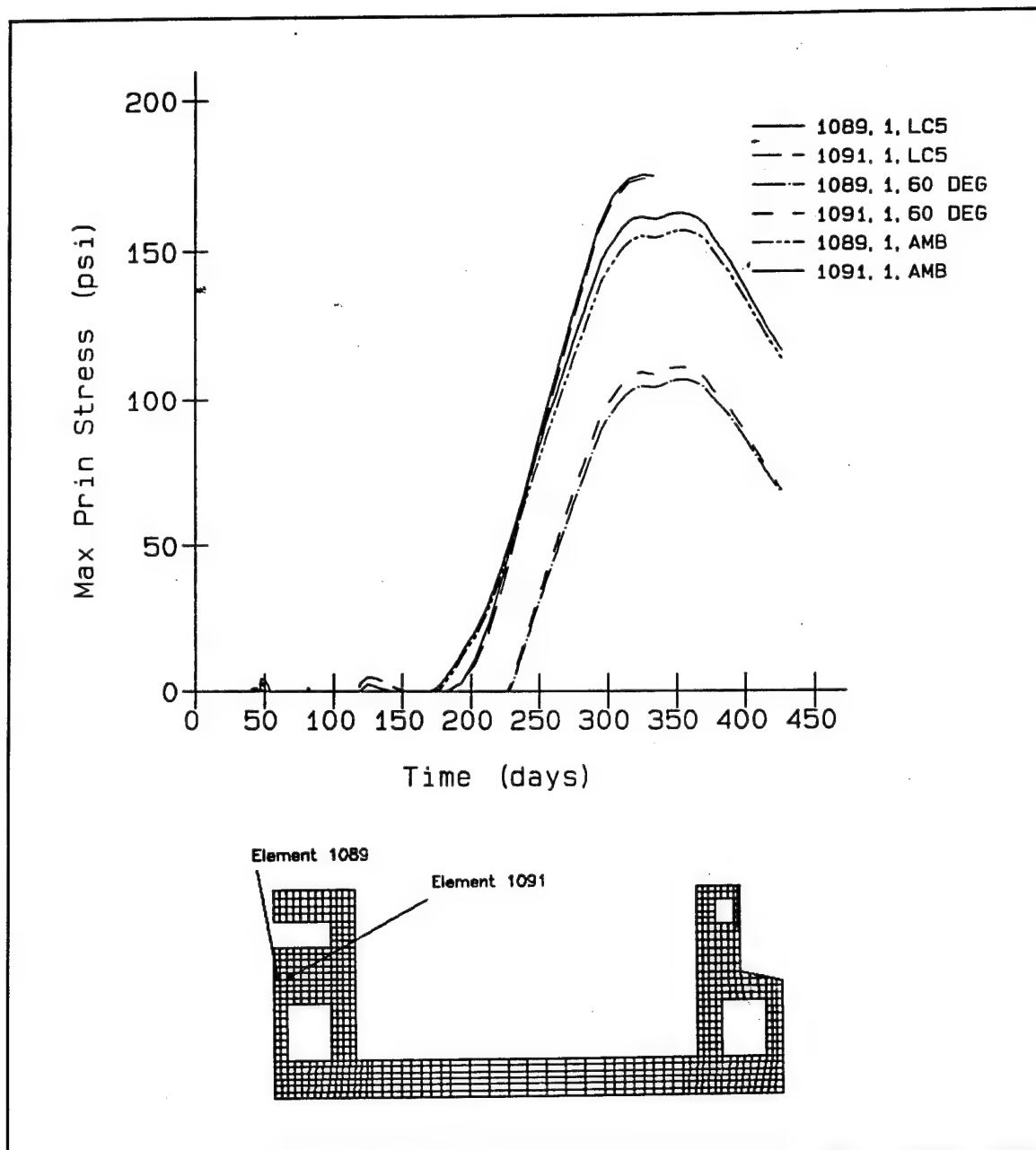
Figure 27.   Maximum principal stresses at center of lifts 10 and 12, load case 5, and increased lift height analyses

the outer face of 2-D elements from load case 5 shown in Figure 31. Three-dimensional plots of surface stresses at 32.5 days are shown in Figure 32. The low stresses in this analysis indicate either that no cracking should occur in this outer wall, or that cracking is caused by some phenomena such as differential settlements of the base that cannot be modeled in our current incremental analysis procedure.

Table 15
Maximum Principal Stresses at Center of Lifts 10 and 12,
Increased Lift Height Analyses

Analysis	Element	Point	Stress (psi)	Day	ETL Allowable (psi)	Percentage of Allowable
Load case 5	1089	1	174.9	324.5	481.9	36.3
60 °F placement	1089	1	104.3	324.5	487.3	21.4
Ambient placement	1089	1	154.8	324.5	487.3	31.8
60 °F placement	1089	1	106.5	351.5	490.6	21.7
Ambient placement	1089	1	156.5	351.5	490.6	31.9
Load case 5	1091	1	173.8	324.5	481.9	36.1
60 °F placement	1091	1	109.1	324.5	487.3	22.4
Ambient placement	1091	1	161.3	324.5	487.3	31.9
60 °F placement	1091	1	110.7	351.5	490.6	22.6
Ambient placement	1091	1	162.4	351.5	490.6	33.1

Conclusions

The time of set for a concrete mixture is an important parameter to the performance of a NISA. Even though the 6-hr time of set analysis proved to be the controlling case for the set time analyses, it is not necessary to evaluate the Olmsted chamber monolith based on these results since test data show that the 12-hr time of set is sufficient.

Changing the material model to accept temperatures from the heat transfer analysis as the stress free temperatures in a newly placed lift from using a single temperature throughout a lift is a valuable modification to the model since the change creates a more realistic model.

Modeling of reinforcement is a key parameter when modeling massive concrete structures for the performance of a NISA. Neglecting the fact that reinforcement is present in a structure limits the capabilities of the designer for developing the most economical structure possible.
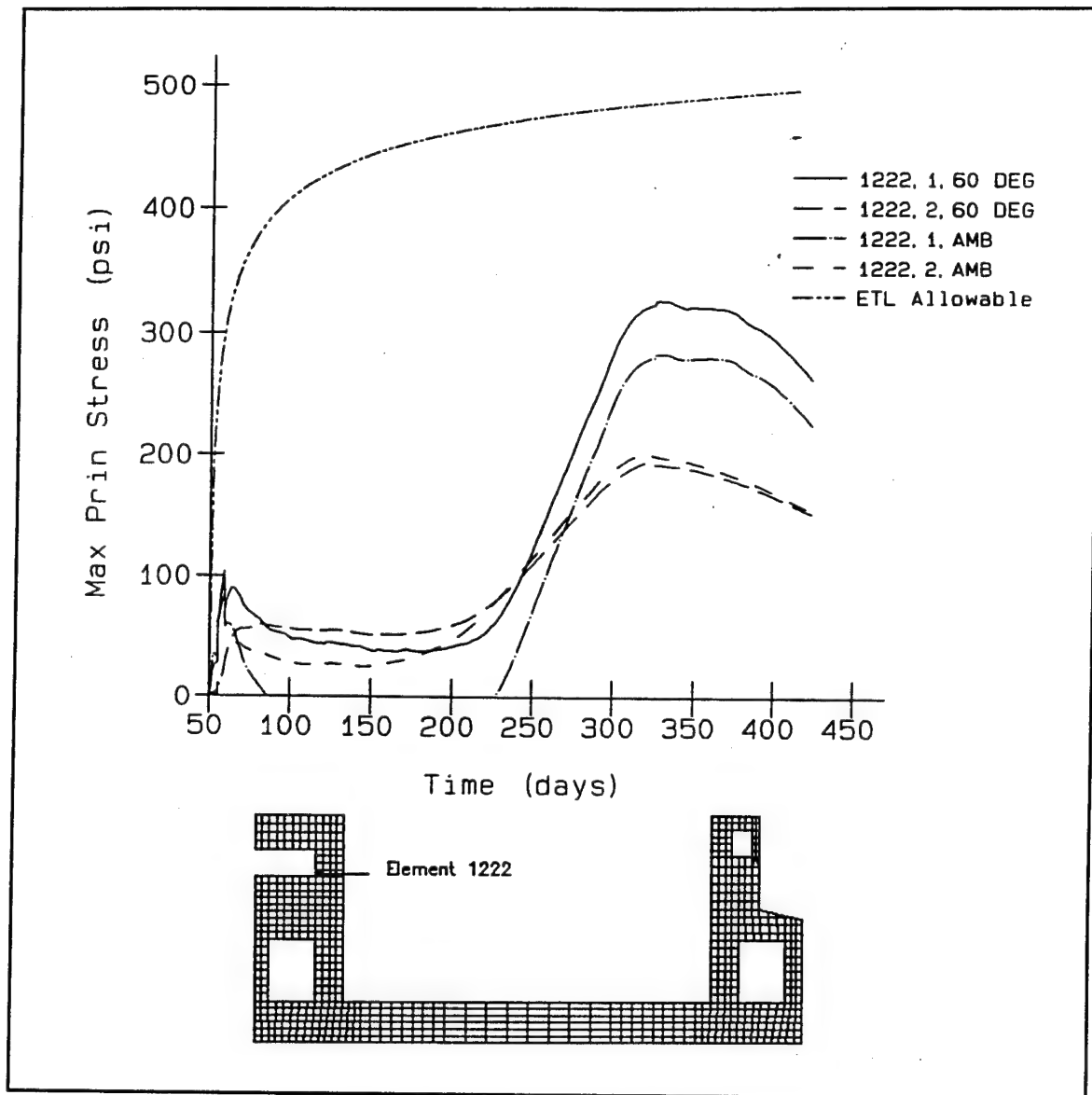
Figure 28.   Maximum principal stresses, element 1222, increased lift height analyses

Table 16
Maximum Principal Stresses, Element 1222, Increased Lift Height Analyses

Analysis	Element	Point	Stress (psi)	Day	ETL Allowable (psi)	Percentage of Allowable
60 °F placement	1222	1	326.6	327.5	486.4	67.1
Ambient placement	1222	1	284.0	327.5	486.4	58.4
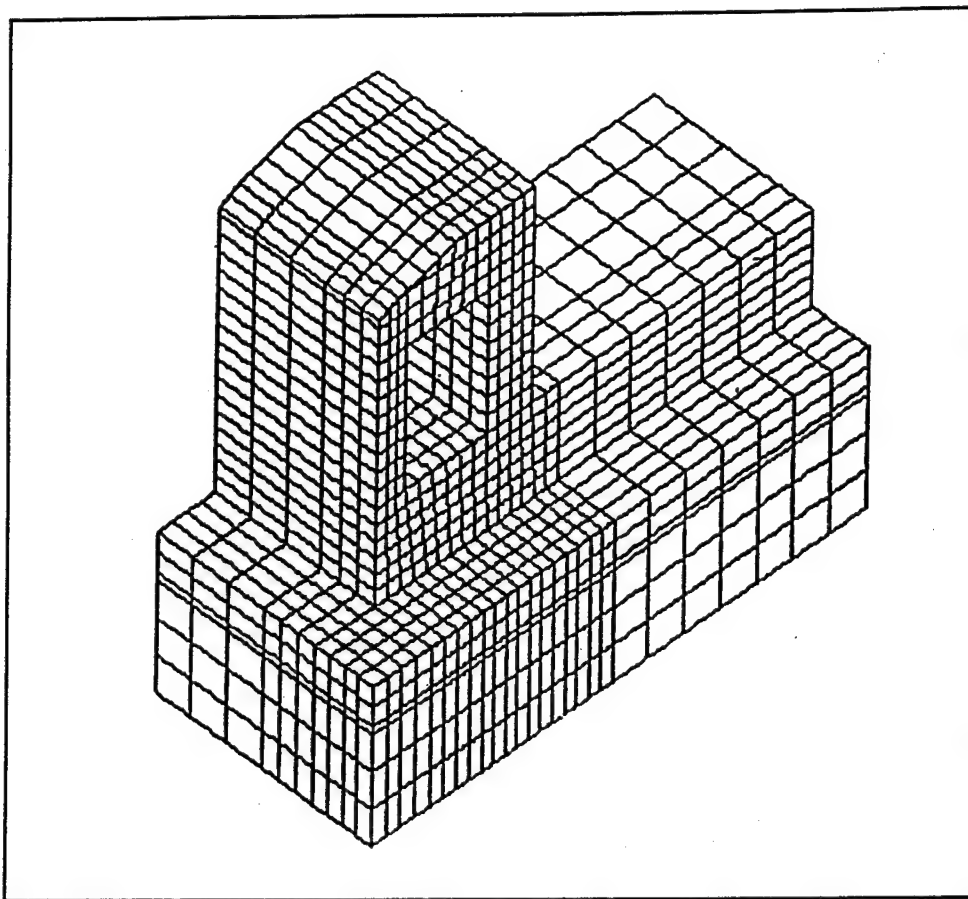
Figure 29.   Grid for 3-D wall analysis

Longer lift placement intervals result in higher stresses in the floor slab due to the increased restraint provided by older supporting lifts. Since the elastic modulus is near its maximum at 30 days, longer lift placement intervals should not cause much increase in tensile stress. Therefore an upper bound is not necessary. Normally tensile stresses that exceed 80 percent of the ETL allowable tensile stress are of concern. However, given the fact that the maximum tensile stresses should peak at around 95 percent of the allowable for lift placement intervals exceeding 30 days and that a higher placement temperature should reduce the tensile stresses in the areas of high tensile stress for the 30-day analyses, the exceeding of this limit is not of great concern.
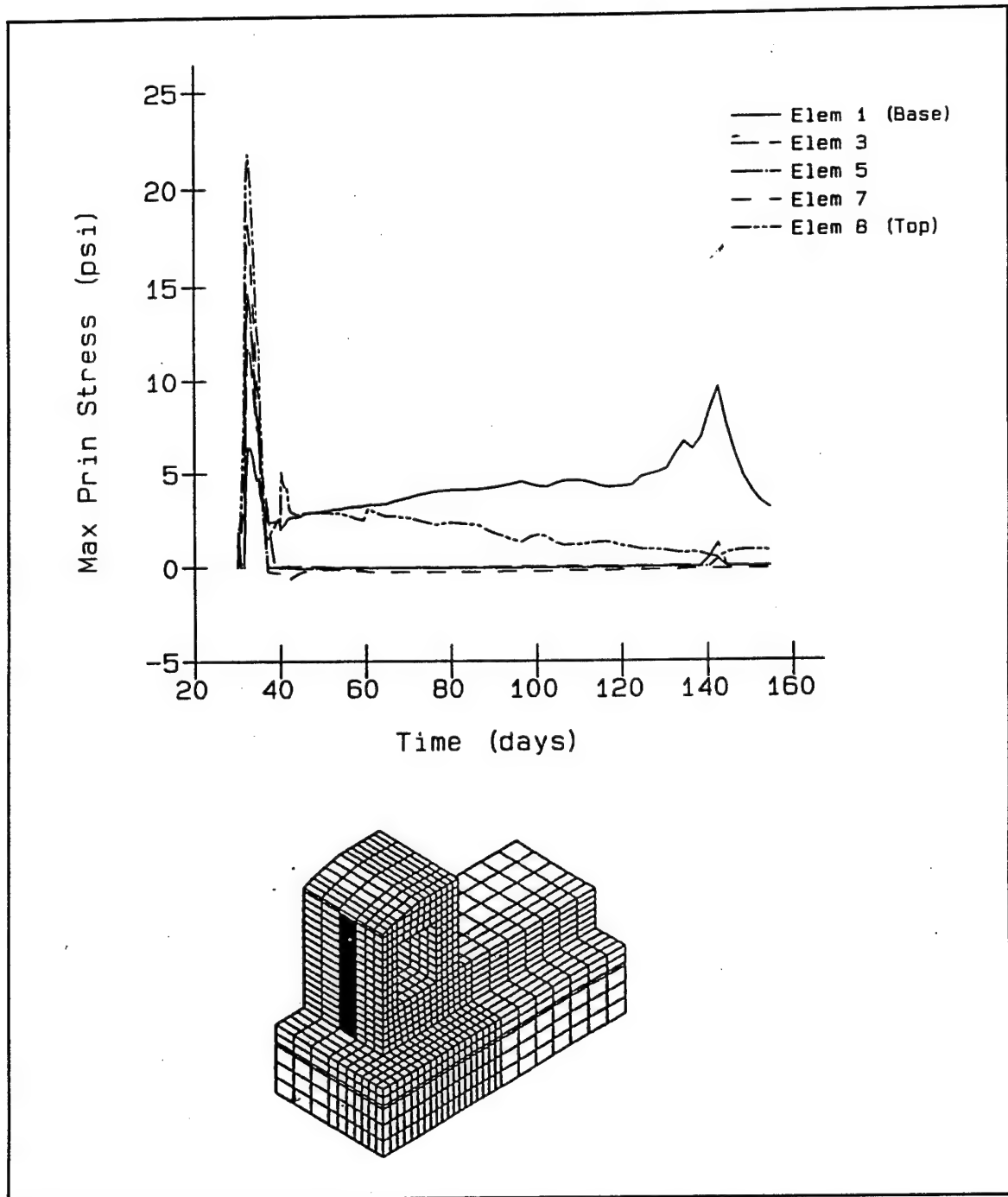
Figure 30.   Maximum principal stresses, outer face of lift 5, 3-D wall analysis
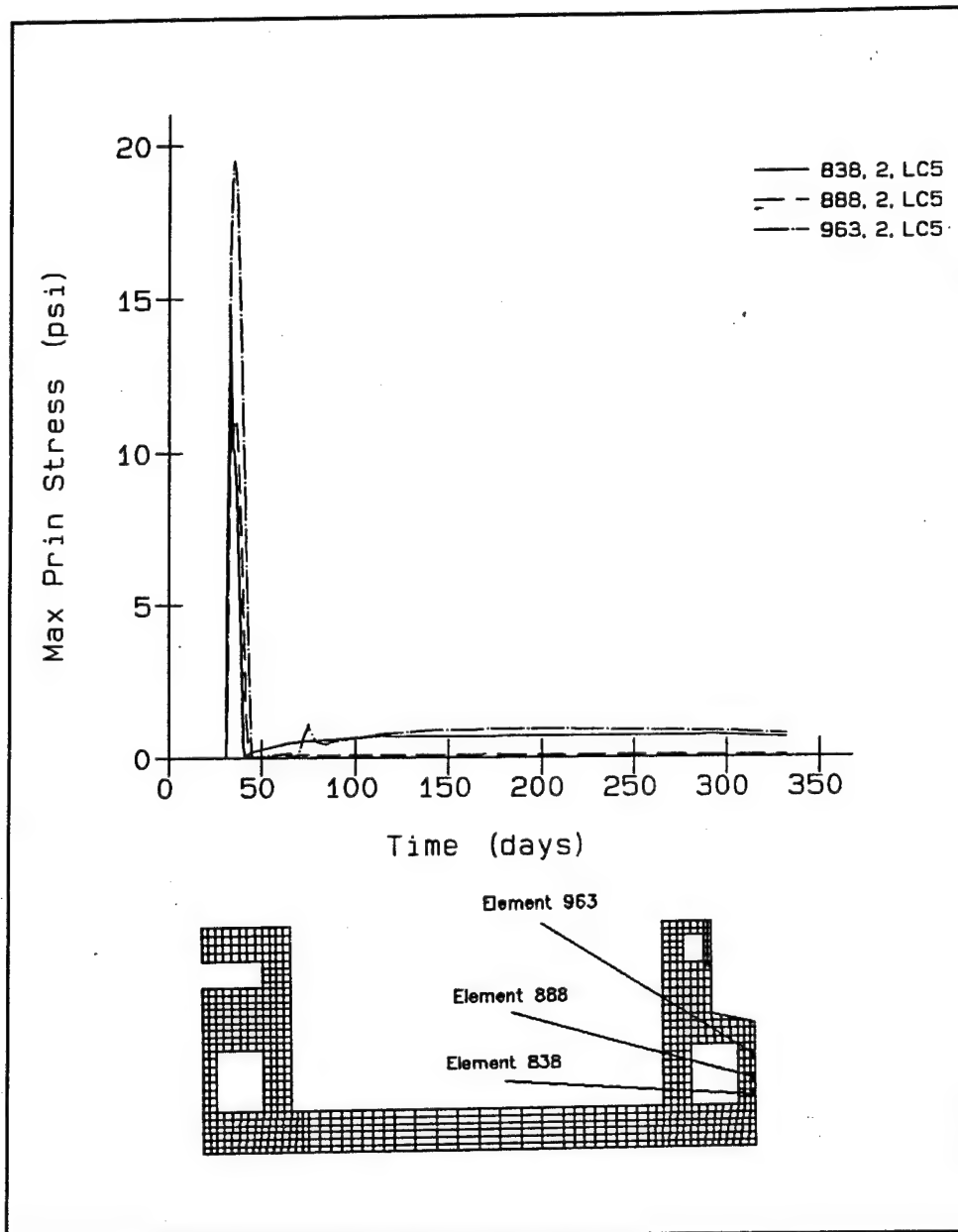
Figure 31.   Maximum principal stresses in lift 5 outer face elements, load case 5
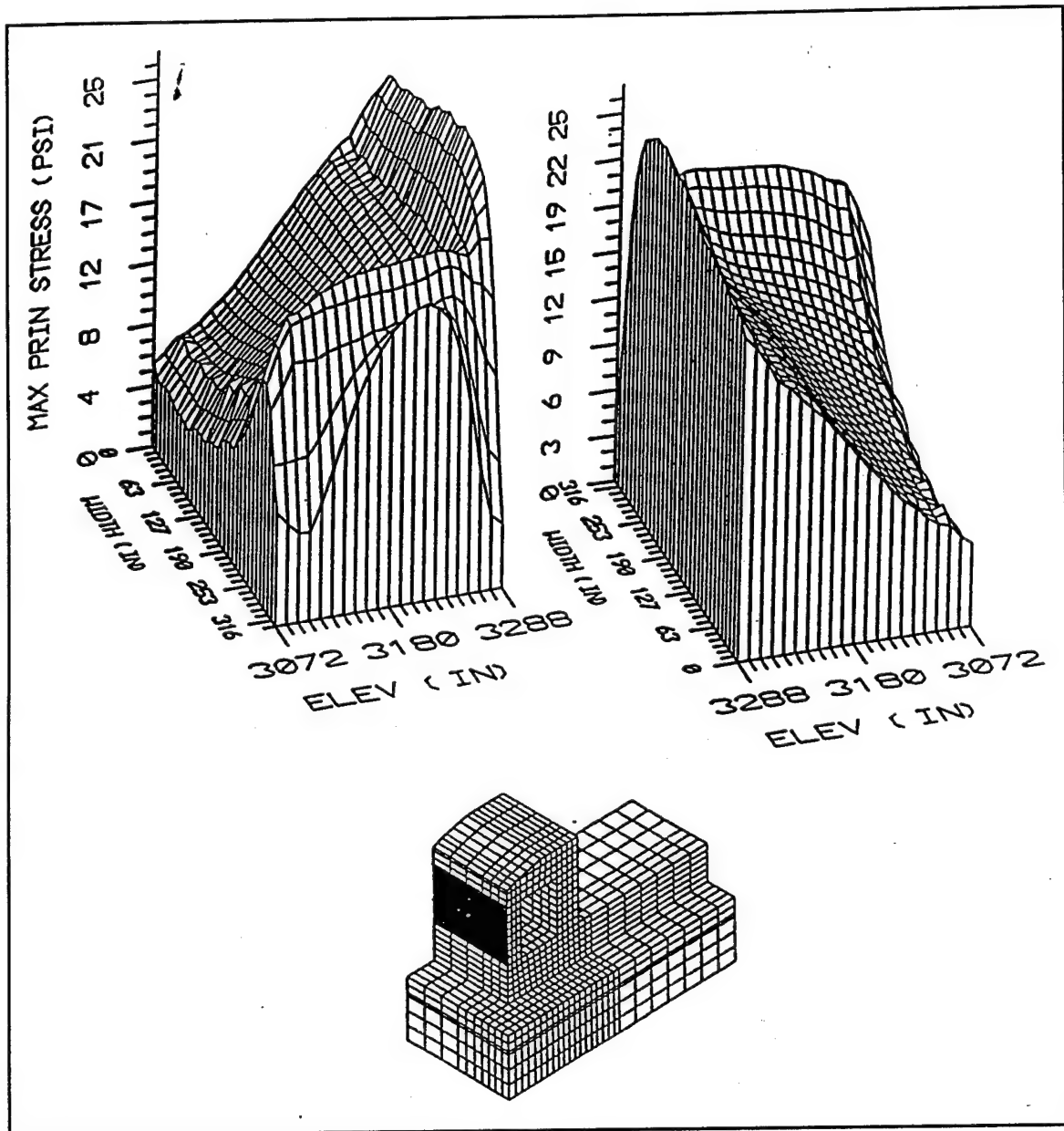
Figure 32.   Maximum principal stresses at outer surface of lift 5, day 32.5

4   Extreme Ambient Condition

Background

As the study progressed, results from the placing temperature analyses were indicating that the best condition for the analyses being performed was the placing scheme which used the ambient conditions for the placing temperature. Since results indicated that the concrete could be placed at ambient conditions there was a concern as to what maximum temperature placing would be allowed and that the results were based on an average daily temperature computed over a 30-year period of time.

A question was raised regarding how the results might change if a hotter than normal summer or a colder than normal winter occurred during construction. In order to account for these possible occurrences it was agreed to review weather data available and find the hottest summer and the coldest winter and develop an ambient temperature curve which would capture the range of temperatures for both extremes. It was felt that such a curve would provide the conservatism necessary for ensuring that selection of an ambient placing temperature scheme would perform satisfactorily. The hot and cold periods chosen were to be extended periods of hot and cold which lasted for a month or longer and not a hot surge or cold snap which only lasted for a few days.

Development of Average Ambient Condition

The curve used for modeling the average ambient conditions was developed from actual daily average temperatures from Paducah, Kentucky. This average is based on 30 years of data. These data were obtained from the National Climatic Data Center of the National Oceanic and Atmospheric Administration located in Asheville, North Carolina.

The curve can be seen in Figure 33. It should be noted that this is the ambient temperature curve that was used throughout Phases I and II of the Olmsted NISA and the curve is based on a Jun 20 start date at time equal to zero. Also shown in Figure 33 are the monthly average temperatures
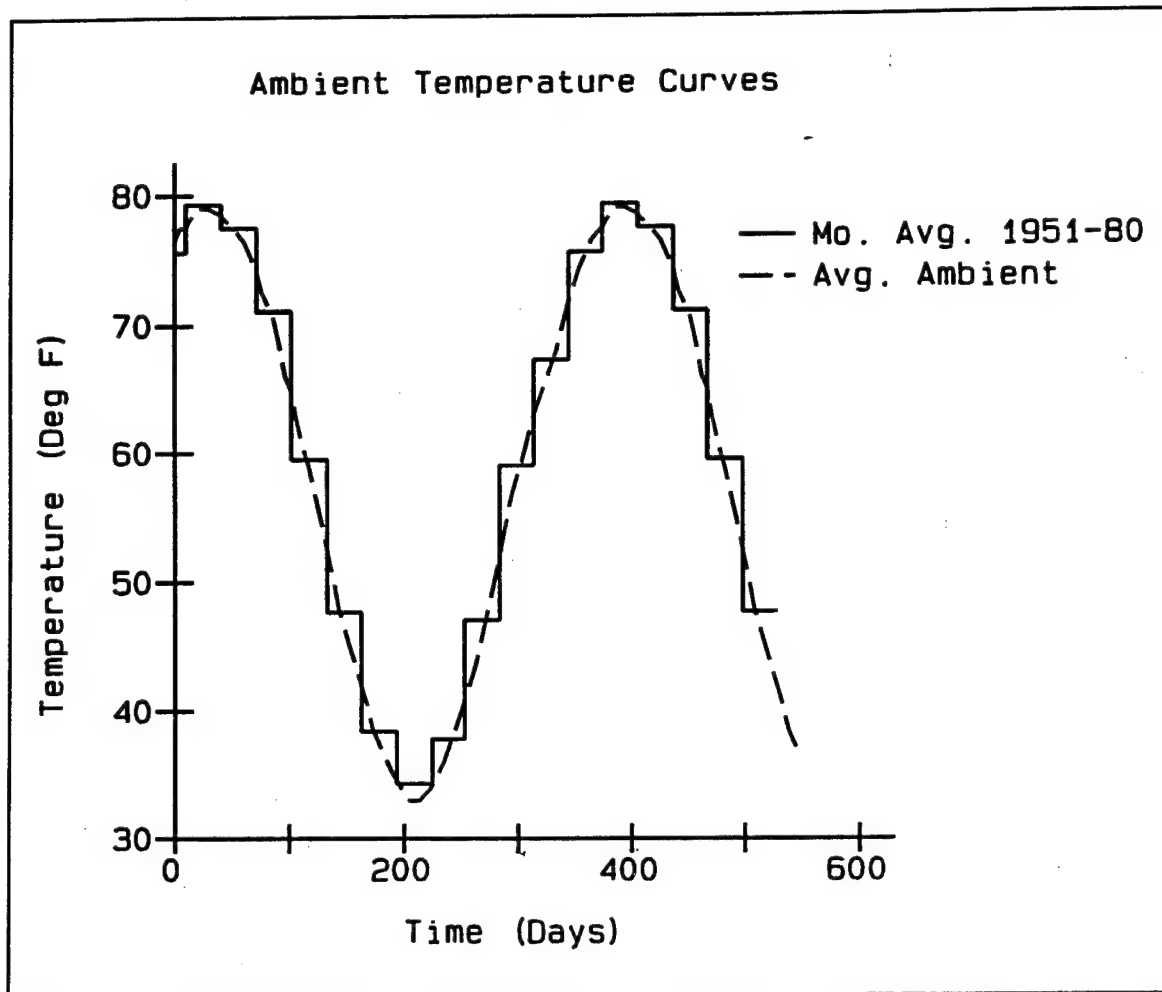
Figure 33.   Average ambient curve and monthly average temperatures associated with the average ambient curve

for the period of 1951 through 1980. As can be seen in Figure 33, the average ambient temperature curve bisects the lines designating the monthly average temperatures on the descending and ascending portions of the curves and reaches its peaks at nearly the midpoint of the month at both the coldest and hottest times of the year. Based on this comparison the monthly average temperatures seem to provide a good estimation of the average ambient temperature.

Development of Extreme Ambient Condition

The objective of developing the extreme ambient curve was to have a curve that would capture the effects of the hottest summer and the coldest winter on record. Therefore, the effects of these hot and cold periods should be for extended periods of time. The data that were received from the National Climatic Data Center contained information from 1939

through 1991 on monthly average temperatures at Paducah, Kentucky. Due to the fact that time was limited and that monthly temperatures would be a suitable indication of extended periods of hot and cold a decision was made to select the extreme ambient temperature curve based on the monthly average temperatures.

Perusal of the data indicated that there were two years which were hotter than others, those being 1987 and 1988. The monthly averages for 1987 and 1988 are shown in Figure 34 and are compared to the average ambient curve. As can be seen in the figure, the maximum temperatures are several degrees higher than the average ambient curve. The coldest year on record was 1985, as shown in Figure 35 and again the monthly averages are compared against the average ambient curve. Calendar year 1985 was colder than the average by more than 10 °F.

Once the extreme years had been selected, a smooth curve which would capture these two extremes needed to be developed. While the average ambient curve was selected from actual data, its shape closely follows that of a sine wave. Because the average ambient curve approximated a sine wave a
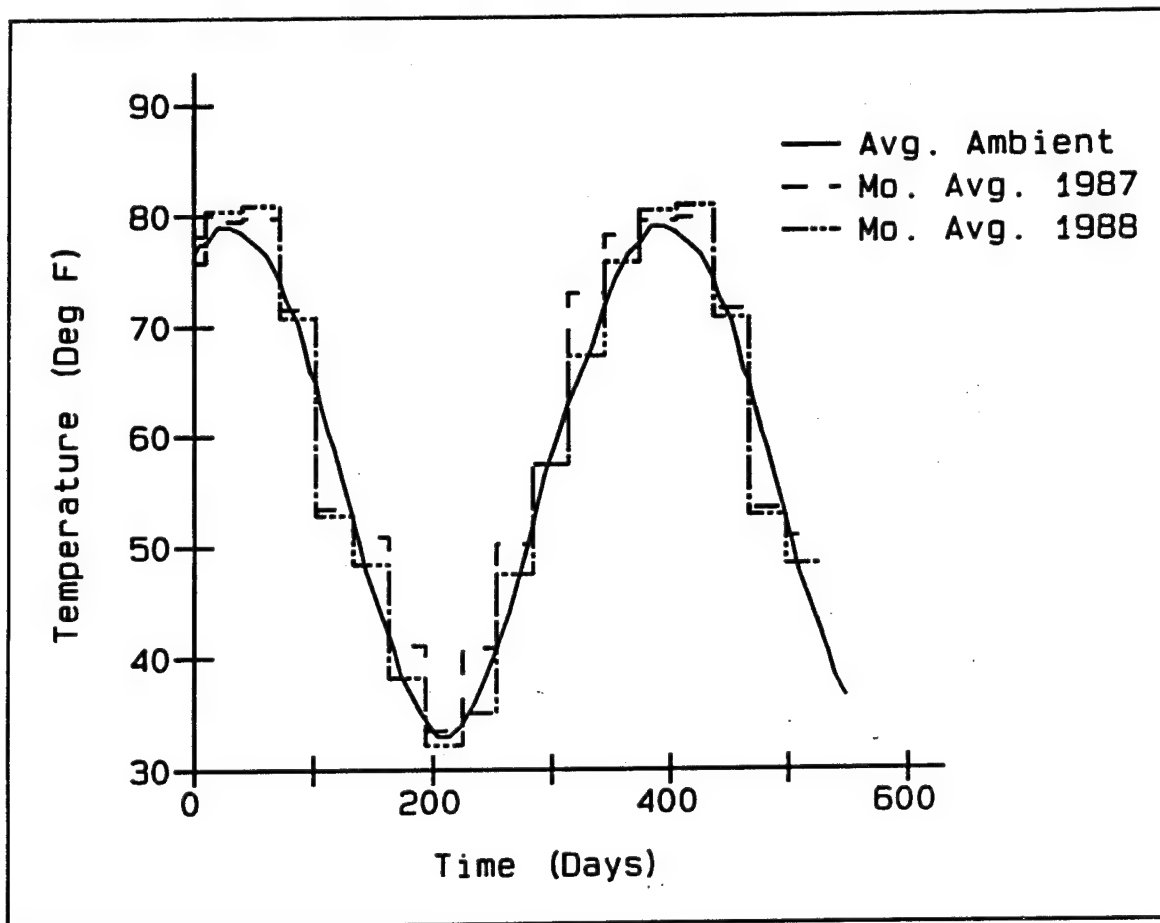
Figure 34.   Average ambient curve and monthly average temperatures for the two hottest years on record
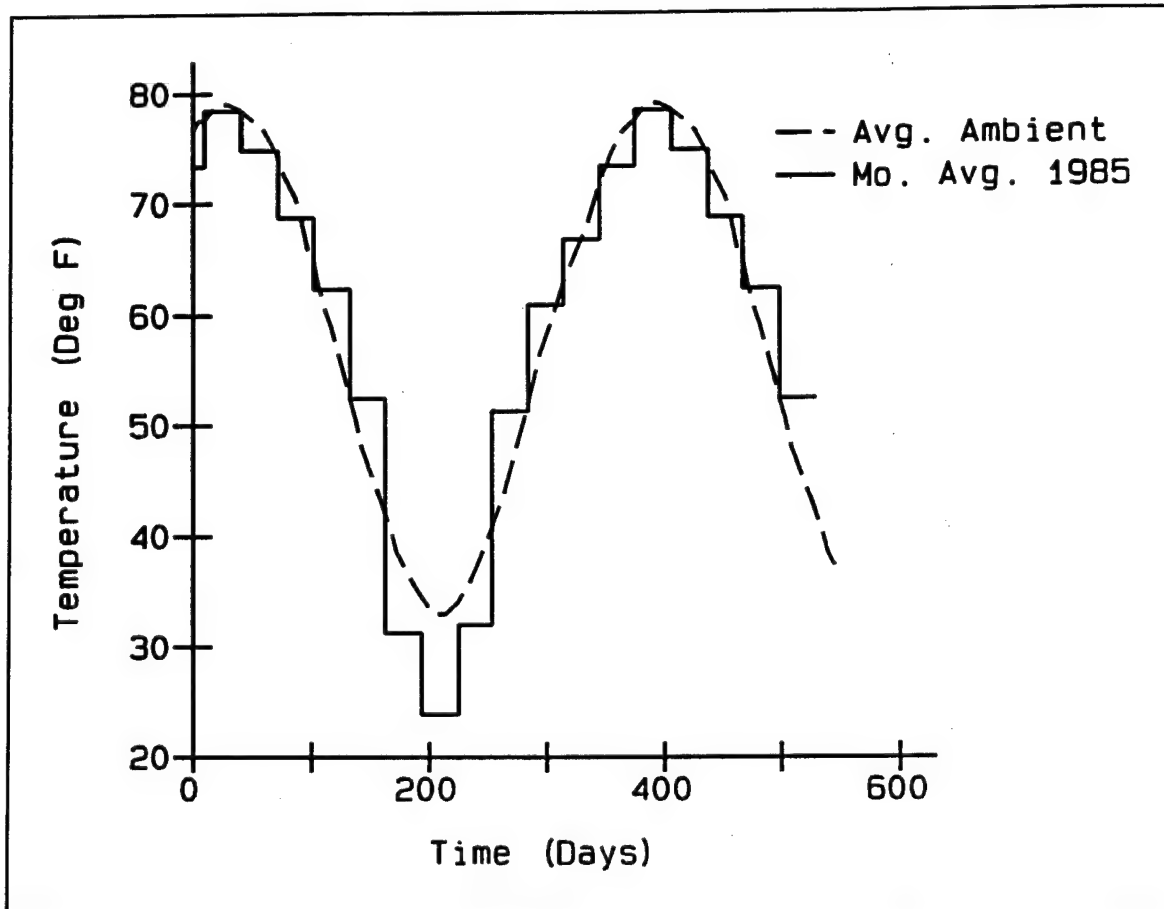
Figure 35.   Average ambient curve and monthly average temperatures for the coldest
year on record

decision was made to model the extreme ambient curve with a sine wave.
Once the sine curve had been selected the only decision which remained
was to select the maximum and minimum of the curve. After some trial
and error the maximum selected was 85 °F and the minimum was 22.5 °F.
This resulted in an equation for the curve of:

Temperature (°F) = 31.25 sin[90 + 180(No. of days)/182.5] + 53.75

The curve is at its maximum on Jul 16 and so the number of days would
be set to zero for Jul 16.

Selection of these values was based on getting the peak months to fall
inside the curve. This can be most clearly seen in Figure 36 where the
curve nearly intersects each end of the coldest month on record. A similar
process was used for the maximum temperature but is not as evident in
Figure 37 since the hottest months on record are offset from the peak. If
the curve were shifted forward by 15 days though, the curve would inter-
sect the ends of the two hottest months shown. It was not necessary to
capture the actual peak monthly temperature since the behavior desired is
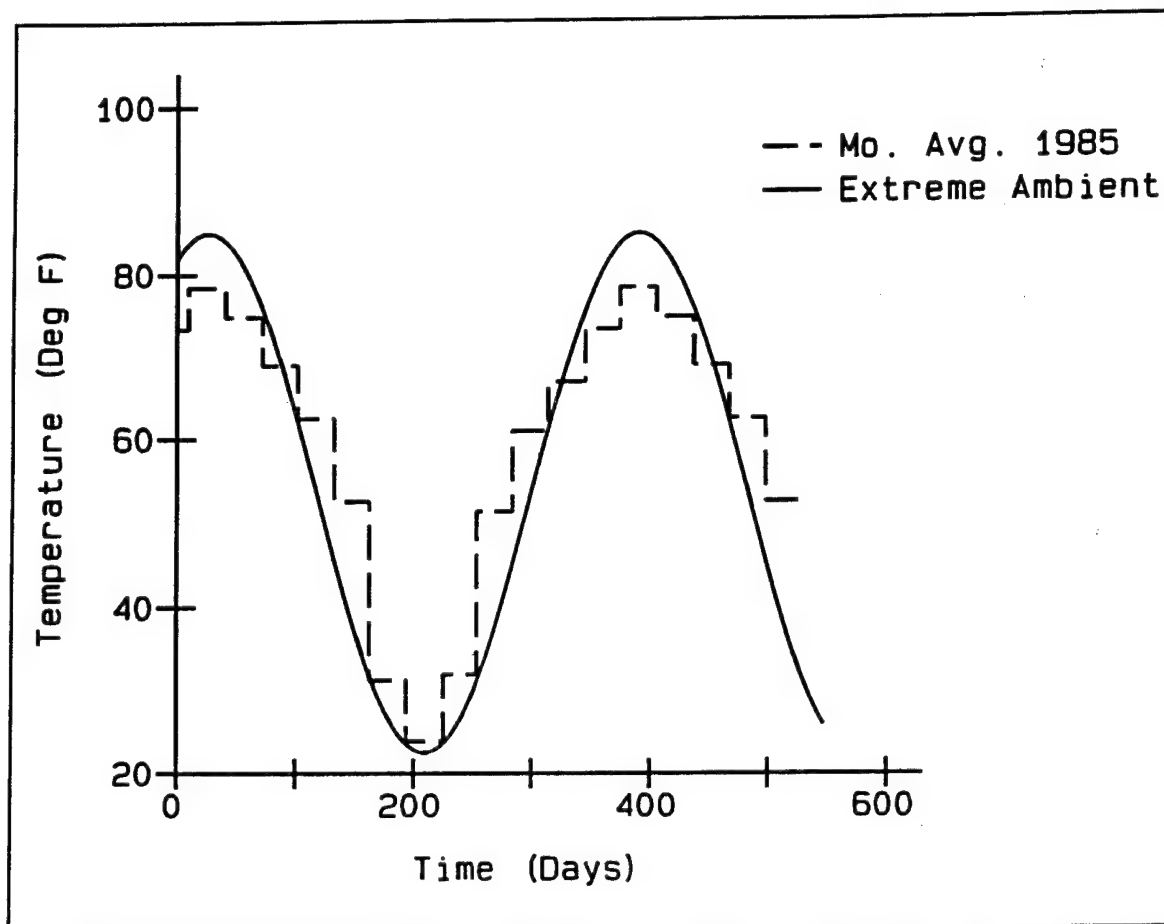
Figure 36.   Extreme ambient curve and monthly average temperatures for the coldest
year on record

a generic behavior and not a specific one. Finally the extreme ambient
curve is compared to the average ambient curve in Figure 38. The curves
follow the same general trends. The extreme curve has a maximum tem-
perature 5 °F higher than the average curve and the minimum temperature
is 10.5 °F colder than the average curve.

Comparison of Average and Extreme Conditions

In order to quantify the effect that the extreme ambient condition com-
pared to the average ambient condition has on the behavior of the struc-
ture, results were plotted from the two analyses to demonstrate the effect
that changing of the ambient conditions would have on the structure.
Comparisons of both temperature and stress will be shown and explana-
tions given for how the behavior changes from the average ambient condi-
tion to the extreme ambient condition. The analyses performed assumed a
placing temperature of 60 °F.
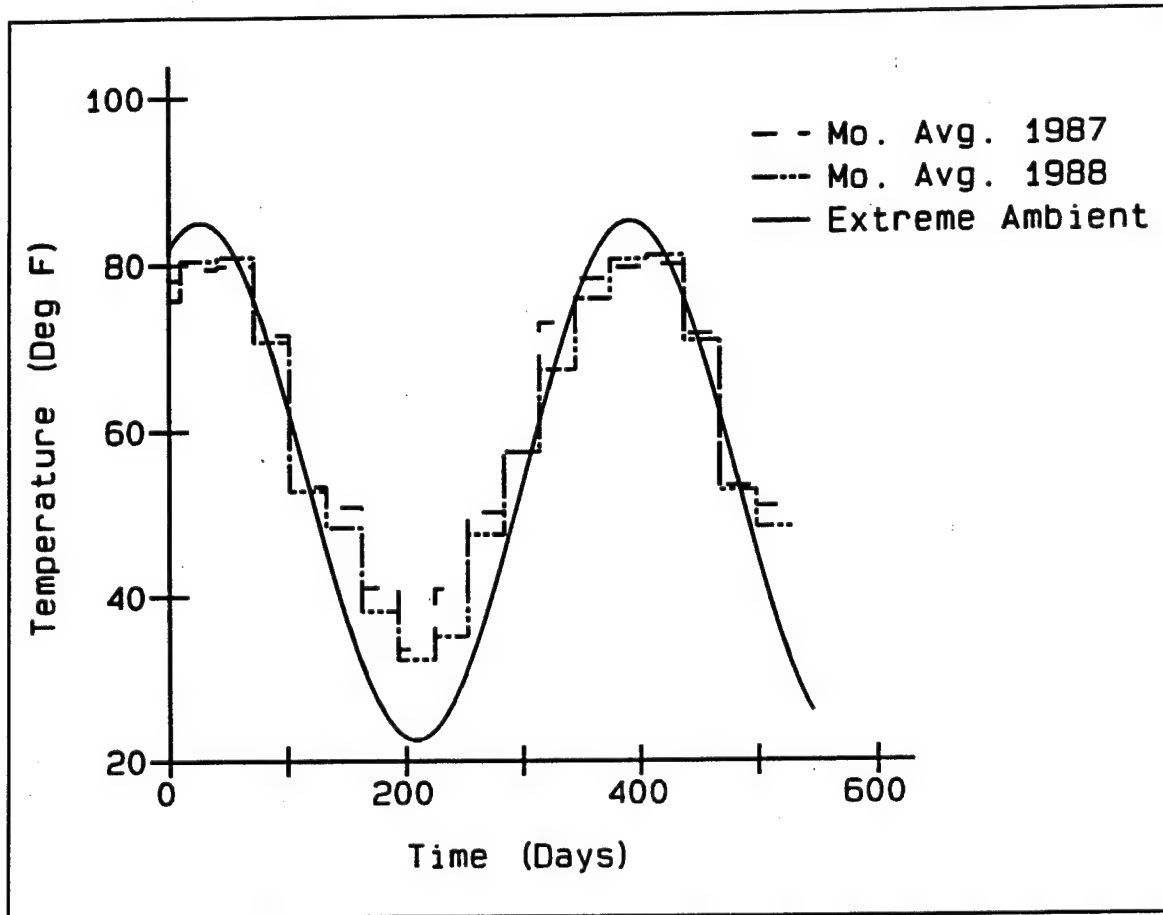
Figure 37.   Extreme ambient curve and monthly average temperatures for the two hottest years on record

Comparison of temperature results

Figures 39-41 are plots of temperatures in the base slab of the chamber monolith. The plots show that use of the extreme ambient condition changes the temperatures near the bottom of the slab (Figure 39), although the difference at the minimum temperature is not as large as near the top of the slab (Figure 41). The fact that the temperature near the bottom of the slab changes less than the temperature near the top of the slab indicates that a larger temperature gradient exists for the extreme condition than for the average condition. It is also readily noticeable how the higher ambient temperatures cause an increase in the maximum temperatures of the concrete.

Figures 42-44 show plots of temperatures in the wall of the chamber monolith. As in the base slab the extreme ambient condition has an effect on the temperature, even at locations that are some distance from the surface of the face of the chamber. Once again, the further away from a convective surface a point resides, the smaller the change in temperature is from the average condition to the extreme condition. The initial temperatures in these plots are nearly identical. This is because at the time the lift
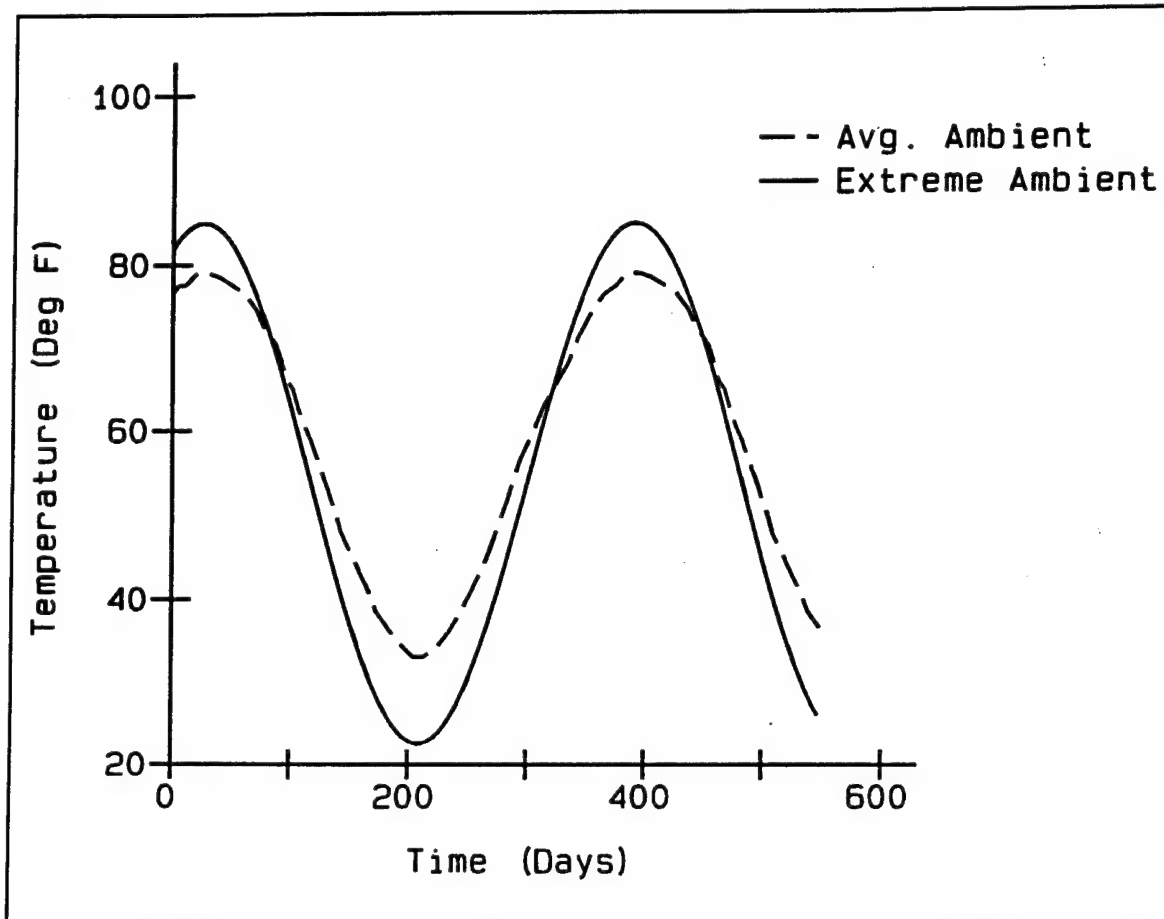
Figure 38.   Comparison of the average ambient and extreme ambient curves

was placed which contains the points shown in Figures 42-44, the temperatures of the two ambient conditions are approximately the same.

Comparison of stress results

Figures 45-48 are time history stress plots of the horizontal stress component for four points near the center of the chamber and are followed by a stress distribution in the slab through these points in Figure 49. Looking first at a point near the bottom of the slab in Figure 45, the change in the ambient condition appears to have little effect on the stresses at the early times, but as expected, at the later times the extreme ambient condition creates a higher compression condition. The trend is similar in Figure 48 which is a time history of a point near the top of the slab except that the extreme condition produces higher tension. Figure 46 shows larger differences at early times than the other three locations shown primarily due to its location with respect to the top of lift 1. All four figures show the general trend which would be expected by increasing the range of ambient temperatures due to the increased temperature gradient across the base
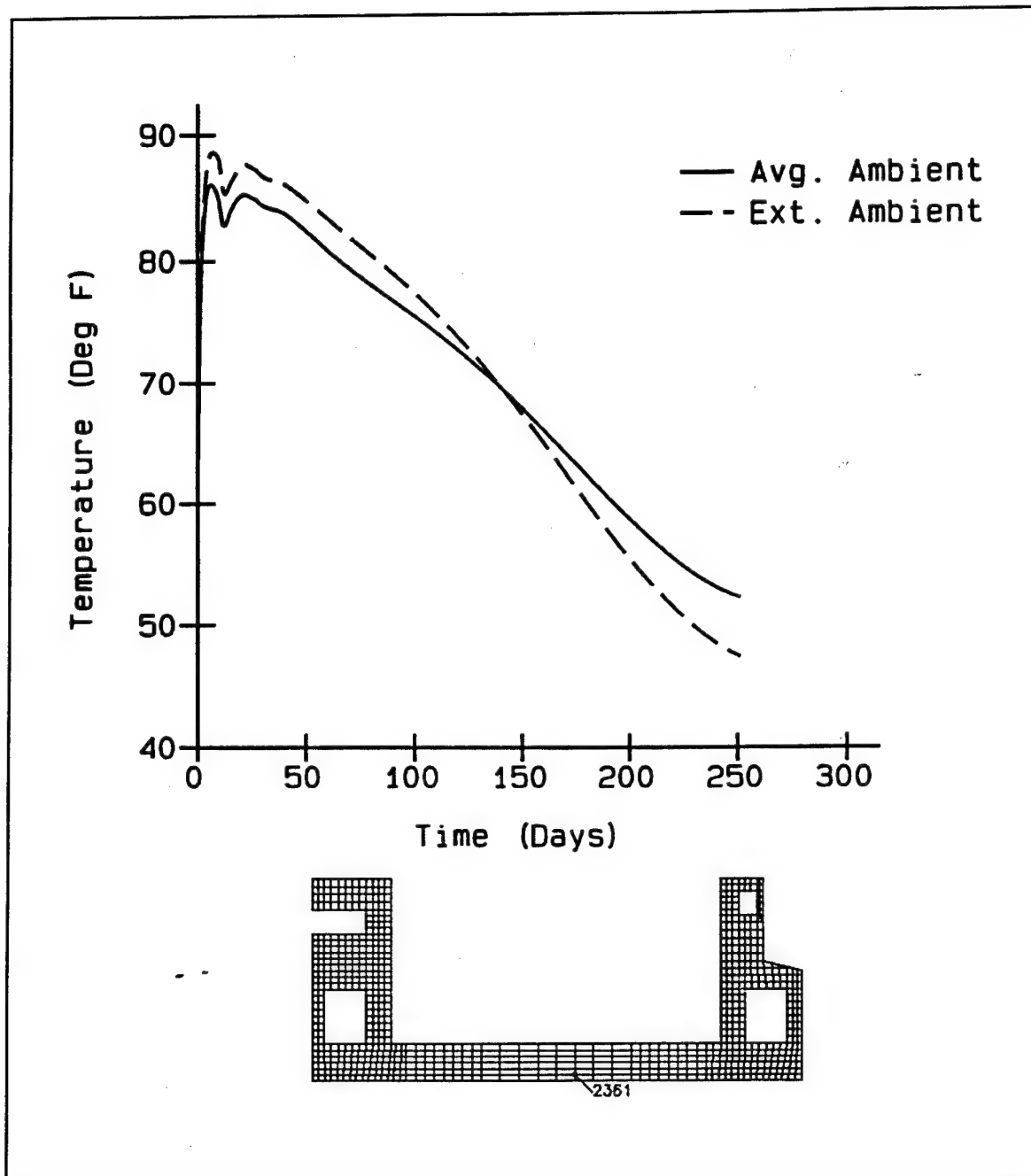
Figure 39.   Temperature time history at node 2361

slab. The effect of the increased temperature gradient across the slab can be seen by the resulting increased stress gradient shown in Figure 49.

Figures 50-52 are time history stress plots at various points across the top of the slab. While the percentage increase in the maximum stresses in these three plots is significant the value remains at a level that is acceptable. For example, in Figure 50 which is a plot of element 756, integration point 3, the increase in the maximum stress from the average ambient
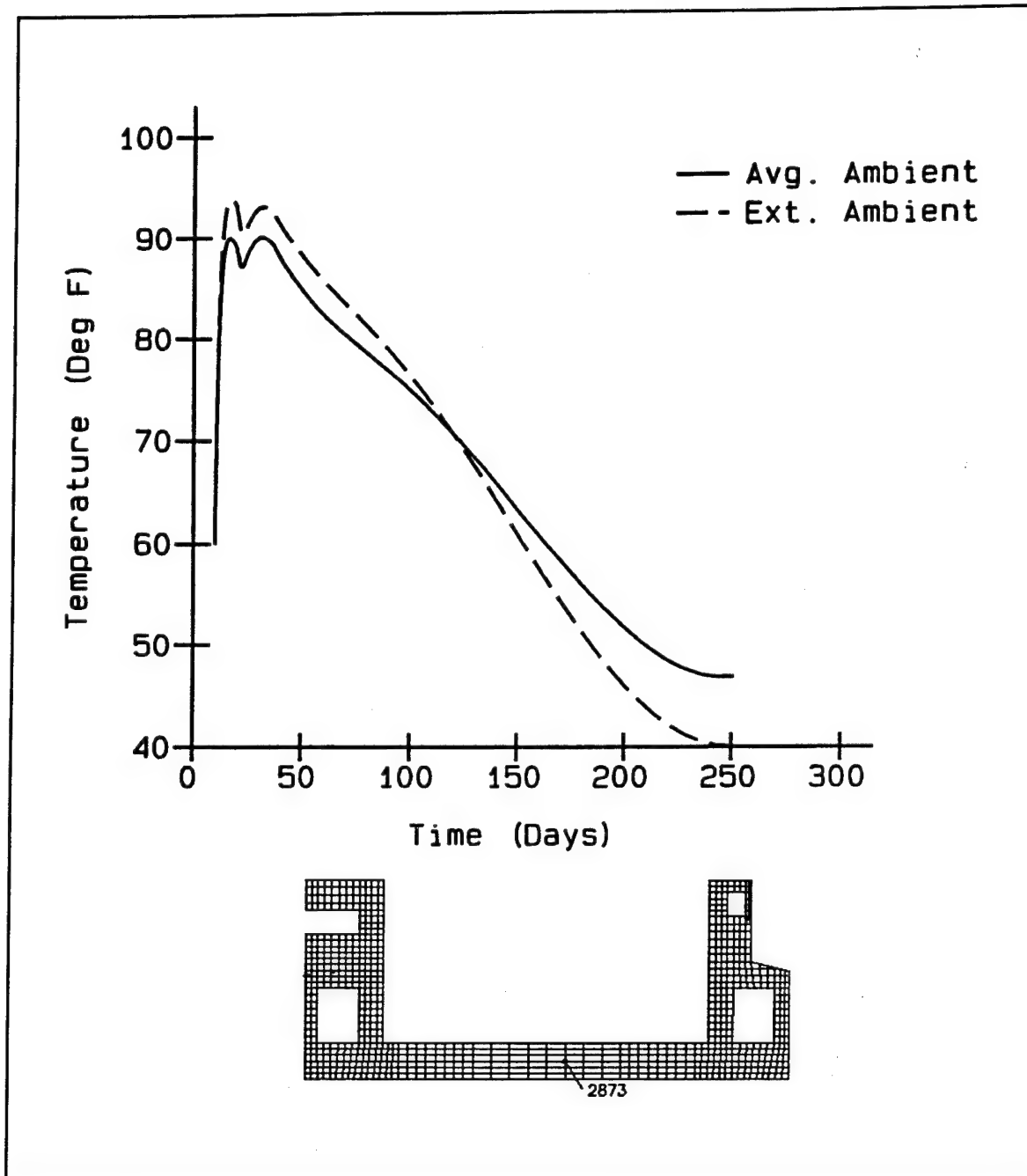
Figure 40.   Temperature time history at node 2873

condition to the extreme ambient condition is 96.7 psi and is a 38 percent
increase in the stress. But the maximum stress for the extreme ambient
curve is 352.2 psi and is 76 percent of the ETL allowable.

Figures 53-56 are time history stress plots of the maximum principal
stress at various points in the center wall. The effects of the changing
ambient conditions can be seen in Figures 53, 54, and 55 by the fact that
the curves diverge at the early times when the ambient temperature is
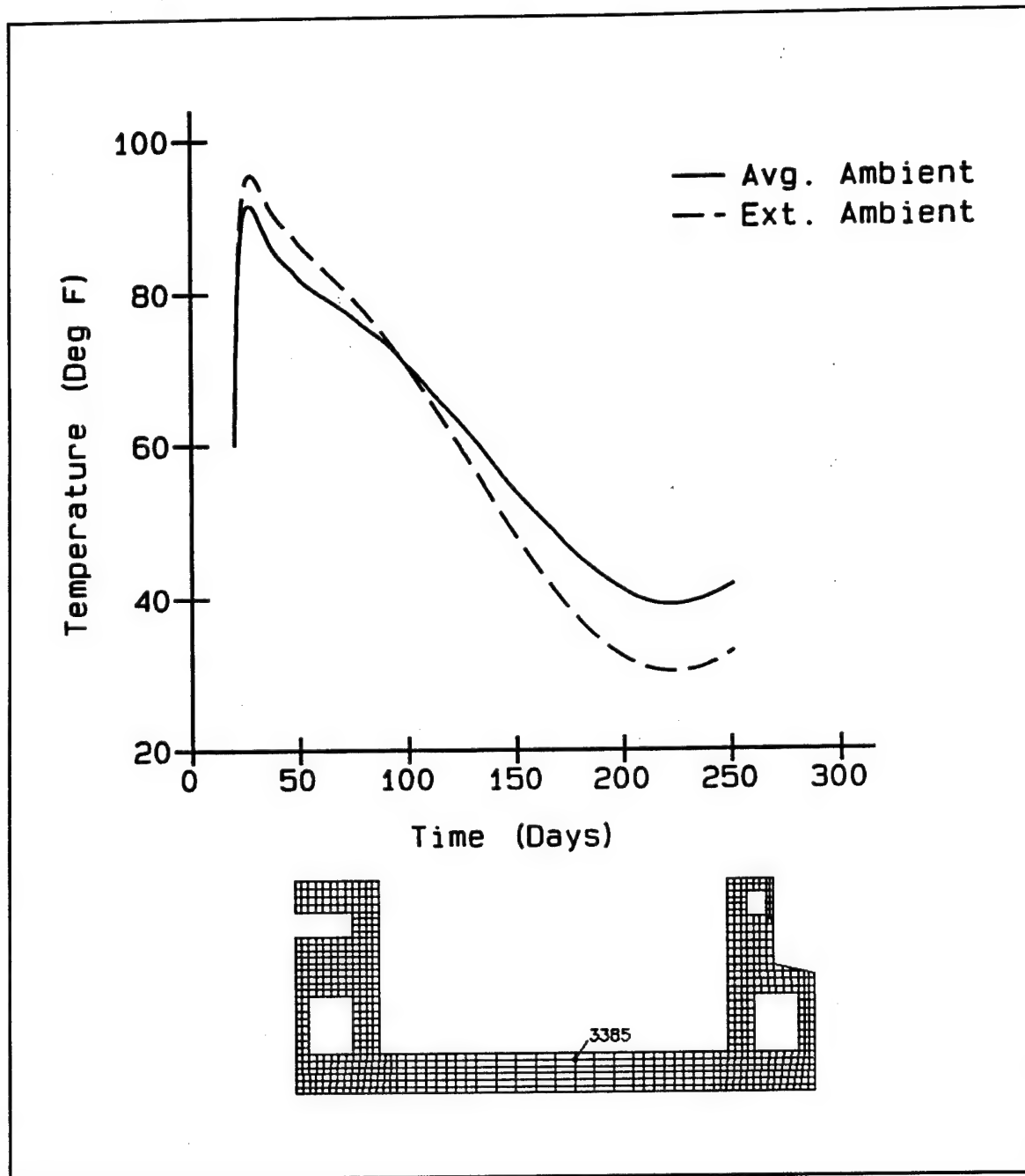
Figure 41.   Temperature time history at node 3385

decreasing but then begin to merge together as the ambient temperature begins to increase. The effects of ambient are less evident in Figure 56 primarily due to the fact that the maximum principal stress at this particular point is less than zero and therefore much of the behavior is lost. There appears to be a difference in behavior in Figures 54 and 55 when compared to the behavior in the slab in that as the ambient temperatures become warmer the tensile stresses increase. This behavior is actually similar to the slab behavior when compared to the behavior of the bottom
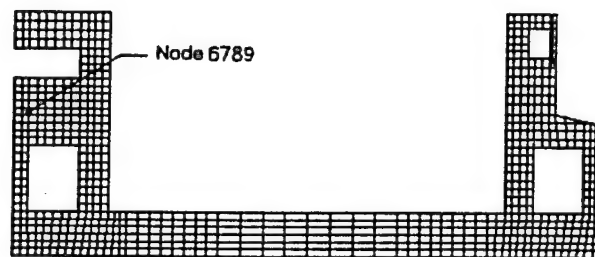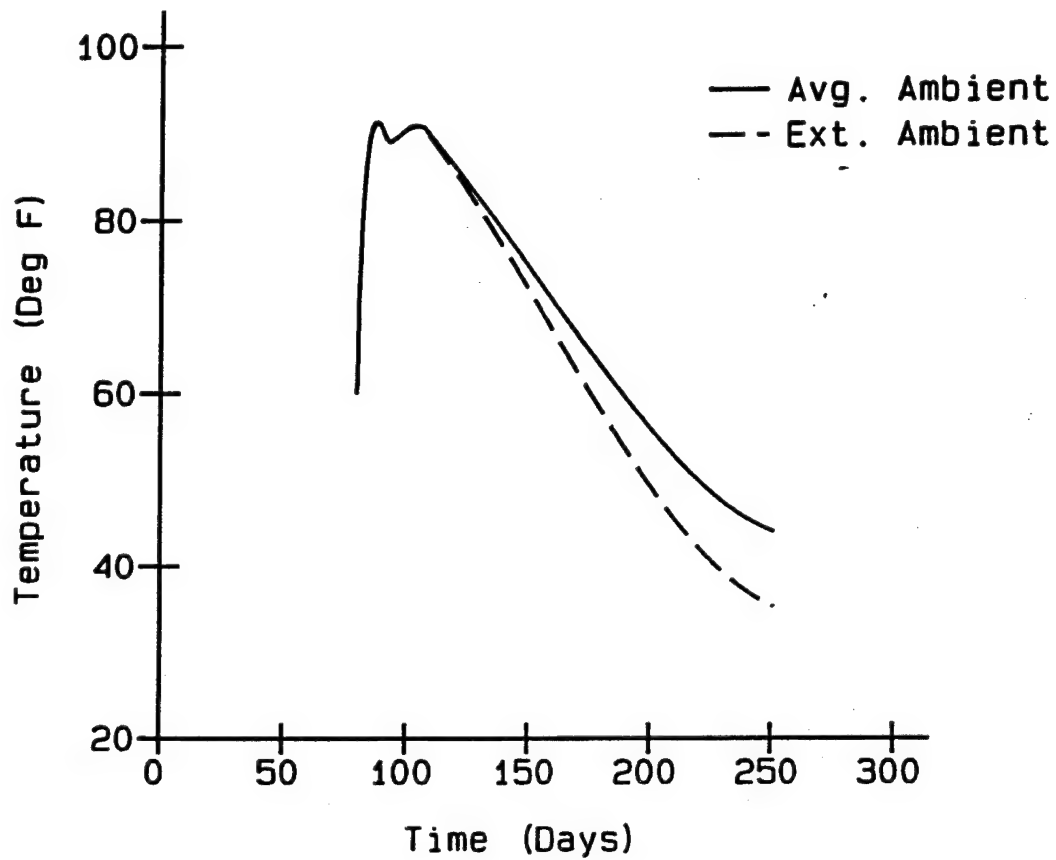
Figure 42.   Temperature time history at node 6789

of the slab which goes into compression as a result of the top of the slab going into tension. The behavior shown in Figures 54 and 55 results from the top of the culvert going into tension and then as the ambient conditions become warmer the stresses in the top of the culvert decrease and eventually go into compression.
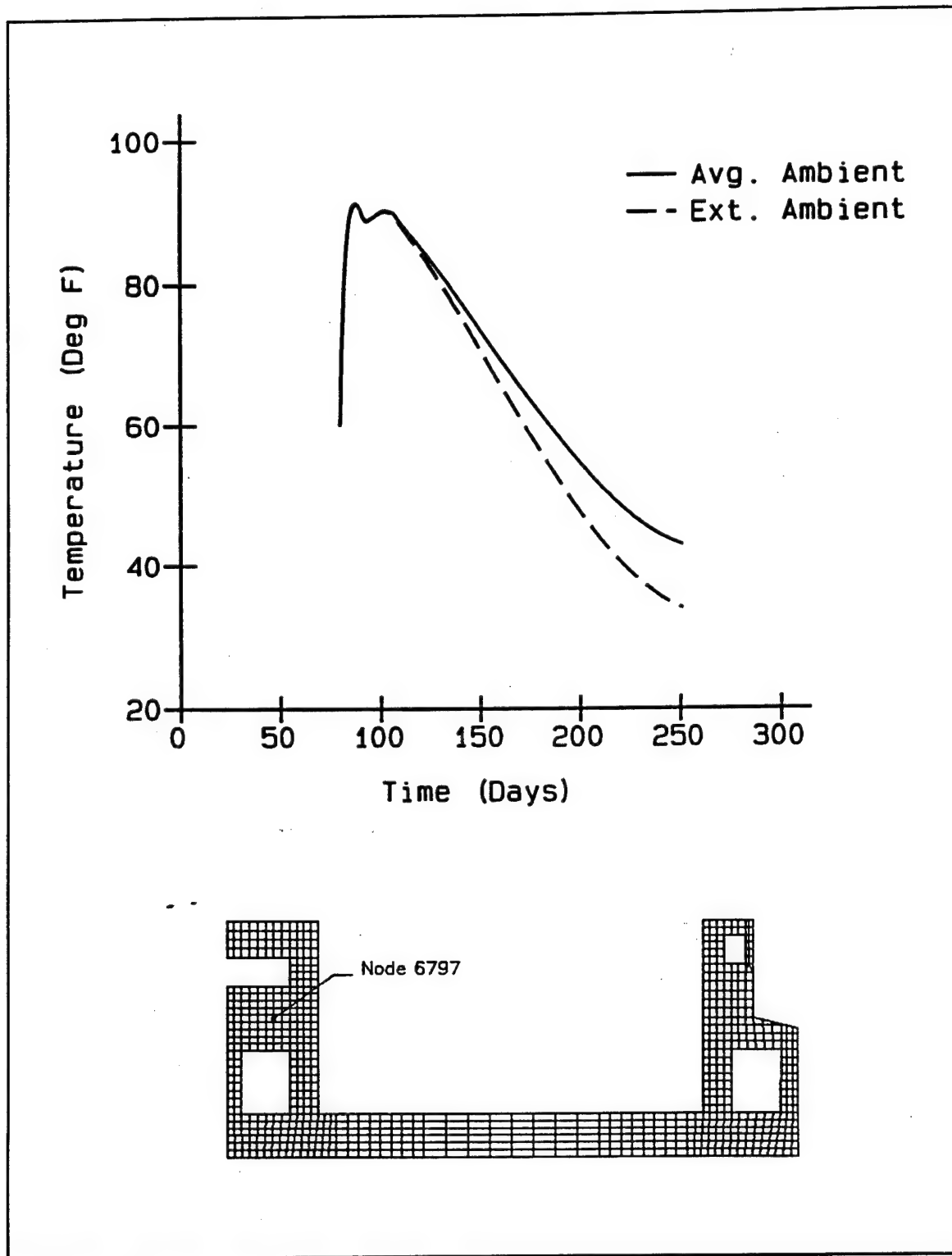
Figure 43.   Temperature time history at node 6797
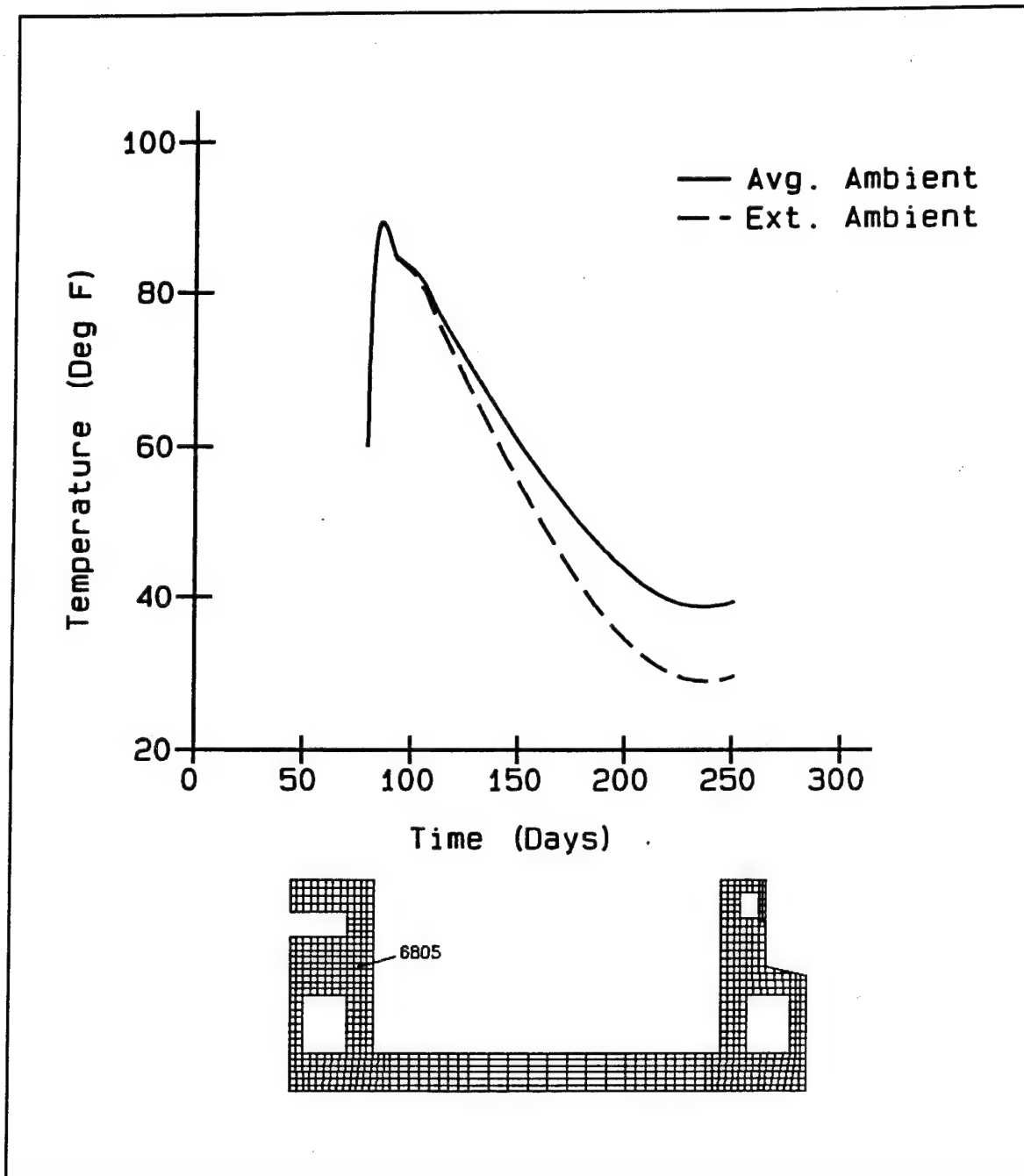
Figure 44.   Temperature time history at node 6805

Evaluation of Results

The results shown in Figures 39-56 clearly indicate that the extreme ambient condition provides a more conservative case than the average ambient condition. Therefore, in order to ensure the results obtained in the placing temperature analyses will be valid for the full range of ambient conditions that may occur, the extreme ambient condition will be used.
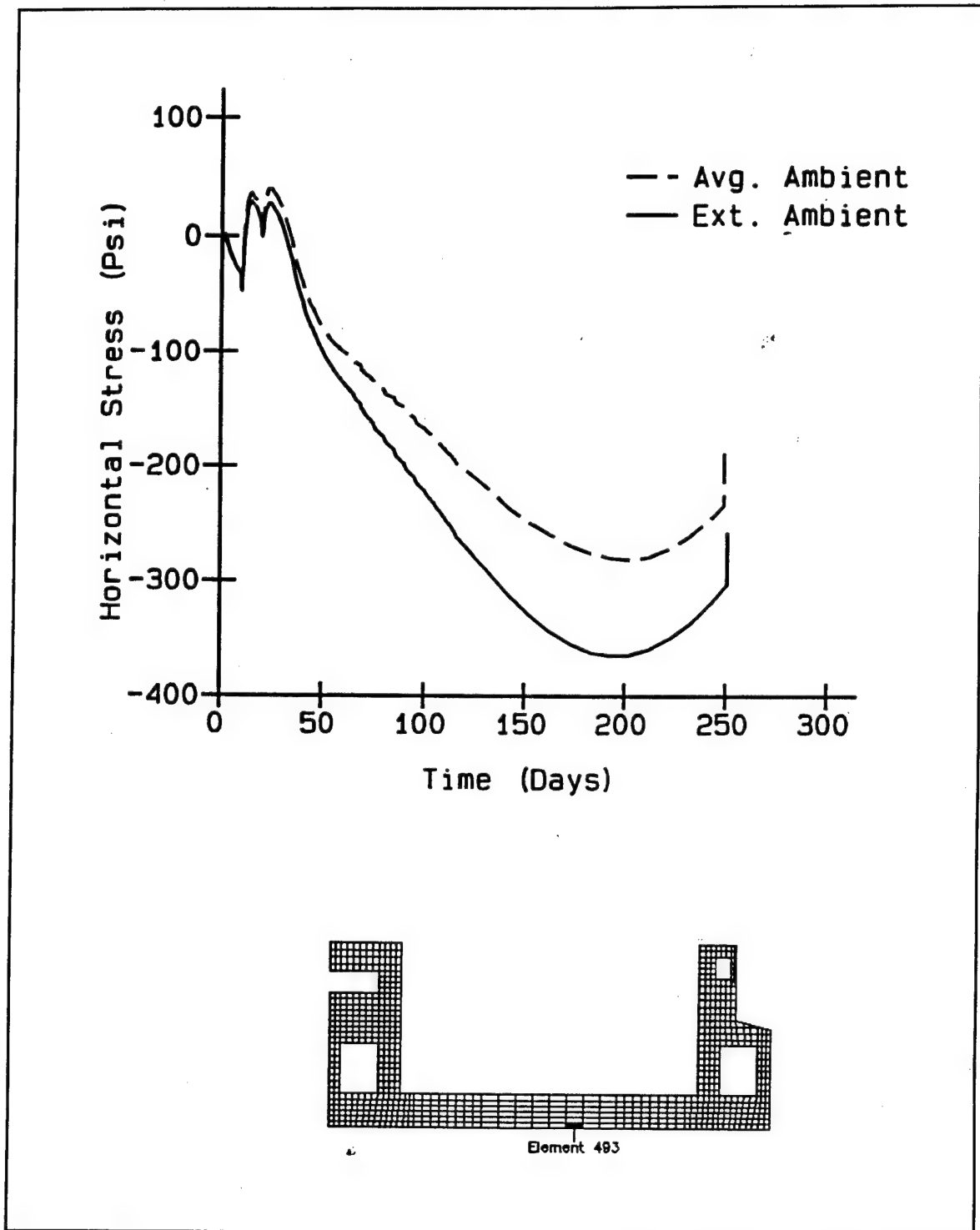
Figure 45.   Time history of horizontal stress at integration point 1 of element 493
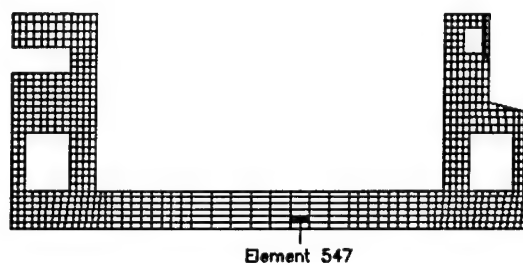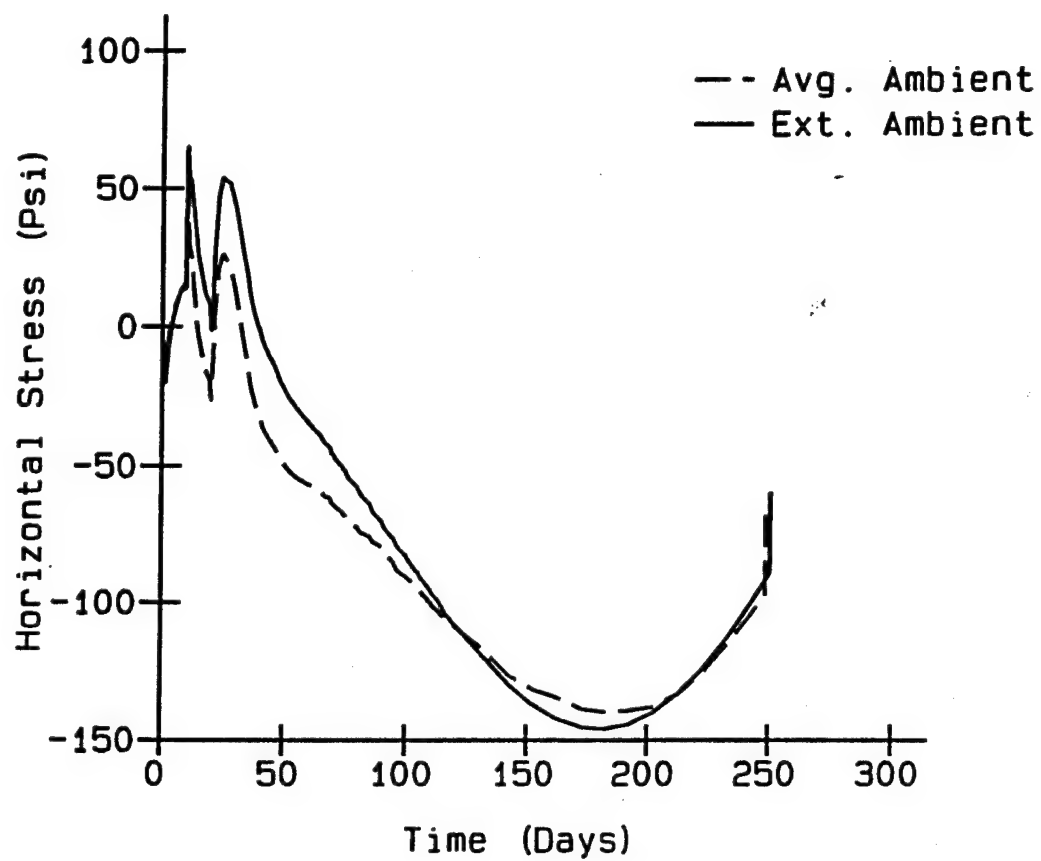
Figure 46. Time history of horizontal stress at integration point 3 of element 547
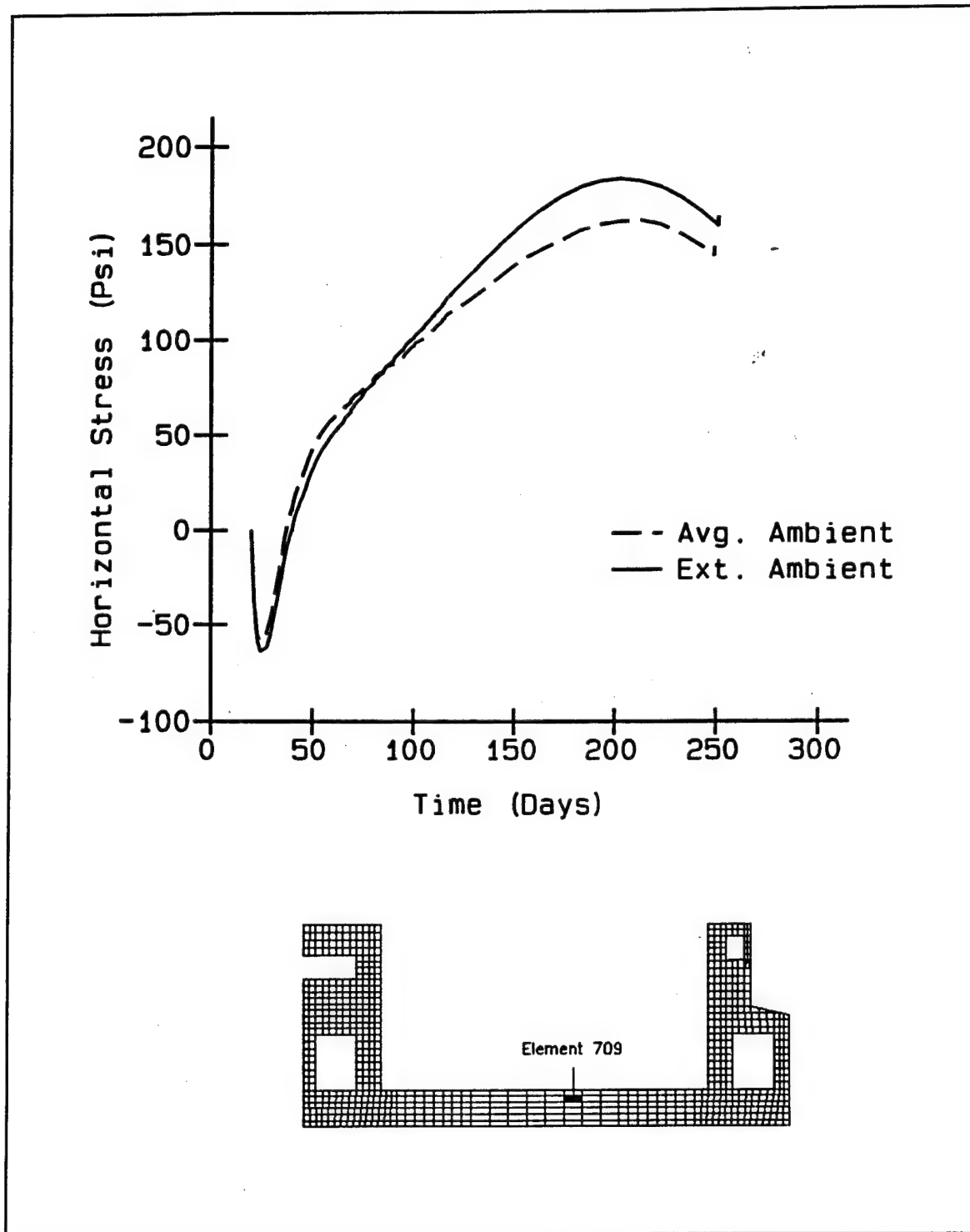
Figure 47.　　Time history of horizontal stress at integration point 1 of element 709
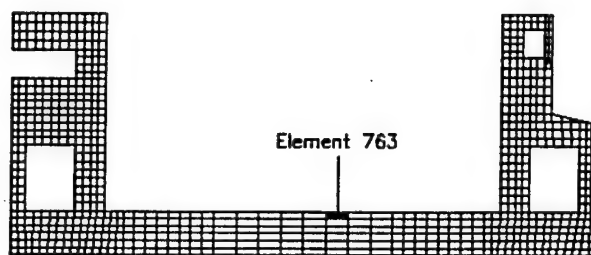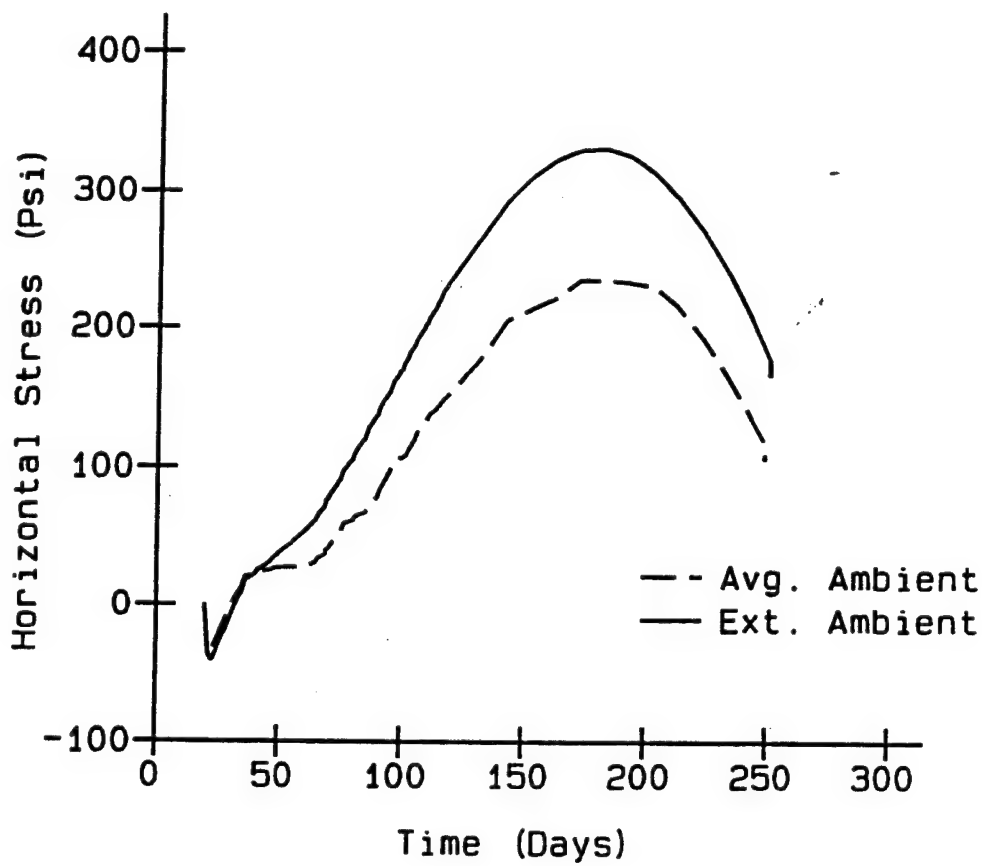
Figure 48.   Time history of horizontal stress at integration point 3 of element 763
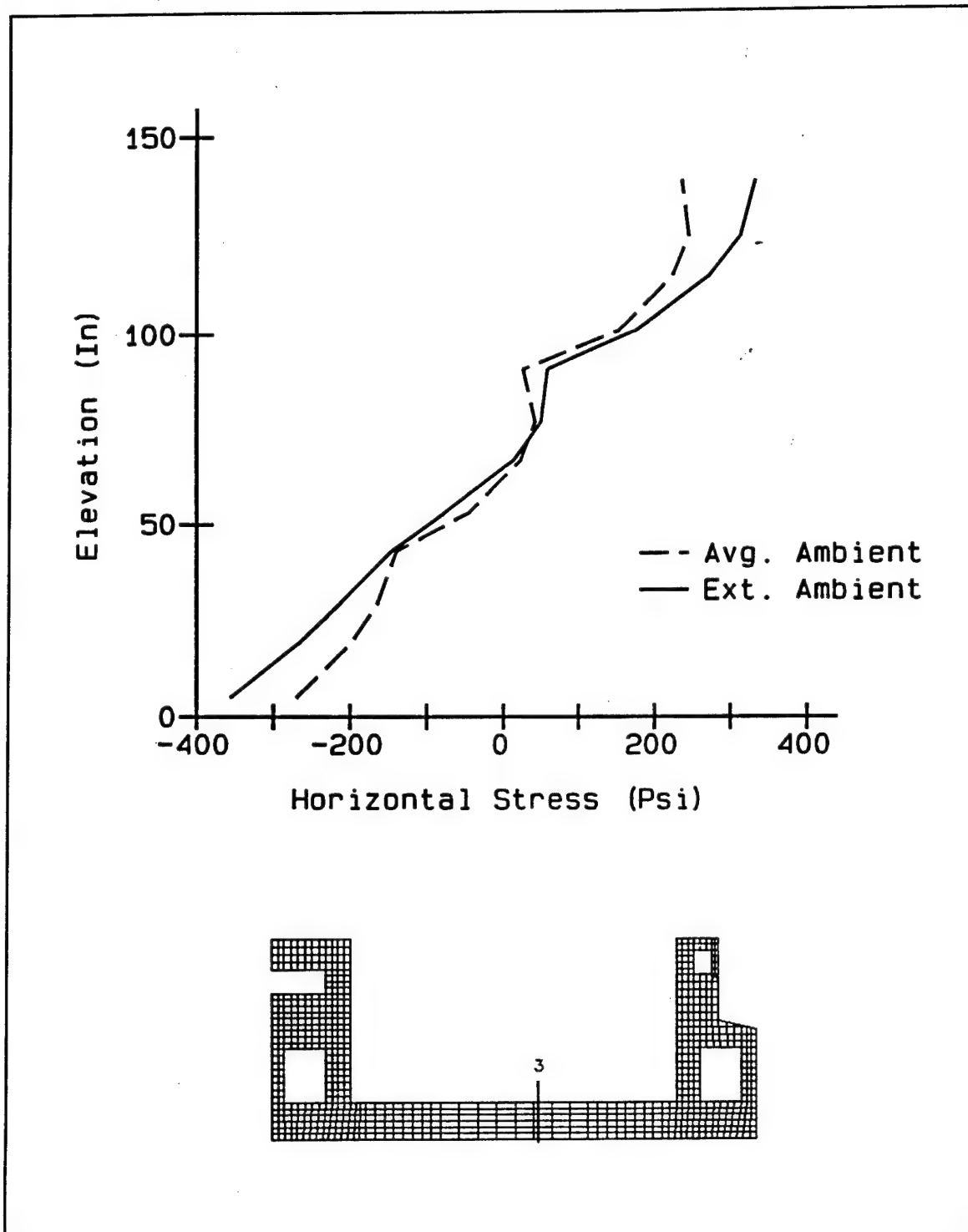
Figure 49.   Stress distribution at section near the center of the base slab at 172.5 days
after the start of construction
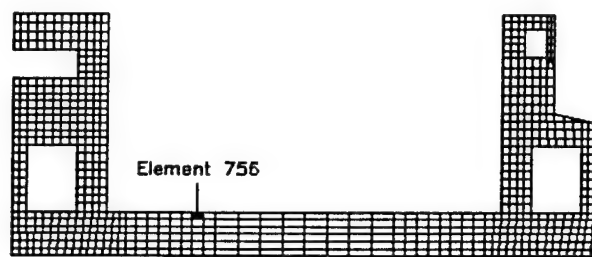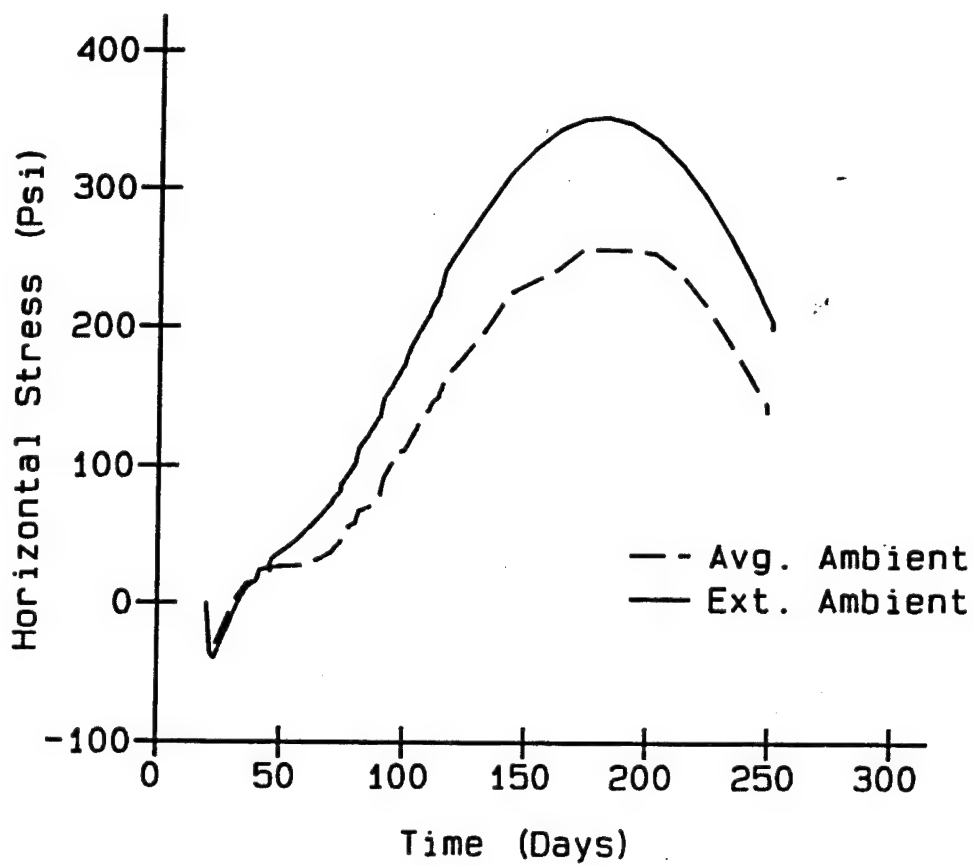
Figure 50. Time history of horizontal stress at integration point 3 of element 756
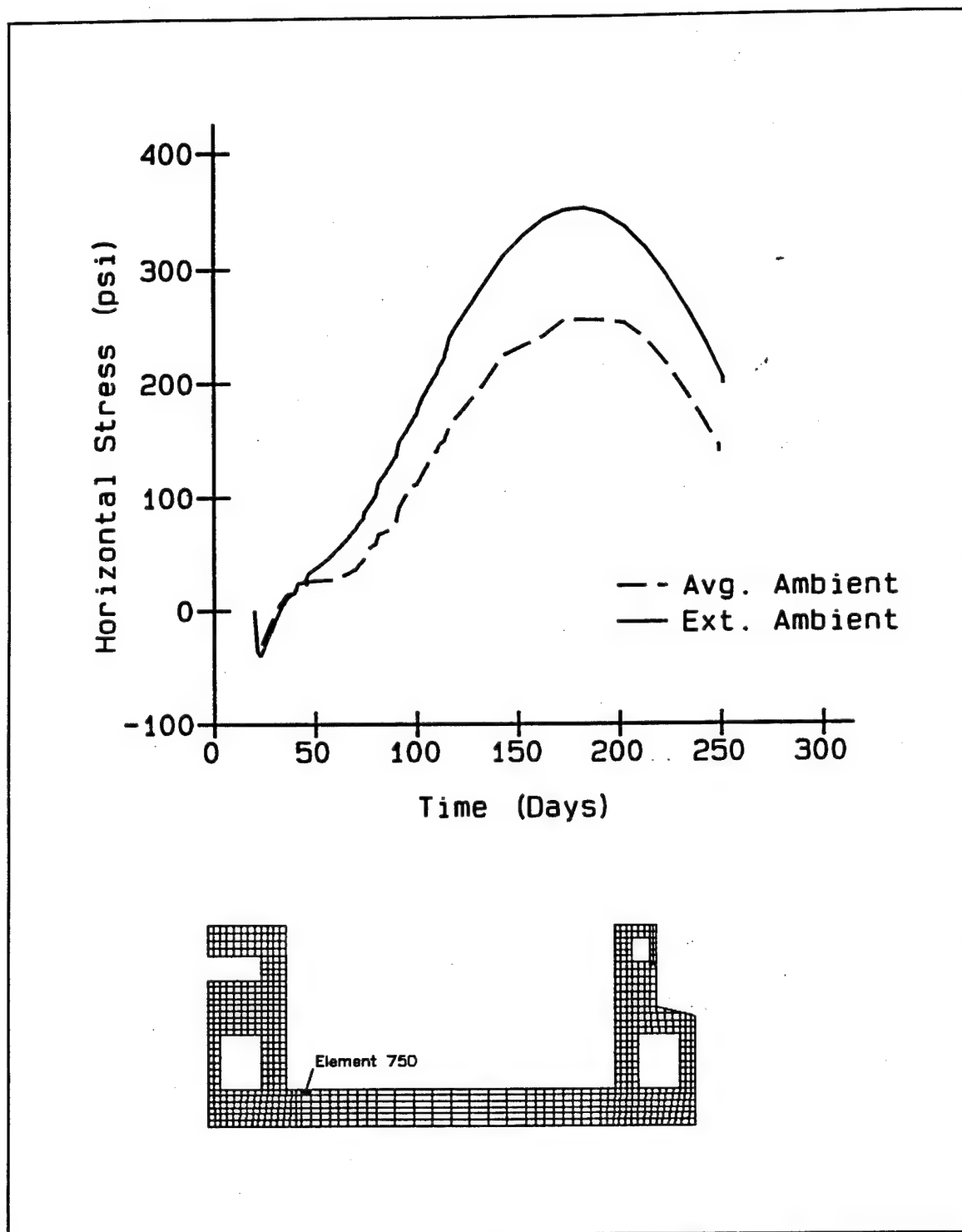
Figure 51.   Time history of horizontal stress at integration point 3 of element 750
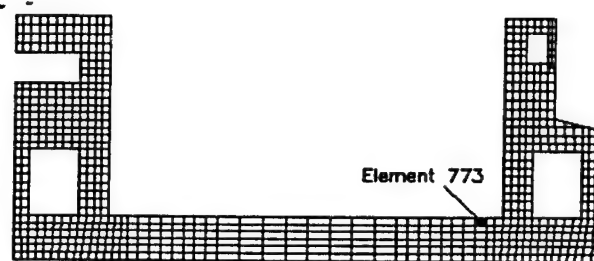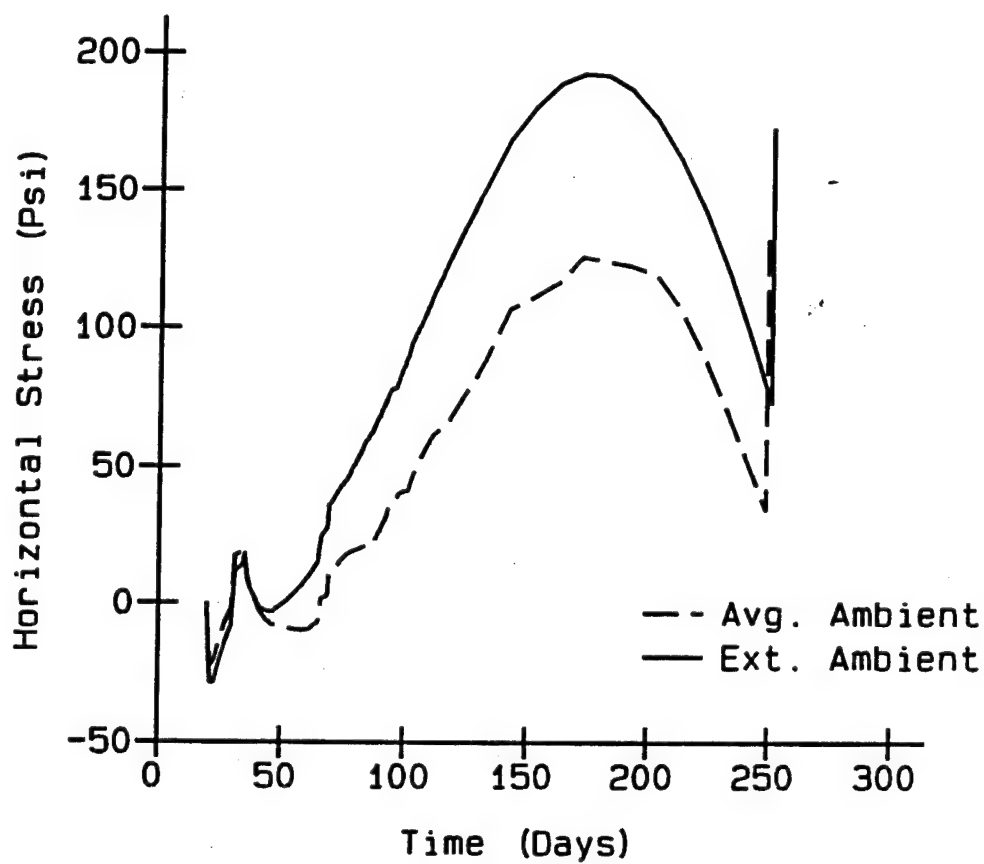
Figure 52.   Time history of horizontal stress at integration point 4 of element 773
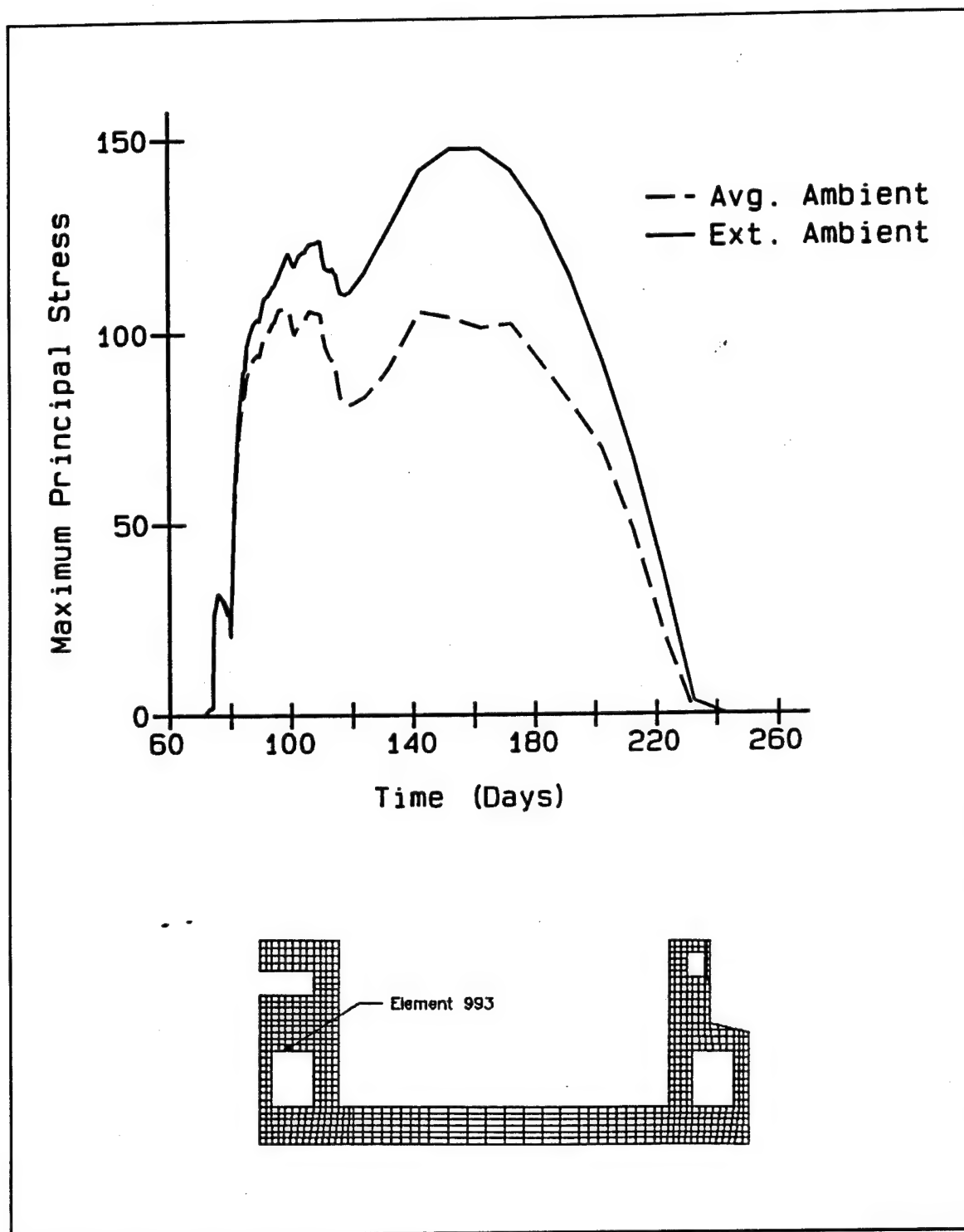
Figure 53.   Time history of maximum principal stress at integration point 2 of element 993
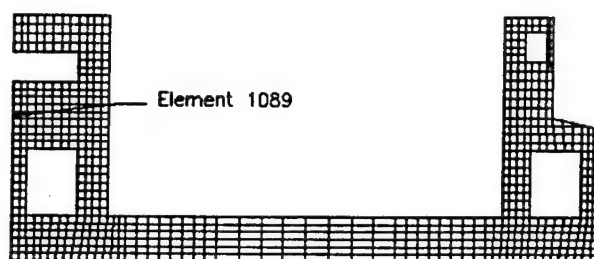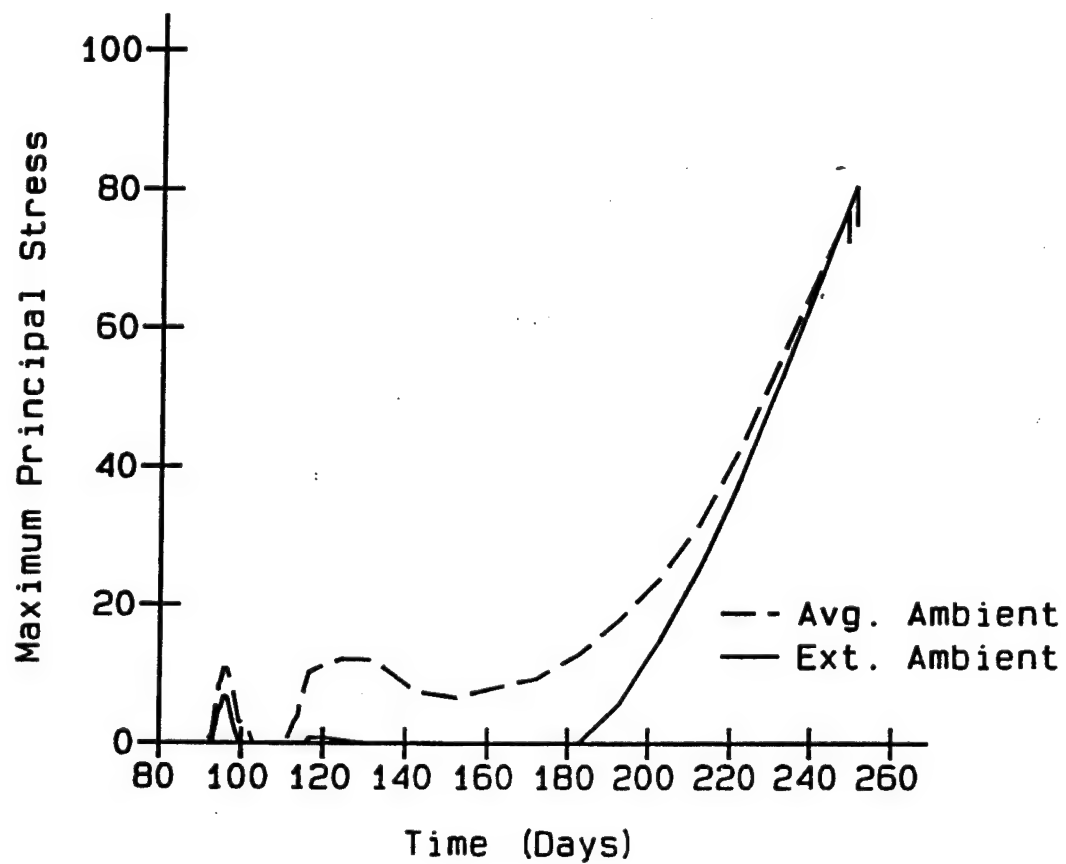
Figure 54.   Time history of maximum principal stress at integration point 2 of element 1089
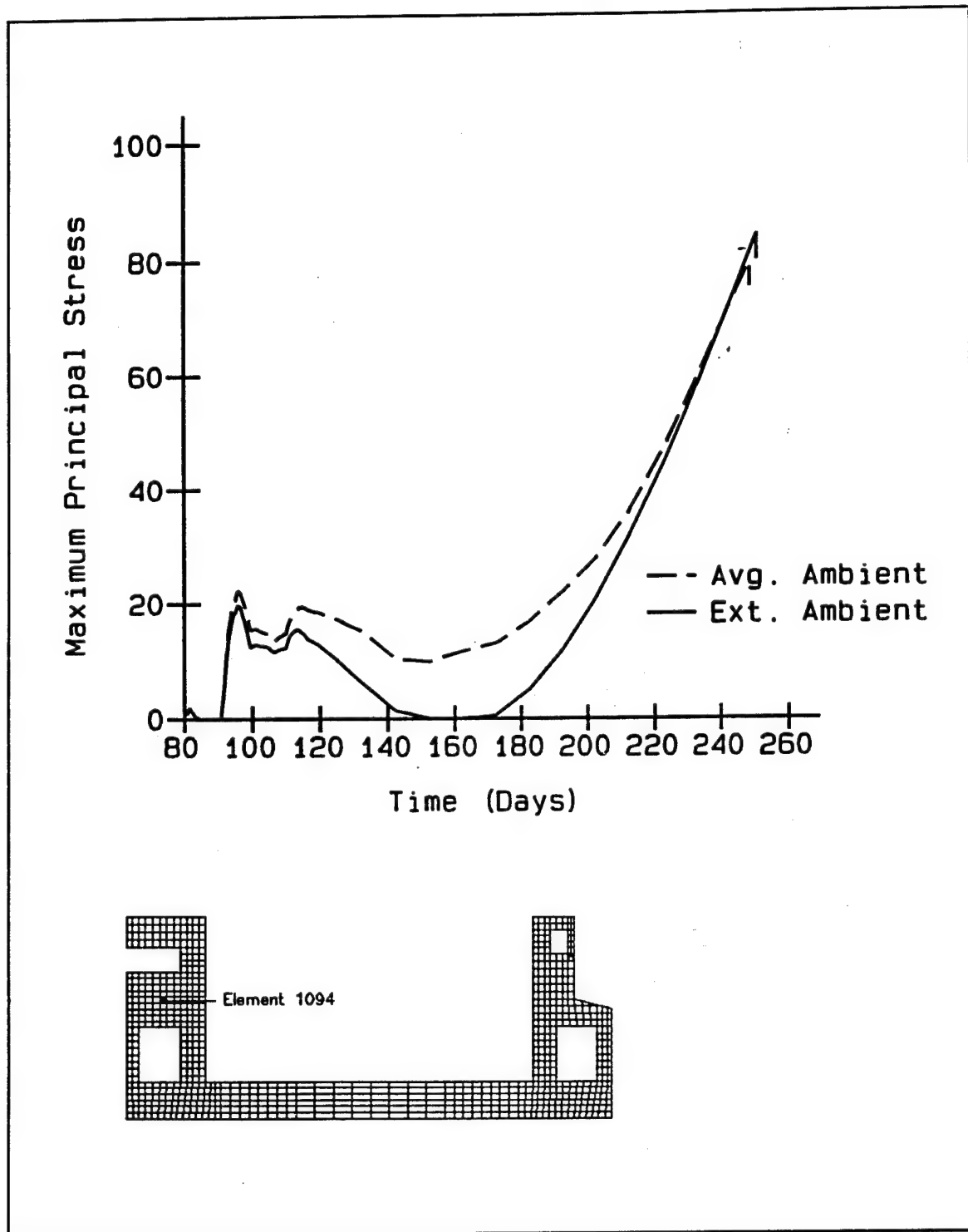
Figure 55.   Time history of maximum principal stress at integration point 1 of element 1094
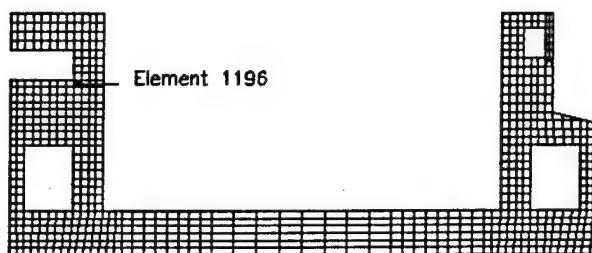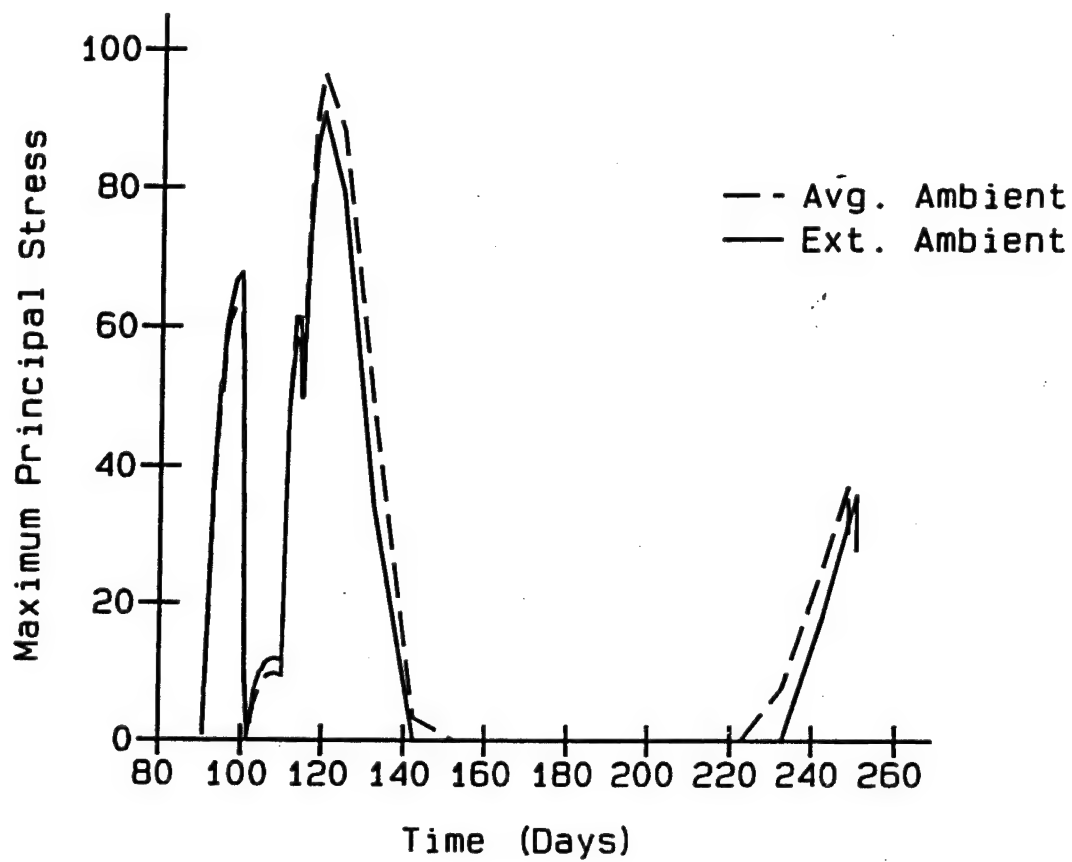
Figure 56.   Time history of maximum principal stress at integration point 4 of element 1196

Conclusions

Results from the slab and wall portions of the placement temperature study are well within the ETL allowable for stress, and no cracking occurred in the typical chamber monolith. For this geometry and concrete mixture, increased placement temperature all the way to extreme ambient conditions had no detrimental effect on structural integrity or performance.

5 Chamber Monolith Placement Temperature Study

Background

Two ways designers can lower project construction costs are through more efficient design or through better utilization of materials. In placing large volumes of mass concrete, much expense can be incurred in controlling the concrete placement temperature. Past experience has shown that cooler placement temperatures help mitigate thermal cracking caused by thermal gradients developed during curing. However, the cost to maintain sufficient temperature control can be expensive. Large monolith placements, like those in the chamber monoliths for Olmsted Locks and Dam, would require a nitrogen cooling system to maintain a 60 °F concrete temperature during summer placements. Allowing a higher placement temperature can lead to significant cost savings through the use of less expensive temperature control methods, i.e. ice, or through the elimination of cooling requirements.

Objective

The objective of this part of the study is to determine a maximum placement temperature that will reduce construction costs by relaxing or eliminating temperature control systems required to regulate concrete placement temperature while maintaining structural integrity and performance.

Analysis Parameters

General

For a given start time, results may not be critical in both the floor slab and wall portions of the W-frame section. In order to assess the impact of placement temperatures, one set of analyses with different placement temperatures and a single start time is inadequate. The study is therefore divided into a floor slab portion and a wall portion. Both portions use load case combination 5 and concrete material properties for mixture 11. Reasons for these selections are discussed in Chapter 1. Finite element meshes for both study portions utilize soil elements for the foundation in heat transfer analyses while replacing the foundation with equivalent springs representing the soil and supporting piles in the stress analyses. The mesh for the W-frame section is identical in both study portions and is similar to the grid used in previous phases (Garner et al. 1992) with the exception being the larger center wall gallery. The typical mesh along with lift designations is shown previously in Figure 2.

Ambient temperature

Initially the average ambient temperature used in previous NISA phases was to be used in the study. However, concern was raised about the possibility of experiencing an unusually warm year while using a high placement temperature. Higher ambient temperatures from an extreme year condition coupled with a high placement temperature may cause excessive thermal cracking in summer placed monoliths. It was determined that, for this objective, assuming an average year temperature was unconservative. All analyses in this study were conducted using the extreme average temperature curve described in Chapter 4. Figure 57 shows the extreme ambient temperature curve used in this study.

Lift interval

Analyses conducted in previous phases utilized a lift interval scheme devised for a 76-ft monolith. This massive size necessitated vertical construction joints in the floor slab. Since analyses were 2-dimensional, it was impossible for the construction lifts to coincide with model lifts. Even though lift intervals in the slab were at 5 days, the time required to account for the out-of-plane placements resulted in 10-day-lift intervals in the model floor slab. Based on recommendations from Phase I, the monolith length was reduced. This resulted in the elimination of the vertical lift joints and allowed the timing of the construction lifts to coincide with that for the model lifts. A lift interval of 5 days is used throughout the analyses in this study.
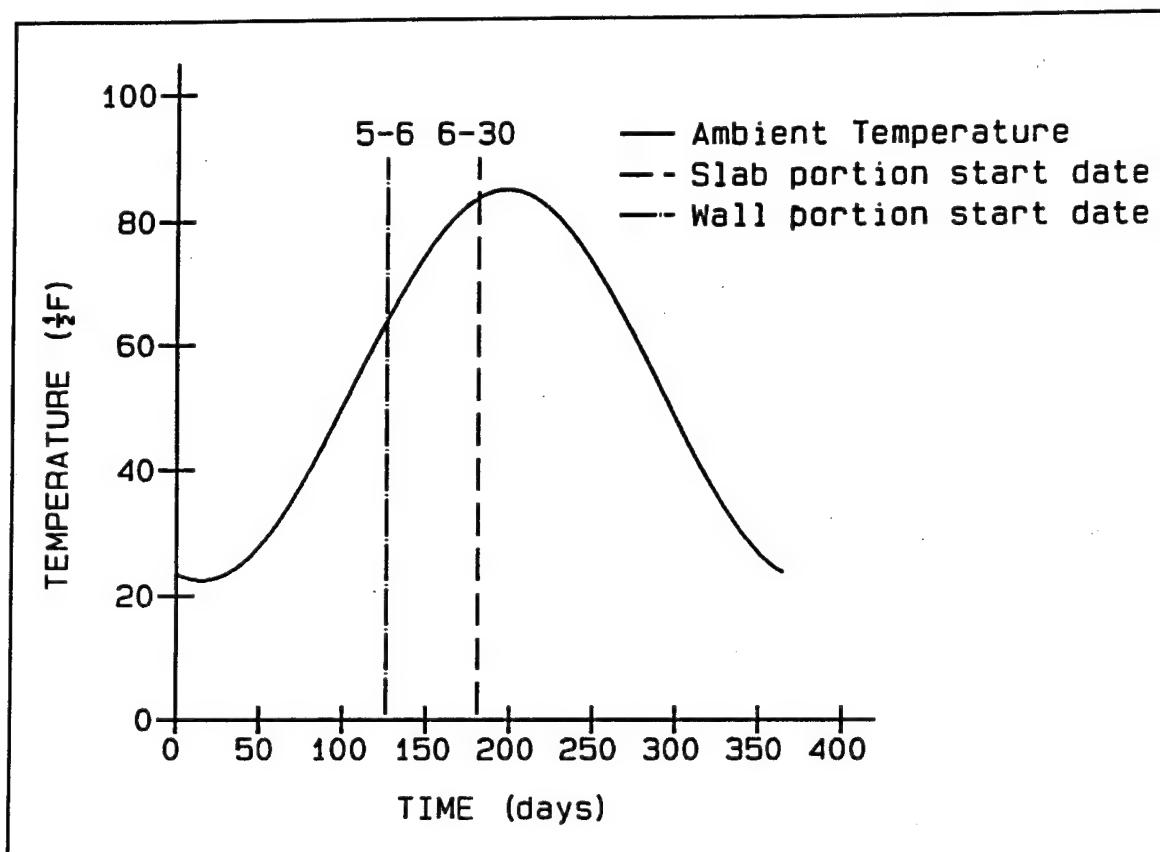
Figure 57.   Extreme ambient temperature with analysis start dates

Start date

For summer starts in previous NISA analyses, floor slab lift 3 was placed during the warmest day of the year and showed the highest tensile stress. If the same summer start date is kept, correcting the floor slab lift interval causes lift 3 to be placed earlier at a cooler ambient temperature. A new start date of Jun 30, previously it was Jun 20, was selected so that lift 3 in the slab study portion would be placed on the warmest day of the year. Lift 10 in the center wall is one of the more massive wall lifts. A start date of May 6 was selected for the wall study portion so lift 10 would be placed during the warmest day of the year.

Placement temperature

Typically, contract specifications, prepared by the Louisville District, place an upper bound of 60 °F for placement of mass concrete. For this reason, the 60 °F analyses are used as the baseline for comparison with other analyses. Average ambient conditions were selected as the upper limit of this study based on results reported in Garner, Hammons, and Bombich (1991). In this report the maximum placement temperature used in analyses was set at 85 °F. Figure 58 shows the 28-day moving average concrete placement along with the actual mean daily air temperature versus
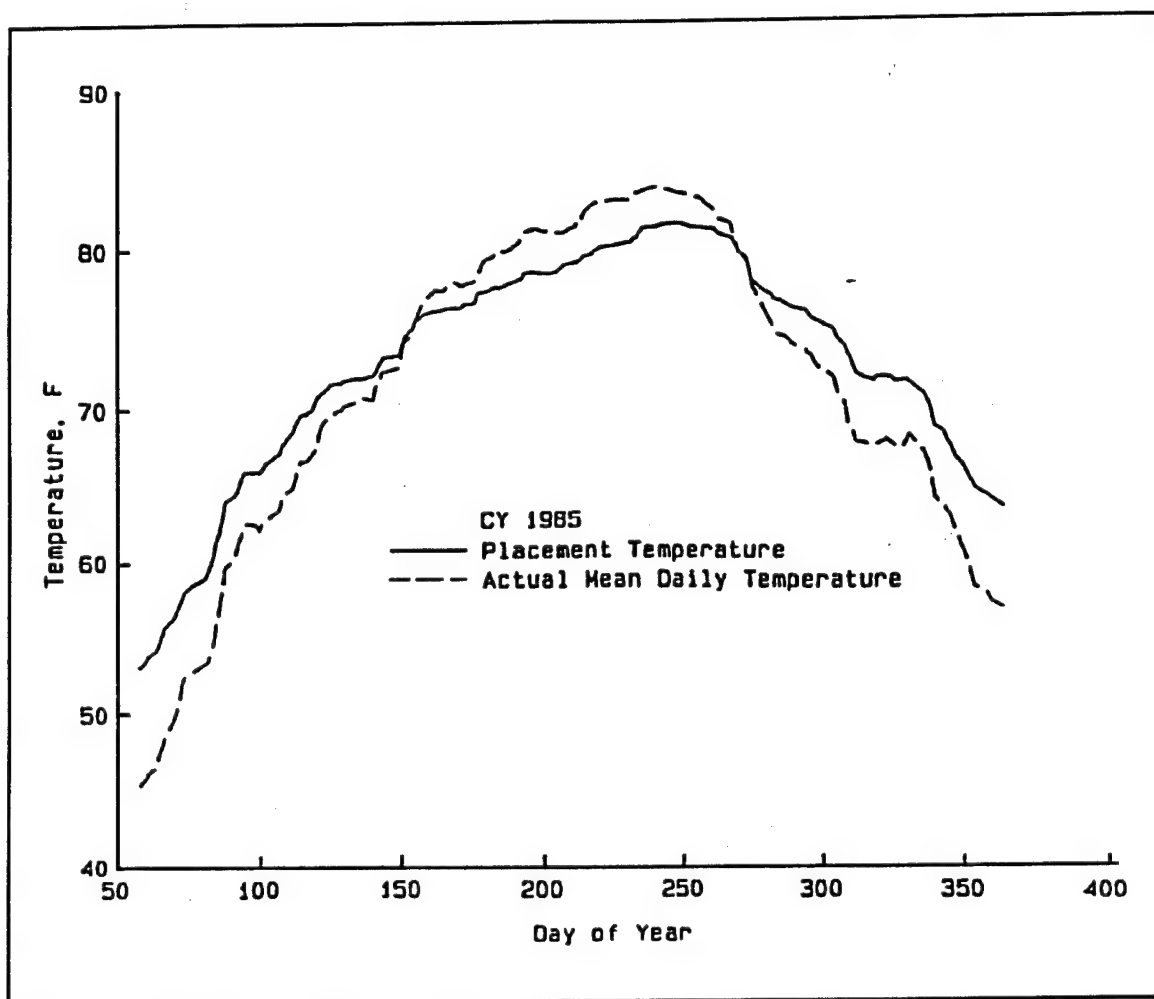
Figure 58.   Twenty-eight-day moving average concrete placement and mean daily air temperature

time at Overton Lock and Dam. The figure shows close correlation between placement temperature and mean daily temperature and further strengthened the decision to use the average ambient condition as an upper limit. Analyses based on 70 °F placement temperature were selected since ice could be added to maintain this temperature and to provide results at an intermediate state between 60 °F and extreme average ambient.

Stress-free temperature

The material model contained in the UMAT subroutine (see Chapter 1) requires the input of a stress-free reference temperature to use in the calculation of the strain. Based on temperature contour plots of the floor slab from Olmsted Phase I NISA, this temperature at 12 hr was estimated to be 6.6 °F higher than the placement temperature. Limitations required the use of one temperature for all nodes in a lift. For 60 °F the stress-free

temperature was 66.6 °F and was 76.6 °F for a 70 °F placement tempera-
ture. Problems arose in preliminary analyses for ambient placement due
to the fact that in many locations the concrete temperature never rose
above the stress-free temperature used to calculate strain. This caused er-
roneous strain computations and much concern about the correctness of
the solution process. UMAT was then modified so the stress-free tempera-
ture would automatically be selected as the temperature obtained from the
first step after lift initialization in the heat transfer analysis. This permit-
ted each point to have a different stress-free temperature and eliminated
the artificial constraint imposed by having elevated stress free temperatures.

Analyses

General

Results of analyses in the slab portion of the study are presented for
section 2 in the slab. Figure 59 shows the location of this section along
with adjacent nodes and elements. Stresses at locations near section 2
were maximum and general trends shown in section 2 results were also ex-
hibited in other locations in the slab. Temperature data are at the nodal
points and stress data are at the element integration points. Results of
analyses in the wall portion of the study are presented at locations of high
tensile stress and locations that better illustrate overall structural behavior.
All resultant data for each analysis were checked and only maximum val-
ues or results in areas of special interest are presented.

Slab study

Heat transfer analyses. Maximum temperatures for nodes near sec-
tion 2, shown in Table 17, show higher values for higher placement tem-
peratures with the maximums for each placement temperature occurring at
the node on the interface between lifts 2 and 3. However, these increases
are not identical to the temperature increase from higher placement tem-
peratures. This is due to more rapid heat loss observed for higher place-
ment temperature. The steeper slopes on the temperature time history
curves for higher placement temperatures shown in Figures 60-66 illustrate
this effect. Locations nearer the surface of the slab show greater influ-
ence from the ambient temperature than those locations further away from
the surface. However, these figures show the dependence of all locations
on the ambient temperature after the initial temperature rise due to hydration.

Stress analyses. Time varying temperature distributions calculated in
the heat transfer analyses for the three placement temperatures were used
as input for the stress analyses. All stresses were compared with the al-
lowable stress computed from ETL 1110-2-324. Tables 18-20 show the
maximum horizontal stresses from the analyses along with their computed
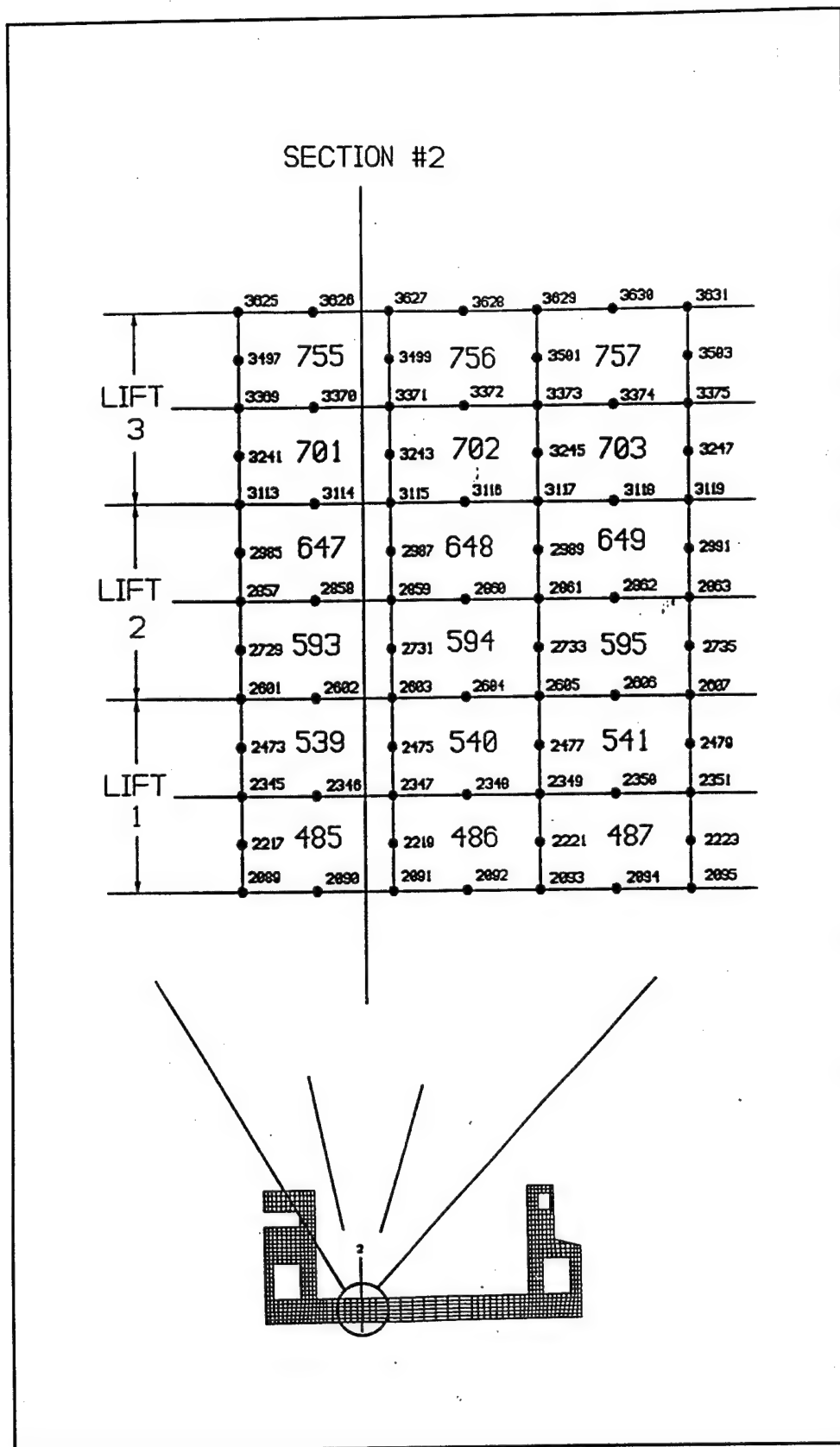
Figure 59.   Locations of presentation for results from slab analyses

Table 17
Nodal Maximum Temperatures

Node	Placement Temp., °F	Time, days	Max. Temp., °F
2091	60	27.0	85.57
	70	27.5	88.95
	Ambient	25.0	93.84
2347	60	15.0	90.89
	70	14.0	95.30
	Ambient	12.0	101.71
2603	60	16.0	95.19
	70	15.0	100.10
	Ambient	15.0	107.02
2859	60	20.0	98.21
	70	19.0	103.12
	Ambient	17.0	110.46
3115	60	19.0	99.65
	70	18.5	104.21
	Ambient	17.0	111.37
3371	60	18.0	97.30
	70	17.0	100.69
	Ambient	15.0	106.46
3627	60	16.0	87.70
	70	16.0	88.46
	Ambient	14.5	89.80
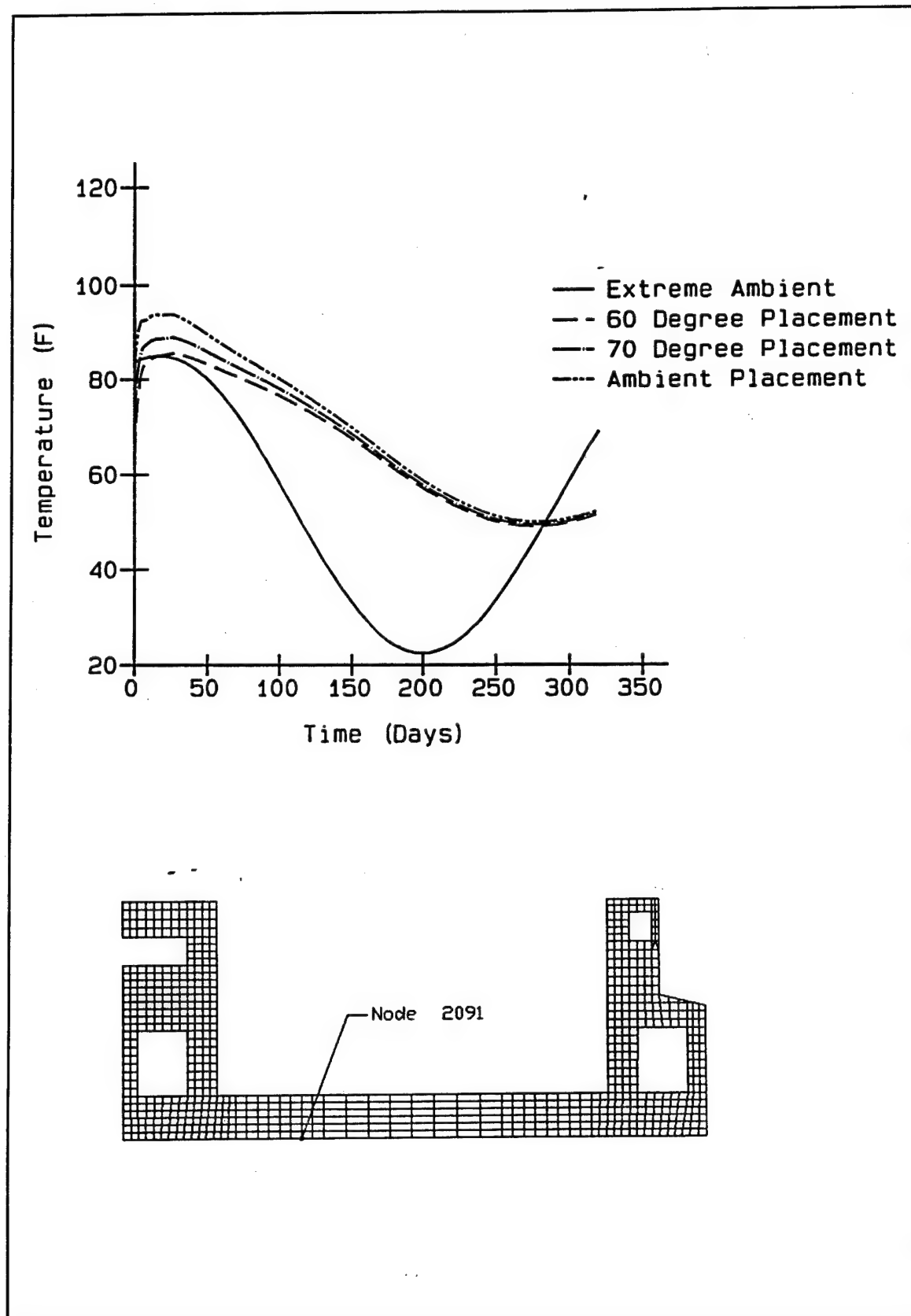
Figure 60.   Temperature time history for node 2091
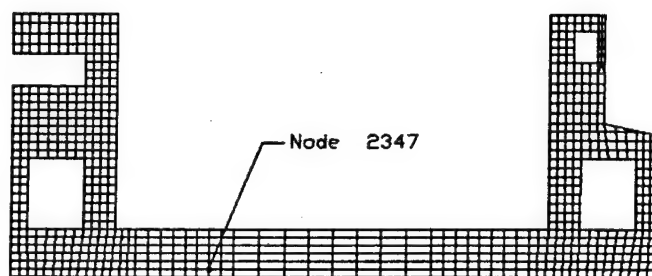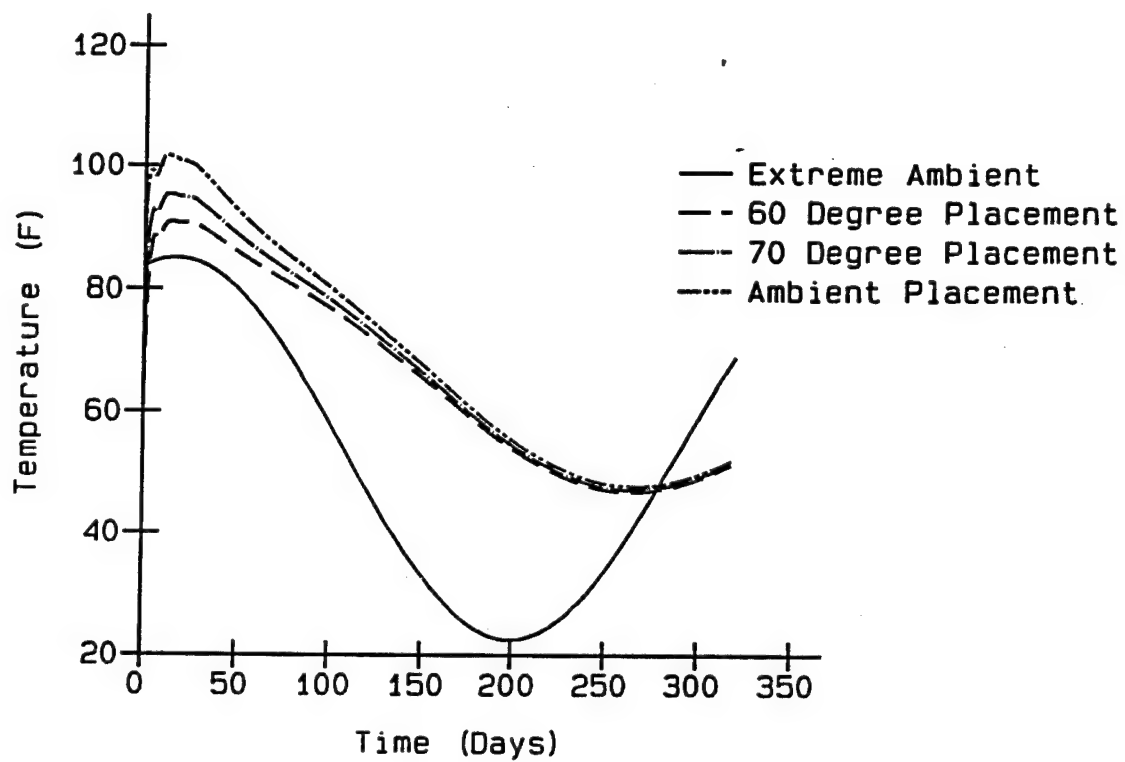
Figure 61.   Temperature time history for node 2347
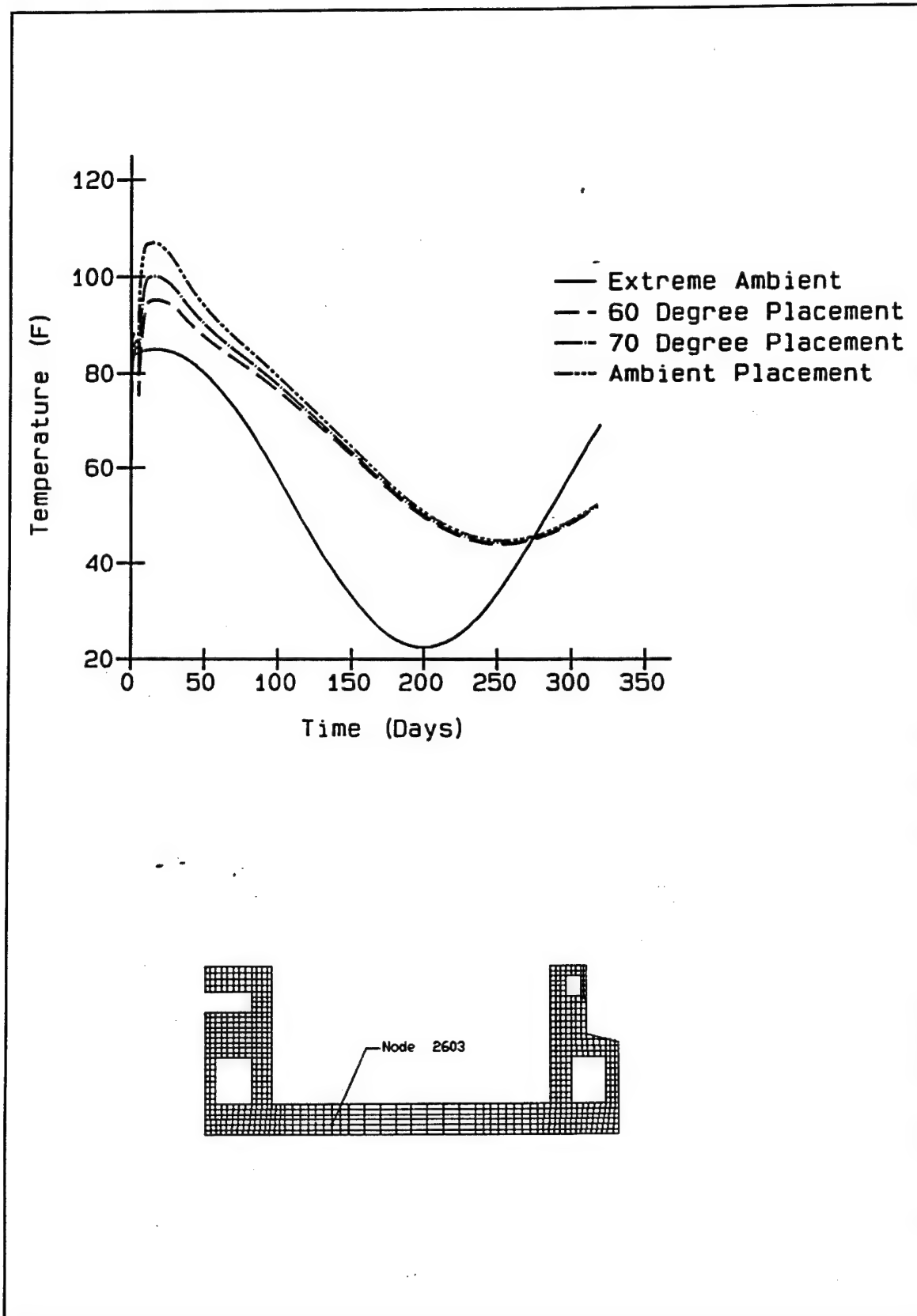
Figure 62.   Temperature time history for node 2603
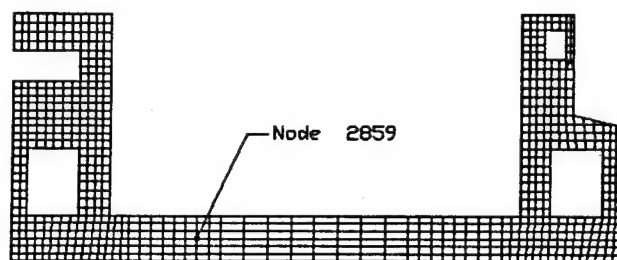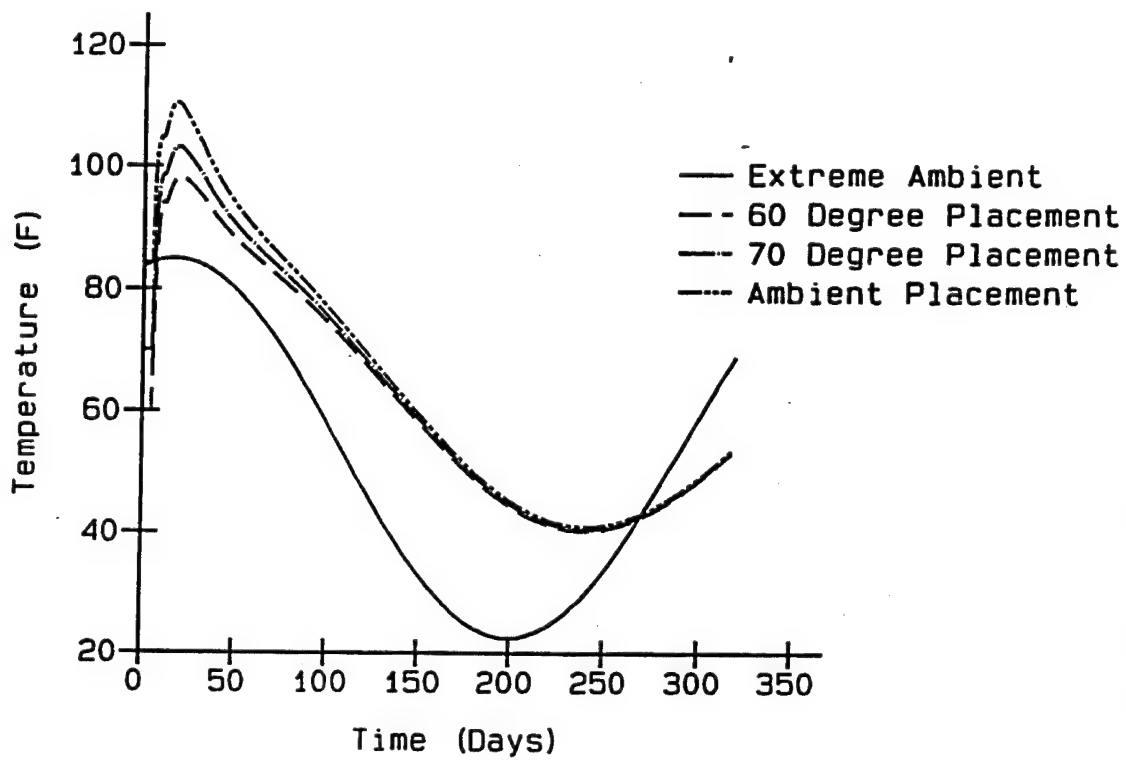
Figure 63.   Temperature time history for node 2859
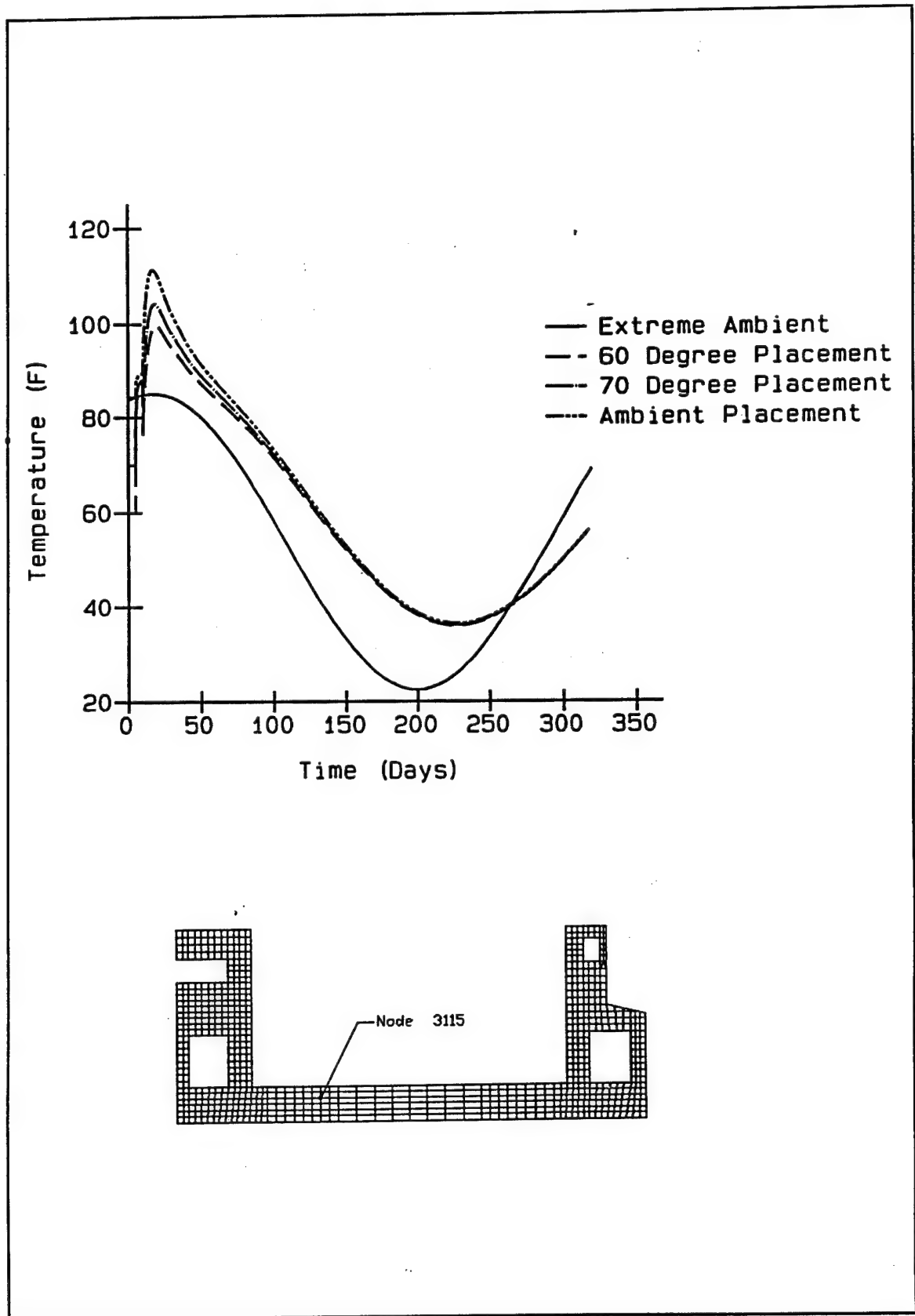
Figure 64.   Temperature time history for node 3115
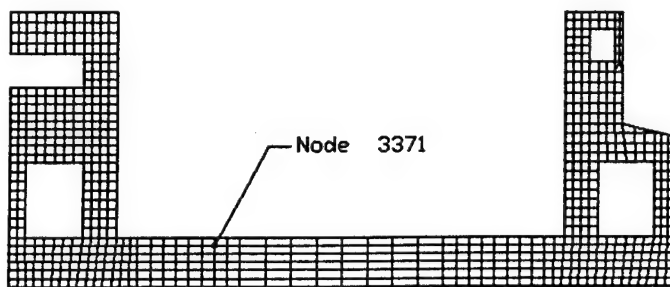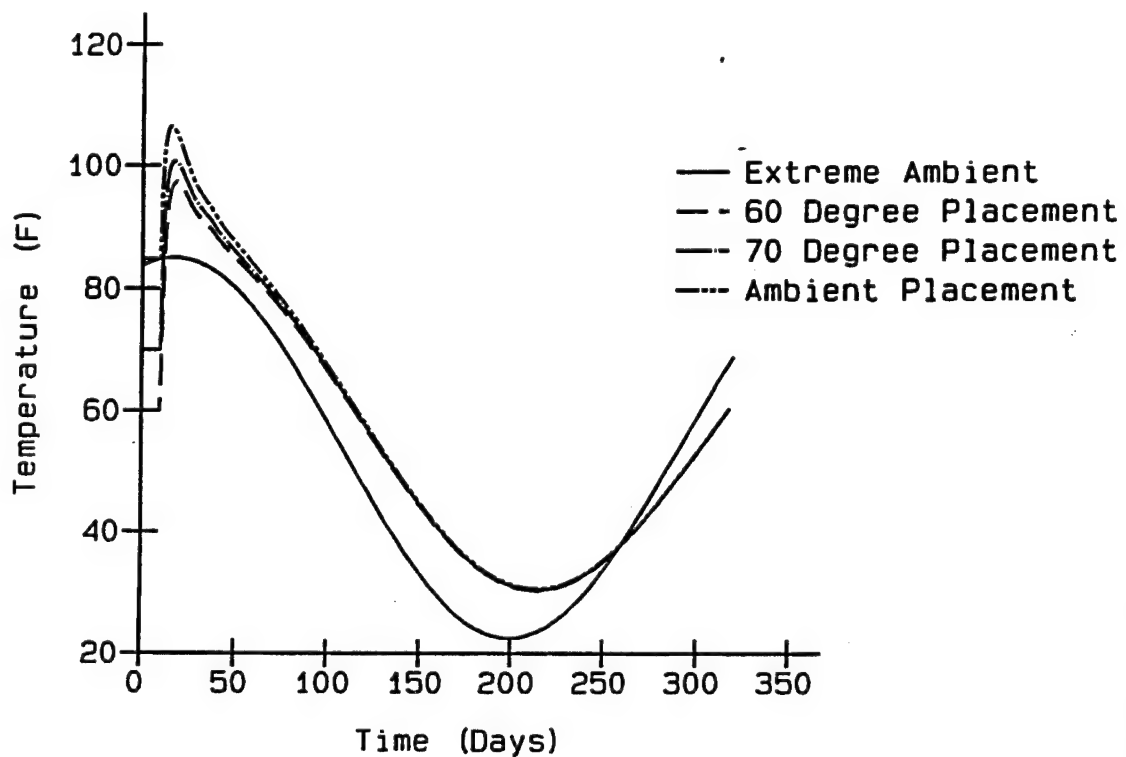
Figure 65.   Temperature time history for node 3371
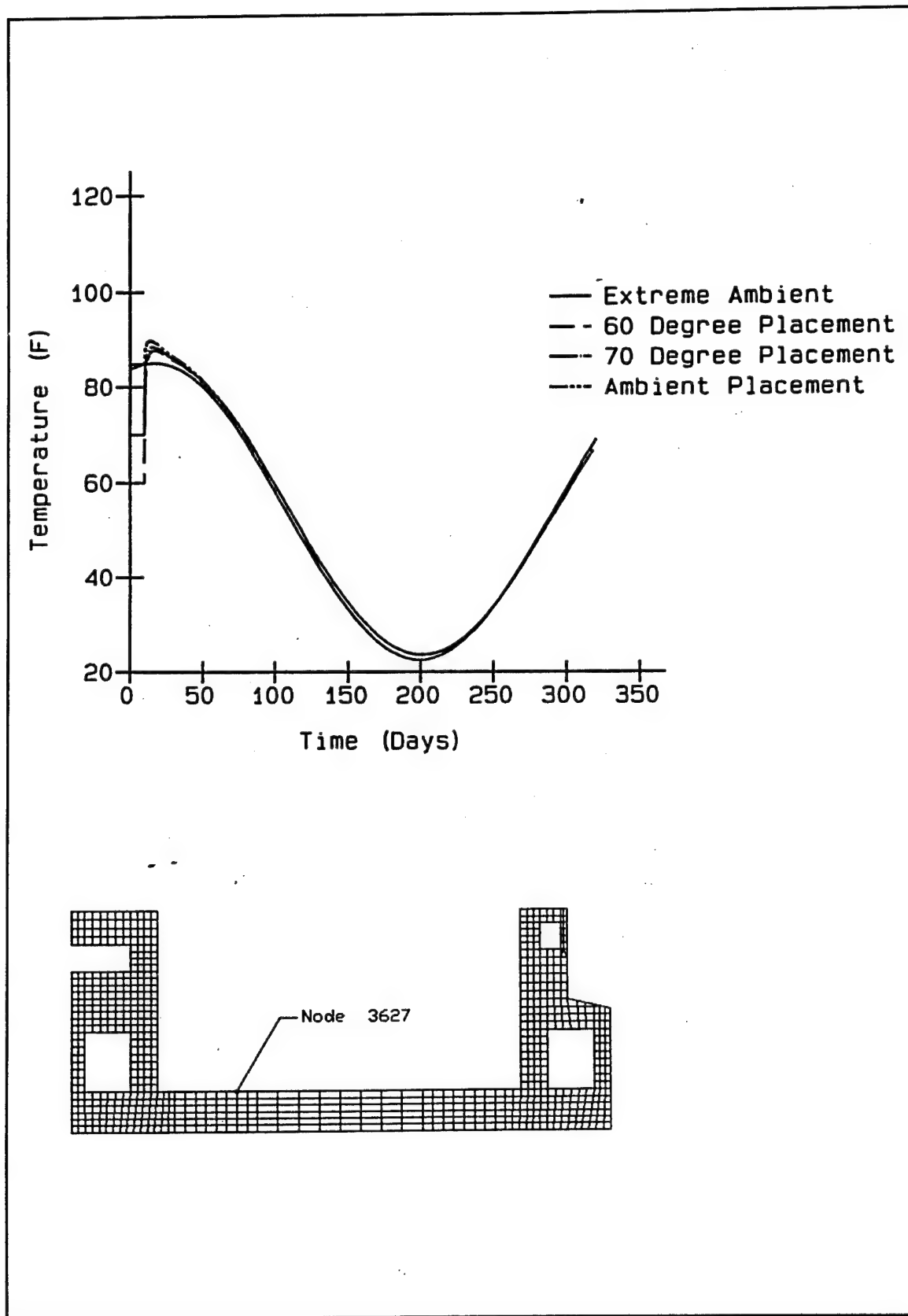
Figure 66.   Temperature time history for node 3627

Table 18
Maximum Floor Slab Stresses (psi) for 60 °F Placement

Element	IP	Day	Horiz. Stress	ETL Allowable	Percent Allowable
737	3	167.5	312.8	464.0	67.4
737	3	177.5	309.1	466.6	66.2
737	3	157.5	308.6	461.2	66.9
756	4	167.5	306.1	464.0	66.0
756	3	167.5	306.0	464.0	66.0
757	3	167.5	305.7	464.0	65.9
755	4	167.5	305.6	464.0	65.9
757	4	167.5	305.0	464.0	65.7
755	3	167.5	304.5	464.0	65.6
756	3	177.5	304.4	466.6	65.2
756	4	177.5	304.3	466.6	65.2
755	4	177.5	304.1	466.6	65.2
757	3	177.5	303.9	466.6	65.1
758	3	167.5	303.7	464.0	65.5
754	4	167.5	303.1	464.0	65.3
755	3	177.5	303.1	466.6	65.0
757	4	177.5	303.1	466.6	65.0
754	4	177.5	301.8	466.6	64.7
758	3	177.5	301.7	466.6	64.7
758	4	167.5	300.8	464.0	64.8

Table 19
Maximum Floor Slab Stresses (psi) for 70 °F Placement

Element	IP	Day	Horiz. Stress	ETL Allowable	Percent Allowable
755	4	167.5	280.3	464.0	60.4
756	3	167.5	280.3	464.0	60.4
756	4	167.5	279.9	464.0	60.3
755	3	167.5	279.8	464.0	60.3
757	3	167.5	279.2	464.0	60.2
754	4	167.5	278.9	464.0	60.1
755	4	177.5	278.6	466.6	59.7
756	3	177.5	278.5	466.6	59.7
755	3	177.5	278.1	466.6	59.6
757	4	167.5	278.0	464.0	59.9
756	4	177.5	277.9	466.6	59.6
754	4	177.5	277.3	466.6	59.4
757	3	177.5	277.2	466.6	59.4
754	3	167.5	276.8	464.0	59.7
758	3	167.5	276.4	464.0	59.6
757	4	177.5	275.9	466.6	59.1
754	3	177.5	275.4	466.6	59.0
756	3	157.5	275.2	461.2	59.7
755	4	157.5	275.2	461.2	59.7
756	4	157.5	274.9	461.2	59.6

Table 20
Maximum Floor Slab Stresses (psi) for Ambient Placement

Element	IP	Day	Horiz. Stress	ETL Allowable	Percent Allowable
755	2	177.5	274.7	466.6	58.9
755	1	177.5	274.6	466.6	58.8
756	1	177.5	274.4	466.6	58.8
754	2	177.5	274.1	466.6	58.7
756	2	177.5	273.7	466.6	58.7
757	1	177.5	273.0	466.6	58.5
754	1	177.5	273.0	466.6	58.5
755	2	167.5	272.5	464.0	58.7
756	1	167.5	272.4	464.0	58.7
755	1	167.5	272.3	464.0	58.7
754	2	167.5	271.8	464.0	58.6
757	2	177.5	271.8	466.6	58.3
756	2	167.5	271.8	464.0	58.6
753	2	177.5	271.6	466.6	58.2
757	1	167.5	271.1	464.0	58.4
754	1	167.5	270.6	464.0	58.3
755	1	187.5	270.5	469.0	57.7
755	2	187.5	270.5	469.0	57.7
758	1	177.5	270.3	466.6	57.9
756	1	187.5	270.2	469.0	57.6

percentage of the ETL allowable stress. No cracking occurred in any of the analyses for this portion on the NISA.

Maximum stress results presented in Tables 18-20 show the maximum stresses and their locations in the floor slab. These tables show that maximum stress decreases as the placement temperature increases. The 60 °F placement analysis shows the maximum stress occurring near the interior corner of the center wall culvert at the integration points nearest the top of the slab. The 70 °F placement analysis shows lower maximum stresses near section 2 and occurring at the integration points closest to the top of the slab. The ambient placement analysis also shows lower maximum stresses near section 2 occurring at the lower integration points in the top element in the model of the floor slab. This reduction and shift in location of the maximum stress can more readily be seen in the stress distribution plot along section 2 shown in Figure 67. Conventional understanding of the behavior of mass concrete dictates that higher tensile stress would be expected at the surface instead of the reduction shown in the stress distribution plot. This phenomenon is more readily explained with the use of stress time history curves for the upper integration point of the top element shown in Figures 68 and 69. Conventional understanding of mass concrete only encompasses the temperature and stresses that result from the initial heat of hydration. The results of concern occur at day 177.5 of the analysis. The driving force at this time is the ambient temperature, not the heat of hydration. During the time driven by the heat of hydration, day 10 to day 25 shown in Figure 69, the results mirror conventional understanding of mass concrete. That is, the higher the placement temperature the higher the tensile stress at the surface. Days 25 to 35 show results that are transitional between hydration driven and ambient driven. In this region creep is relieving the higher tensile stresses of the ambient placement more than those for the 70 °F analysis and the higher 70 °F placement tensile stresses more than those for the 60 °F placement analysis. This results in a steeper declining stress gradient for the ambient placement stress than the 70 °F stress and a steeper declining gradient for the 70 °F stress than the 60 °F stress. After day 35 the ambient air temperature is driving the results. Due to the lesser slope on the stress gradient in the transitional time range, the stress gradient for the 60 °F results was more quickly returned to an increasing tensile gradient by the ambient air temperature load than the 70 °F and ambient placement results. This resulted in higher tensile values at the integration point nearest the surface of the floor for the 60 °F placement temperature stress and lower tensile values for the ambient placement temperature stress. However, higher tensile stresses were predicted for the ambient placement than those for the 70 °F placement and higher 70 °F tensile stresses than those for the 60 °F in the interior of the lift away from the surface. Figure 70 shows the stress time history for element 755, integration point 2, that confirms higher interior stresses occur with higher placement temperatures. This also conforms to conventional understanding of how mass concrete behaves. Vertical sections taken at other locations in the slab exhibit similar tendencies.
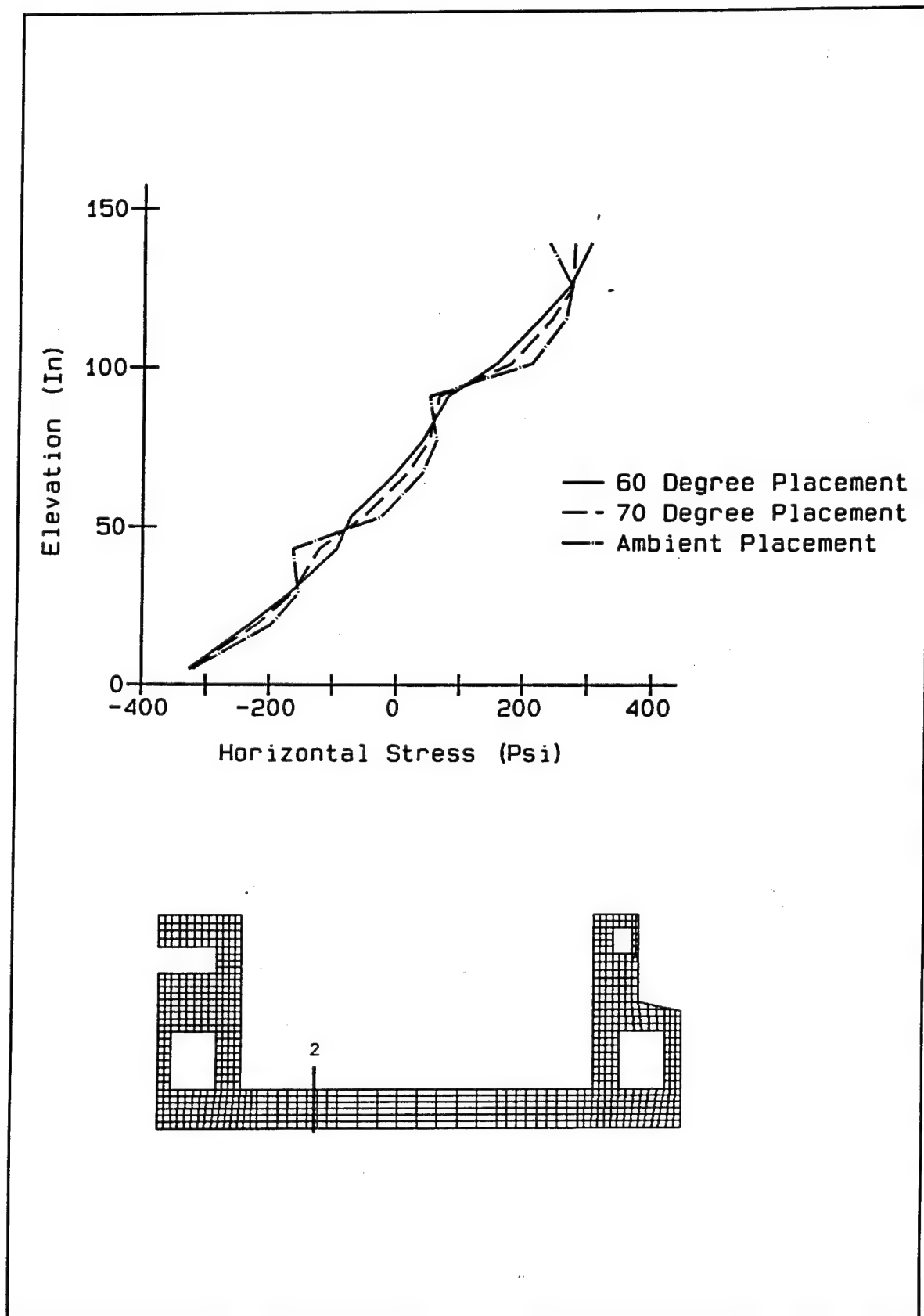
Figure 67.　Stress distribution at day 177.5 for section 2
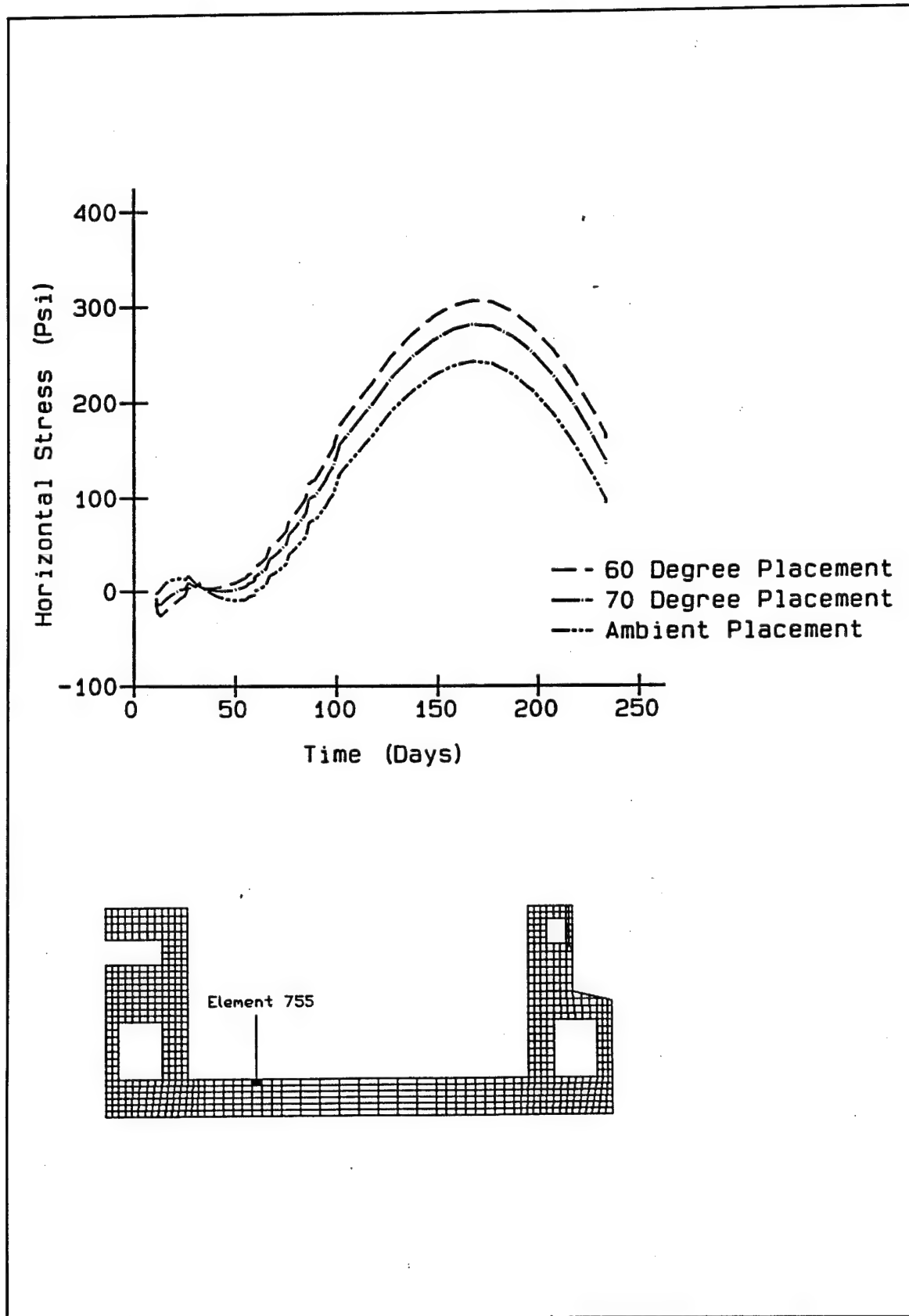
Figure 68.   Stress time history for element 755, integration point 4
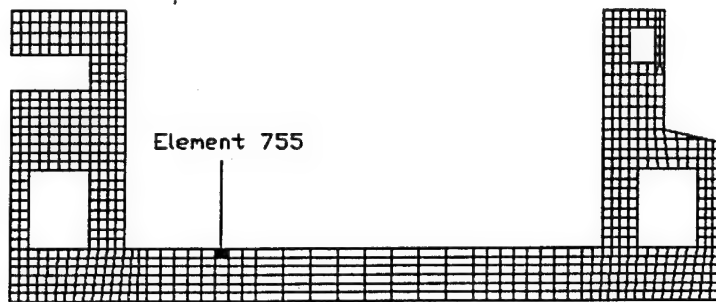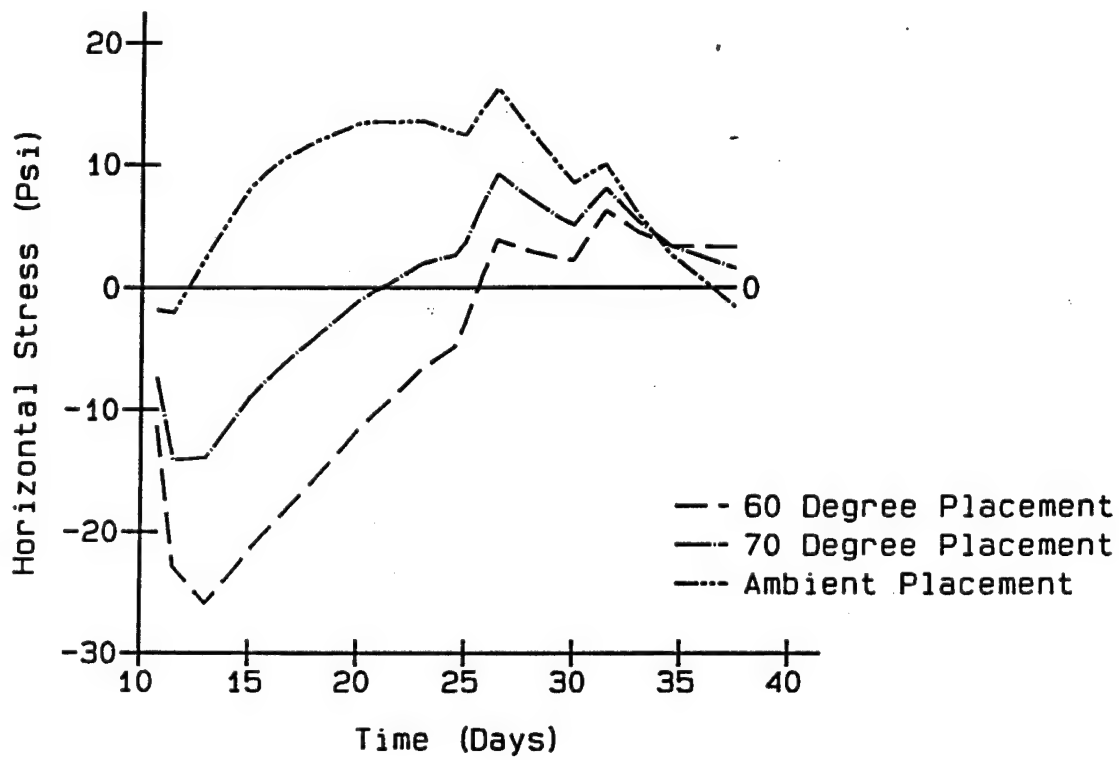
Figure 69.   Enlargement of stress time history for element 755, integration point 4
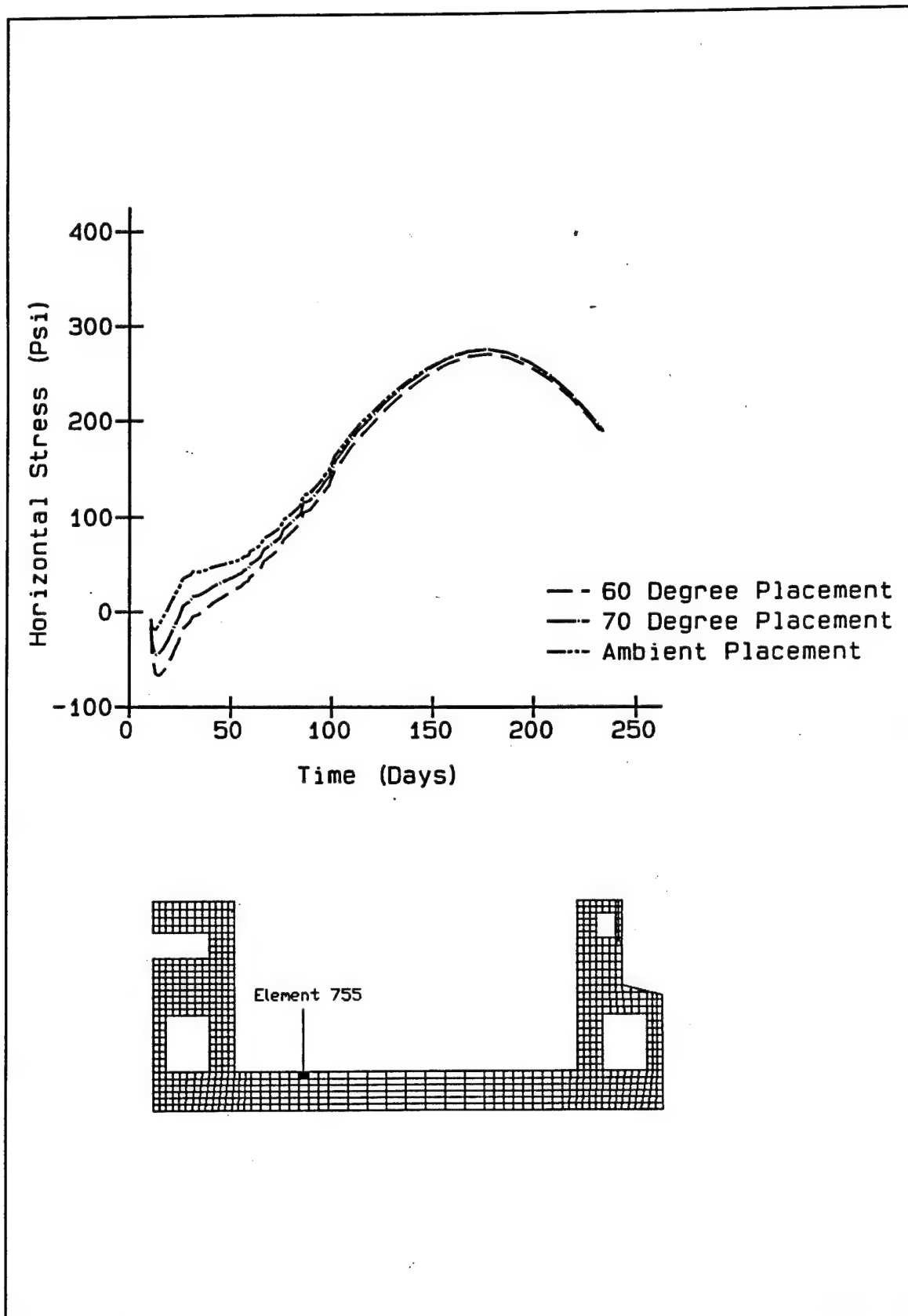
Figure 70.   Stress time history for element 755, integration point 2

Wall study

Stress analyses. Time varying temperature distributions calculated in the heat transfer analyses for the three placement temperatures were used as input for the stress analyses. All stresses were compared with the allowable stress computed from ETL 1110-2-324. Tables 21-23 show the maximum principal stresses from the analyses along with their computed percentage of the ETL allowable stress. For locations like the lock walls where stress in one direction is not predominate, maximum principal stresses are more appropriate from which to draw conclusions. Figure 71 shows the location of these maxima.

Table 21					
Maximum Wall Principal Stresses (psi) for 60 °F Placement					
Element	IP	Day	Stress	ETL Allowable	Percent Allowable
801	1	233.5	250.1	476.4	52.5
991	1	207.5	249.0	462.6	53.8
991	1	197.5	247.6	459.7	53.9
800	2	233.5	243.8	475.5	51.3
991	1	217.5	240.8	465.3	51.8
991	1	187.5	239.0	456.6	52.3
790	2	233.5	237.7	474.5	50.1
991	2	207.5	229.4	462.6	49.6
991	2	197.5	227.6	459.7	49.5
991	1	227.5	225.3	467.8	48.2
991	2	217.5	223.4	465.3	48.0
992	1	207.5	221.8	462.6	47.9
992	1	197.5	220.1	459.7	47.9
991	2	187.5	220.0	456.6	48.2
991	1	177.5	217.6	453.1	48.0
992	1	217.5	216.2	465.3	46.5
992	2	207.5	216.0	462.6	46.7
992	2	197.5	214.5	459.7	46.7
993	1	207.5	214.1	462.6	46.3
992	1	187.5	213.1	456.6	46.7

Table 22
Maximum Wall Principal Stresses (psi) for 70 °F Placement

Element	IP	Day	Stress	ETL Allowable	Percent Allowable
800	2	233.5	272.6	475.5	57.3
801	1	233.5	252.5	476.4	53.0
790	2	233.5	215.5	474.5	45.4
991	1	207.5	200.5	462.6	43.3
991	1	197.5	200.1 .	459.7	43.5
991	2	207.5	197.3	462.6	42.7
991	2	197.5	196.5	459.7	42.7
992	1	207.5	194.9	462.6	42.1
992	1	197.5	194.1	459.7	42.2
992	2	207.5	193.5	462.6	41.8
992	2	197.5	192.9	459.7	42.0
993	1	207.5	192.8	462.6	41.7
991	1	187.5	192.8	456.6	42.2
993	1	197.5	192.4	459.7	41.8
991	1	217.5	191.6	465.3	41.2
790	2	217.5	191.0	471.2	40.5
790	2	227.5	191.0	473.3	40.3
991	2	217.5	190.5	465.3	40.9
991	2	187.5	189.9	456.6	41.6
993	2	207.5	189.8	462.6	41.0

The maximum principal stresses shown in Tables 21-23 are less than stresses in the slab shown in Tables 18-20 except for the location of stress concentration where the center wall intersects the floor slab for ambient placement conditions. Figure 72 shows, that for this location, the maximum principal stress occurs when the service loads are applied. The slab deflects more under the walls than in the center which results in larger tensile forces at the corner. No compressive (negative) stress is shown on maximum principal stress plots since by definition they are zero or tensile (positive).

Table 23
Maximum Wall Principal Stresses (psi) for Ambient Placement

Element	IP	Day	Stress	ETL Allowable	Percent Allowable
800	2	233.5	313.4	475.5	65.9
801	1	233.5	258.9	476.4	54.3
800	2	227.5	200.3	474.3	42.2
800	2	233.5	200.2	475.5	42.1
800	1	233.5	197.7	475.5	41.6
800	2	217.5	194.3	472.3	41.1
790	2	233.5	185.0	474.5	39.0
800	2	207.5	183.2	470.1	39.0
1314	3	227.5	178.5	456.6	39.1
1314	3	217.5	178.5	453.1	39.4
1314	3	223.5	177.9	458.5	38.8
1314	3	233.5	177.7	458.5	38.7
1314	3	207.5	176.9	449.3	39.4
799	2	233.5	176.2	475.5	37.1
1314	3	197.5	173.7	445.1	39.0
1314	3	187.5	168.8	440.3	38.3
800	2	197.5	165.8	467.8	35.4
1314	4	233.5	163.9	458.5	35.8
1314	4	227.5	163.8	456.6	35.9
1314	4	233.5	163.7	458.5	35.7

Figure 73 shows principal stress time history at a location not near a stress concentration. The location, at the center of the upper gallery in the center wall, is one expected to be of significance. The higher stress at a more interior integration point rather than one closer to the surface is due to the same surface effects explained in the stress analyses section for the slab portion. Higher stresses for the extreme ambient, reverse of the trend shown at a free surface in the slab, are due to less restraint being provided by the gallery wall as compared to the restraint provided lift 3 by lift 2. Figures 74 and 75 are horizontal stress time histories for element 1314, integration point 2, and for element 1389, integration point 3. These locations are along a vertical section through the roof of the gallery nearest
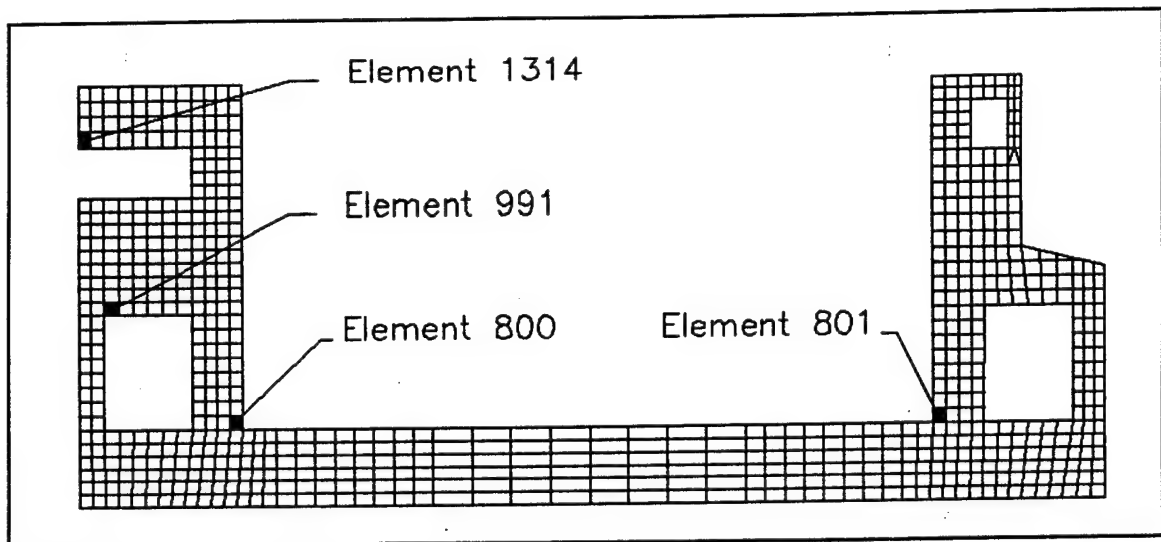
Figure 71.   Locations of maximum principal stress in the lock walls

the centerline of the model. As the extreme ambient temperature cools, compression forms at the top of the section and tension forms at the bottom of the section. This indicates that gallery roof stress is dominated by thermally induced bending.

Conclusions

The extreme ambient condition appears to be a valuable tool for evaluating structures for which ambient conditions are controlling the behavior. Use of the extreme ambient curve will increase the confidence of the materials engineer that the possible range of temperatures that may occur has been accounted for. Compilation of the extreme ambient curve is also a fairly simple procedure.
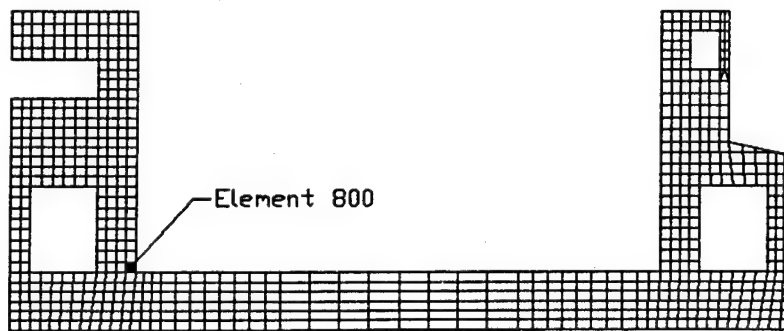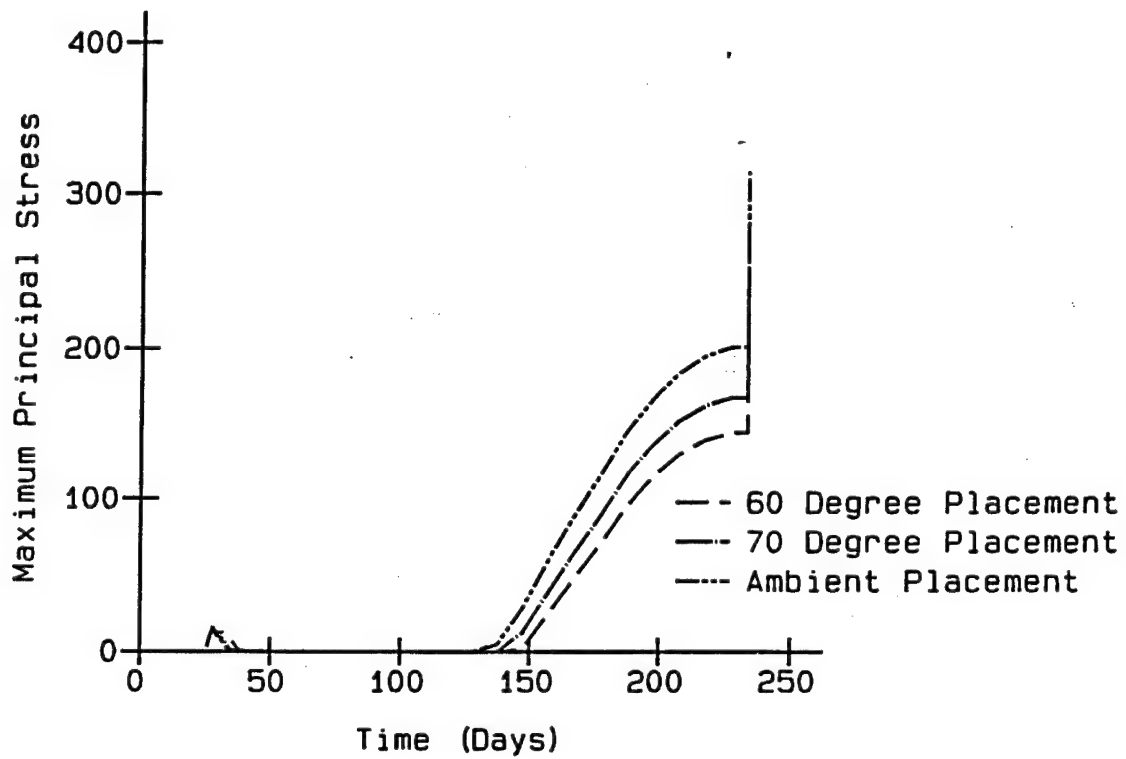
Figure 72.   Maximum principal stress time history for element 800, integration point 2
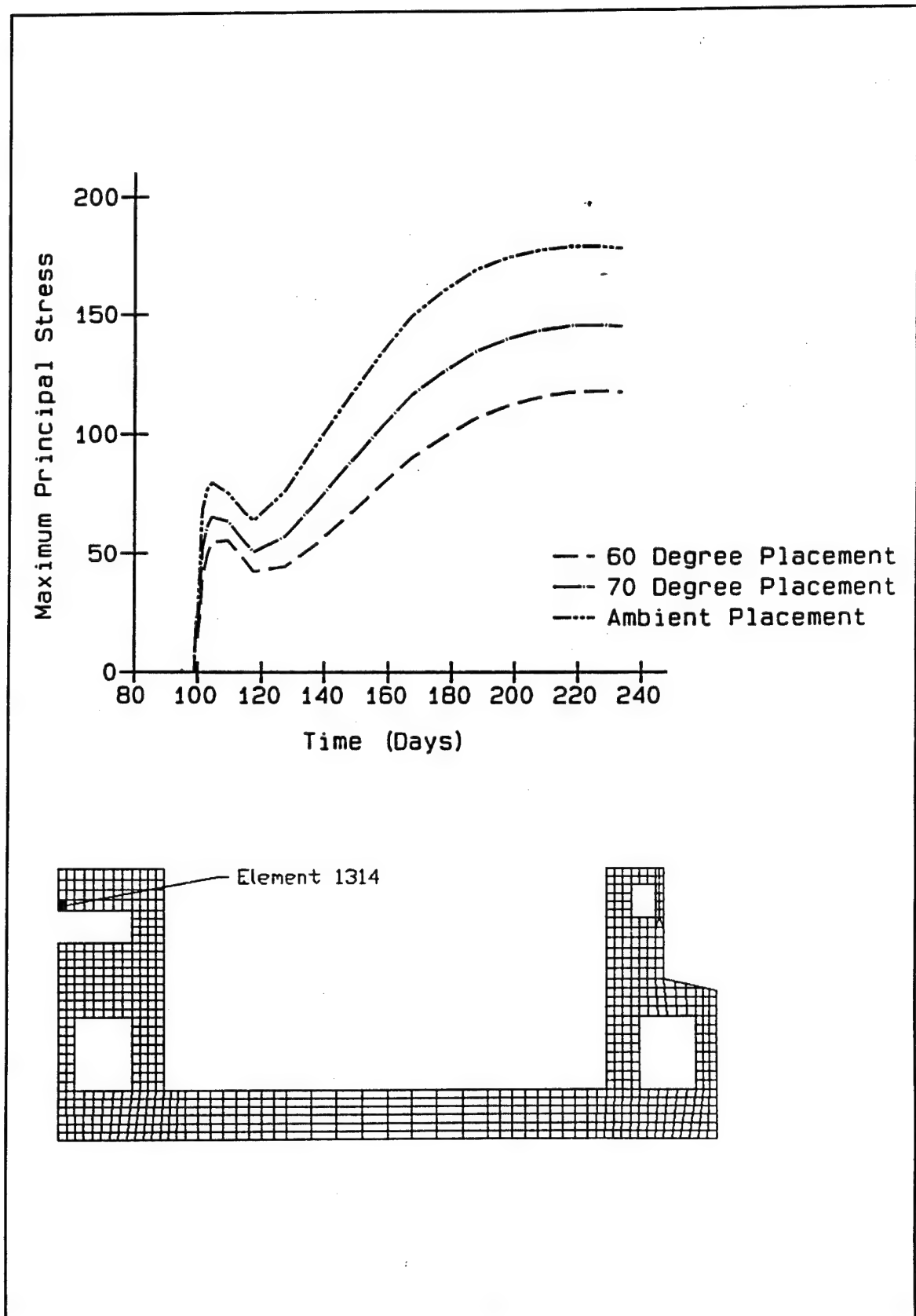
Figure 73.   Maximum principal stress time history for element 1314, integration point 3
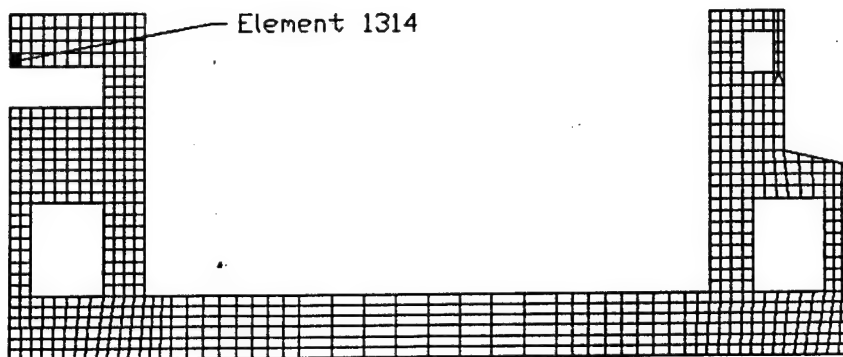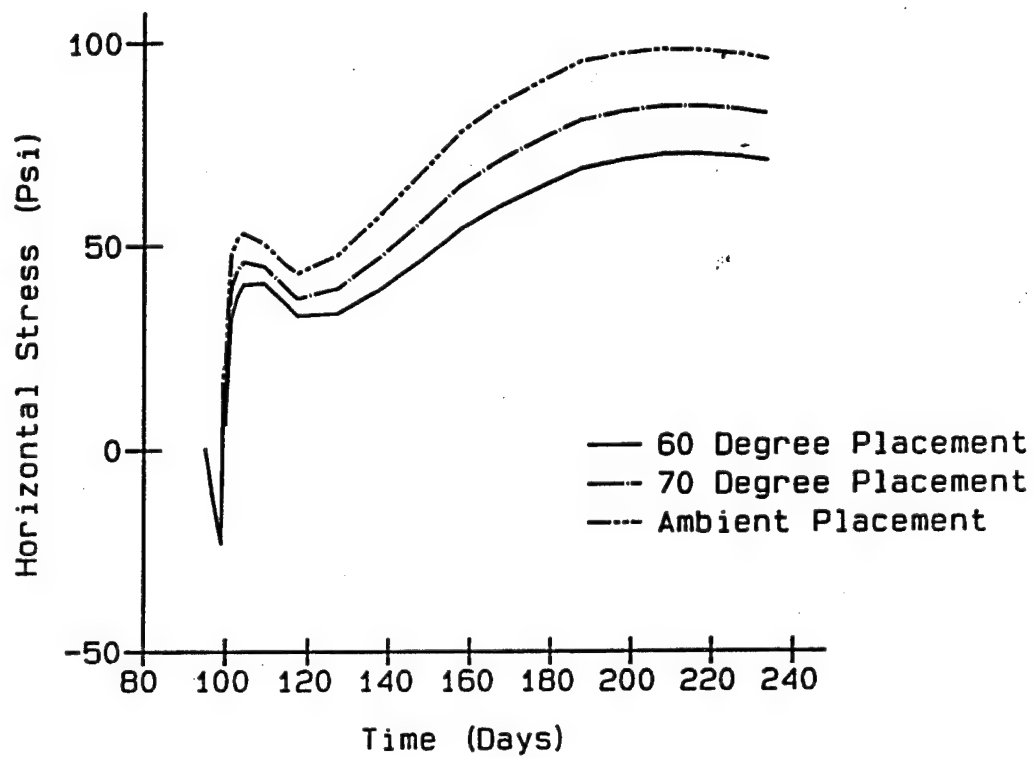
Figure 74.   Stress time history for element 1314, integration point 1
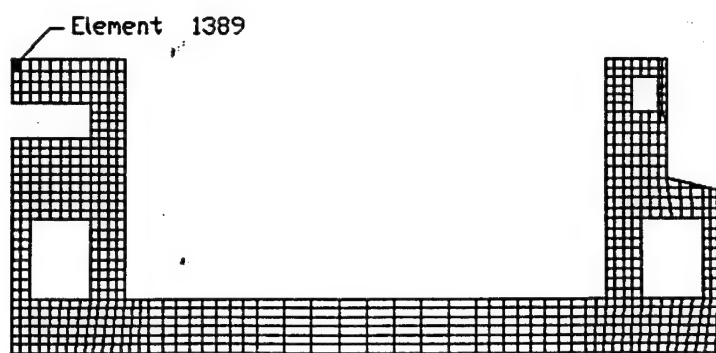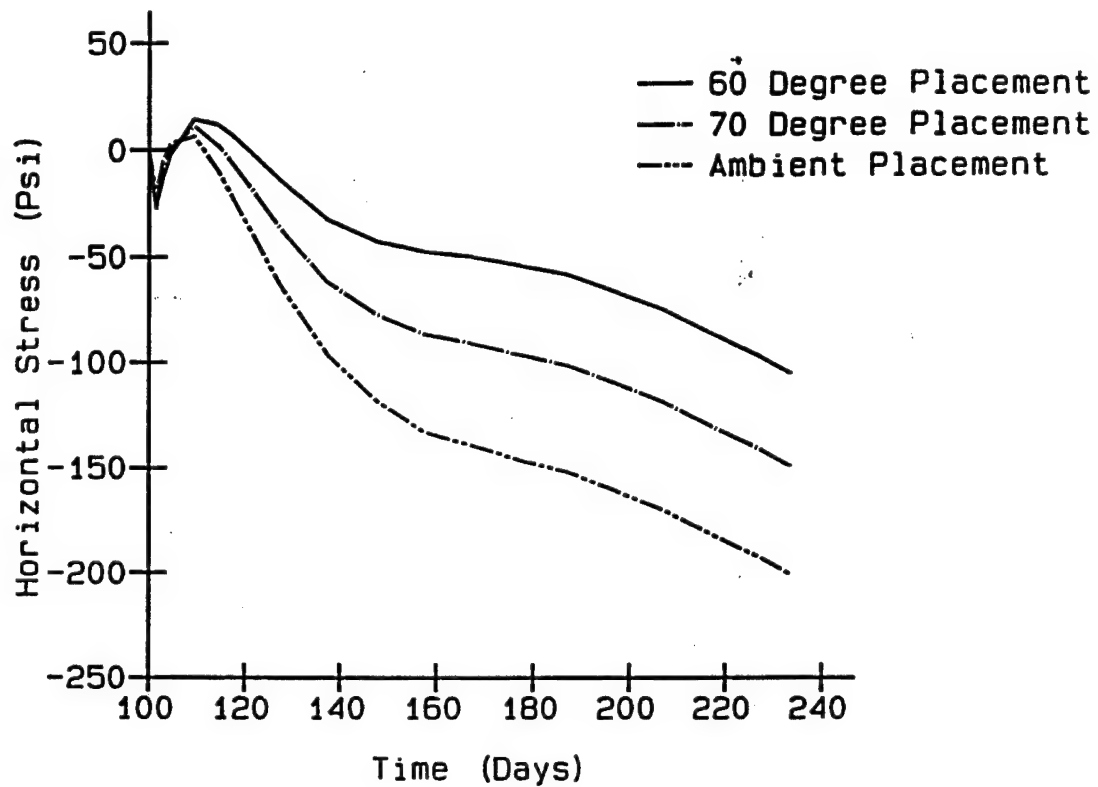
Figure 75.   Stress time history for element 1389, integration point 3

6 Miscellaneous Parameters

Background

The parametric studies and analyses discussed in Chapters 2 through 5 were performed to demonstrate the potential for changing construction methods which could be translated into construction cost savings. These items included parametric analyses of insulation periods, lift heights, and placing temperatures. Some of the other analyses discussed in Chapters 2 through 5 were performed to support and verify the conclusions drawn from the primary set of analyses. These included analyses of various start times and evaluation of the extreme ambient condition. Additional parametric studies were performed on various other items in the Phase III study as discussed briefly in the following paragraphs. A detailed discussion of each parametric study and its results is provided in the following sections.

A comparison was made between using a time of set of 12 hr against a time of set of 6 hr to determine how substantial the effects for a different time of set will be. The study of set times was a result of discussions in the Phase III periodic meetings on how aging characteristics change with temperature and how these changes might affect the results.

Another parameter which was evaluated was the temperature used in the analyses as the stress-free temperature. NISAs to this point have been performed using a single temperature value for each lift. This single value had to be determined by an estimate taken from a temperature contour plot and was an input value into the material subroutine UMAT. Since it is known that initial temperatures 12 hr after placement will vary throughout a lift, it was determined during the course of the study that a means for using the temperature values from the heat transfer analysis as the initial temperatures at the beginning of the stress analysis should be incorporated into UMAT. This feature was incorporated and a comparison between the two methods of applying initial temperatures was made.

Reinforcement is an integral part of a W-frame lock structure, but prior to the Phase III study the capability for using reinforcement in an analysis had not been developed by the Corps of Engineers. The use of reinforcement

in a NISA was developed in this study and is reported in full in a WES Report (Fehl and Merrill in preparation). The final portion of reinforcement development was the use of reinforcing in the chamber monolith of the Olmsted locks. The results of the study of the reinforced structure will be compared with those from the unreinforced structure. Effects of cracking will also be presented.

Finally, concerns were raised over the placement intervals being used in the slab. Phase II of the Olmsted NISA study used 10-day intervals between placement where typically 5-day intervals have been used. To determine the effects of different interval times in the slab placement, analyses were performed with 5-, 10- and 30-day intervals.

Time of Set Analyses

Introduction

During the course of the Phase III study the time of set of 12 hr which had been used in the first two phases of the study came into question. Questions were raised concerning the time of set because as concrete becomes warmer the aging process accelerates and as it cools the aging process slows down. Since set times are determined from tests typically performed at approximately 70 °F, concern existed about how the concrete might actually be aging at early times when temperatures can approach 100 °F near the center of the mass.

In an effort to quantify this effect an analysis was performed which assumed a time of set of 6 hr as opposed to a time of set of 12 hr used in all other analyses. This change requires that the input parameter in the UMAT model for specifying the age at loading be changed from 12 hr to 6 hr. In addition, an extra quarter-day increment must be added to the beginning of each time step in the stress analysis when a lift is added and must ensure the proper temperature value is used from the heat transfer analysis for the new increment. The heat transfer analysis is unaffected by this change. Both analyses in this parametric study used a 60 °F placing temperature, load case 5, mixture 11 properties, 10-day placing intervals in the slab and 5-day intervals in the wall, and stress-free temperatures as defined by the heat transfer analysis.

Discussion of results

Results comparing the two analyses are shown in Figures 76-85. A quick perusal of the results indicates that using a 6-hr time of set is the critical case. In all but two of the time history plots the maximum compressive stress occurs in the 6-hr time of set condition. In Figure 80, the
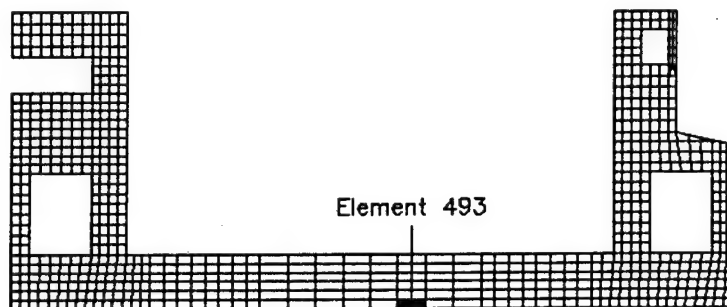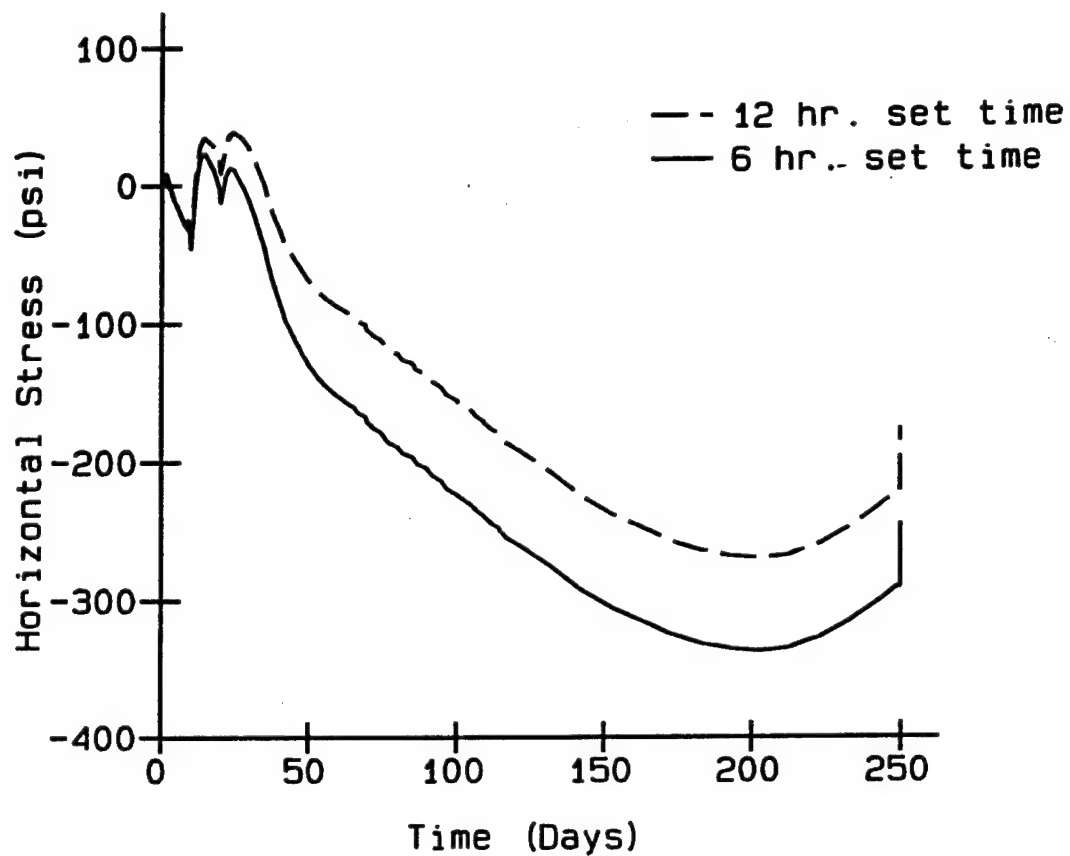
Figure 76.   Time history of horizontal stress at integration point 1 of element 493
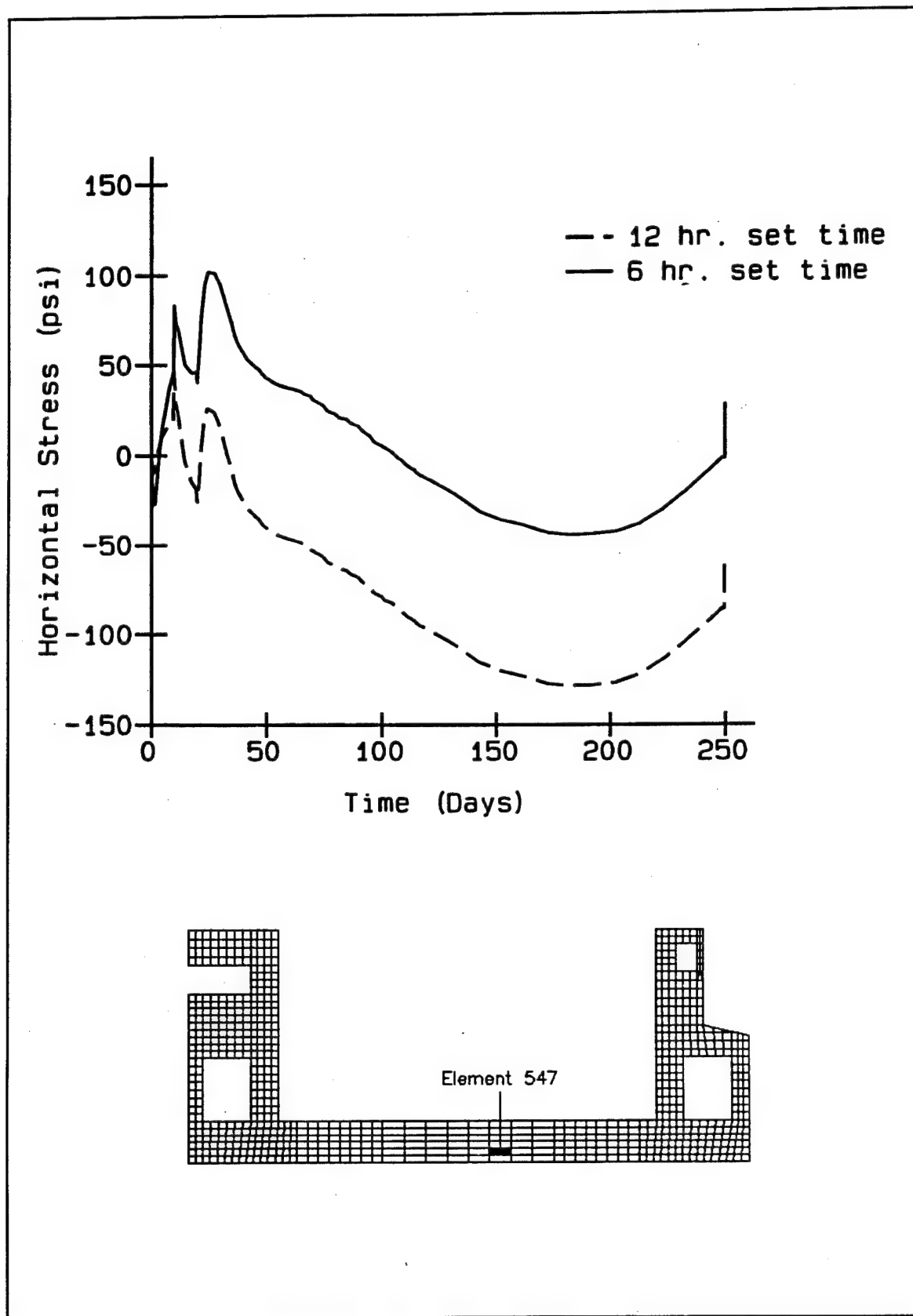
Figure 77.   Time history of horizontal stress at integration point 3 of element 547
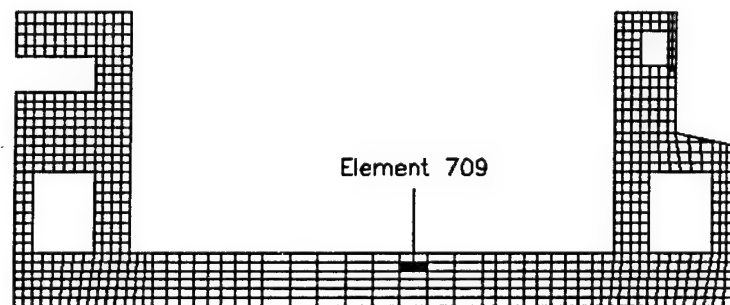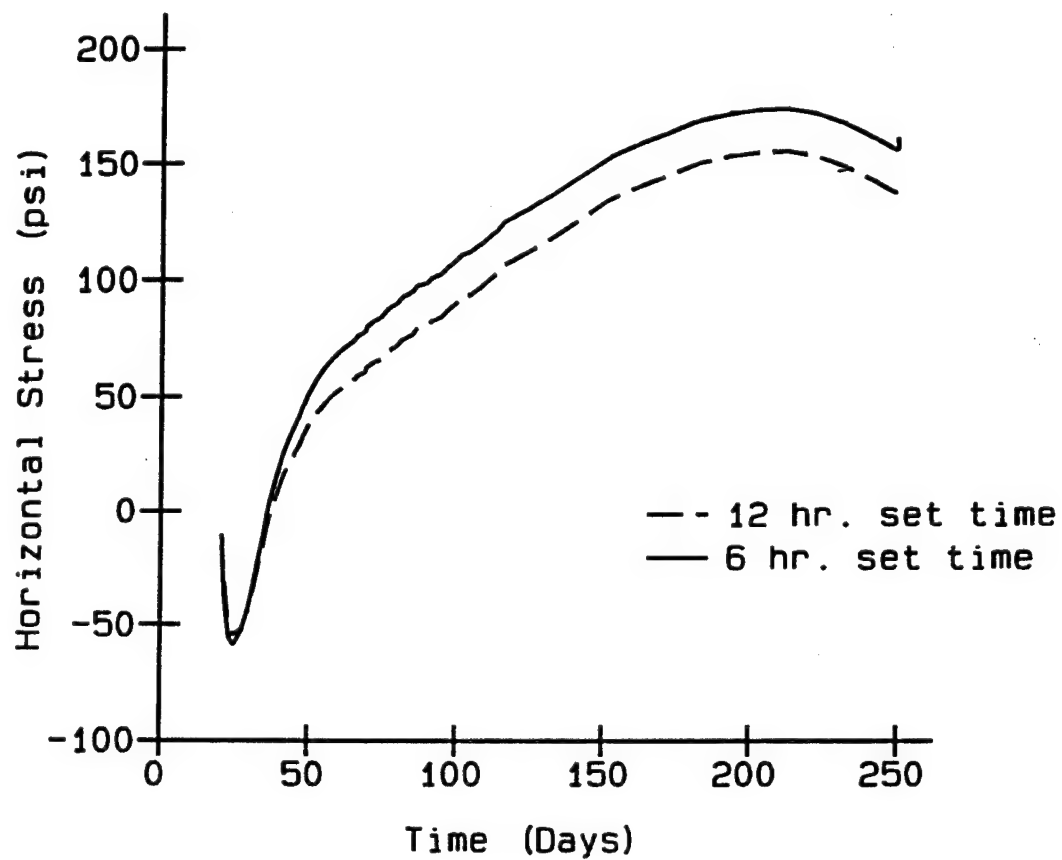
Figure 78.   Time history of horizontal stress at integration point 1 of element 709
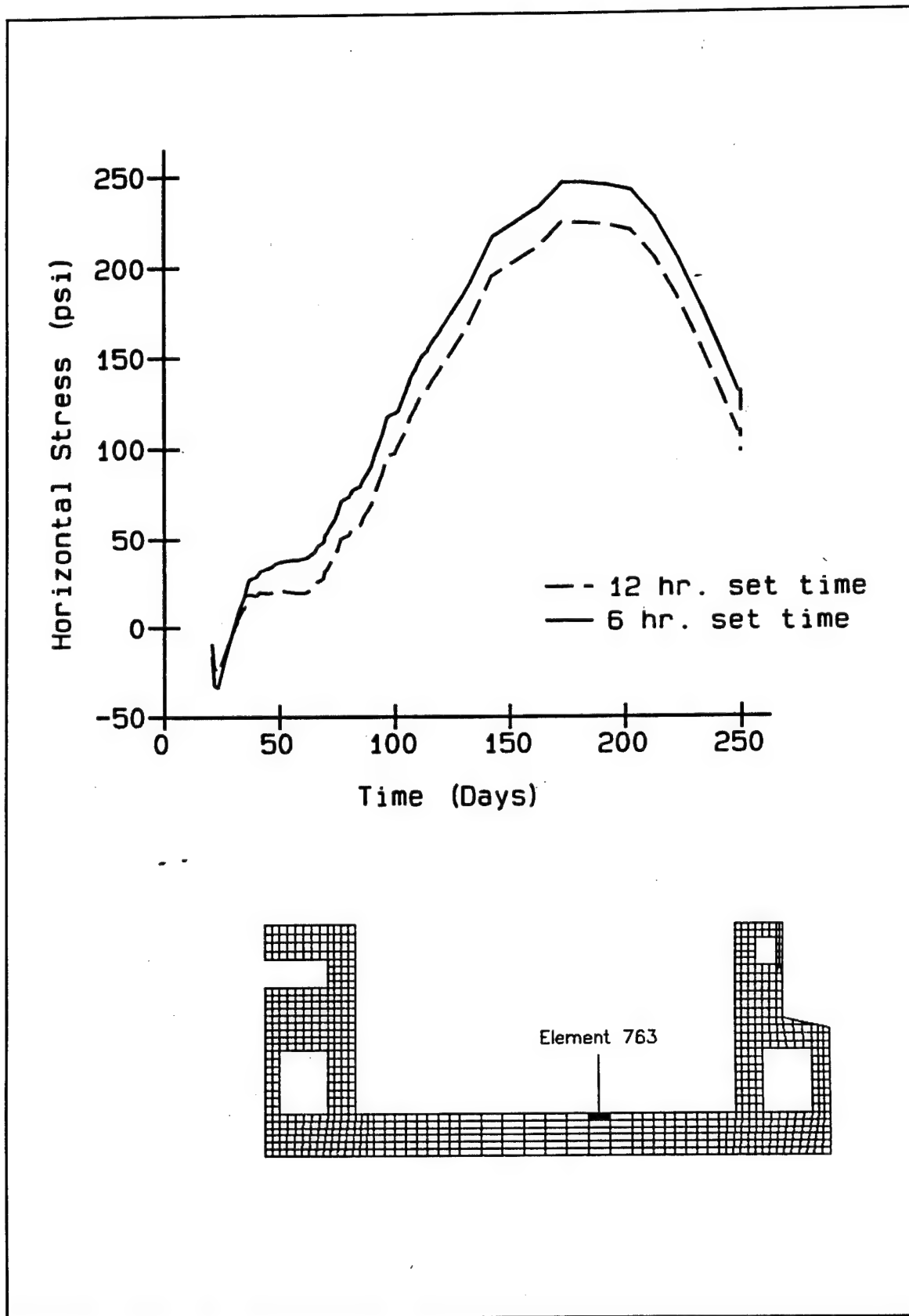
Figure 79. Time history of horizontal stress at integration point 3 of element 763
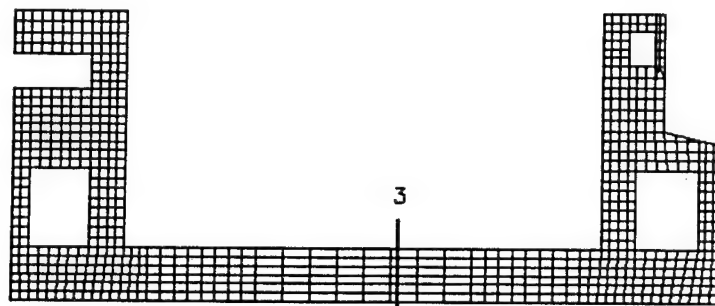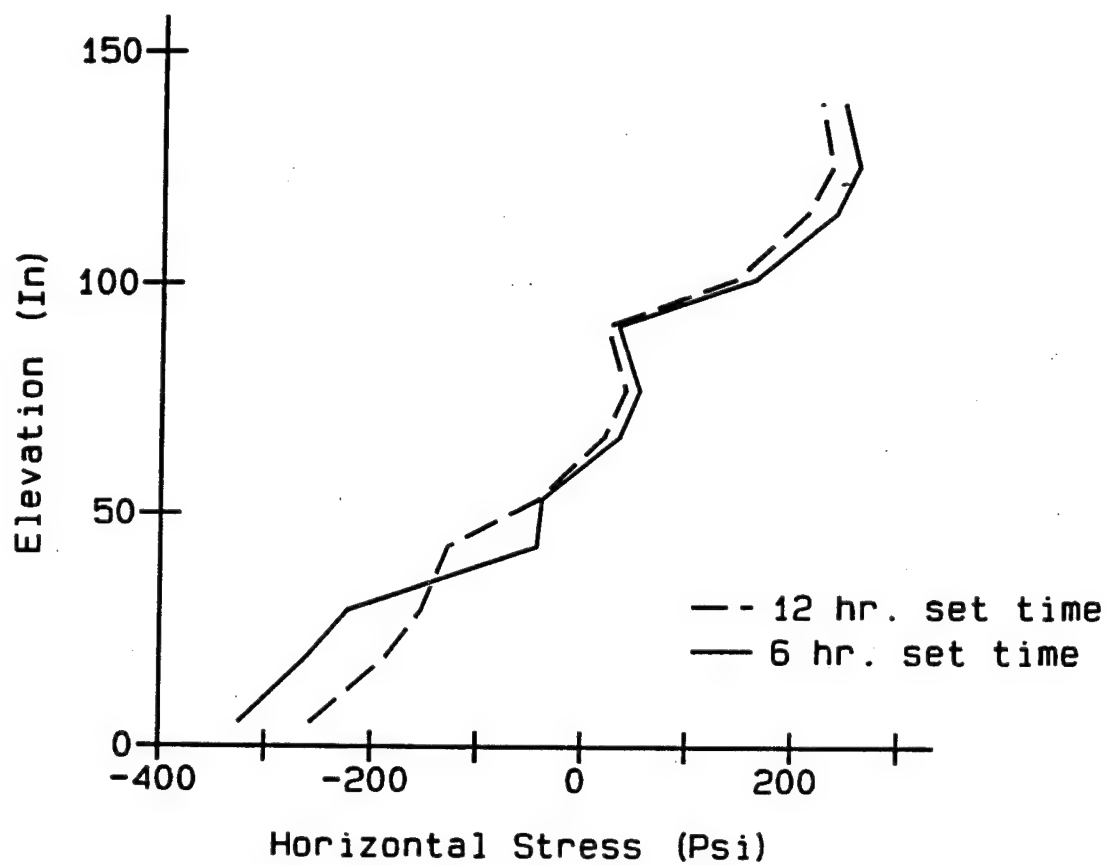
Figure 80. Stress distribution at section through base slab

Figure 81.   Time history of horizontal stress at integration point 3 of element 756
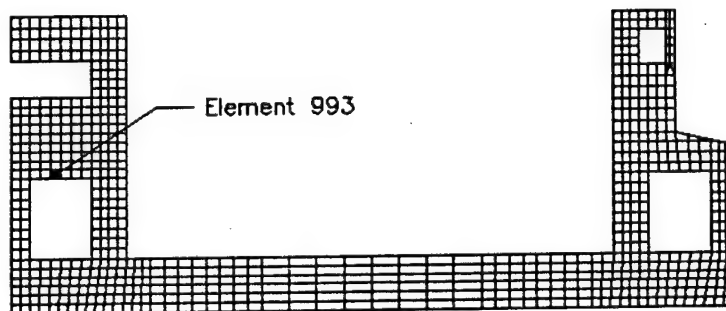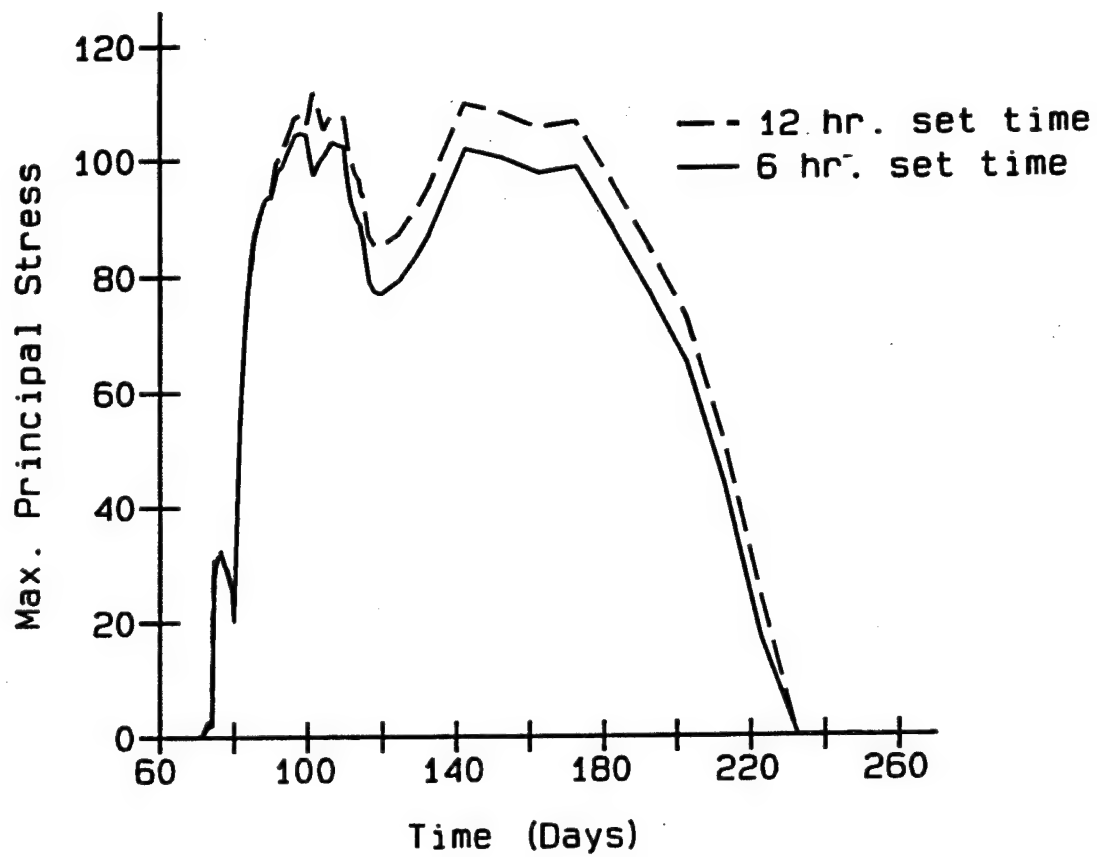
Figure 82.   Time history of maximum principal stress at integration point 2
of element 993
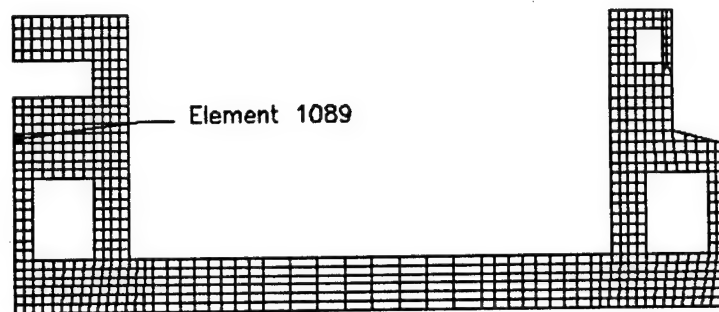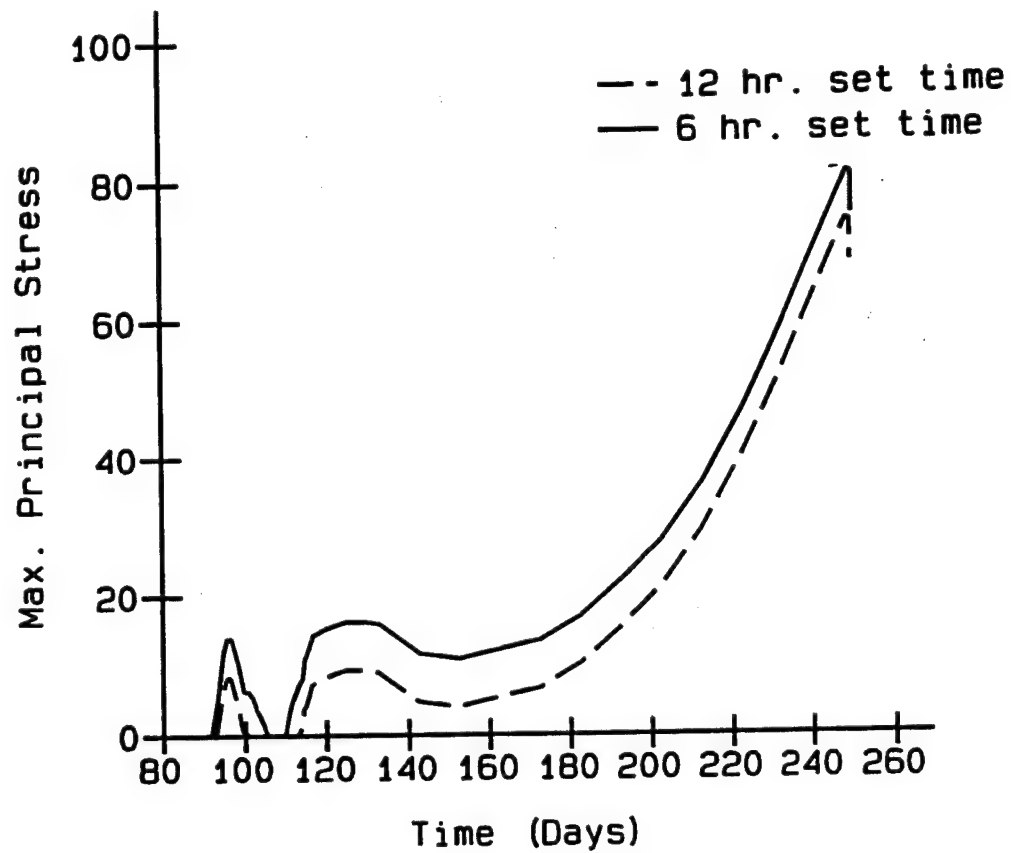
Figure 83.   Time history of maximum principal stress at integration point 2
of element 1089

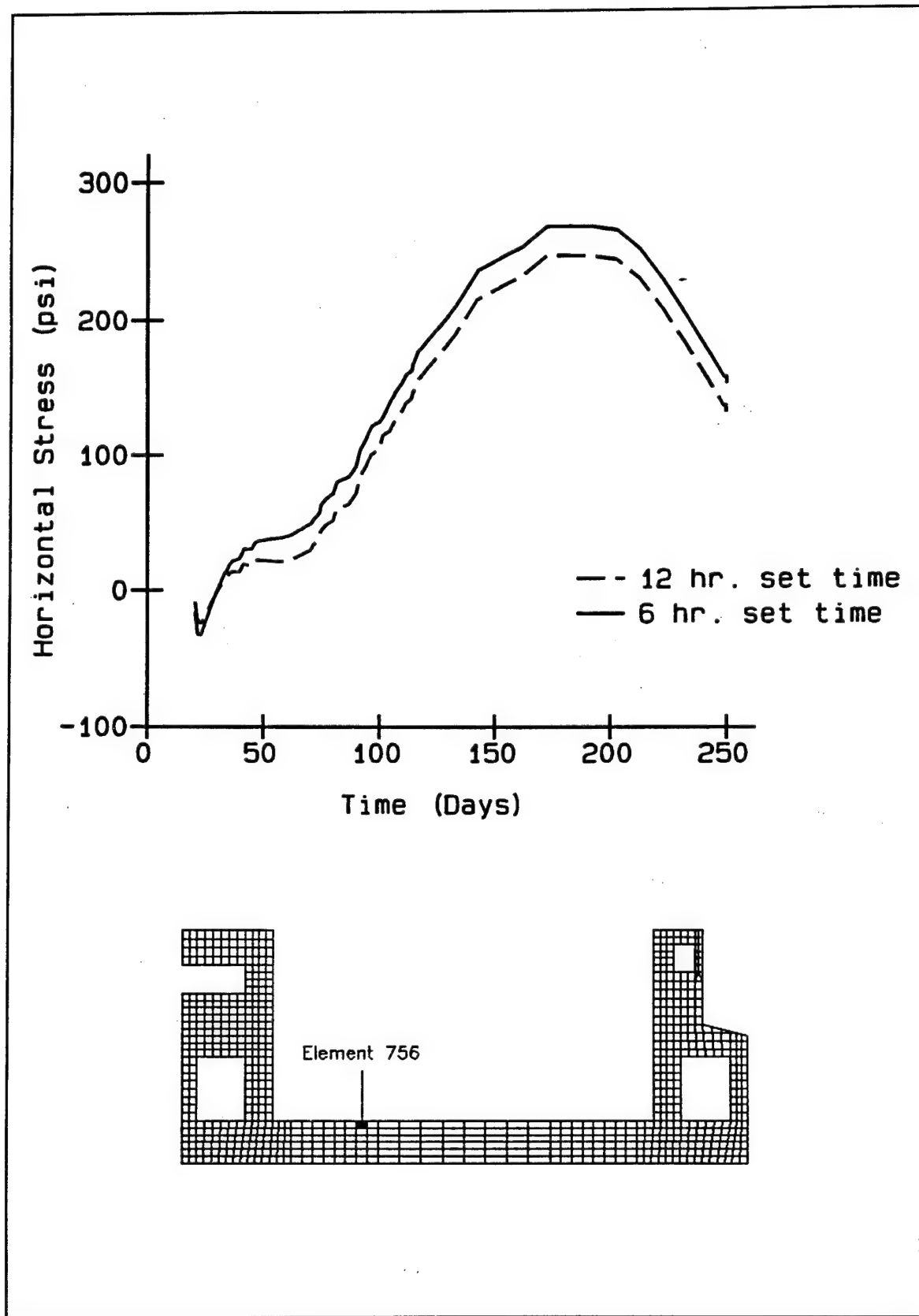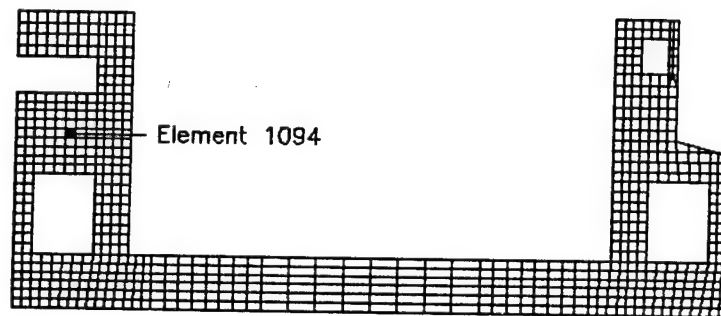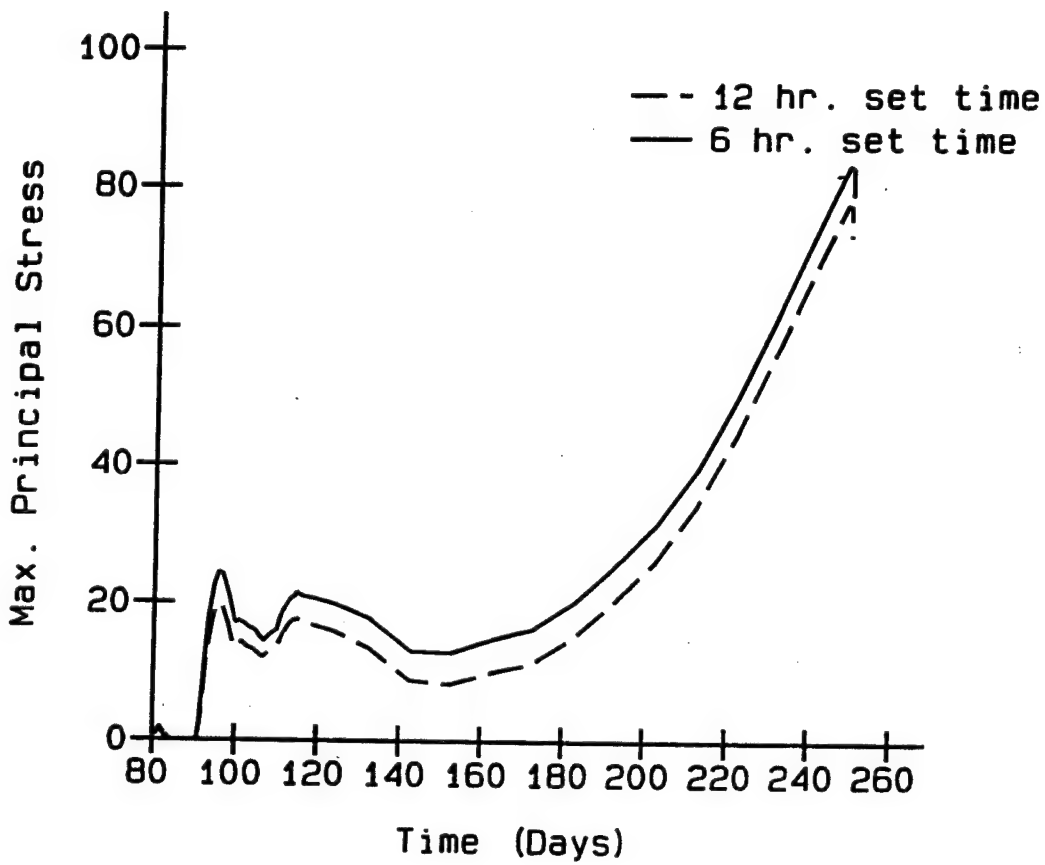Figure 84. Time history of maximum principal stress at integration point 1
of element 1094
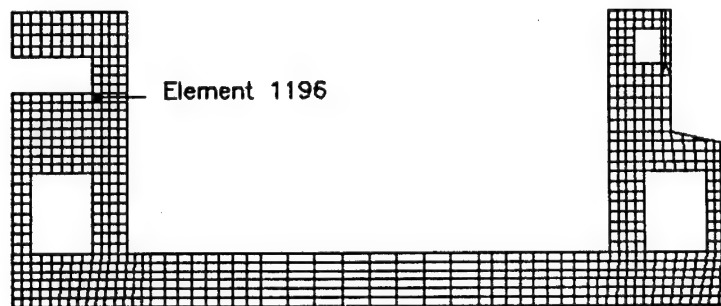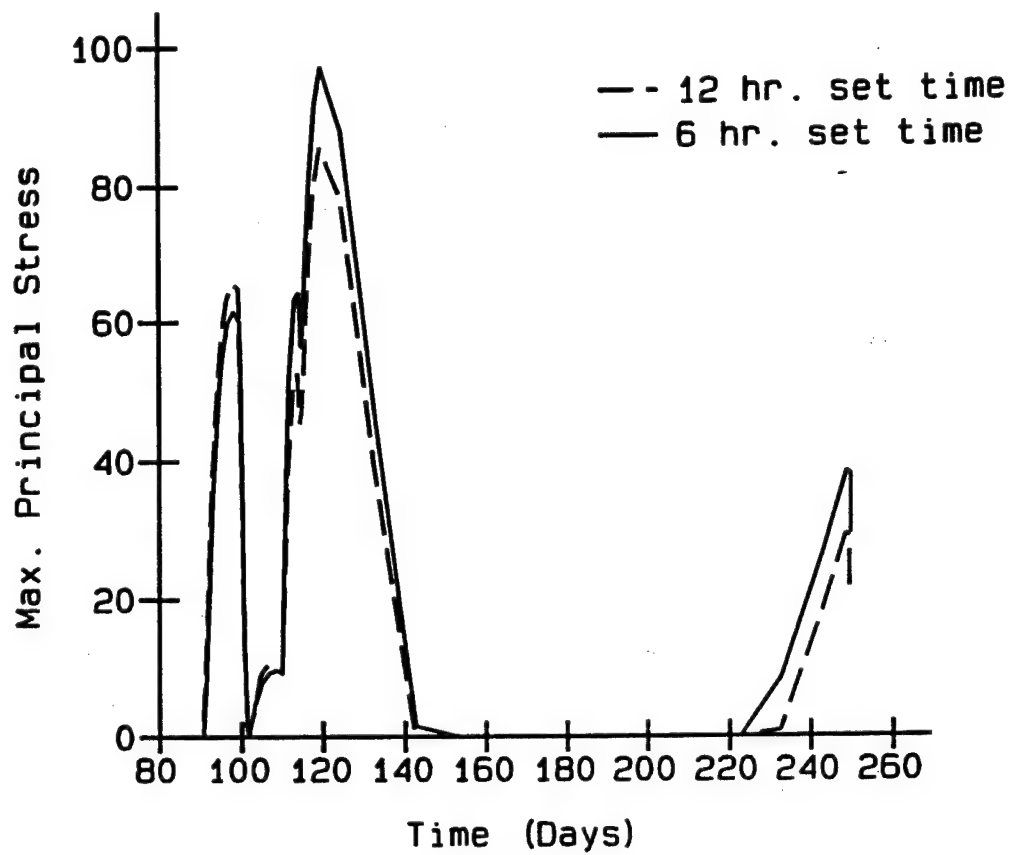
Figure 85.   Time history of maximum principal stress at integration point 4
of element 1196

stress gradient also is larger for the 6-hr time of set case. Only in Figures 77 and 82 does the 12-hr case control.

In Figure 77 this reversal in the general trend can be explained by what occurs in the first 10 days after the lift is placed. Since the 6-hr case begins taking load earlier than the 12-hr case, the structure can undergo larger deformations since the total change in temperature will be greater if the structure begins taking load at 6 hr rather than at 12 hr. With these deformations are, of course, associated stresses. This explains why the 6-hr case goes further into compression than the 12-hr case. It must also be remembered that creep has its largest effect at early times; therefore, the tensile stresses occurring in the first 2 days will be affected by creep the most and the 6-hr case will be influenced by this more than the 12-hr case. As the concrete begins to cool, the point in Figure 77 starts to go into compression and the same magnitude of deformations which created the tension must occur as the concrete goes into compression. Again, the 6-hr case went through a larger deformation and will, therefore, go through more of a transition to the compression side and will exceed the total compression of the 12-hr case due to the creep which occurred at the early times.

In Figure 82 the difference appears to be more a result of what occurred in the second lift above the culvert (lift 12). Because the 6-hr case for the placement of lift 12 initially goes into a higher tension than the 12-hr case (see Figures 83 and 84), a higher tensile value is imparted into the lift above the culvert (lift 10). Because of the culvert, a stress gradient results from the application of this tensile force and creates compression at the bottom of the lift 10. This resulting compression can be seen in Figure 82 by the fact that the 12-hr case has the higher tensile values.

While results indicate that the 6-hr case may be more critical than the 12-hr case for most points in the structure, the differences are not large. In Figure 76 the difference in the maximum compression values is approximately 25 percent and represents the largest difference between the two analyses. At the top of the slab where tension is occurring the differences between the two analyses is less than 10 percent at both elements 763 and 756 (Figures 79 and 81). At element 993 in the wall the largest difference is about 7 percent.

Evaluation of results

Based on the results presented, using a set time of 6 hr would be conservative. Partially due to the fact that the differences between the two analyses were not excessively large, especially in the tensile regions, it was decided that analyses could continue using a time of set of 12 hr. In addition, during the course of Phase III some additional testing was performed for time of set, and for mixture 11 results indicated that for a 70 °F temperature the initial time of set was 9 hr and 43 min while the final time of set was 13 hr and 44 min. It was agreed that the final time of

set is the time in which the concrete can begin to carry load and, therefore, the 12-hr time of set is sufficient. Finally, the test data also revealed that if the concrete was at 40 °F then the initial time of set would be 31 hr and 5 min and the final time of set would be 50 hr and 55 min. When this is taken into consideration, the use of the 40 °F case which better approximates winter conditions, the 12-hr time of set will likely provide conservative results.

While use of the 12-hr time of set was determined to be satisfactory for this set of analyses, consideration should be given on other projects to different time-of-set values. Also, the time of set should not be limited to having to start on quarter-day intervals. Finally, when considering the time of set, the fact that concrete ages as a function of time and temperature must be kept in mind. As noted above, the time of set for the 40 °F case was quite lengthy and an analysis could be performed using the information from the time-of-set test data but it should also be kept in mind that the shapes of the curves for the various material properties will also change and, therefore, changing only the time-of-set value may not be appropriate.

Stress-Free Temperature Analyses

Introduction

The stress-free temperature used in a NISA is the initial set of temperatures used to compute the first set of stresses in the analysis. The stress-free temperature is assumed to occur at the time the concrete matures enough to carry load. Prior to the work performed in Phase III the stress-free temperature had to be determined for each lift by approximating the average temperature for the lift at the time of set based on a temperature contour plot at that particular time. While this method of selection was not exact it did appear to be generally accurate for the center portions of the lift.

During a periodic meeting of the Phase III study personnel, results near lift surfaces began to come into question and the fact that the stress-free temperature was considerably different from the temperatures at the surface of the lift was noted as a possible reason for some of the behavior observed. It was then decided that modifications to the material model were needed such that the stress-free temperature could be obtained for each node from the heat transfer analysis. This modification was implemented and is now part of the UMAT subroutine in the ANACAP-U software (ANATECH Research Corp. 1992).

Discussion of results

Once the modifications for using temperatures from the heat transfer analysis as the stress-free temperatures were completed an analysis was performed for the purpose of comparing the affect of the change. Figures 86-92 are plots comparing analyses from the two different methods of applying the stress-free temperature. The analysis denoted "Single Temp." in the figures is the analysis which used a single temperature in a lift as the stress-free temperature; the analysis denoted "Multi Temp." uses the temperatures from the heat transfer analysis.

Figures 86-89 are points in the base slab, and for each point shown the original method of stress-free temperatures provides the more conservative set of results. The effects of the modification are not significantly large, particularly at the points near the bottom (Figure 86) and top (Figure 89) of the slab. The difference between the two analyses for the maximum values are 6 percent for element 493 and 10 percent for element 763.

Figures 90-92 are points from the wall of the monolith. For these points no trend is evident as to whether one method is any more conservative than the other. Despite the fact that no general trend has been established in the walls, it should be noted that the differences between the two analyses are very small. The differences between the two analyses are always less than 10 psi.

Evaluation of results

The change in the method of calculating the stress-free temperature did not make a particularly large difference in the results. Despite this fact, the modification was necessary because the modified method of using the temperatures from the heat transfer analysis more closely approximates what actually occurs in the field. It is important to implement changes to the NISA process when it is known that the change more accurately predicts the actual behavior.

Reinforcement and Cracking Analyses

Introduction

As previously stated, reinforcing is an integral part of a W-frame lock. Ignoring the fact that reinforcing exists in a structure when performing an analysis will provide conservative results but the full benefits of performing a NISA when cracking is present cannot be realized until reinforcement is integrated into the analysis. For this reason and with the knowledge that some of the more massive monoliths at the Olmsted Locks were likely to require inclusion of reinforcement in the analysis to

Figure 86.   Time history of horizontal stress at integration point 1 of element 493

Figure 87.   Time history of horizontal stress at integration point 3 of element 547

Figure 88.   Time history of horizontal stress at integration point 1 of element 709
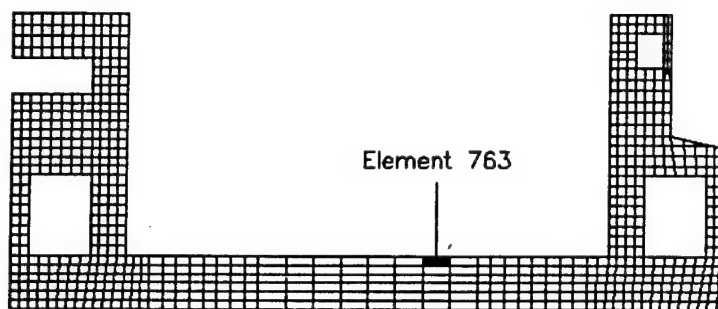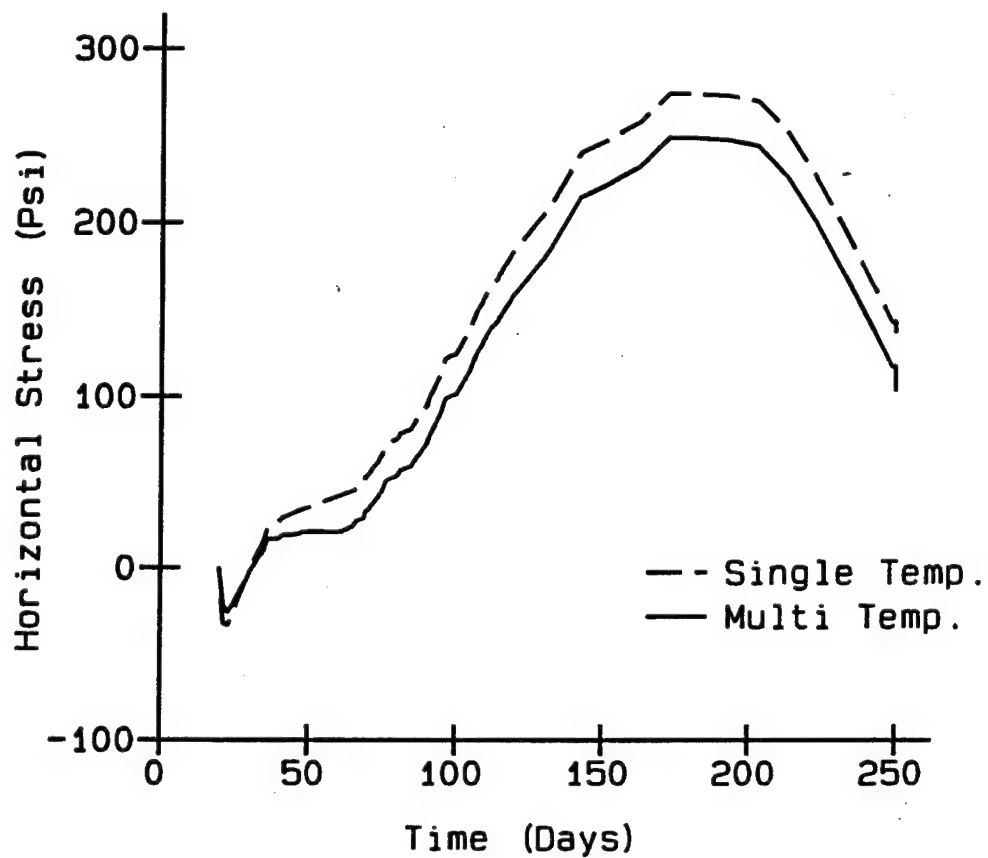
Figure 89.   Time history of horizontal stress at integration point 3 of element 763
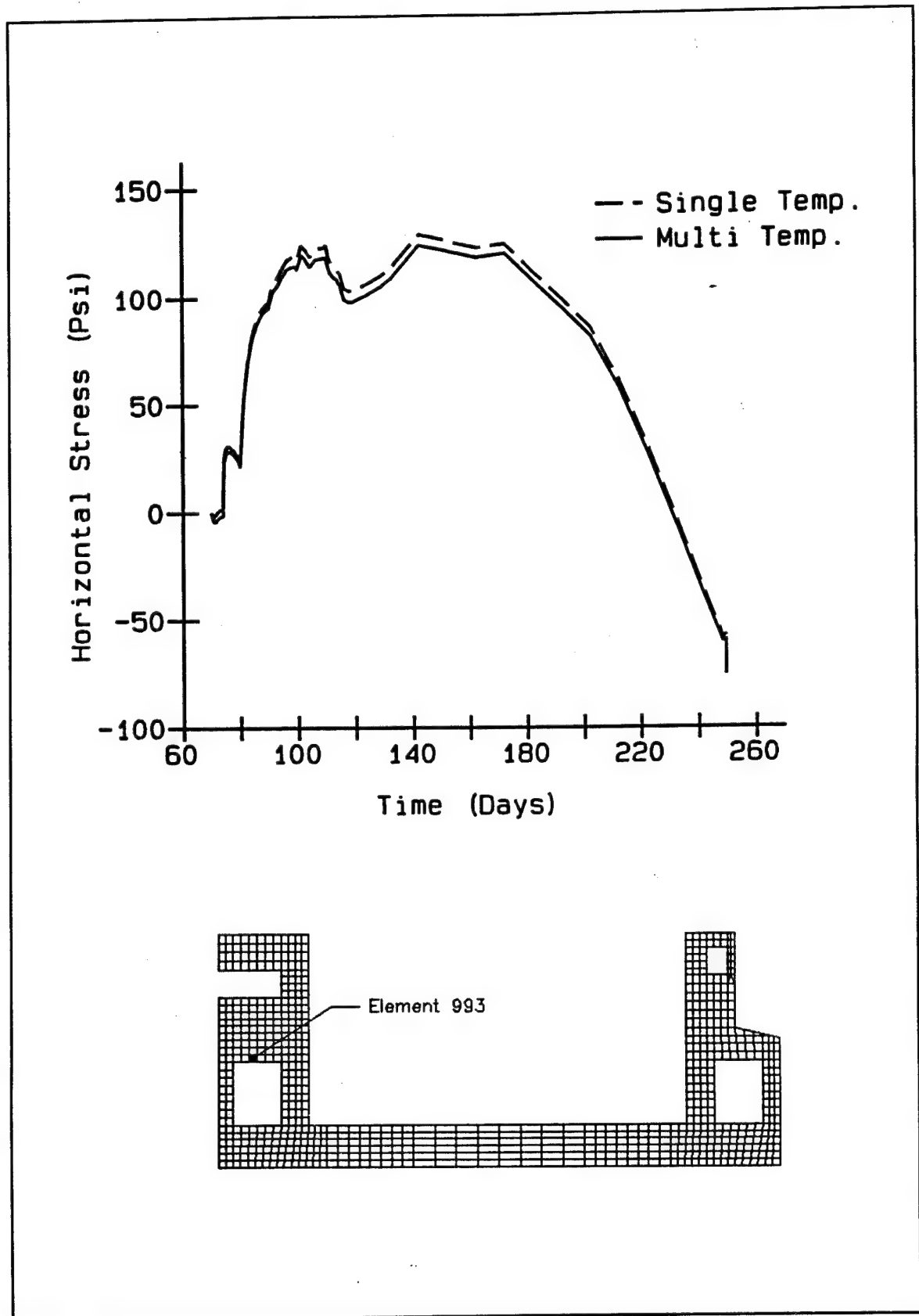
Figure 90.   Time history of horizontal stress at integration point 2 of element 993
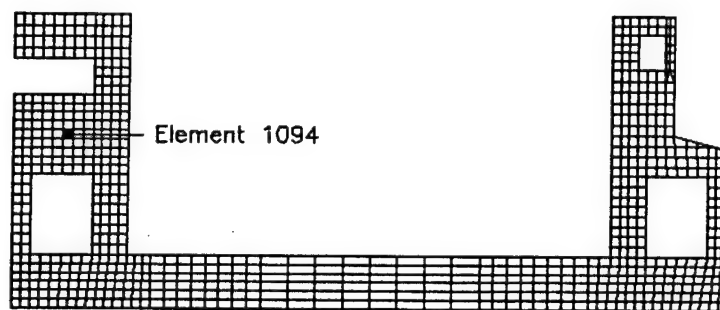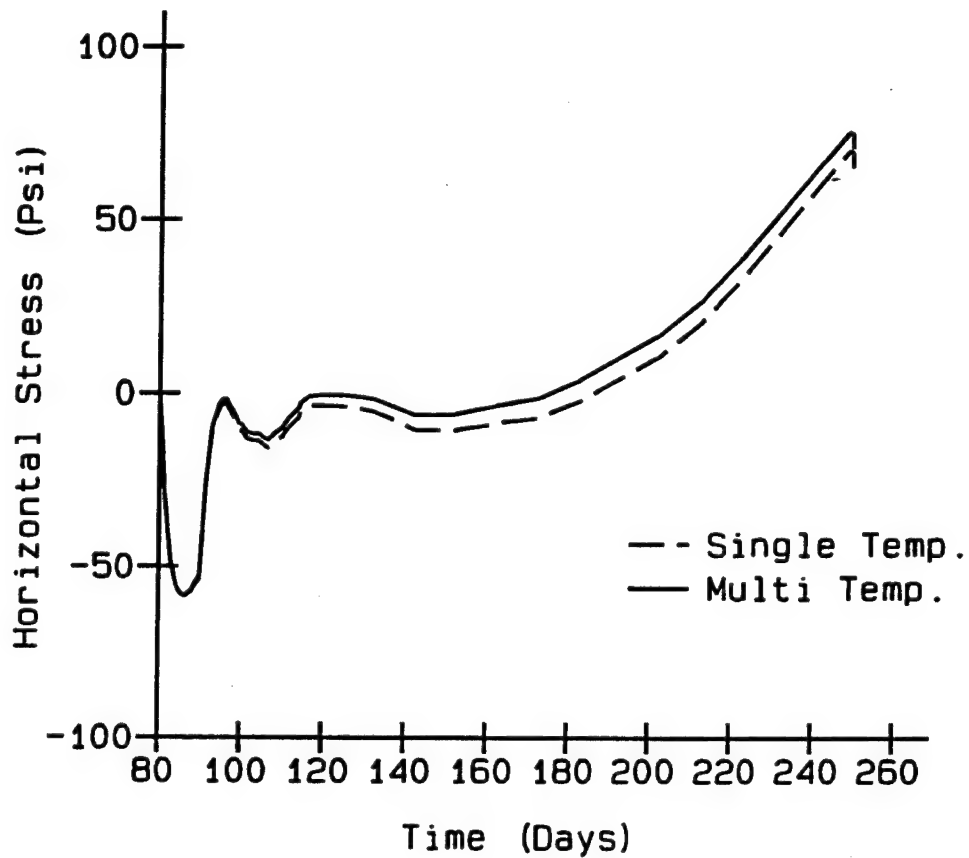
Figure 91.   Time history of horizontal stress at integration point 1 of element 1094
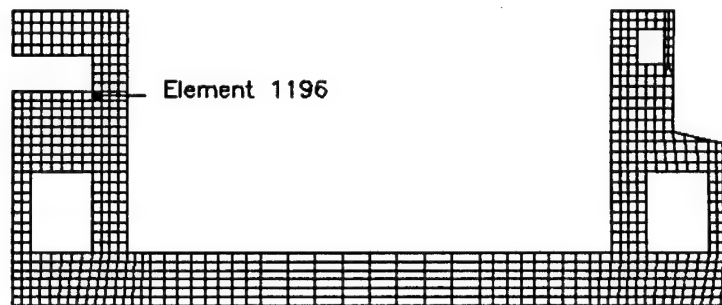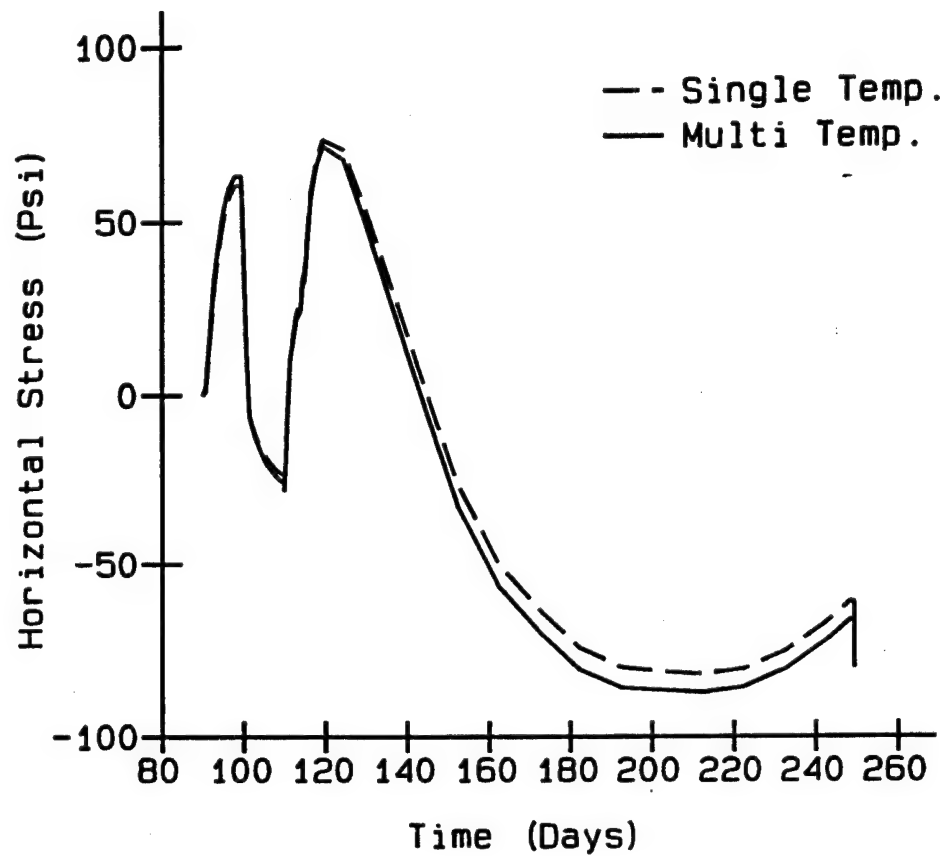
Figure 92.   Time history of horizontal stress at integration point 4 of element 1196

demonstrate constructability, a decision was made to develop a capability for including reinforcement in a NISA.

Simple problems were performed initially and compared with closed form hand solutions and are reported in a WES Report (Fehl and Merrill, in preparation). The final portion of the development was to include reinforcement in the chamber monolith at Olmsted and evaluate its effects on the structural behavior. The reinforcement added to the model was based on the layout of reinforcing as shown in Figure 93. It should also be noted that the reinforcing was modeled using the ABAQUS option *REBAR instead of discrete truss elements. The *REBAR option in ABAQUS simply changes the stiffness of the existing element integration points based on the amount of reinforcing added to the model.
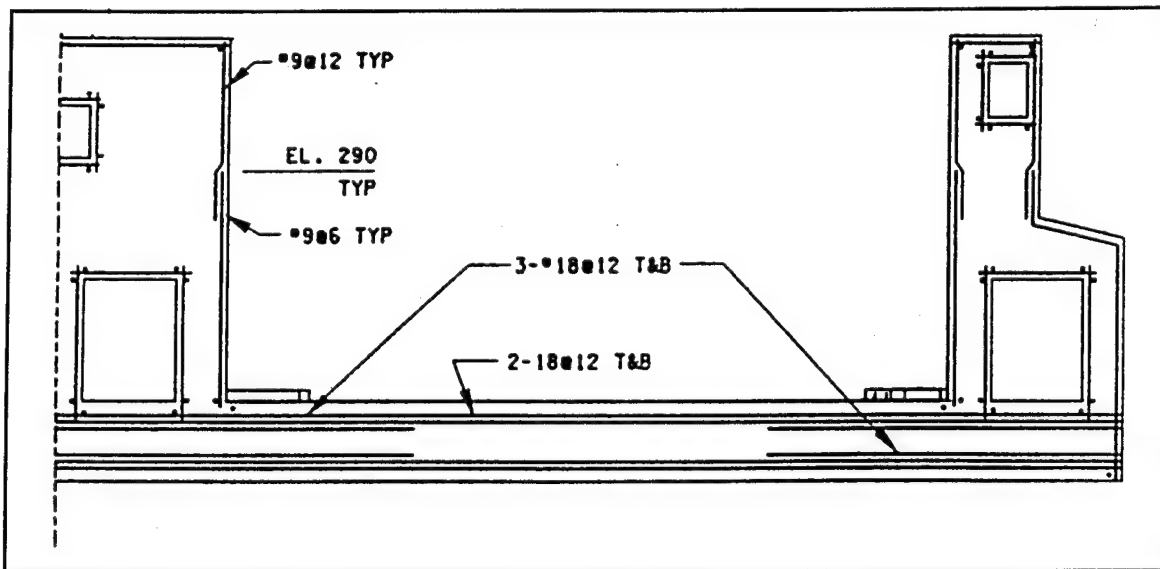
Figure 93.   Reinforcement layout for chamber monolith

While it may be important to include reinforcing in a NISA, the effects of reinforcing on the structural behavior are minimal until cracking occurs. Therefore, in order to understand the full effect of the reinforcing on the structural behavior it was necessary to incrementally change the reinforcing analyses until cracking occurred. This approach required that several analyses be performed. Five analyses were compared, beginning with the results from the Phase II analysis and leading up to the case where the cracking criteria were reduced to induce cracking into the structure.

Discussion of results

Results from the reinforcing analyses are presented in Figures 94-110. Figures 94-104 present time history stresses in the concrete. Five separate analyses were performed and are compared for each point in the figures. The five analyses being compared are:
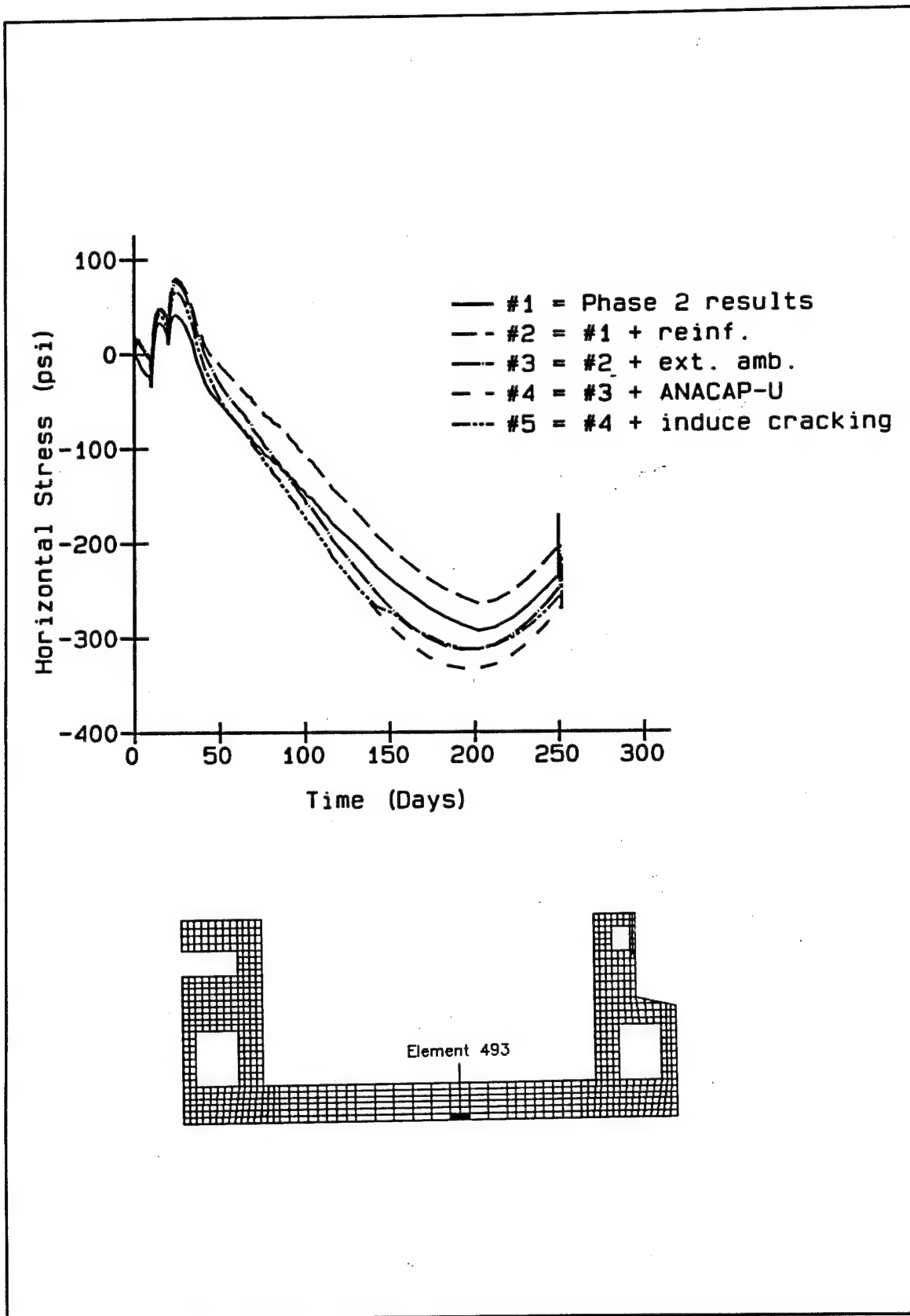
Figure 94.   Time history of horizontal stress at integration point 1 of element 493
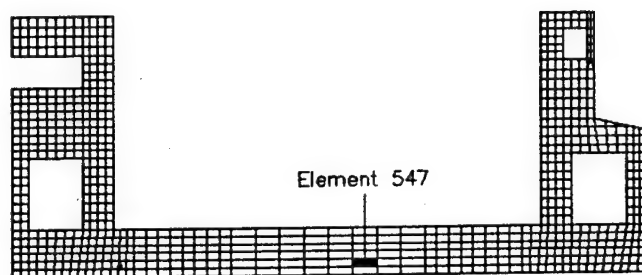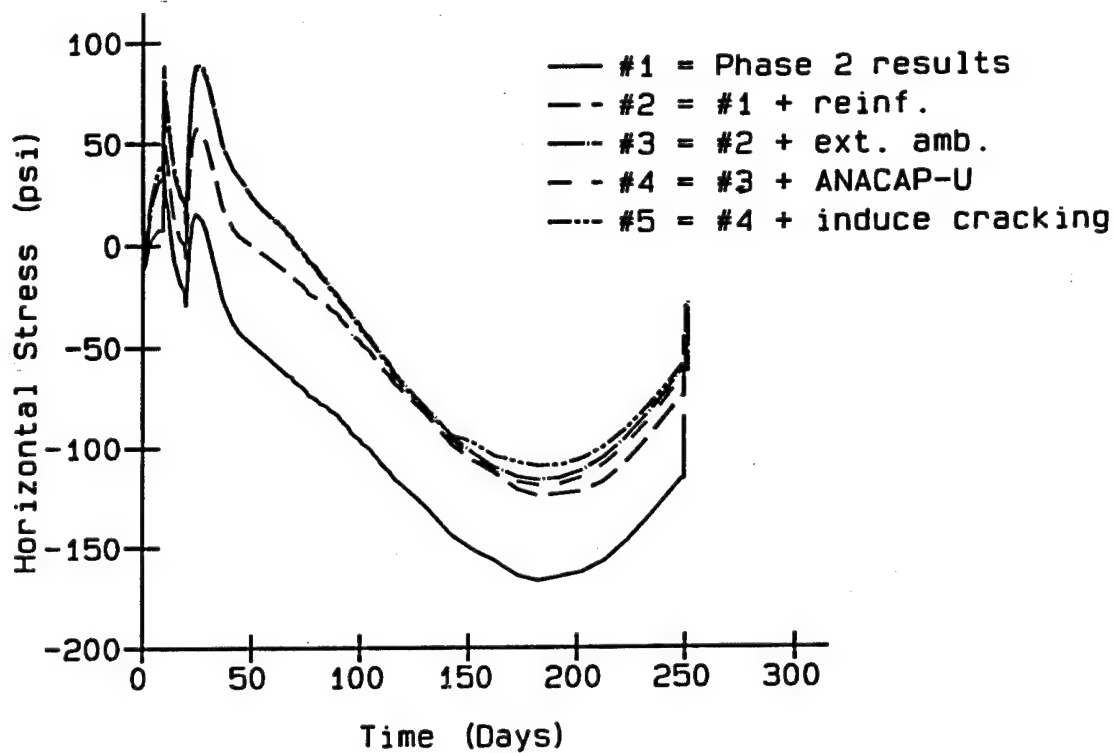
Figure 95.   Time history of horizontal stress at integration point 3 of element 547
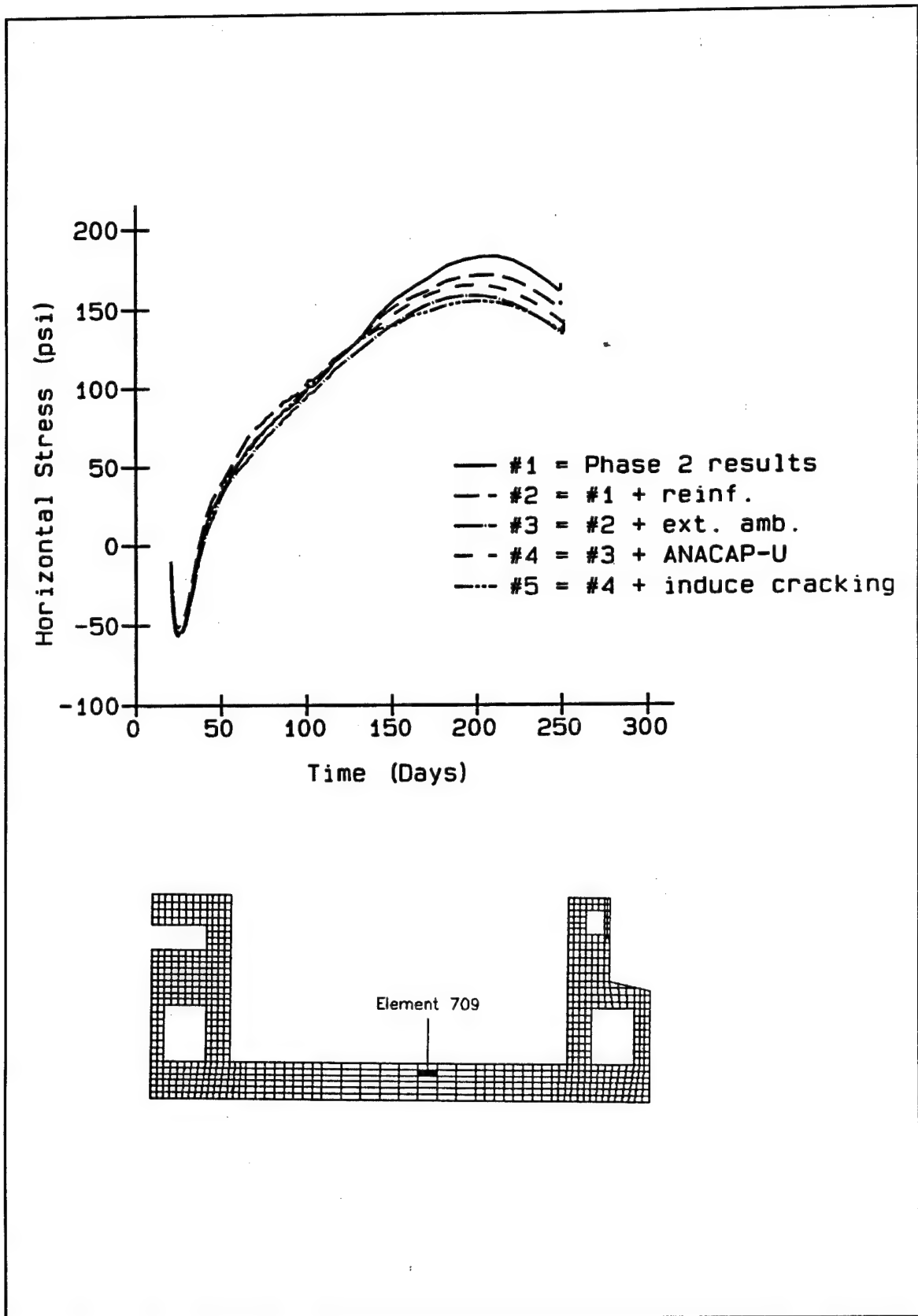
Figure 96.   Time history of horizontal stress at integration point 1 of element 709
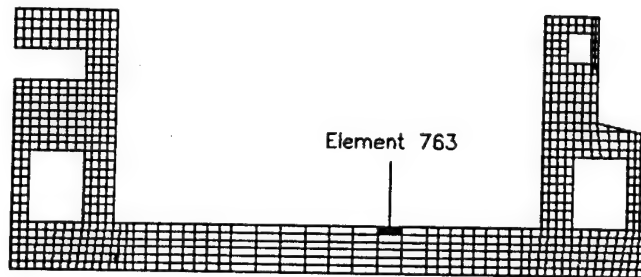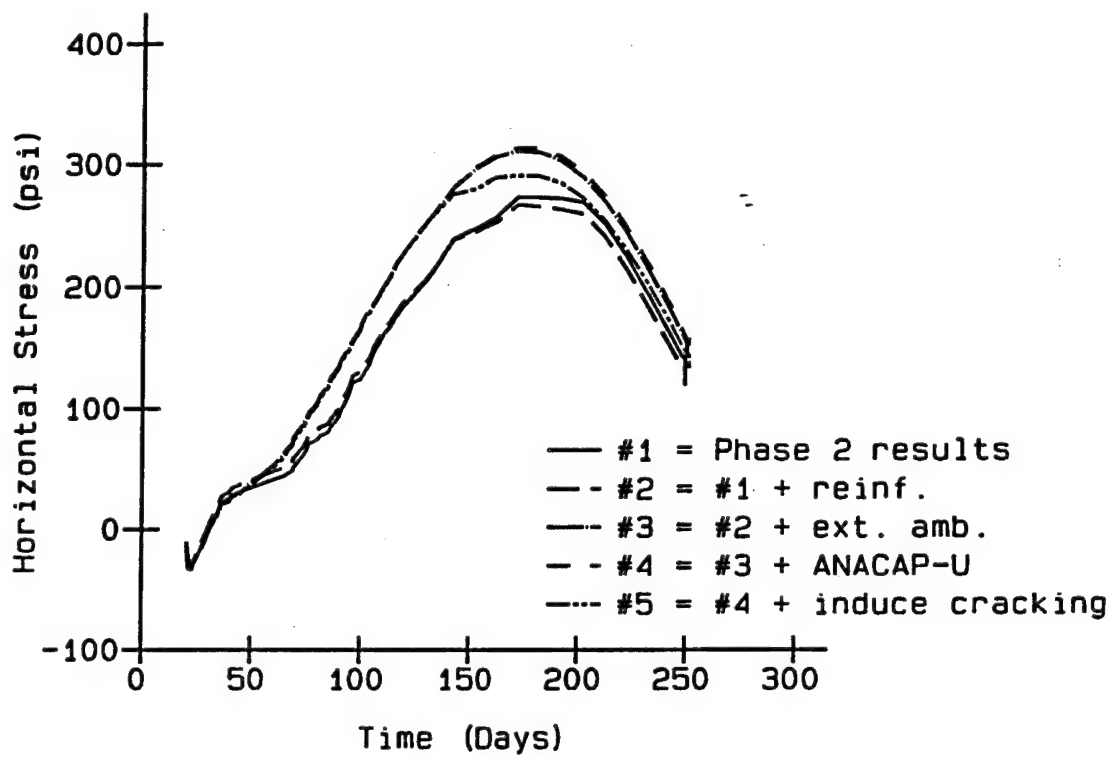
Figure 97.   Time history of horizontal stress at integration point 3 of element 763
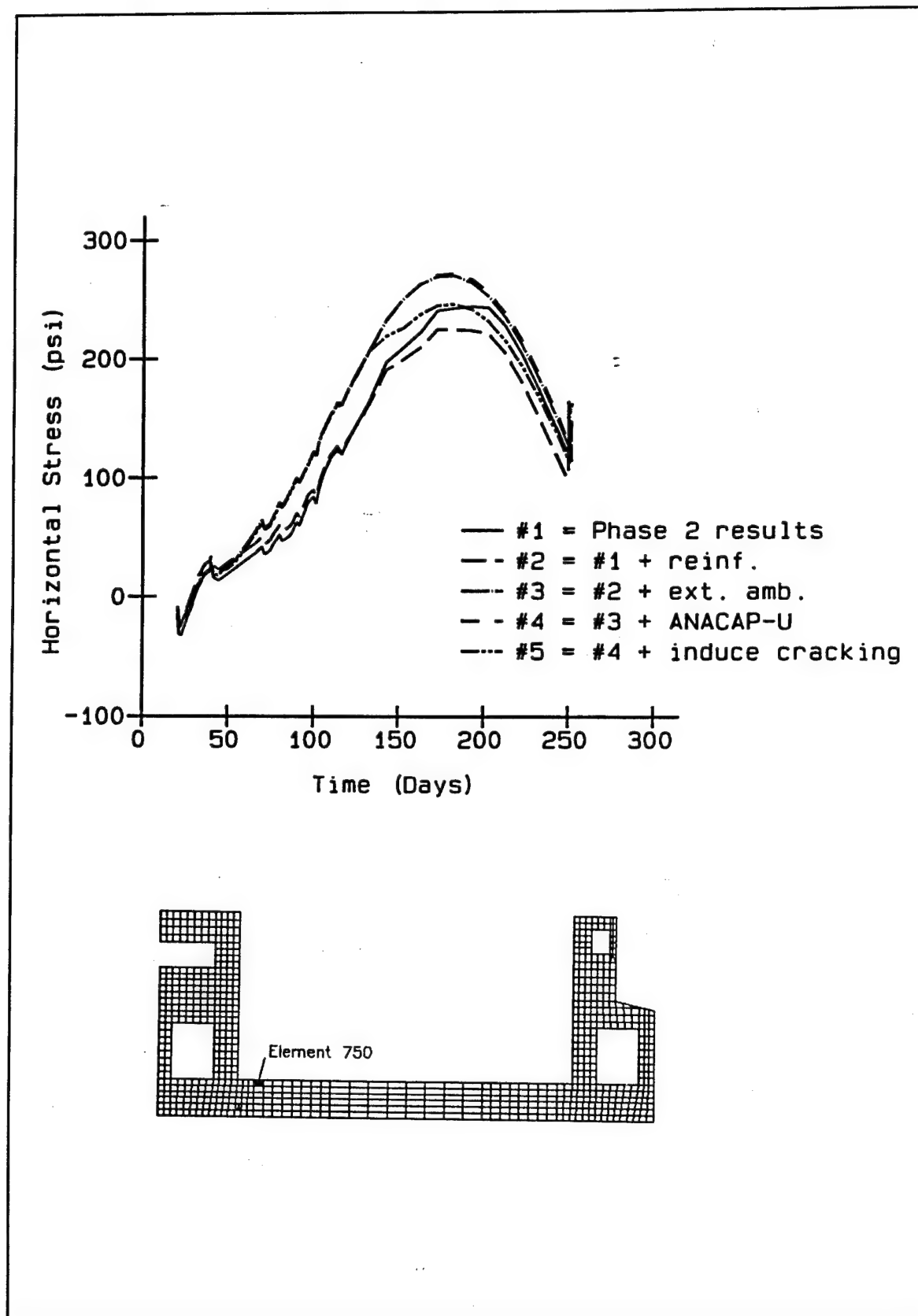
Figure 98.   Time history of horizontal stress at integration point 3 of element 750
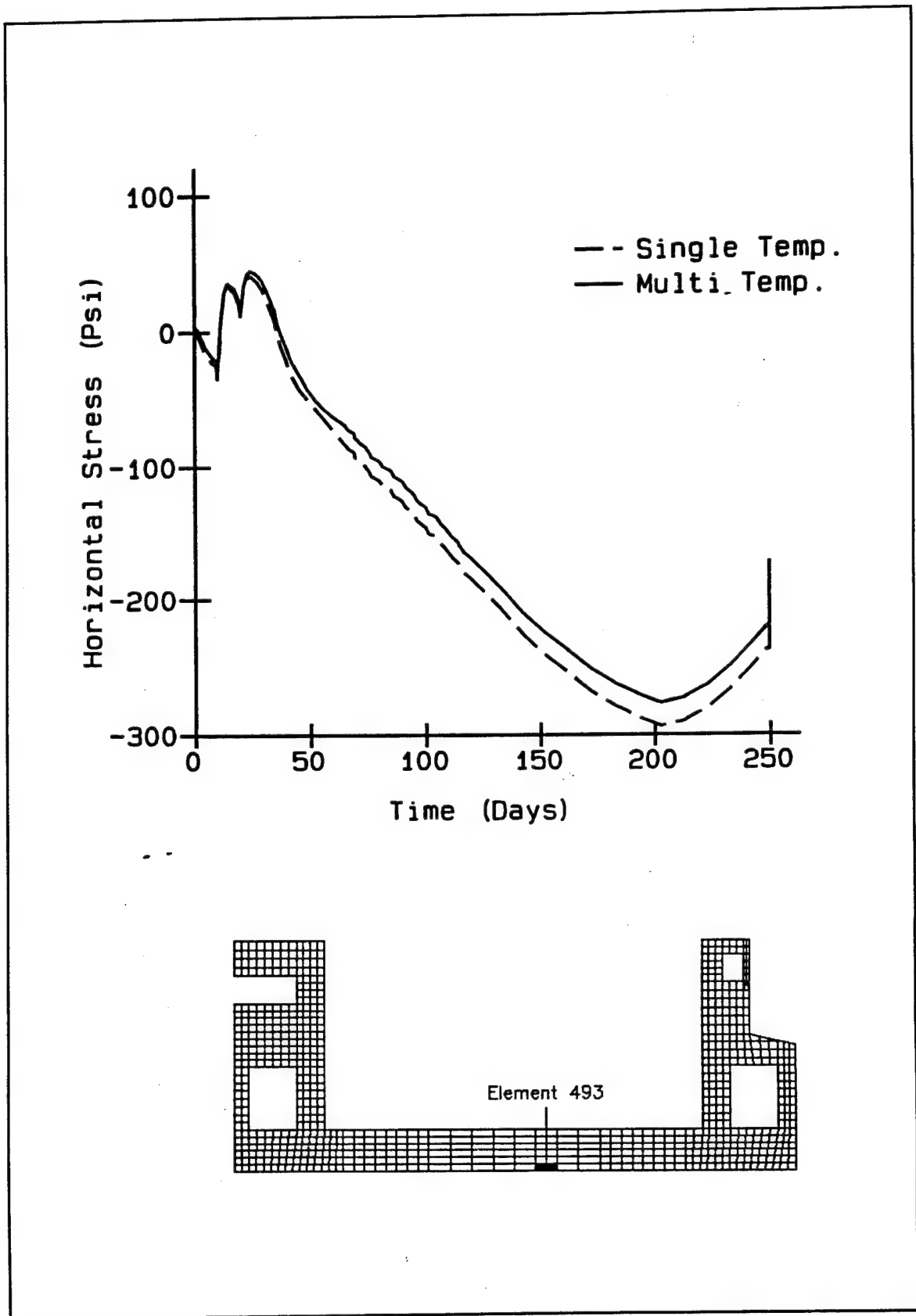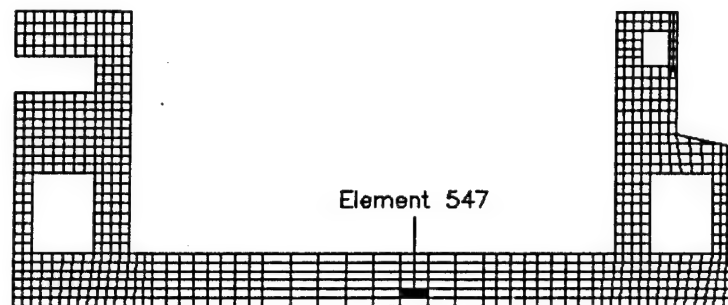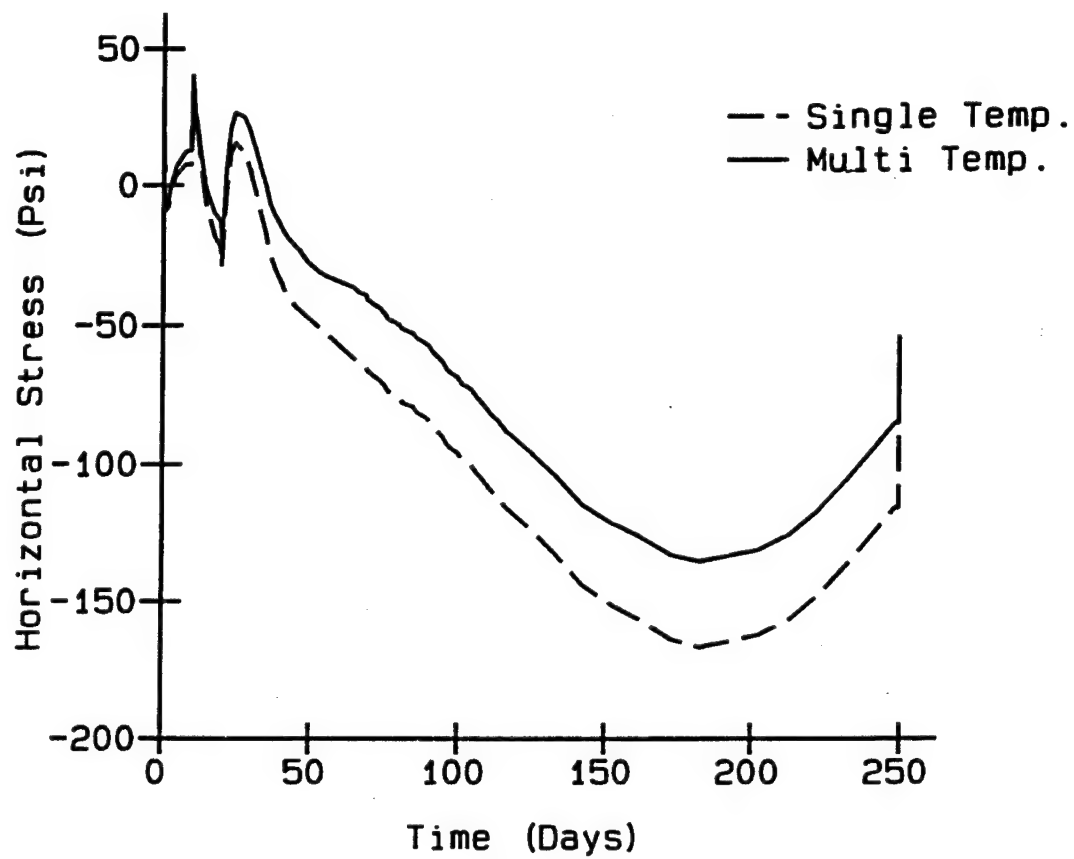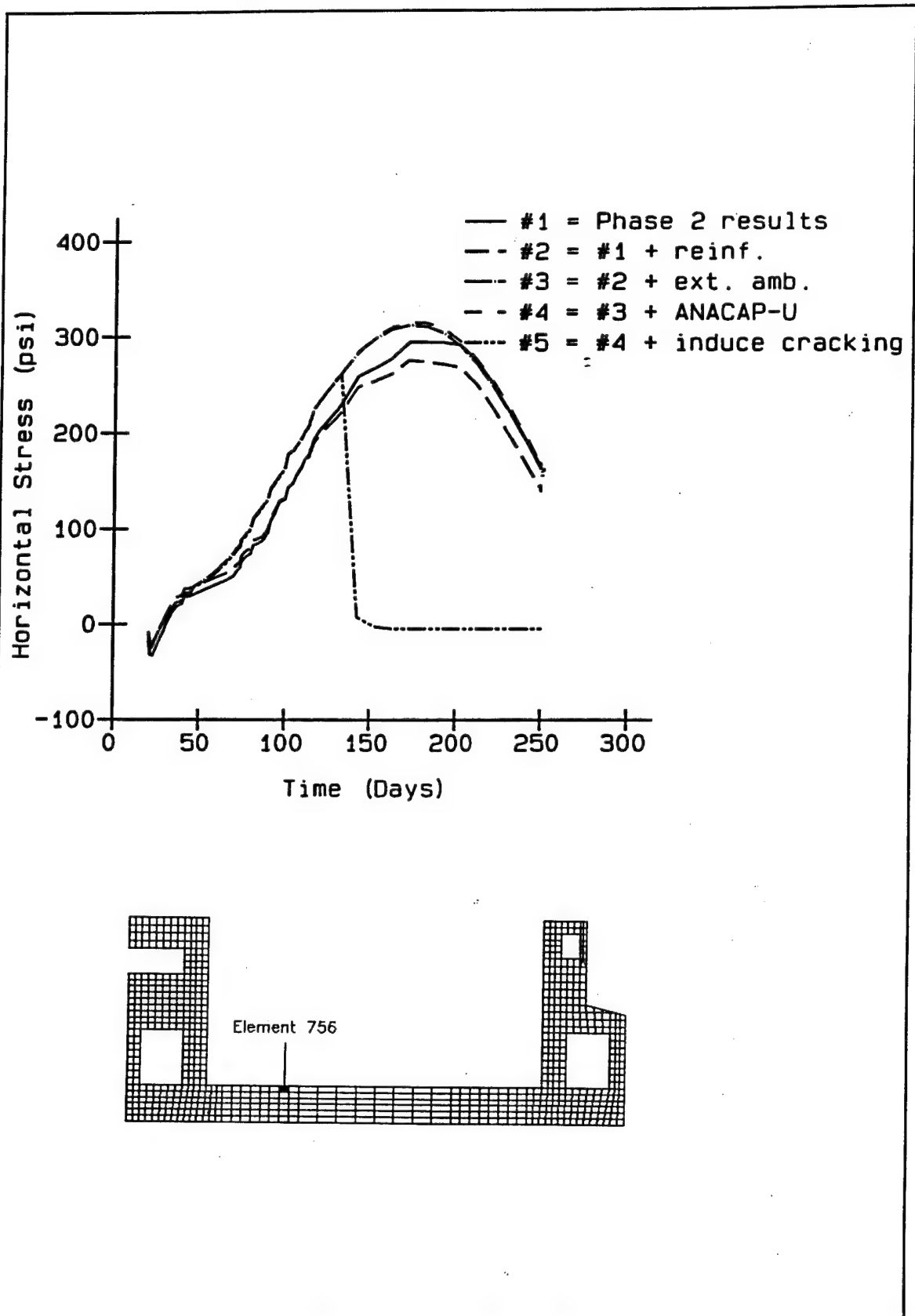
Figure 99.   Time history of horizontal stress at integration point 3 of element 756
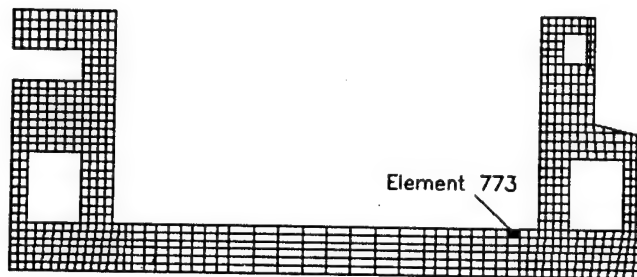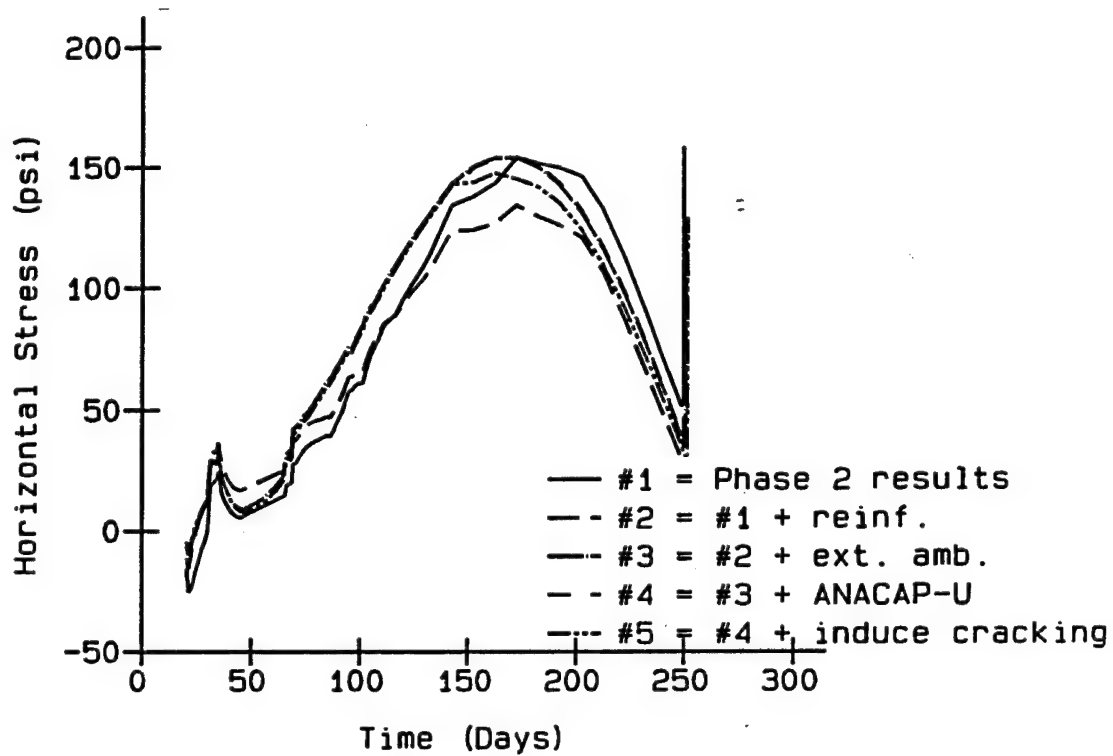
Figure 100. Time history of horizontal stress at integration point 4 of element 773

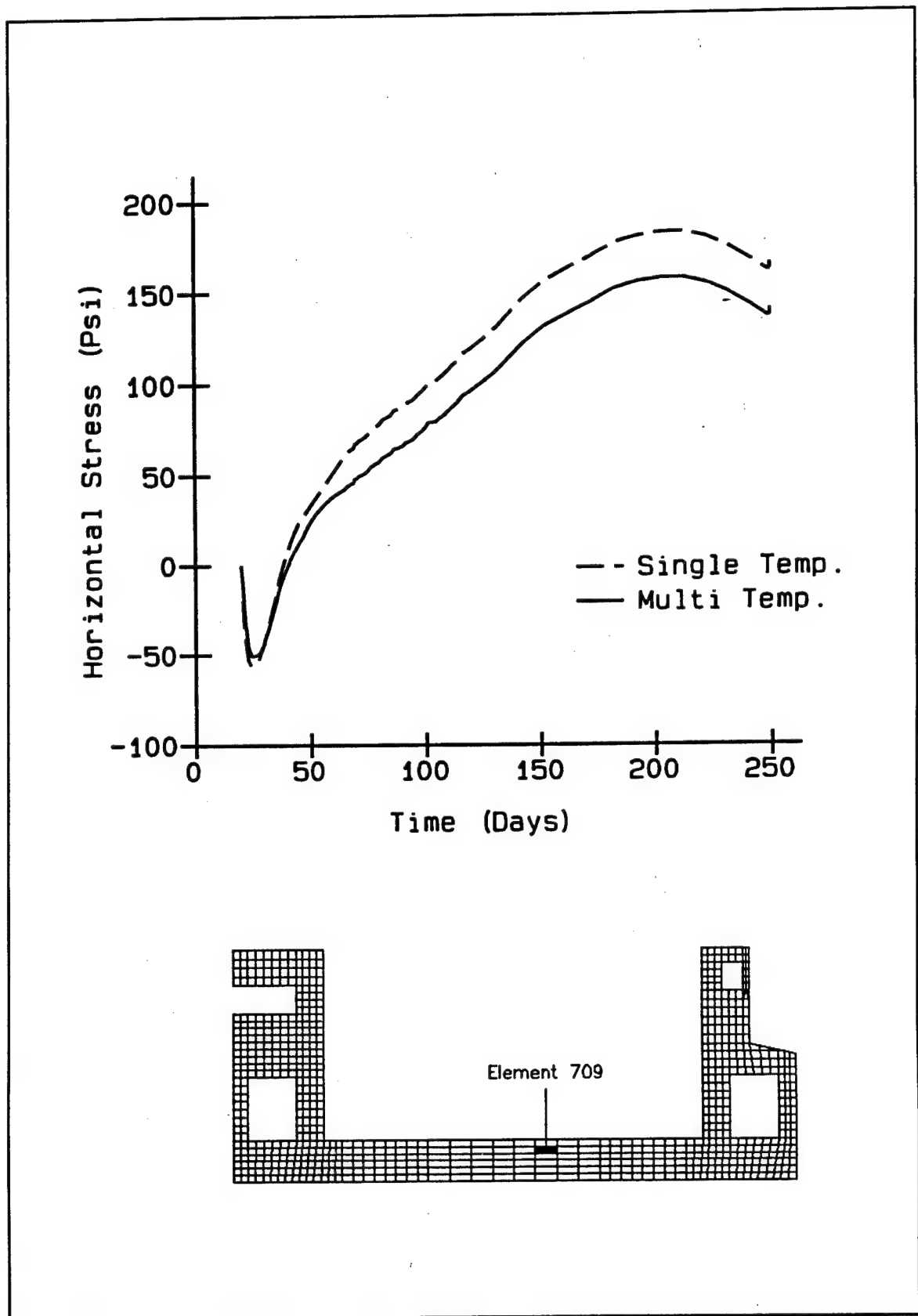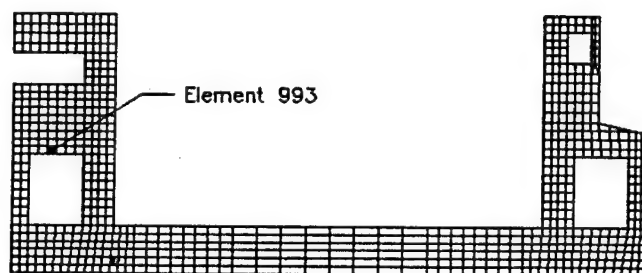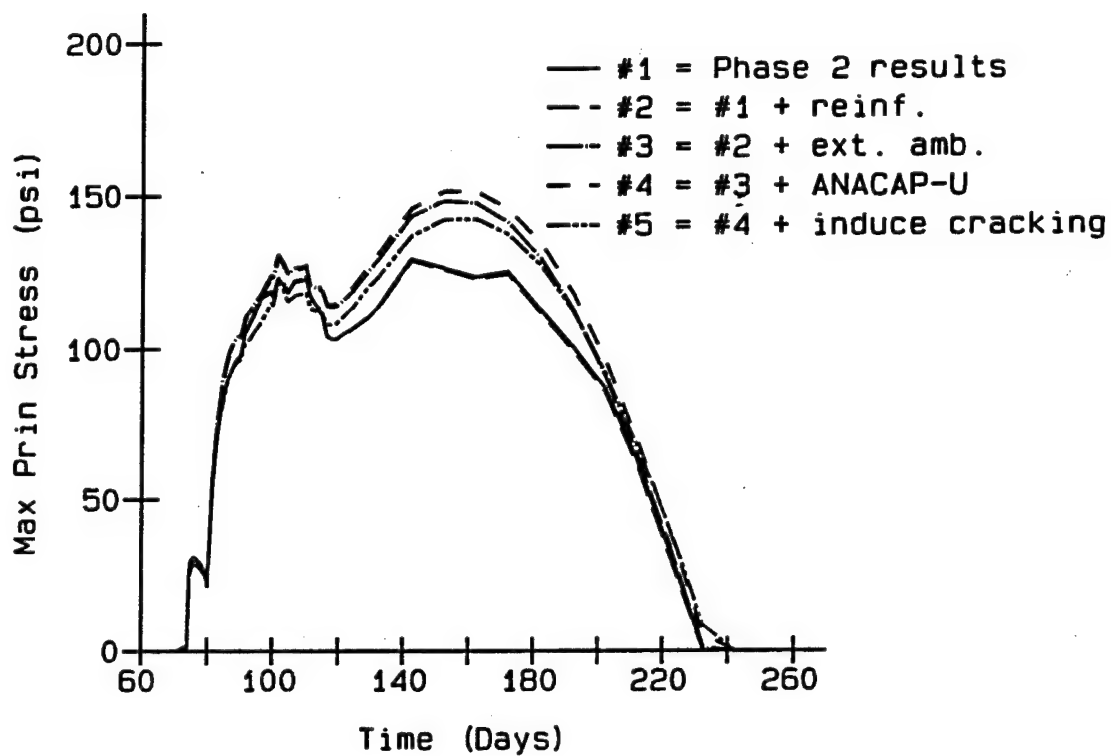Figure 101. Time history of maximum principal stress at integration point 2
of element 993
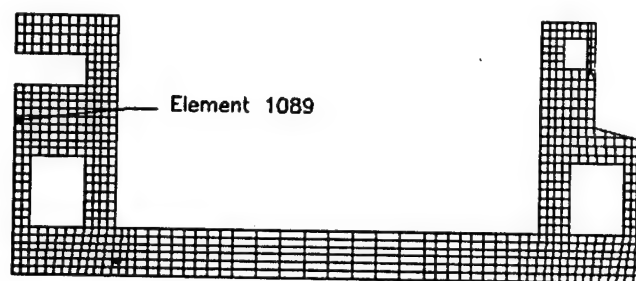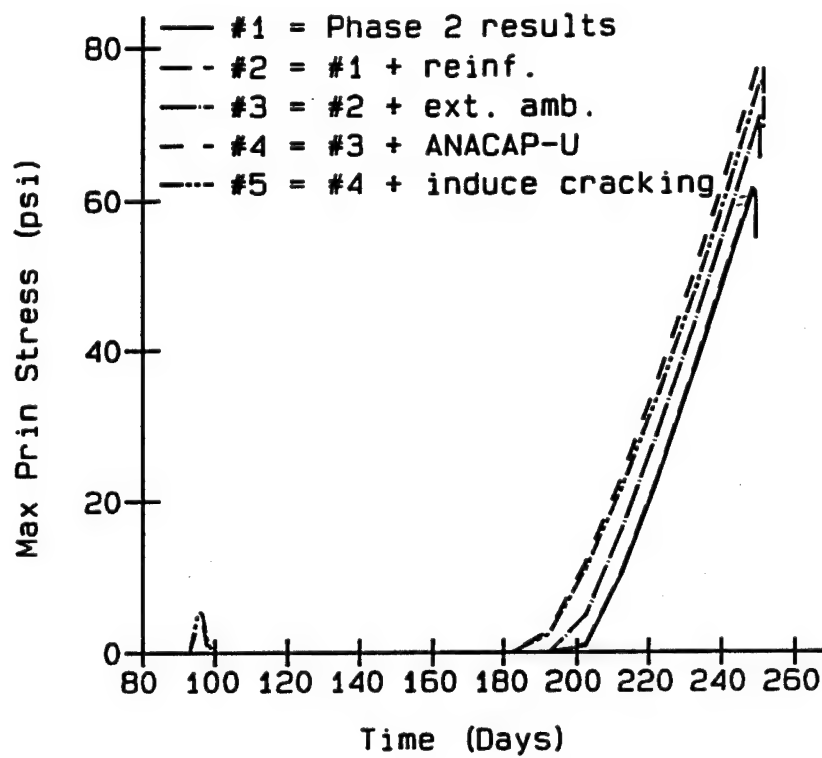
Figure 102. Time history of maximum principal stress at integration point 2 of element 1089
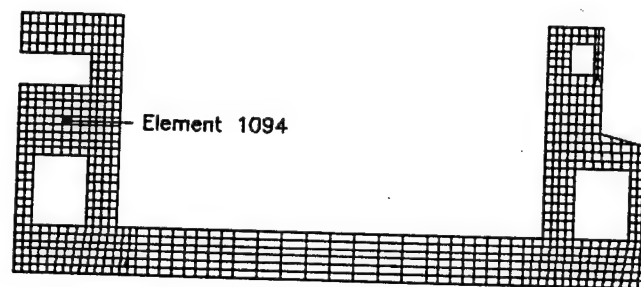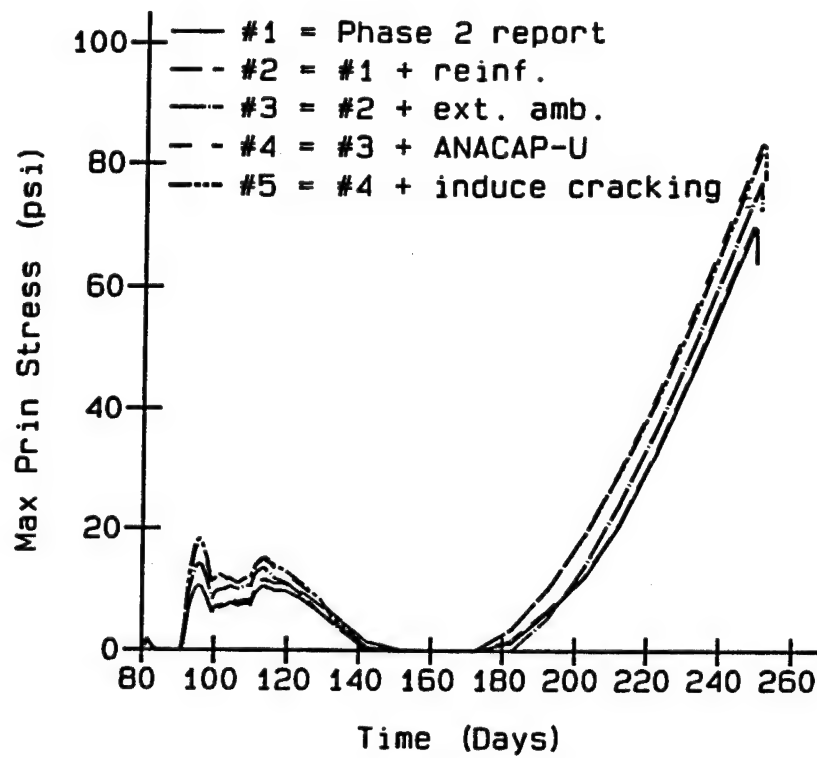
Figure 103. Time history of maximum principal stress at integration
point 1 of element 1094
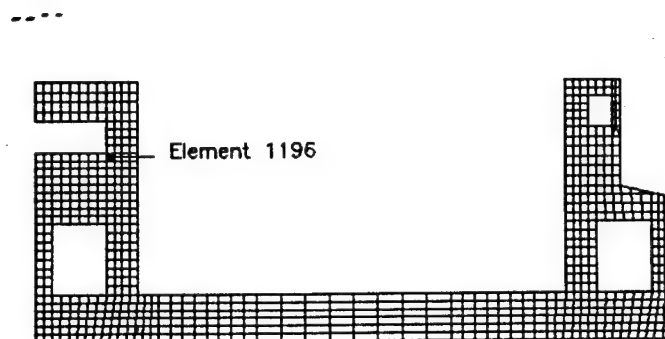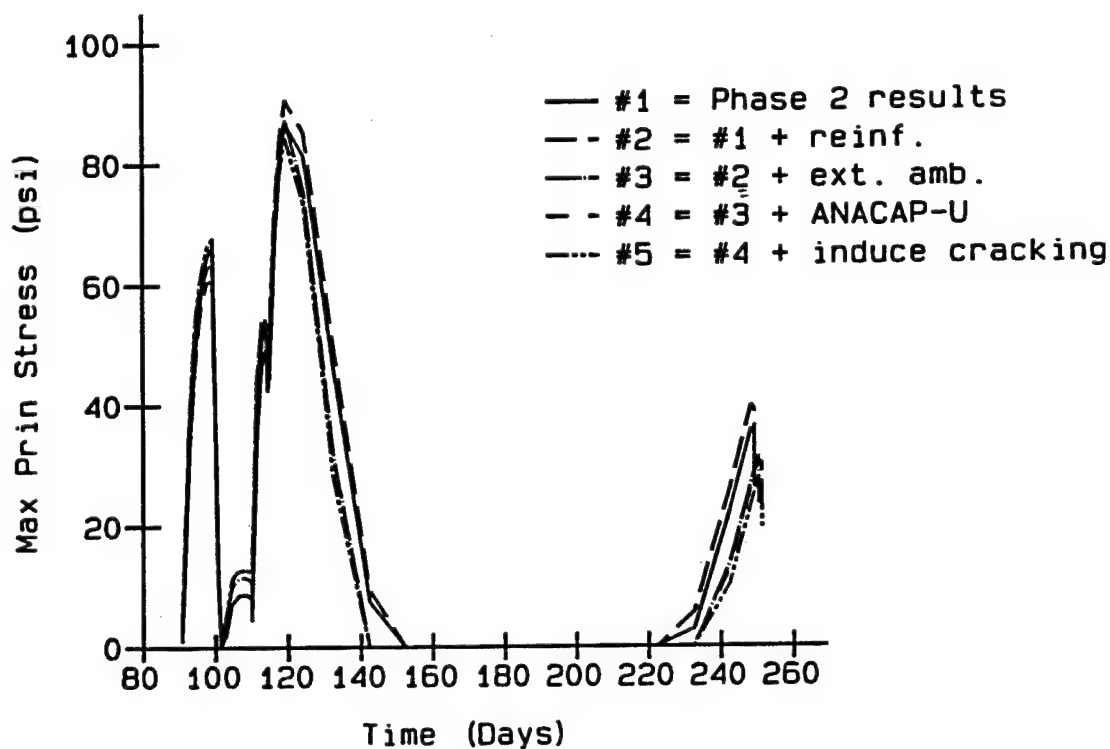
Figure 104.   Time history of maximum principal stress at integration point 4
of element 1196
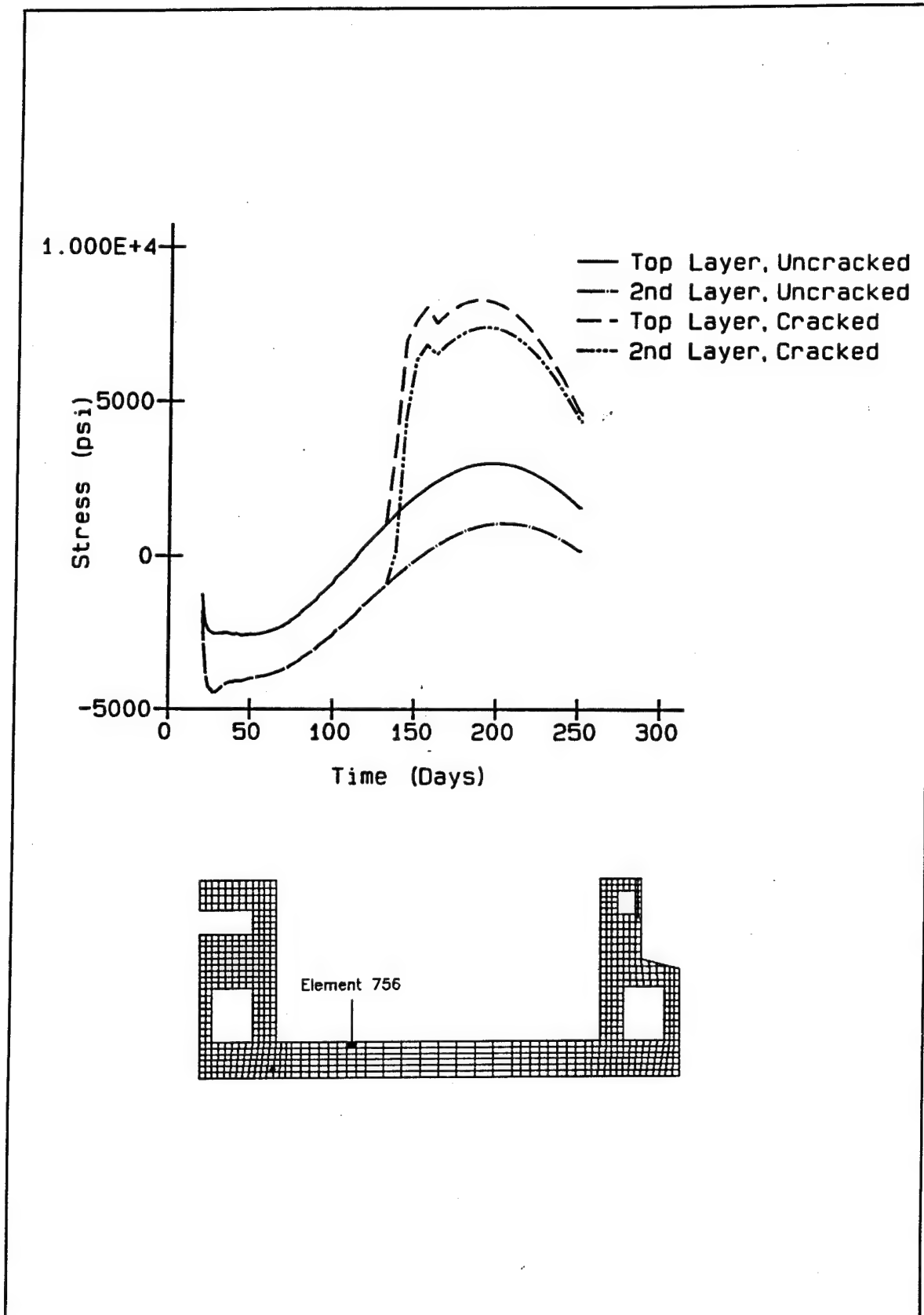
Figure 105. Time history of stress in reinforcement for element 756
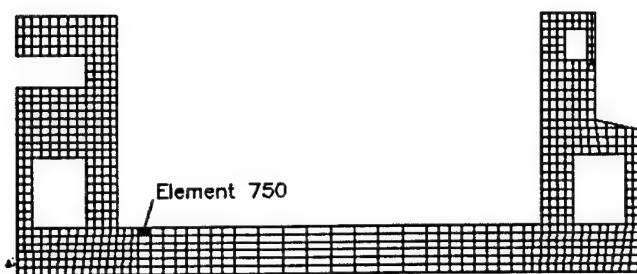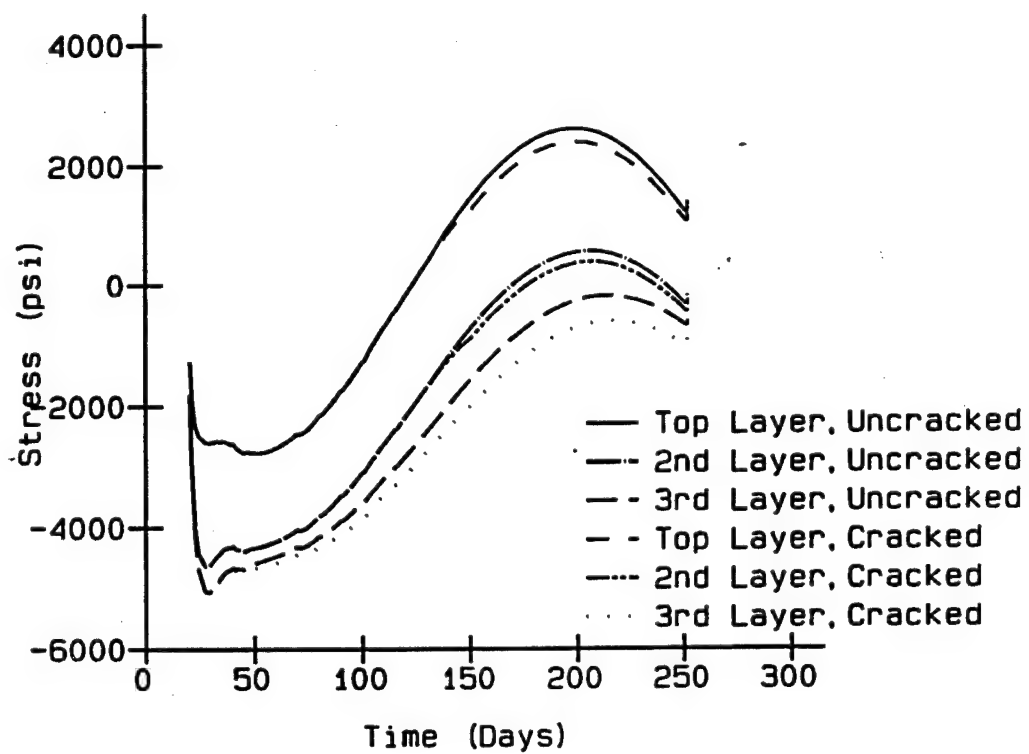
Figure 106.   Time history of stress in reinforcement for element 750
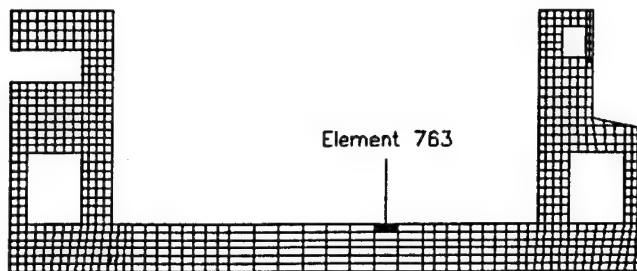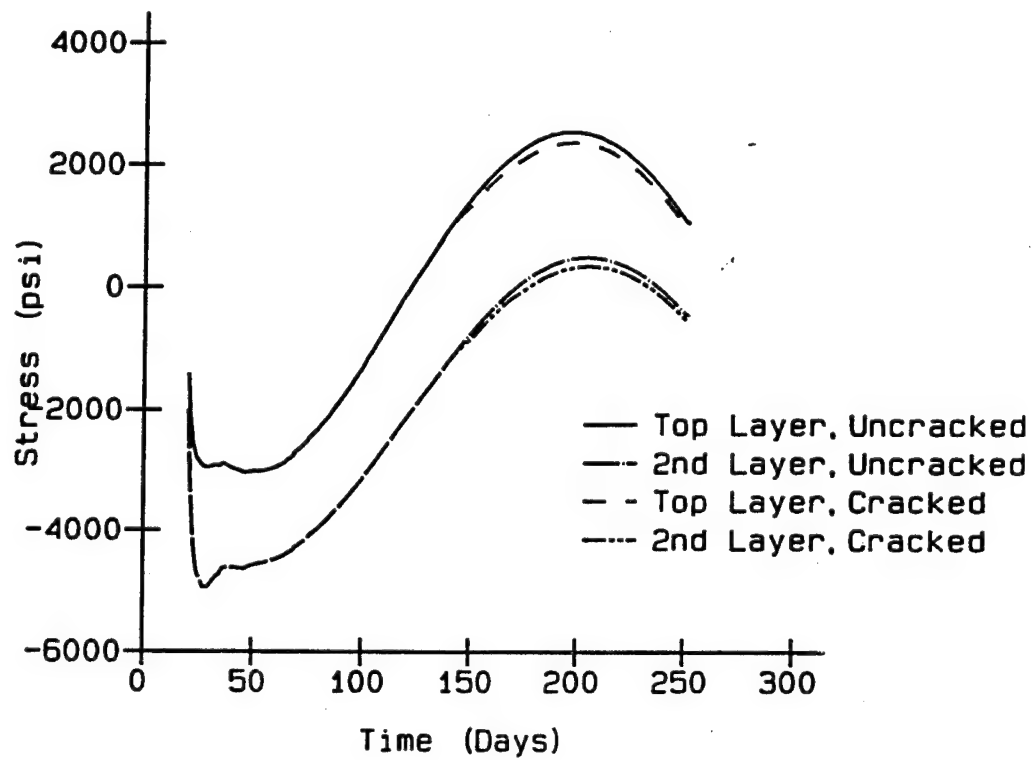
Figure 107.   Time history of stress in reinforcement for element 763
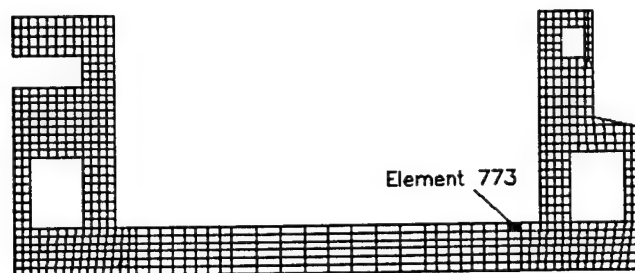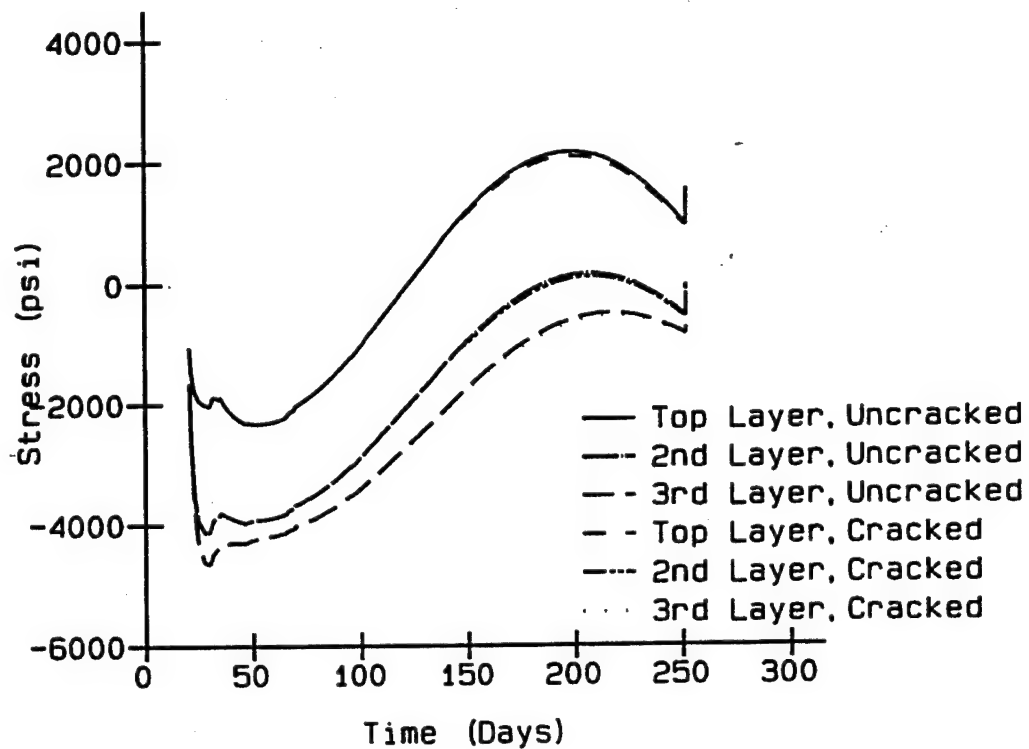
Figure 108.   Time history of stress in reinforcement for element 773
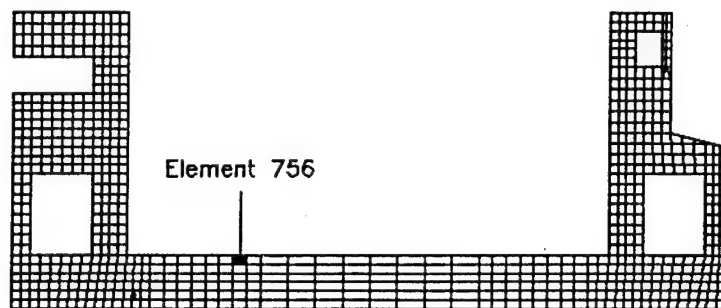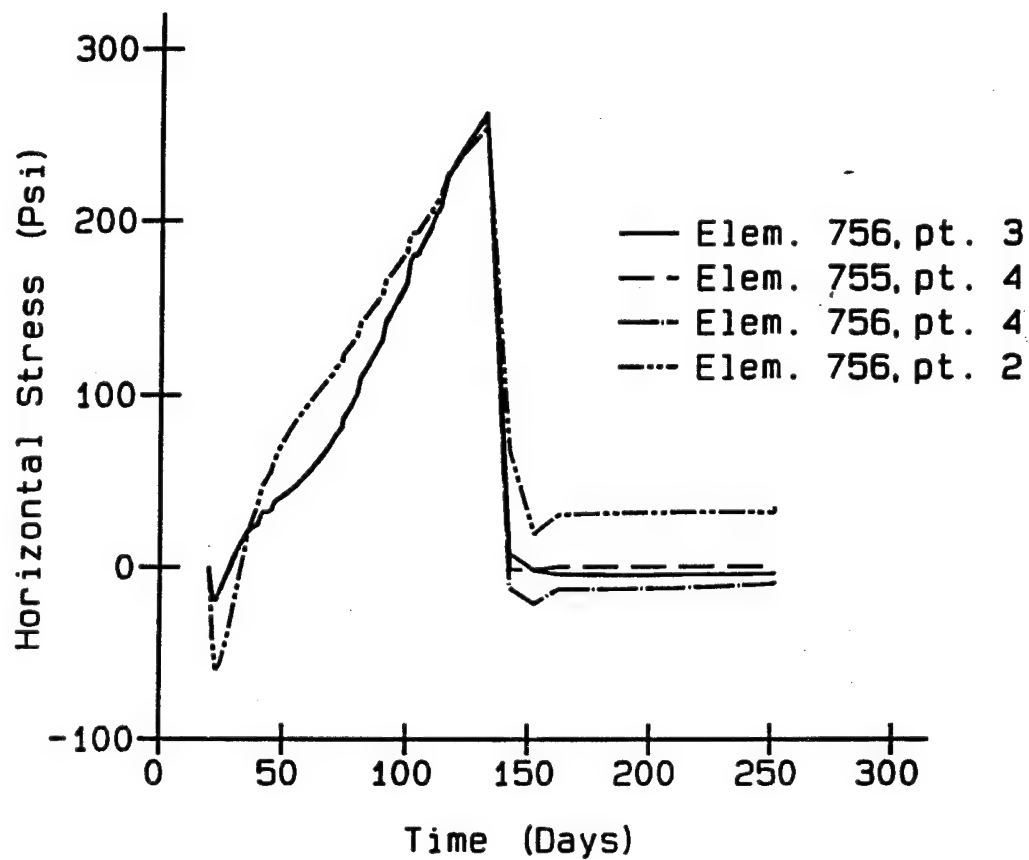
Figure 109.   Time history of stress in concrete around crack location
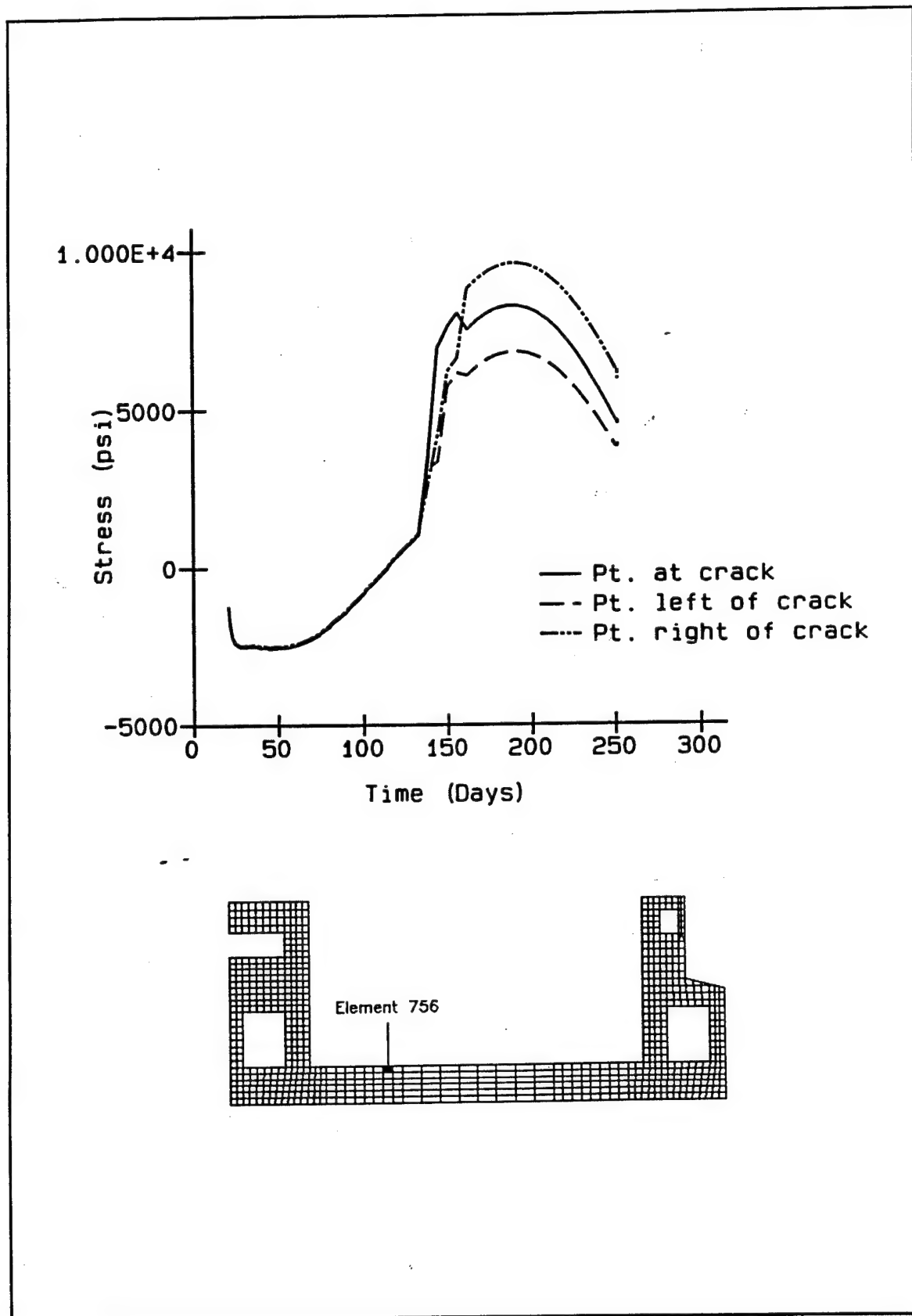
Figure 110. Time history of stress in reinforcement around crack location

Analysis 1 -   Results from Phase II Olmsted NISA study using mix-
               ture 11, load case 5, average ambient conditions, no rein-
               forcement, 100 microns for cracking strain, WES
               UMAT material model

Analysis 2 -   Analysis 1 parameters except reinforcing is added

Analysis 3 -   Analysis 2 parameters with extreme ambient conditions
               instead of average ambient conditions

Analysis 4 -   Analysis 3 parameters except the WES UMAT is re-
               placed with the UMAT licensed from ANATECH Re-
               search Corp.

Analysis 5 -   Analysis 4 parameters except the cracking strain is re-
               duced from 100 microns to 50 microns

Close examination of the figures will indicate that the addition of rein-
forcing in Analysis 2 did reduce maximum stresses to some degree. The
effect of the reinforcing is much more evident in Figures 94-100 which
are time history plots in the base slab. Some differences can be recog-
nized between Analyses 1 and 2 in Figures 101-104 for points in the wall
but the change is very small. The change is larger in the slab because the
amount of reinforcing added is significantly higher than was used in the
walls and, therefore, the stiffness added from the reinforcement is signifi-
cantly higher.

Comparison of Analysis 2 and Analysis 3 should correlate directly with
comparisons made in Chapter 4 when comparing the average ambient con-
dition and the extreme ambient condition. This change, of course, has a
significant effect on the results but since these changes were discussed in
Chapter 4 no further discussion will be given for these two analyses.

Small changes exist when looking at the differences between Analy-
ses 3 and 4. The change between these two analyses is simply a change
in the material model used in the analysis. Analyses 1, 2, and 3 all used
the WES version of the UMAT material model which was developed by
ANATECH Research Corp. and purchased by WES in 1987. Since that
time ANATECH has updated the code and Analysis 4 makes use of the up-
dated code. Differences noted in the plots between Analyses 3 and 4 can
be primarily attributed to changes in some of the algorithms used in the
program. One of the reasons for performing the reinforcing and crack
analyses with the new version of the material model was because the up-
dated version incorporated changes which corrected inconsistencies in the
failure criteria used in the previous version.

Significant differences between Analyses 4 and 5 can be seen in some
of the plots. Analysis 5 lowers the threshold of cracking by 50 percent so
that the effect of cracking could be evaluated with respect to how the rein-
forcing behaves after cracking. The primary crack occurs in the slab at

144

integration point 3 of element 756 at approximately 140 days into the analysis. Crack plots show the crack for the first time at day 143 and the initial cracks in the slab can be seen in Figure 111. Figure 112 shows the cracks 20 days later (day 163) and how they have propagated. The cracking pattern seen in Figure 112 does not change throughout the remainder of the analysis. A more detailed look at the cracking which occurs in this portion of the slab is shown in Figure 113. In addition, Figure 114 shows cracking which begins occurring in the land wall side of the slab at day 163. Figure 115 shows the cracking 20 days later. As in the other side of the slab the crack stops propagating after the second set of cracks form. Figure 116 shows an enlarged view of the cracks seen in Figure 115.

In the time history analyses the effect of the crack on the stresses is most apparent in Figure 100 where the stress drops off to zero after the
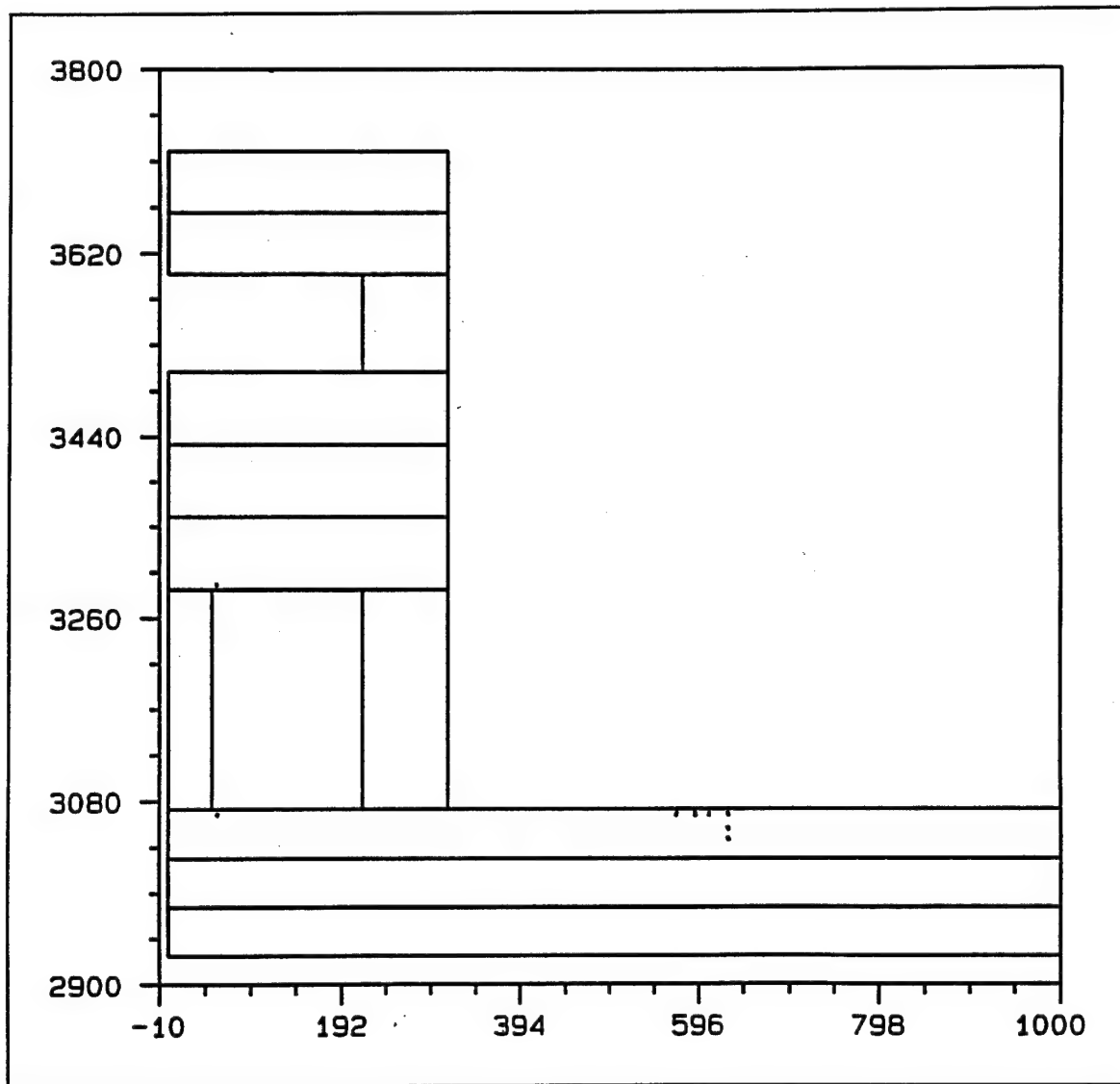
Figure 111. Crack pattern at day 143 of the center wall half of the monolith
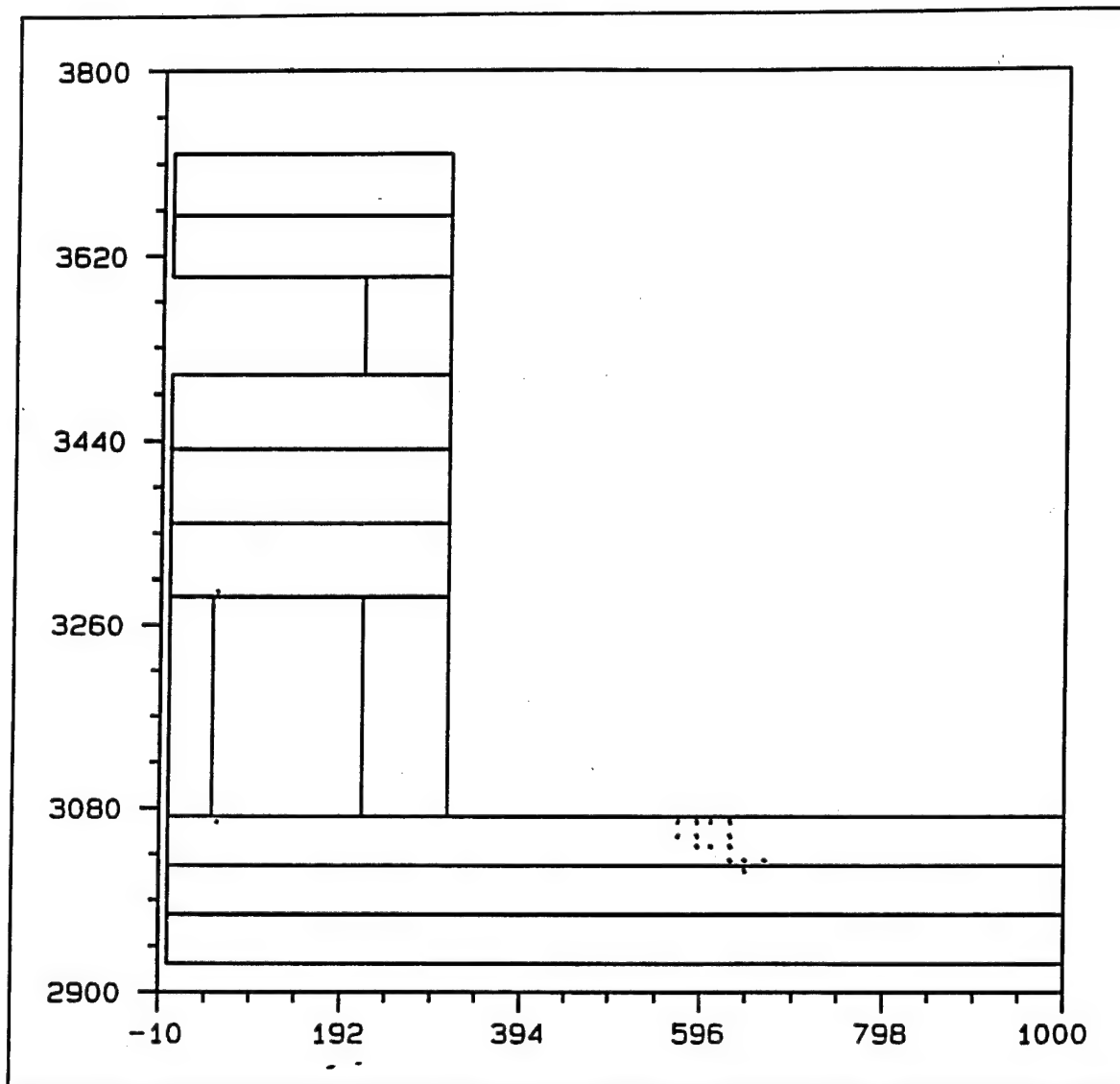
Figure 112.   Crack pattern at day 163 of the center wall half of the monolith

crack occurs. The affect of the crack can also be seen at other points such as in Figures 94, 97, 98, and 100. Results from Analyses 4 and 5 coincide until the point at which the crack occurs. Once the crack occurs, a drop in stress occurs at each one of the points shown in the previously mentioned figures. This drop in stress is a result of the fact that the stresses in the slab are primarily thermal induced and, therefore, when a crack occurs the energy stored is simply released and does not have to be carried by a different point in the structure as would be the case for a mechanically induced load. Therefore, when a crack occurs at the top of the slab all of the remaining points in the slab will undergo some reduction in stress.

A crack also occurs in the center wall at the corner of the culvert as seen in Figure 117 at approximately 85 days into the analysis. In the time history plots shown of the wall, the effect of this crack can be seen primarily in Figure 101 where after day 83 of the analysis the plot for Analyses 4

146
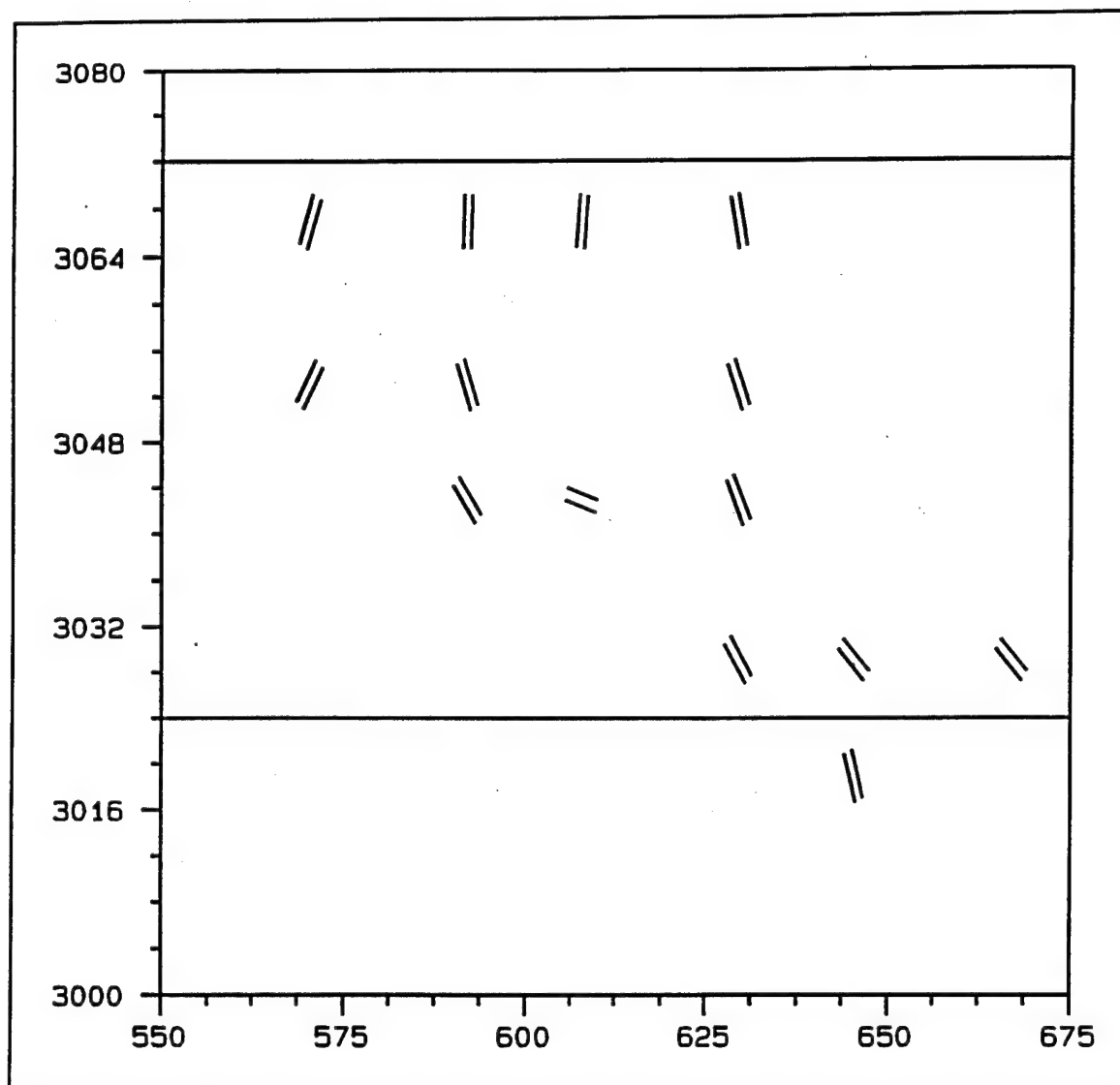
Figure 113.   Enlarged view of the final crack pattern in the slab of the center wall half of the monolith

and 5 separate. Smaller differences can be seen in Figures 102-104. If actual criteria were being used in Analysis 5, the crack shown in Figure 117 would not be a major concern since it does not propagate. A good remedial measure to take during construction of the monolith would be to place diagonal bars at the corners of the culvert to ensure a crack such as this one does not propagate.

A crack also shows up underneath the culvert at day 133 of the analysis as seen in Figure 118 but it also does not propagate past the point shown in the figure. In addition, effects of this crack forming do not appear to affect resulting stresses in the chamber portion of the slab or the wall based on the time histories presented.
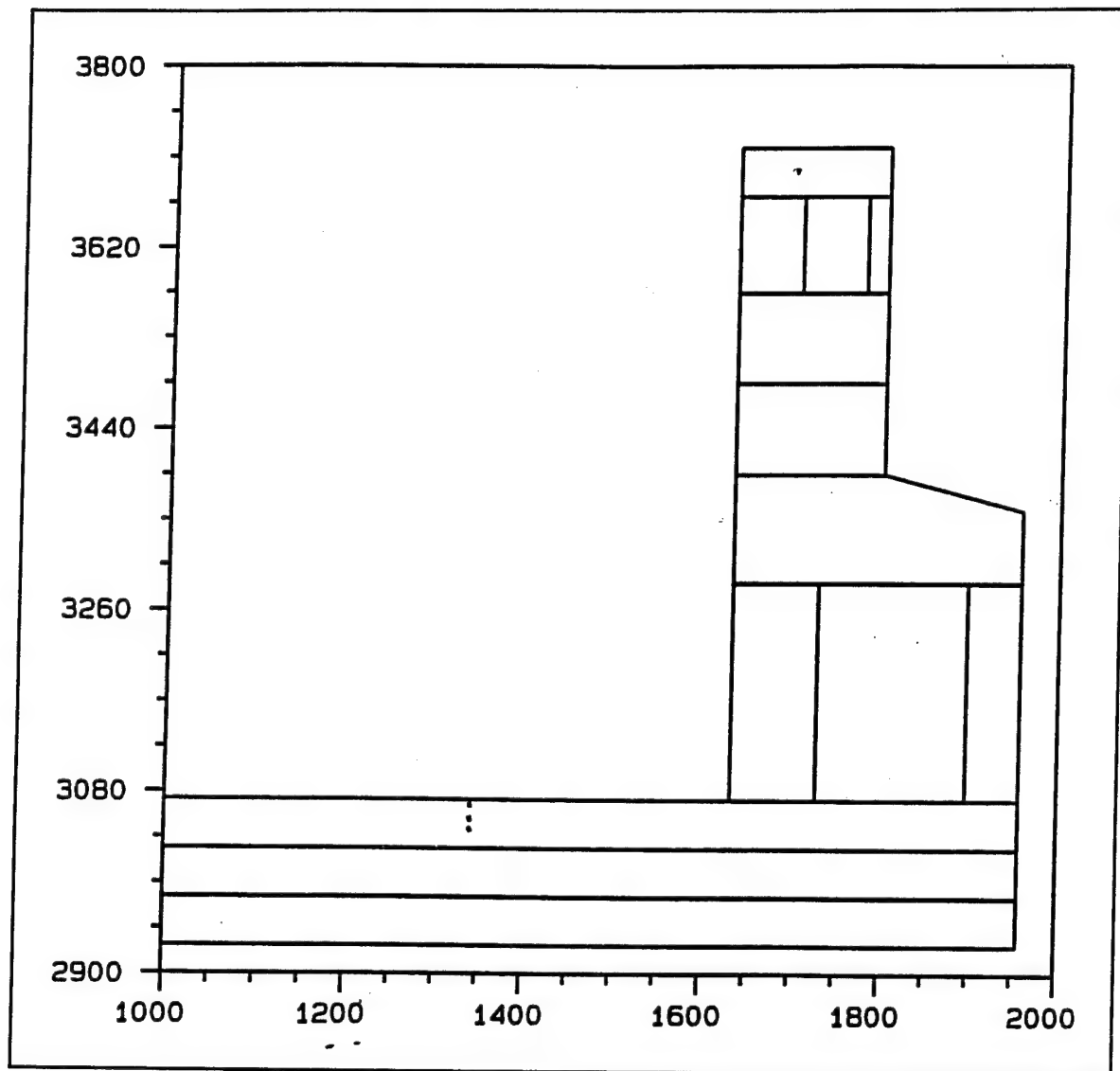
Figure 114. Crack pattern at day 163 of the land wall half of the monolith

Stresses in the reinforcing can also be evaluated. Figures 105-108 are time history plots of the stress in the reinforcement for both Analysis 4 (uncracked) and Analysis 5 (cracked). The most discernible affect of the reinforcing can be seen in Figure 105 which is a plot of the reinforcing at the actual location of the crack in the slab. As can be seen in this figure, for the uncracked case the stresses in the reinforcing follow the same trend due to ambient conditions as was observed for the concrete stresses. For the cracked case, though, the time when the crack occurs is obvious and the increase in stress is due to the release of the load that was in the concrete into the reinforcement. Once the crack occurs and the solution stabilizes, then the stresses in the reinforcement again begin to be driven by the ambient conditions. Away from the crack, the stresses in the reinforcing are relieved when the crack occurs (Figures 115-117) for the same reason the stresses were relieved in the concrete when the crack occurred.
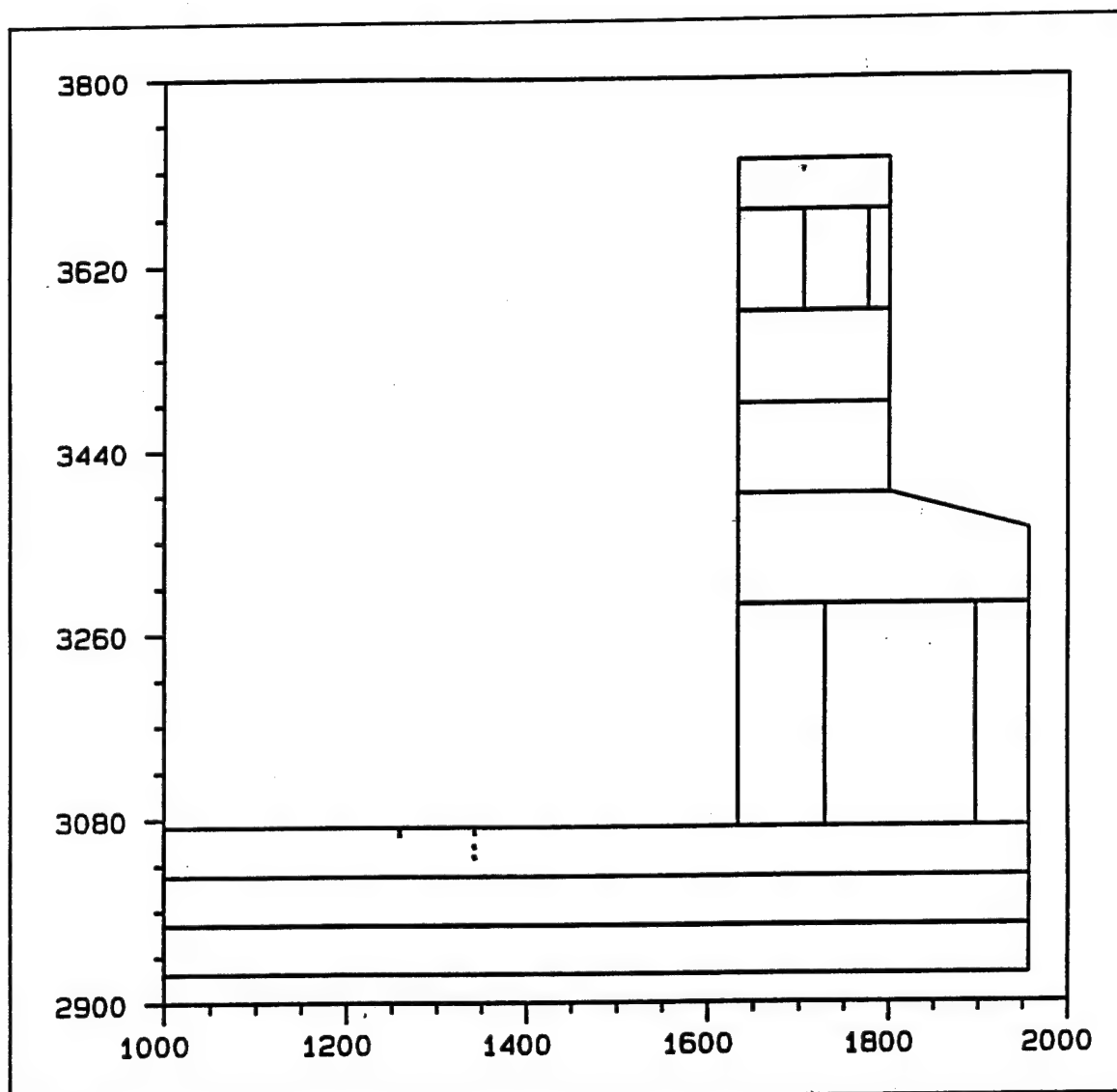
Figure 115.   Crack pattern at day 183 of the land wall half of the monolith

Finally, some points around the crack location are plotted for the concrete (Figure 109) and for the reinforcement (Figure 110). As can be seen in Figure 109, even though integration point 3 of element 756 was the point that cracked, the stresses immediately around this point also went to zero as well. Likewise, in Figure 110 it can be seen that reinforcing at points next to the crack location had significantly increased stresses at the time the crack occurred.

Evaluation of results

The results of the reinforcement and cracking study indicate that reinforcement is a valuable tool for including in a NISA. The reinforcing behaved in a manner that was expected and provided the capability for which it is intended. It should also be noted that when the crack did occur
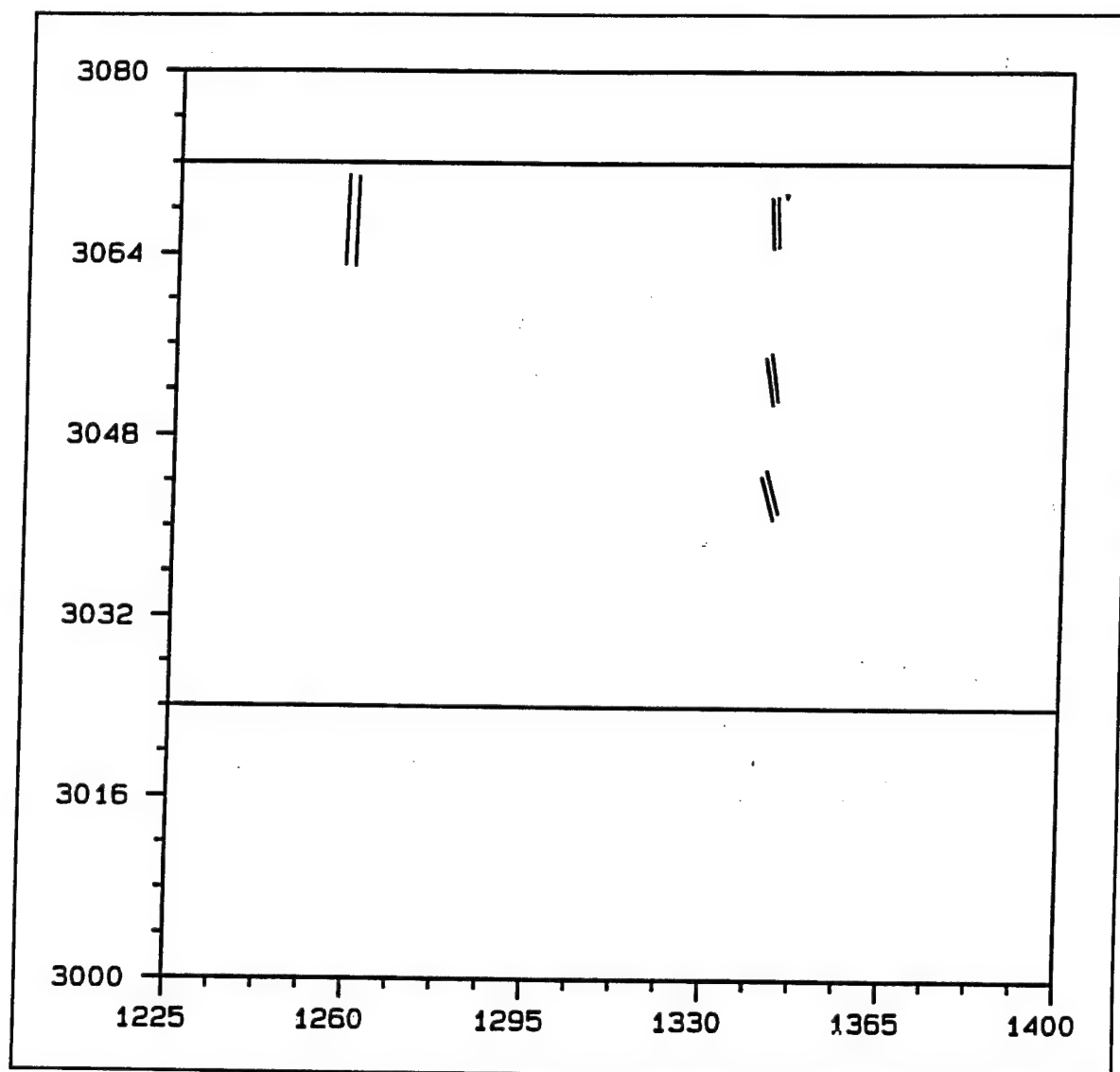
Figure 116. Enlarged view of the final crack pattern in the slab of the land wall half of the monolith

in the slab that the resulting stresses in the reinforcing were not excessive. The maximum stress observed in the reinforcing was approximately 10 ksi. Reinforcing with a yield strength of 60 ksi is typically used in construction and, therefore, a stress of 10 ksi in the reinforcing is of little consequence to the behavior of the structure.

If the criteria being used to predict the cracks shown were the actual criteria being used to evaluate the structure instead of the 50 percent reduced value, the cracks shown in Figures 111-116 would have to be evaluated carefully. During such an evaluation, a decision would have to be made as to whether the cracking shown was acceptable or if a change in construction parameters (e.g. placing temperature) was needed. A part of this decision-making process would be, of course, the resulting stresses observed in the reinforcing. In this particular case, the fact that stresses in

150
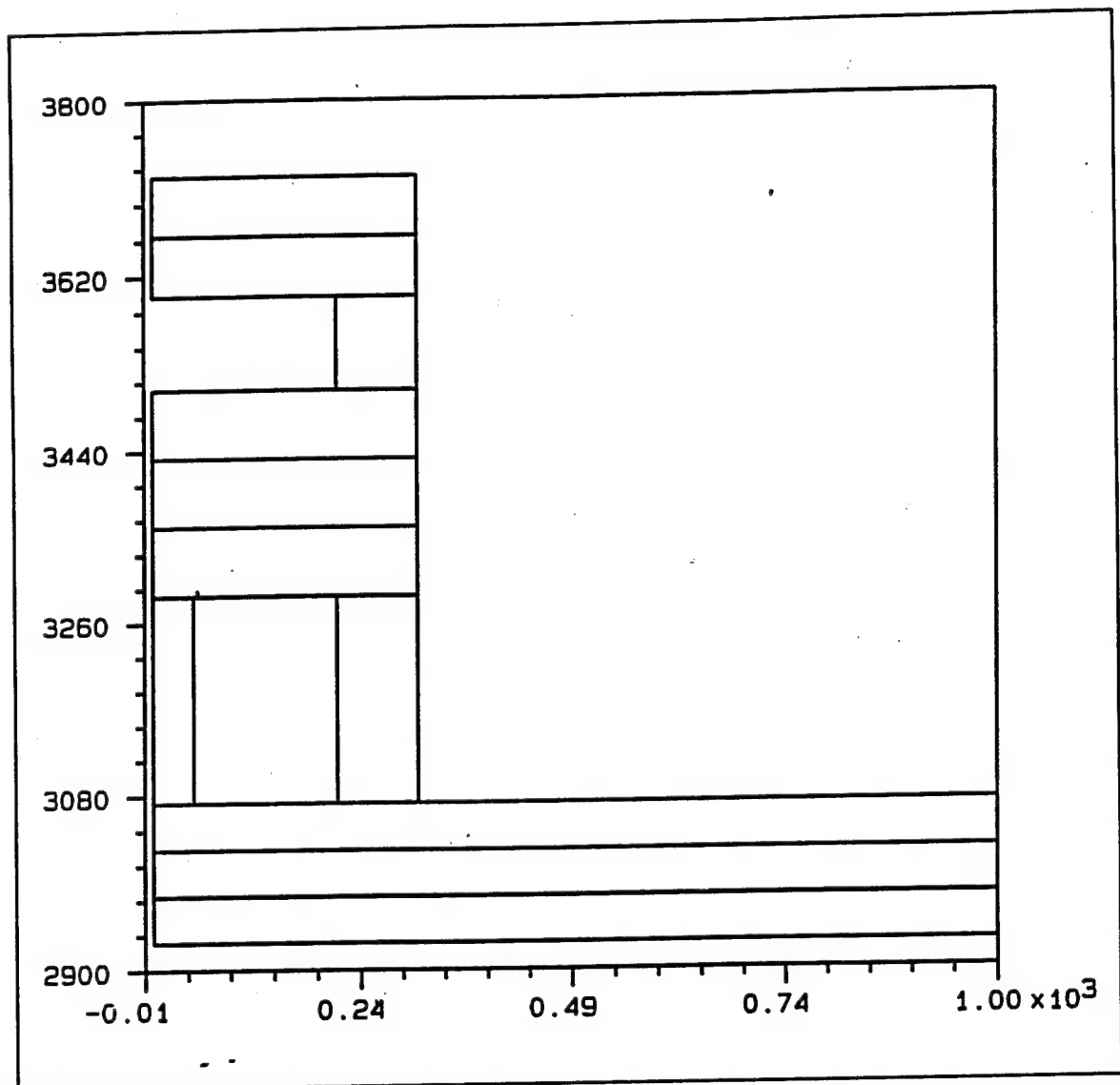
Figure 117. Crack pattern at day 85 of the center wall half of the monolith

the reinforcing were low compared to allowable stresses would have to be weighed against the magnitude of cracking occurring at the one location in the slab.

Lift Placement Interval Study

Lift placement intervals not only affect the time required to construct a chamber monolith but also the stresses within the structure. The effect on stress was observed when the lift interval in the floor slab was reduced from 10 days to 5 days. This reduction was possible when the monolith length was shortened in order to eliminate the vertical construction joints in the floor slab. This study evolved from 5- and 10-day interval comparisons to include analyses for 30-day lift intervals. The 30-day interval was
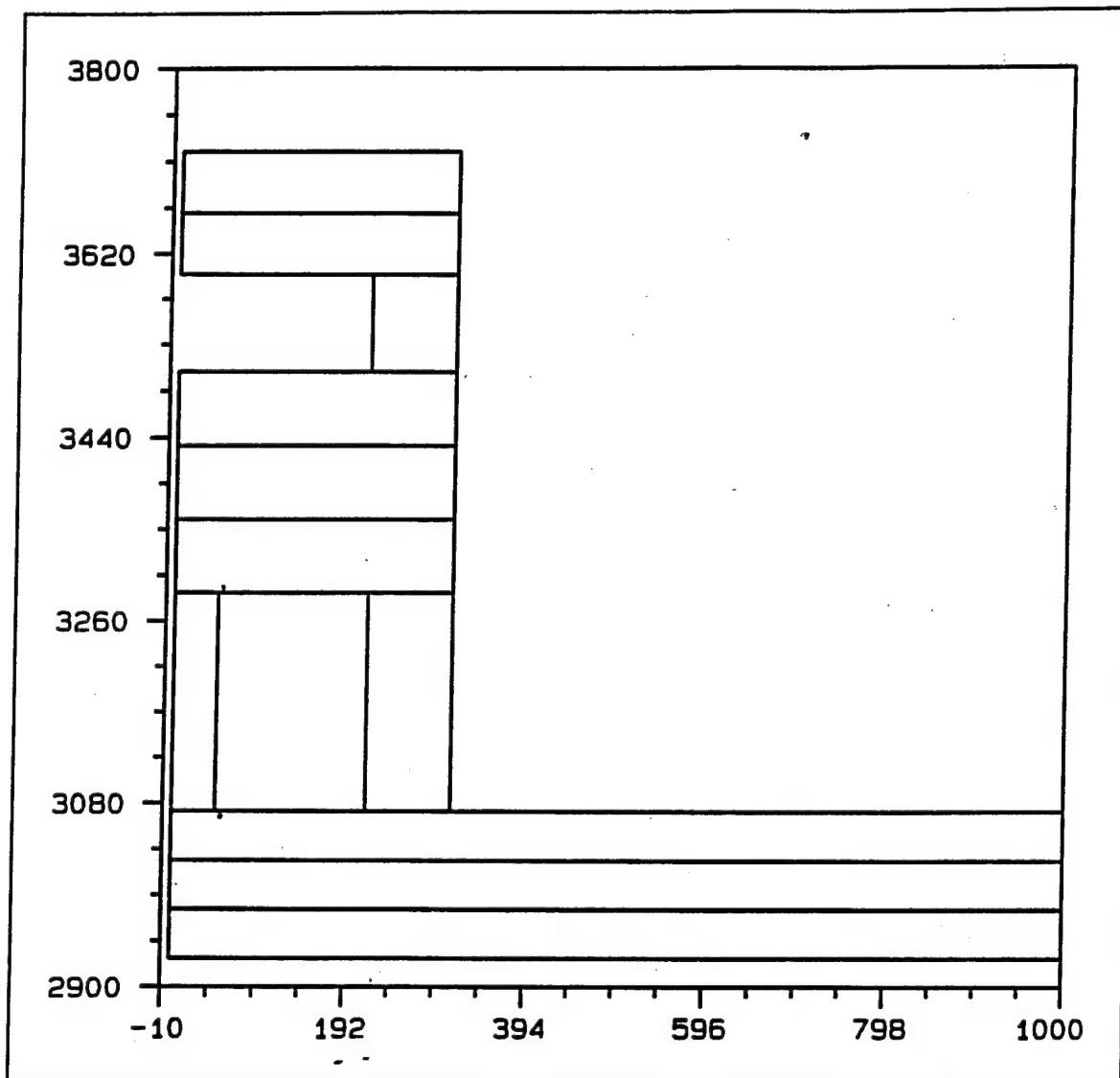
Figure 118. Crack pattern at day 133 of the center wall half of the monolith

selected to account for variations in placement intervals due to contractor construction schemes and delays during construction.

Objective

The objective of this part of the study is to determine the effect lift placement intervals have on structural performance and to recommend interval limits based on these findings.

Analysis parameters

The following parameters were used in all analyses conducted for this study. Load case 5, concrete mixture 11 properties, as discussed in

Chapter 1, and the UMAT subroutine modified to automatically select the stress-free temperature as the temperature obtained from the first step after lift initialization were also used in each analysis.

Ambient temperature. Analyses for this study used the same average ambient temperature curve as used in Olmsted NISA Phases I and II and not the extreme ambient temperature curve described in Chapter 4. The average ambient temperature curve is shown in Figure 119.
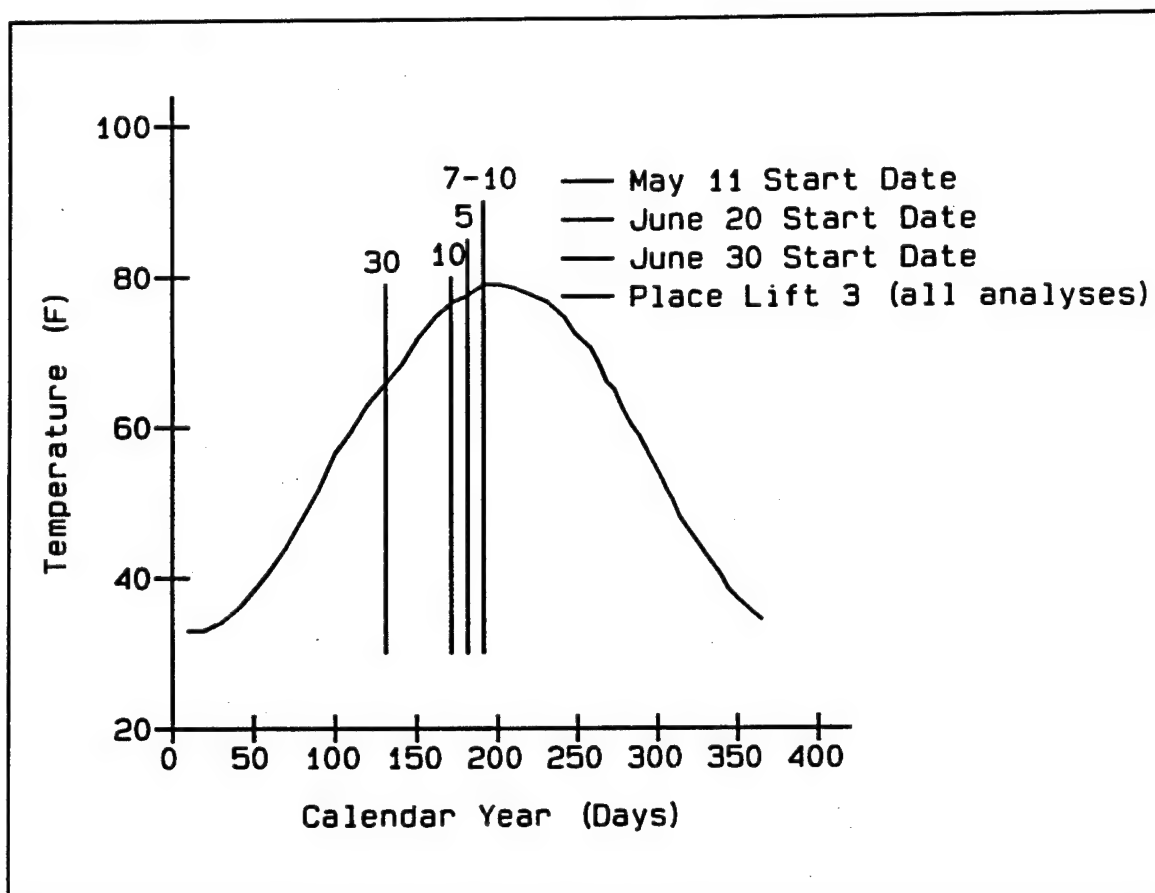
Figure 119. Average ambient temperature curve with start dates

Lift interval. Wall lift intervals were prescribed to be 5 days while floor slab lift intervals varied from 5, 10, and 30 days for analyses in this study.

Start date. In order to minimize the affect of changing ambient temperature, different start dates for each lift interval analysis were determined. Lift 3 in the floor slab was fixed to be placed on Jul 10 for all analyses, the same day as in Olmsted Phases I and II. Placement of this lift at this time resulted in high tensile stresses in lift 3. Once the placement of lift 3 was set, new start dates based on lift placement intervals were calculated for each analysis. Table 24 shows the start date, placement day, and ambient temperature for each analysis. Figure 119 graphically

Table 24
Lift Interval Analysis Parameters

Model Lift	5-Day Interval			10-Day Interval			30-Day Interval		
	Start Date	Placement Day	Temp. °F	Start Date	Placement Day	Temp. °F	Start Date	Placement Day	Temp. °F
1	30 Jun	0	77.5	20 Jun	0	76.5	11 May	0	65.75
2	5 Jul	5	78.25	30 Jun	10	77.5	10 Jun	30	74.5
3	10 Jul	10	79.0	10 Jul	20	79.0	10 Jul	60	79.0

shows the start dates and date of lift 3 placement superimposed on the average ambient temperature curve.

Placement temperature. Placement temperature of 60 °F was specified. Based on results presented in Chapter 5, this placement temperature should yield conservative stresses in the floor slab.

Analyses

Results of analyses are presented for nodes 3117 and 3629 and for elements 702 and 756 in the slab. Figure 59 shows these locations. Time history plots of temperature and stress have been plotted relative to the placement of lift 3, day 0. This permits easier interpretation of results since the time axis aligns properly for all placement interval data after relative placement day 0. Temperature data are at the nodal points and stress data are at the element integration points.

All resultant data for each analysis were checked and only maximum values or results in areas of special interest are presented.

Heat transfer analyses. Figures 120 and 121 show temperature time histories for nodal points 3117 and 3629, respectively. Node 3117 is located at the interface between lifts 2 and 3 while node 3629 is directly above node 3117 on the slab surface. Due to longer lift intervals allowing more heat to dissipate, the shorter lift interval analyses show higher internal temperatures. Node 3629, being a surface node, is more dependent on the ambient temperature, and temperatures from the three lift interval analyses show little difference. Both locations eventually follow the ambient temperature with a slight time shift and reduced amplitude with depth into the slab. The temperature time history for node 3117 begins to follow the trend set by the ambient temperature curve at approximately relative day 100 while temperatures at node 3629 follow the ambient temperature trend at approximately relative day 10.
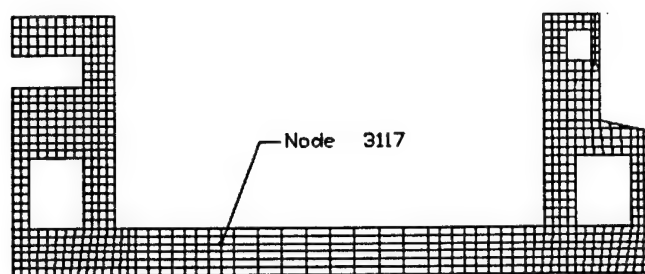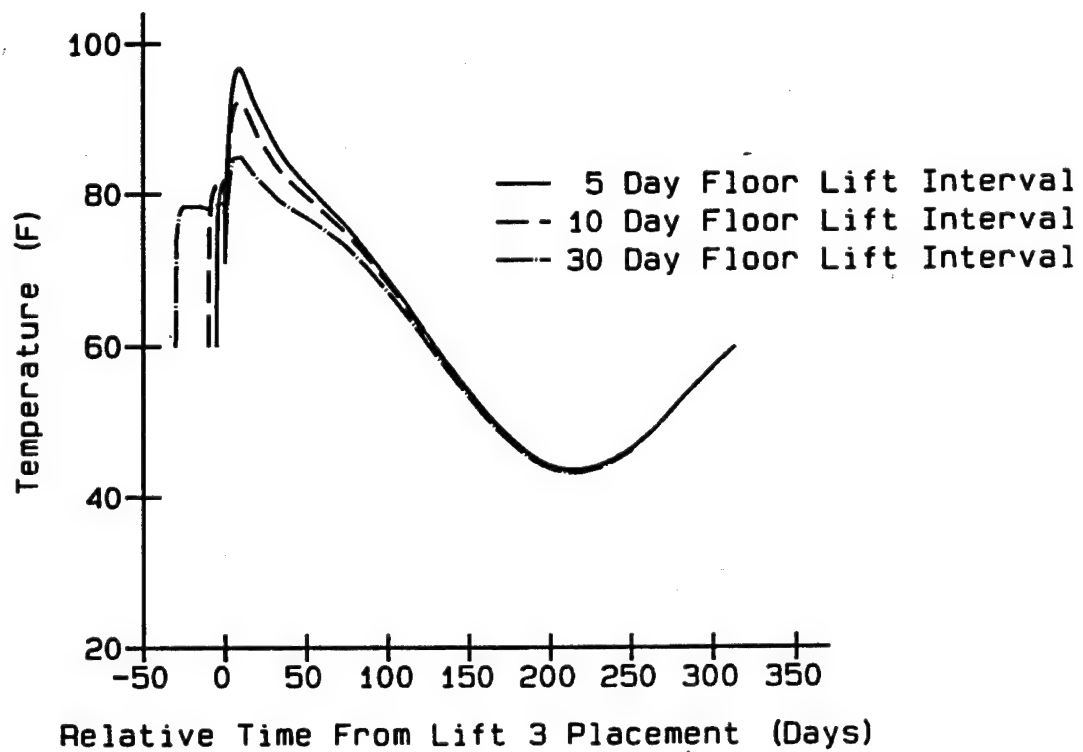
Figure 120.   Temperature time history for node 3117
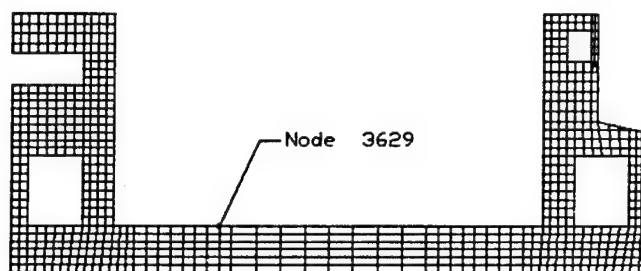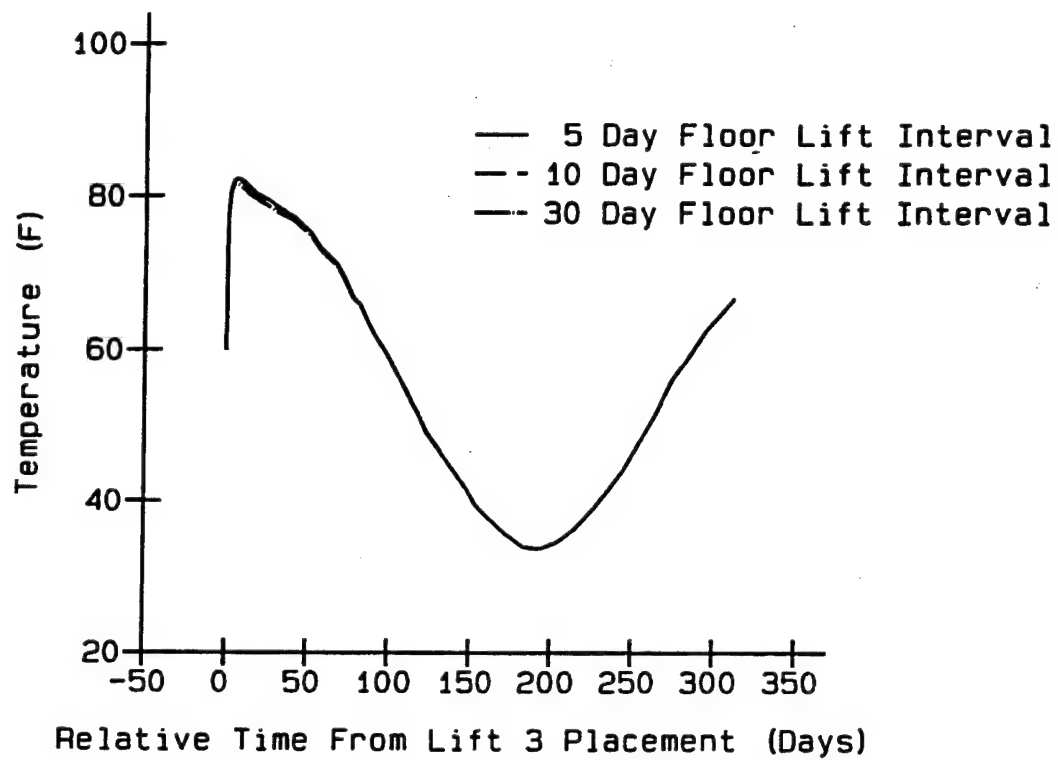
Figure 121.   Temperature time history for node 3629

Stress analyses. Time varying temperature distributions calculated in the heat transfer analyses for the three lift intervals were used as input for the stress analyses. All stresses were compared with the allowable stress computed from ETL 1110-2-324. Tables 25-27 show the maximum horizontal stresses from the analyses along with their computed percentage of the ETL allowable stress. No cracking occurred in any of the analyses for this portion on the NISA.

Maximum stress results ranked by percent of ETL 1110-2-324 allowable tensile stress are shown in Tables 25-27. These results show increased tensile stresses with increased lift placement interval. Tensile stresses reached 93.2 percent of the allowable for a 30-day lift placement interval with lesser percentages for the 10- and 5-day lift placement interval tensile stresses. Stress time histories for element 756, integration point 4, are typical of the high tensile stress regions in the slab away from regions of stress concentrations due to sharp corners at wall intersections (Figure 122). Mixture 11 concrete properties are such that the critical condition was caused by the ambient air temperature and not the heat of hydration. Therefore, the added restraint provided by previously placed lifts due to the aging increased modulus of elasticity (Figures 123-125) was a greater influence than heat retained by placing lifts at a faster rate. Longer placement intervals had similar effects on creep and shrinkage. For the 30-day interval these effects had nearly saturated when lift 3 was placed. Since lift 2 was no longer experiencing movement due to creep and shrinkage, it served as a restraint to movements in lift 3 due to these factors. This, coupled with the stiffer modulus of lift 3 compared to lift 2, resulted in higher tensile stresses at the surface of the floor slab for 30-day lift intervals at later times than stresses for 10-day lift intervals.

The same concrete aging effects in lifts 3 and 2 also resulted in higher stresses for the 10-day placement interval than the stresses for the 5-day placement interval. The differences in tensile stresses for the 10- and 5-day placement intervals were not as large as the differences in tensile stresses for the 30- and 10-day placement intervals. This was due to the smaller age difference of lifts 2 and 3 concrete (5 days) as opposed to a 20-day age difference between the longer placement intervals. The disparity in ages of the lifts also resulted in the creep and shrinkage of the previously placed lift being closer to the saturation point, maximum possible for the material, for the 30-day interval than the 10-day interval and the 10-day interval closer to saturation than the 5-day interval. These results also reflect conventional wisdom when considering the longer placement interval more closely reflects an overlay condition. However, unlike typical overlays where cracking initiates due to higher tensile stresses at the interface and progresses upward, the tensile stress is higher at the floor slab surface. Figure 126 shows the stress time history for element 702, integration point 2, which is located at the interface of lifts 2 and 3 directly below element 756, integration point 4. The maximum tensile stress value for element 702 is approximately 275 psi while the maximum tensile stress for element 756 is approximately 420 psi. This shows a tendency for a crack, if one formed, to propagate downward from the top through

Table 25
Maximum Floor Stresses (psi) for 5-Day Lift Placement Interval Analysis

Element	IP	Day	Horizontal Stress	ETL Allowable	Percent Allowable
756	4	167.5	204.4	464.0	44.0
756	3	167.5	204.3	464.0	44.0
756	2	177.5	205.4	466.6	44.0
756	1	177.5	205.3	466.6	44.0
757	3	167.5	204.0	464.0	44.0
757	1	177.5	205.1	466.6	44.0
755	4	167.5	203.9	464.0	43.9
755	2	177.5	205.0	466.6	43.9
757	2	177.5	204.5	466.6	43.8
756	1	187.5	205.5	469.0	43.8
756	2	187.5	205.5	469.0	43.8
757	4	167.5	203.3	464.0	43.8
756	2	167.5	203.2	464.0	43.8
756	1	167.5	203.1	464.0	43.8
757	1	187.5	205.2	469.0	43.8
755	2	187.5	205.2	469.0	43.8
757	1	167.5	203.0	464.0	43.7
755	1	177.5	204.0	466.6	43.7
756	3	177.5	204.0	466.6	43.7
756	4	177.5	204.0	466.6	43.7

Table 26
Maximum Floor Stresses (psi) for 10-Day Lift Placement Interval Analysis

Element	IP	Day	Horizontal Stress	ETL Allowable	Percent Allowable
756	4	172.5	267.1	462.6	57.7
756	3	172.5	267.1	462.6	57.7
757	3	172.5	266.8	462.6	57.7
755	4	172.5	266.7	462.6	57.7
757	4	172.5	266.0	462.6	57.5
755	3	172.5	265.6	462.6	57.4
756	3	182.5	266.9	465.3	57.4
756	4	182.5	266.9	465.3	57.4
755	4	182.5	266.6	465.3	57.3
757	3	182.5	266.5	465.3	57.3
758	3	172.5	264.7	462.6	57.2
754	4	172.5	264.2	462.6	57.1
755	3	182.5	265.6	465.3	57.1
757	4	182.5	265.6	465.3	57.1
756	3	192.5	266.4	467.8	56.9
756	4	192.5	266.2	467.8	56.9
755	4	192.5	266.1	467.8	56.9
754	4	182.5	264.4	465.3	56.8
757	3	192.5	265.8	467.8	56.8
758	3	182.5	264.2	465.3	56.8

Table 27
Maximum Floor Stresses (psi) for 30-Day Lift Placement Interval Analysis

Element	IP	Day	Horizontal Stress	ETL Allowable	Percent Allowable
737	3	212.5	431.4	462.6	93.2
737	3	222.5	429.9	465.3	92.4
737	3	232.5	426.9	467.8	91.3
756	4	212.5	419.6	462.6	90.7
737	3	202.5	416.9	459.7	90.7
756	3	212.5	419.5	462.6	90.7
757	3	212.5	419.3	462.6	90.6
755	4	212.5	419.1	462.6	90.6
757	4	212.5	418.6	462.6	90.5
756	3	222.5	420.9	465.3	90.5
756	4	222.5	420.9	465.3	90.4
755	4	222.5	420.6	465.3	90.4
757	3	222.5	420.5	465.3	90.4
755	3	212.5	417.9	462.6	90.3
758	3	212.5	417.5	462.6	90.2
757	4	222.5	419.7	465.3	90.2
755	3	222.5	419.6	465.3	90.2
756	3	232.5	421.3	467.8	90.1
754	4	212.5	416.6	462.6	90.0
755	4	232.5	421.1	467.8	90.0

160
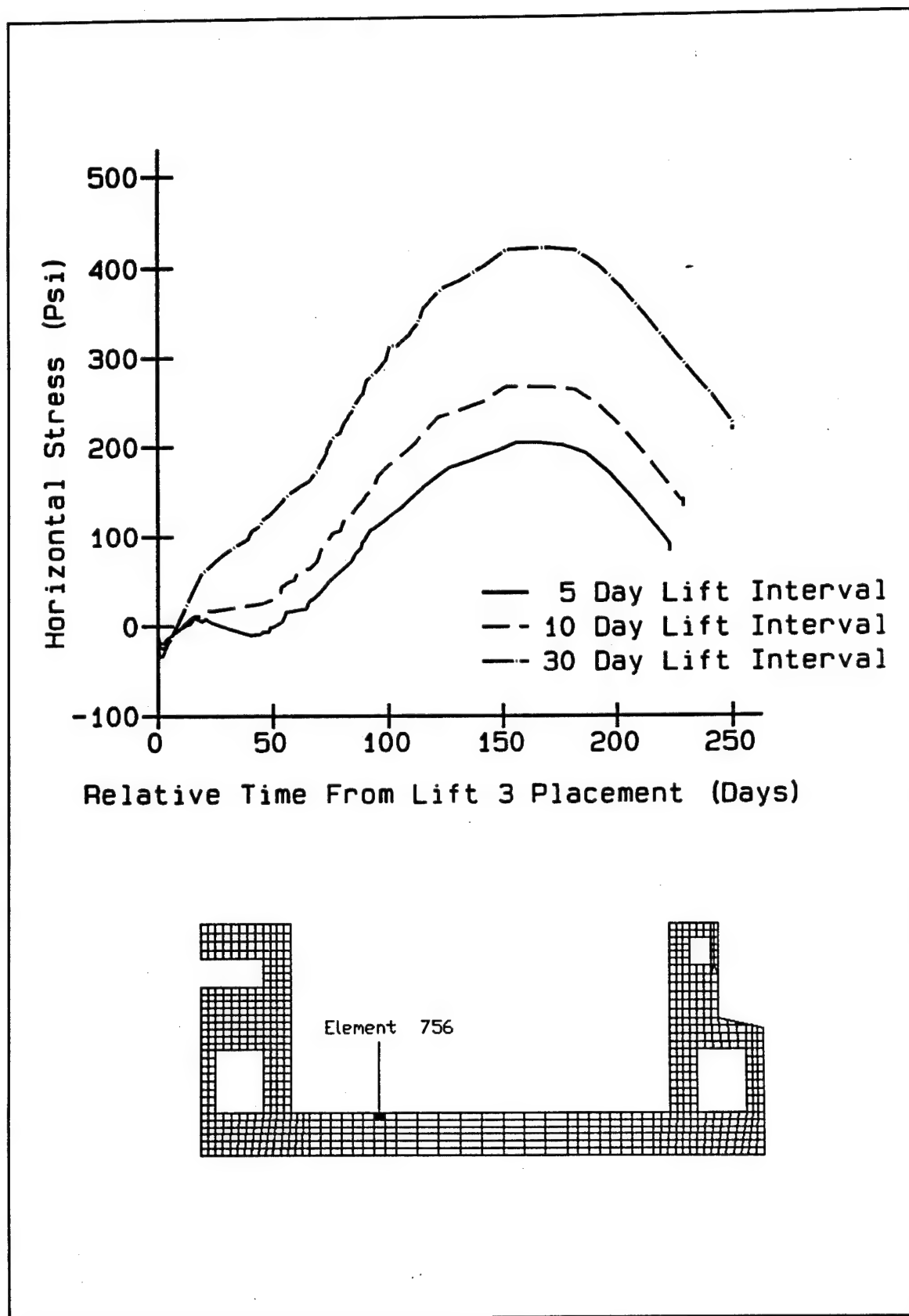
Figure 122.   Stress time history for element 756, integration point 4
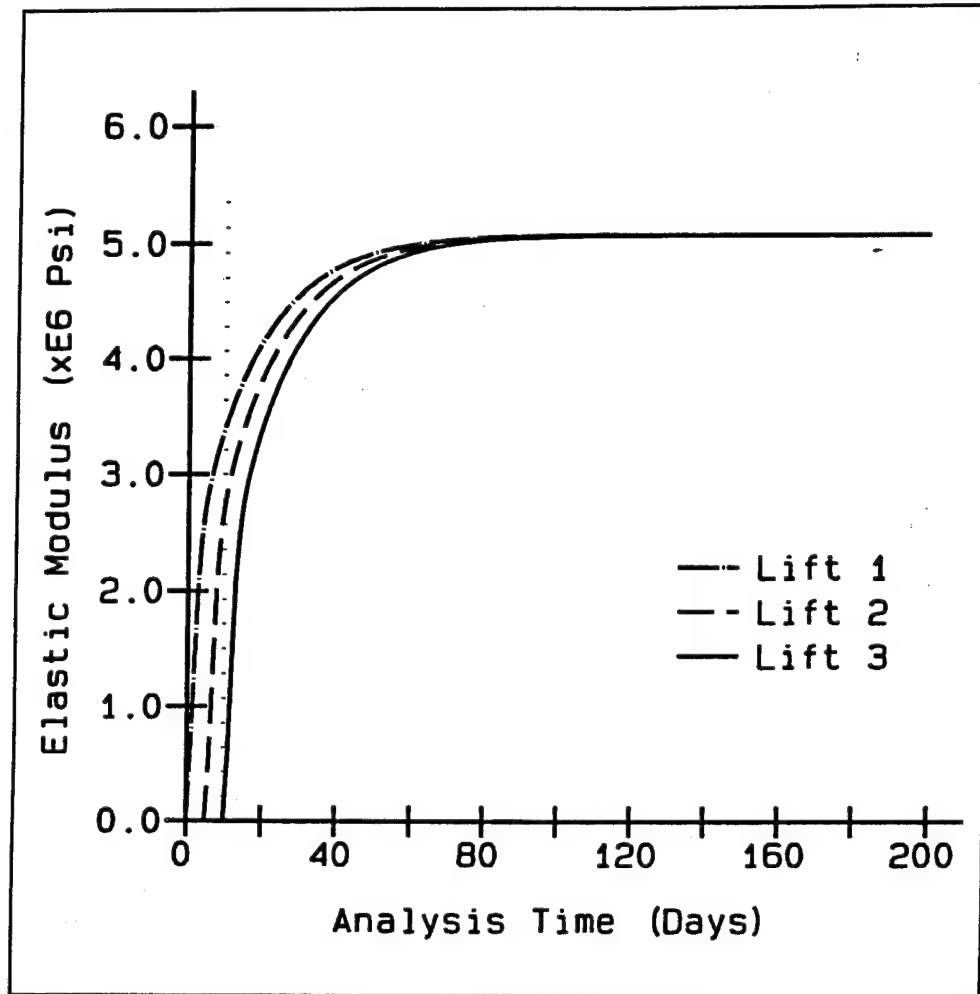
Figure 123. Elastic moduli for 5-day lift placement interval

lift 3 instead of upward from the interface which typically occurs when cracks form in overlays.

Conclusions

When the height of center wall lift 10 was increased from 6 to 12 ft in summer placement analyses, initial temperature differentials across the wall section were increased. Initial temperature differentials increased more for the analysis with ambient temperature placement than for the analysis with a maximum 60 °F placement. However, by approximately 50 days after placement, temperature differentials across the lift were similar for all analyses, regardless of placement temperature or lift height. Maximum wall stresses in the thick section of the chamber monolith center wall consisting of lifts 10 and 12 were approximately equal for the two increased lift height analyses, but location of maximum stress changed with placement temperature. For the analysis with a maximum 60 °F

Figure 124.   Elastic moduli for 10-day lift placement interval

placement temperature, maximum stresses occurred at the top of lift 10. When wall lifts were placed at ambient temperature, the location of maximum stress shifted to the center of lift 10. Maximum stresses in this section were slightly higher in the load case 5 analysis (Garner et al. 1992) than in the increased lift height analyses, possibly due to the thicker gallery wall used in the 1992 analyses. This thicker wall should result in less heat loss through the gallery. The maximum wall stress in the two increased lift height analyses occurred at the lower corner of the gallery and was about 15 percent higher in the 60 °F placement analysis than in the ambient placement analysis. The maximum principle stress at this location (element 1222, integration point 2) was 67 percent of the ETL allowable stress. Based on these analyses, maximum wall lift heights of 10 to 12 ft seem to be acceptable.

Stresses in the outer wall of the chamber monolith riverwall culvert were low in the 3D analysis. Maximum principle stresses near the outside of the wall peaked approximately 2.5 days after placement, while interior stresses peaked at a later time. Maximum principle stresses were less than
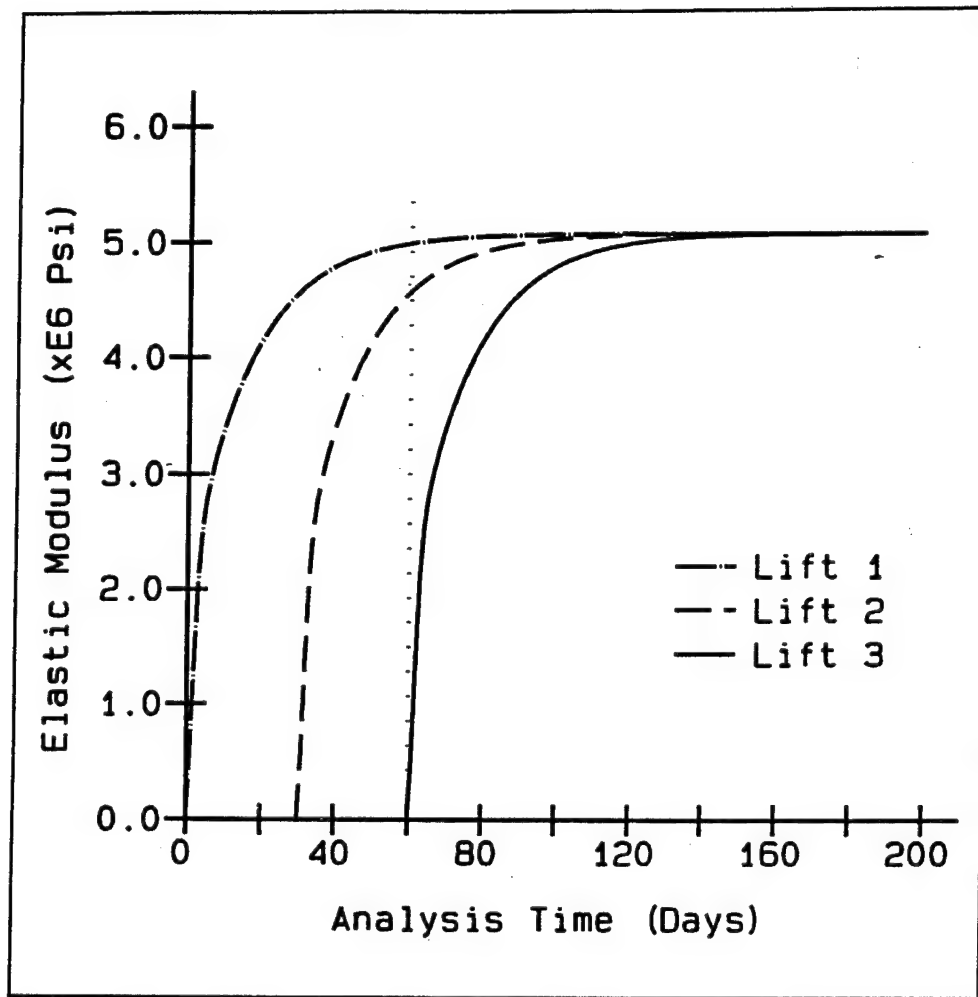
Figure 125. Elastic moduli for 30-day lift placement interval

25 psi at all times in the analysis, and no cracking of the thin outer wall seems likely to occur.
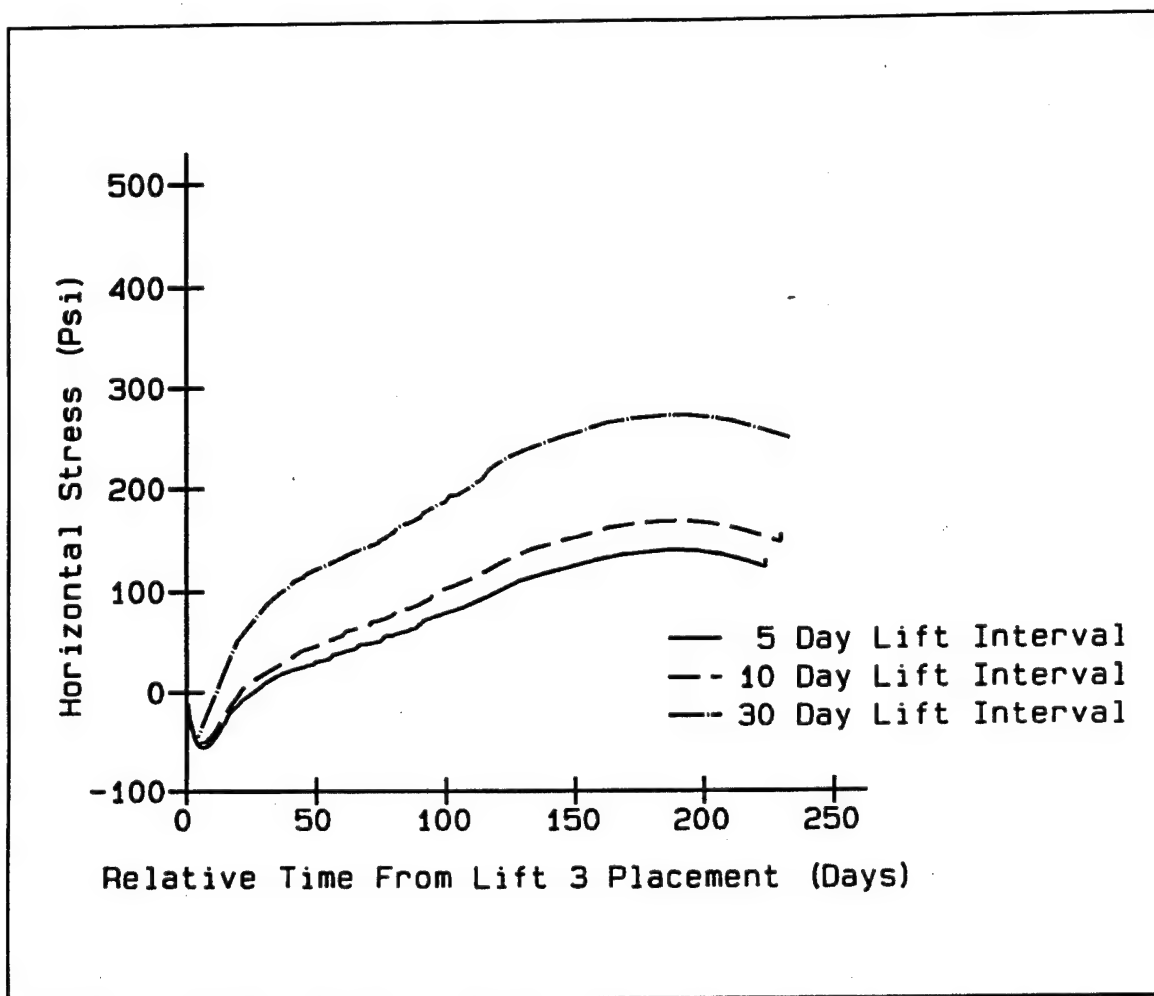
Figure 126.   Stress time history for element 702, integration point 2

7 Conclusions and Recommendations

Conclusions

During the course of the Phase III studies a substantial number of analyses were performed providing information for the Louisville District to evaluate construction of the Olmsted locks as well as for the researchers at WES to be used on future NISAs. Enumerated below are the conclusions drawn from the analyses.

a. Modeling closed culverts with air elements as suggested in ETL 1110-2-324 rather than using a low film coefficient at all interior surfaces results in higher temperatures at the interior of culverts, larger temperature differentials across wall sections, and wall stresses that represent a larger percentage of the ETL allowable stress. Results from the two methods are similar enough that the ETL method does not appear to be overly conservative, although either method should produce acceptable results.

b. During cold fronts, temperatures at the surface of the concrete can drop to 8 °F to 10 °F below ambient, or well below freezing. However, stresses calculated in the walls were within acceptable limits when wall insulation was removed at an age of 30 days. Maximum wall stresses from the winter analyses occurred at the lower corner of the center wall gallery and were approximately 50 percent of the ETL allowable stress. Surface stresses were always well below ETL allowable stresses, even when cold fronts were simulated. Based on these analyses, insulation to a concrete age of 30 days seems to be adequate for chamber monolith walls.

c. Maximum horizontal stresses in the floor remained at acceptable levels for all winter analyses using the daily average ambient temperature curve and an Oct 1 start-of-placement date. However, when later placement times were simulated in conjunction with a cold front at the time that insulation was removed and a concrete age at removal of 30 days, horizontal stresses near the surface of the

floor exceeded the ETL allowable. When the insulation was removed at an age of 90 days, the maximum horizontal stress near the surface of the floor was only about 77 percent of the ETL allowable stress. Based on these analyses, winter floor insulation should remain in place until the concrete has reached an age of 90 days.

d. Analyses of an uninsulated floor using the extreme daily ambient temperature curve rather than the daily average ambient resulted in higher horizontal stresses near the top of the floor, but all floor stresses remained within the ETL allowable. When cold fronts were simulated, maximum horizontal stresses near the surface of the floor exceeded the ETL allowable. This provides further evidence that 90 days of insulation is preferable for the chamber monolith floor.

e. Wall stresses were within the ETL allowable when the extreme ambient temperature curve with cold fronts was used. The maximum stress occurred at the corner of the center wall gallery and was approximately 64 percent of the ETL allowable stress.

f. When the height of center wall lift 10 was increased from 6 to 12 ft in summer placement analyses, initial temperature differentials across the wall section were increased. Initial temperature differentials increased more for the analysis with ambient temperature placement than for the analysis with a maximum 60 °F placement. However, by approximately 50 days after placement, temperature differentials across the lift were similar for all analyses, regardless of placement temperature or lift height. Maximum wall stresses in the thick section of the chamber monolith center wall consisting of lifts 10 and 12 were approximately equal for the two increased lift height analyses, but location of maximum stress changed with placement temperature. For the analysis with a maximum 60 °F placement temperature, maximum stresses occurred at the top of lift 10. When wall lifts were placed at ambient temperature, the location of maximum stress shifted to the center of lift 10. Maximum stresses in this section were slightly higher in the load case 5 analysis (Garner et al. 1992) than in the increased lift height analyses, possibly due to the thicker gallery wall used in the 1992 analyses. This thicker wall should result in less heat loss through the gallery. The maximum wall stress in the two increased lift height analyses occurred at the lower corner of the gallery and was about 15 percent higher in the 60 °F placement analysis than in the ambient placement analysis. The maximum principal stress at this location (element 1222, integration point 2) was 67 percent of the ETL allowable stress. Based on these analyses, maximum wall lift heights of 10 to 12 ft seem to be acceptable.

g. Stresses in the outer wall of the chamber monolith riverwall culvert were low in the 3-D analysis. Maximum principal stresses near the outside of the wall peaked approximately 2.5 days after placement, while interior stresses peaked at a later time. Maximum principal

stresses were less than 25 psi at all times in the analysis, and no cracking of the thin outer wall seems likely to occur.

h. The extreme ambient condition described in Chapter 4 appears to be a valuable tool for evaluating structures for which ambient conditions are controlling the behavior. Use of the extreme ambient curve will increase the confidence of the materials engineer that the possible range of temperatures that may occur has been accounted for. Compilation of the extreme ambient curve is also a fairly simple procedure.

i. Results from the slab and wall portions of the placement temperature study are well within the ETL allowable for stress, and no cracking occurred in the typical chamber monolith. For this geometry and concrete mixture, increased placement temperature all the way to extreme ambient conditions had no detrimental effect on structural integrity or performance.

j. The time of set for a concrete mixture is an important parameter to the performance of a NISA. Even though the 6-hr time of set analysis proved to be the controlling case for the set time analyses, it is not necessary to evaluate the Olmsted chamber monolith based on these results since test data show that the 12-hr time of set is sufficient.

k. Changing the material model to accept temperatures from the heat transfer analysis as the stress-free temperatures in a newly placed lift from using a single temperature throughout a lift is a valuable modification to the model since the change creates a more realistic model.

l. Modeling of reinforcement is a key parameter when modeling massive concrete structures for the performance of a NISA. Neglecting the fact that reinforcement is present in a structure limits the capabilities of the designer for developing the most economical structure possible.

m. Longer lift placement intervals result in higher tensile stresses in the floor slab due to the increased restraint provided by older supporting lifts. Since the elastic modulus is near its maximum at 30 days, longer lift placement intervals should not cause much increase in tensile stress. Therefore an upper bound is not necessary. Normally tensile stresses that exceed 80 percent of the ETL allowable tensile stress are of concern. However, the fact that the maximum tensile stresses should peak at around 95 percent of the allowable for lift placement intervals exceeding 30 days and that, based on Chapter 5 data, a higher placement temperature should reduce the tensile stresses in the areas of high tensile stress for the 30-day analyses, the exceeding of this limit is not of great concern.

Recommendations

Based on the results for analyses of the typical chamber monolith presented in this report several recommendations are in order as delineated below. Changes from the assumed parameters used to perform the analyses in this study may require additional analyses to ensure proper prediction of the structure's behavior.

a. Winter insulation can be removed from walls at a concrete age of 30 days. Floor insulation should remain in place until the concrete has reached an age of 90 days. The floor insulation requirement applies to the chamber monolith and all floor sections of similar thickness.

b. Wall lift heights of 10 to 12 ft can be used. This applies to all walls except those in the gate bay and tainter gate monoliths. Wall heights in these areas may be affected by analyses that are still in progress.

c. The extreme ambient condition should be used on any future NISAs when ambient conditions are expected to be or are found to be controlling the behavior of a structure.

d. Due to the uncertainty of ambient temperature throughout the construction cycle, it is unwise to relax all control of placement temperature. An extreme ambient event may occur and with no controls on placement temperature, the Government may be exposed to costly construction claims. Although analyses show that placement temperatures tied to the extreme ambient curve showed no detrimental effects on structural integrity or performance, it is difficult to place temperature limits on an oscillating value. Therefore, a constant upper limit on placement temperature is more realistic and enforceable during construction. Based on analyses, placing this limit at 60 °F is too conservative and would result in higher construction costs due to cooling requirements. The best option for temperature control lies between 70 °F and ambient temperature. For these reasons, a constant upper placement temperature of 75 °F is recommended for all typical chamber monolith concrete placement.

e. Time-of-set use in a NISA should be determined from test data. Therefore, time-of-set tests should be a part of any testing program for material properties to be used in the performance of a NISA.

f. Reinforcement should be included in all future NISAs for structures which have a high potential for cracking or when early analyses indicate cracking will occur. In addition, definitive criteria should be established which allow some cracking provided it can be shown that the crack will arrest after a given time and that the reinforcing

at which the crack occurs is capable of carrying the loads transferred into it.

References

ANATECH Research Corp. (1992). "ANACAP-U, ANATECH concrete analysis package user's manual, version 92-2.2." San Diego, CA.

Fehl, B. D., and Merrill, C. A. (in preparation). "Use of reinforcement in a nonlinear incremental structural analysis," Technical Report -94- , U.S. Army Engineer Waterways Experiment Station, Vicksburg, MS.

Garner, S., and Hammons, M. (1991). "The development and use of a time-dependent cracking model for concrete," Technical Report SL-91-7, U.S. Army Engineer Waterways Experiment Station, Vicksburg, MS.

Garner, S., Bombich, A. A., Norman, C. D., Merrill, C. A., Fehl, B. D., and Jones, H. W. (1992). "Nonlinear incremental structural analysis of Olmsted Lock and Dam," Technical Report SL-92-28, U.S. Army Engineer Waterways Experiment Station, Vicksburg, MS.

Garner, S., Hammons, M., and Bombich, A. (1991). "Red River Waterways thermal studies; Report 2, Thermal stress analysis," Technical Report SL-90-8, U.S. Army Engineer Waterways Experiment Station, Vicksburg, MS.

Hibbit, Karlsson, and Sorensen, Inc. (1988). "ABAQUS user's manual, version 4.8," Providence, RI.

U.S. Army Corps of Engineers. (1990). "Special design provisions for massive concrete structures," Engineer Technical Letter 1110-2-324, Washington, D.C.

REPORT DOCUMENTATION PAGE

Public reporting burden for this collection of information is estimated to average 1 hour per response, including the time for reviewing instructions, searching existing data sources, gathering and maintaining the data needed, and completing and reviewing the collection of information. Send comments regarding this burden estimate or any other aspect of this collection of information, including suggestions for reducing this burden, to Washington Headquarters Services, Directorate for Information Operations and Reports, 1215 Jefferson Davis Highway, Suite 1204, Arlington, VA 22202-4302, and to the Office of Management and Budget, Paperwork Reduction Project (0704-0188), Washington, DC 20503.

1. AGENCY USE ONLY (Leave blank)	2. REPORT DATE January 1995	3. REPORT TYPE AND DATES COVERED Final report

4. TITLE AND SUBTITLE
Nonlinear, Incremental Structural Analysis of Olmsted Locks: Phase III

5. FUNDING NUMBERS

6. AUTHOR(S)
Chris A. Merrill, Barry D. Fehl, Sharon Garner

7. PERFORMING ORGANIZATION NAME(S) AND ADDRESS(ES)
U.S. Army Engineer Waterways Experiment Station
3909 Halls Ferry Road, Vicksburg, MS 39180-6199

8. PERFORMING ORGANIZATION REPORT NUMBER
Technical Report ITL-95-1

9. SPONSORING/MONITORING AGENCY NAME(S) AND ADDRESS(ES)
U.S. Army Engineer District, Louisville
Louisville, KY 40201-0059

10. SPONSORING/MONITORING AGENCY REPORT NUMBER

11. SUPPLEMENTARY NOTES
Available from National Technical Information Service, 5285 Port Royal Road, Springfield, VA 22161.

12a. DISTRIBUTION/AVAILABILITY STATEMENT
Approved for public release; distribution is unlimited.

12b. DISTRIBUTION CODE

13. ABSTRACT (Maximum 200 words)

The Olmsted Locks and Dam will be constructed on the Ohio River at mile 964.4. Since the design of the locks is the unprecedented W-frame type structure, extensive studies have been undertaken to determine the constructability of the lock.

This report is part of the third phase of a study evaluating the constructability of the Olmsted locks using nonlinear, incremental structural analysis methods outlined in ETL 1110-2-324, "Special Design Provisions for Massive Concrete Structures." The first two phases of the study, which led to the third phase, evaluated parameters such as plane stress versus plane strain analysis, creep, shrinkage, placing schemes, and two concrete mixtures and are reported in a WES report "Nonlinear, Incremental Structural Analysis of Olmsted Locks and Dams."

Contained in this third phase report are results of parametric studies on insulation, placing temperatures, placement intervals, various ambient conditions, and different concrete set times. Results of analyses performed led to recommending higher placing temperatures than originally planned and shorter insulation periods for portions of a chamber monolith.

14. SUBJECT TERMS

Aging	Finite element	Shrinkage
Cracking	Mass concrete	
Creep	Nonlinear analysis	

15. NUMBER OF PAGES
187

16. PRICE CODE

17. SECURITY CLASSIFICATION OF REPORT UNCLASSIFIED	18. SECURITY CLASSIFICATION OF THIS PAGE UNCLASSIFIED	19. SECURITY CLASSIFICATION OF ABSTRACT	20. LIMITATION OF ABSTRACT